Universidade de Aveiro Departamento de Biologia
2015

ISABEL OLIVEIRA FERNANDES

Mecanismo de infecção de *Diplodia corticola*

Infection mechanism of *Diplodia corticola*

A tese foi realizada em regime de co-tutela com a Universidade de Ghent na Bélgica.

The thesis was realized in co-tutelle regime (Joint PhD) with the Ghent University in Belgium.

Universidade de Aveiro Departamento de Biologia
2015

ISABEL OLIVEIRA FERNANDES

Mecanismo de infecção de *Diplodia corticola*

Infection mechanism of *Diplodia corticola*

Tese apresentada à Universidade de Aveiro para cumprimento dos requisitos necessários à obtenção do grau de Doutor em Biologia, realizada sob a orientação científica da Doutora Ana Cristina de Fraga Esteves, Professora Auxiliar Convidada do Departamento de Biologia da Universidade de Aveiro e co-orientações do Doutor Artur Jorge da Costa Peixoto Alves, Investigador Principal do Departamento de Biologia da Universidade de Aveiro e do Doutor Bart Devreese, Professor Catedrático do Departamento de Bioquímica e Microbiologia da Universidade de Ghent. A tese foi realizada em regime de co-tutela com a Universidade de Ghent.

Apoio financeiro da FCT e do FEDER através do programa COMPETE no âmbito do projecto de investigação PROMETHEUS.

Bolsas com referência:
PTDC/AGR-CFL/113831/2009
FCOMP-01-0124-FEDER-014096

Apoio financeiro da FCT e do FSE no âmbito do III Quadro Comunitário de Apoio.

Bolsa com referência BD/66223/2009

FCT Fundação para a Ciência e a Tecnologia
MINISTÉRIO DA EDUCAÇÃO E CIÊNCIA

POPH PROGRAMA OPERACIONAL POTENCIAL HUMANO

QREN QUADRO DE REFERÊNCIA ESTRATÉGICO NACIONAL PORTUGAL 2007.2013

UNIÃO EUROPEIA
Fundo Social Europeu

Perguntaste-me um dia o que pretendia fazer a seguir,
Respondi-te simplesmente que gostaria de ir mais além,
Assim fiz!

Gostava que me perguntasses de novo...

Ao meu pai,

You asked me one day what I intended to do next,
I simply answered you that I would like to go further,
I did so!

I would like you ask me again...

To my father,

O júri

Presidente

Prof. Doutora Anabela Botelho Veloso
Professora Catedrática do Departamento de Economia, Gestão e Engenharia Industrial da Universidade de Aveiro, Portugal

Prof. Doutor Bart Devreese
Full Professor in the Department of Biochemistry and Microbiology of Ghent University, Belgium

Prof. Doutor Nelson Manuel Viana da Silva Lima
Professor Catedrático do Centro de Engenharia Biológica da Universidade do Minho, Portugal

Prof. Doutor António Carlos Matias Correia
Professor Catedrático do Departamento de Biologia da Universidade de Aveiro, Portugal

Doutora Rebeca Cobos Román
Research Scientist in the Instituto de Investigación de la Viña y el Vino de la Universidad de León, Spain

Doutora Sónia Cláudia Morgado Gonçalves
Investigadora Principal do Centro de Biotecnologia Agrícola e Agro-Alimentar do Alentejo, Portugal

Prof. Doutora Ana Cristina de Fraga Esteves
Professora Auxiliar Convidada do Departamento de Biologia da Universidade de Aveiro, Portugal

Doutora Katarzyna Ciesielska
Postdoctoral Researcher in the Department of Biochemistry and Microbiology of Ghent University, Belgium

Agradecimentos

A apresentação desta dissertação de doutoramento representa o culminar de uma etapa académica, havendo contributos que gostaria que não passassem despercebidos. Por este motivo, desejo expressar os meus sinceros agradecimentos:

À Dra. Ana Cristina Esteves, minha orientadora, que me concedeu a oportunidade de desenvolver este trabalho científico em simultâneo nas Universidades de Aveiro e Gent. Muito obrigada pelos votos de confiança.

Ao Prof. Bart Devreese, que me acolheu no seu grupo de trabalho, no qual aprendi imenso, tendo igualmente tido a oportunidade de transmitir aquilo que aprendi. Foi uma experiência nem sempre fácil, mas bastante positiva.

Ao Dr. Artur Alves pela confiança.

Ao Prof. António Correia por me ter concedido a oportunidade de desenvolver este trabalho no Microlab (CESAM).

A toda a equipa do L-Probe, sempre atenciosos.

Ao Isaak por toda a paciência dispendida para comigo. A conclusão deste trabalho deve-se em grande parte ao que me transmitiu e às dicas que me foi sugerindo ao longo do tempo.

À Nádia, pela amizade e pelas muitas frustrações partilhadas.

À Andreia, pela amizade e pela partilha de conhecimentos. Foram muitas vezes cruciais para a prossecução do trabalho.

À Maria, conhecemo-nos por mero acaso sem nunca pensar-mos que vínhamos do mesmo país. Ainda bem que assim foi!

Aos amigos do coração, Sandra, Zé e Ana, longe, perto, nada muda!

À minha família, mantiveram sempre o seu apoio incondicional ao longo deste percurso.

Por último, mas longe, muito longe de ser o último, ao Gonçalo, meu amigo e galanteado. Por toda a paciência e tenacidade que mantiveste ao longo destes anos repletos de vicissitudes. Tenho a maior das gratidões pela incansável dedicação, carinho e afeição com que me enlaçaste.

Acknowledgments

The presentation of this doctoral dissertation represents the culmination of an academic step, whereby there are contributions that I would like did not pass unnoticed. For this reason, I wish to express my sincere thanks:

To Dr. Ana Cristina Esteves, my advisor, that gave me the opportunity to develop this scientific work simultaneoulsy at the Universities of Aveiro and Ghent. Thank you for the votes of confidence.

To Prof. Bart Devreese, that received me in his working group, wherein I learned a lot and where I had also the opportunity transmit what I have learned. It was an experience not always easy, but extremely positive.

To Dr. Artur Alves for the trust.

To Prof. António Correia for giving me the opportunity to develop this work in the Microlab (CESAM).

To all the team of L-Probe, always kind.

To Isaak for all the patience spent with me. The conclusion of this work owes largely to the knowledge that he conveyed me and to the tips suggested along the time.

To Nádia, for her friendship and for all the shared frustrations.

To Andreia, for her friendship and for the sharing of knowledge. It was often crucial for the work progress.

To Maria, we knew each other by chance without ever imagine that we came from the same country. Thankfully it was like that!

To my dearest friends, Sandra, Zé e Ana, far, near, nothing changes!

To my family, that always kept their unconditional support along this journey.

And lastly, but far, far from being the last, to Gonçalo, my friend and gallant. For all the patience and tenacity that you maintained along these years full of vicissitudes. I have the greatest gratitude for the tireless dedication, fondness and affection with which you enlaced me.

Palavras-chave

Diplodia corticola, *Botryosphaeriaceae*, declínio do sobreiro, proteoma, secretoma, sequenciação *de novo*

Resumo

Diplodia corticola é considerado o fungo mais virulento associado ao declínio do sobreiro, infectando não só espécies de *Quercus* (na maioria *Q. suber* e *Q. ilex*), como também videiras (*Vitis vinifera*) e eucaliptos (*Eucalyptus* sp.). Este fungo endofítico é também um patógeno, cuja virulência se manifesta reiteradamente com o aparecimento de *stress* na planta. Considerando que a infeção culmina frequentemente na morte do hospedeiro, a sua propagação gera uma crescente preocupação a nível ecológico e socio-económico. Os mecanismos moleculares da infeção permanecem até agora largamente desconhecidos.

Por conseguinte, o objectivo deste estudo é revelar potenciais fatores de virulência implicados na infeção de *D. corticola*. Este conhecimento é essencial para delinear a estrutura molecular que lhe permite invadir e proliferar nos seus hospedeiros, causando doença. Como os efetores utilizados são na sua maioria proteínas, adoptou-se uma abordagem proteómica.

Foram realizados testes de patogenicidade *in planta* para seleccionar duas estirpes de *D. corticola* com graus de virulência distintos, para os estudos que se subseguiram.

À semelhança de outros fungos filamentosos, *D. corticola* secreta concentrações diminutas de proteínas *in vitro*, assim como elevados níveis de polissacáridos, duas características que dificultam a análise do secretoma. Assim, compararam-se vários métodos de extracção de proteínas extracelulares para averiguar o seu desempenho e compatibilidade com a separação electroforética por 1D e 2D. A precipitação de proteínas com TCA-acetona e TCA-fenol foram os métodos mais eficientes, tendo-se seleccionado o primeiro para os estudos ulteriores.

As proteínas foram extraídas, separadas por 2D-PAGE, digeridas com tripsina e os péptidos resultantes analisados por MS/MS. A sua identificação foi efetuada por sequenciação *de novo* e/ou por pesquisa no MASCOT. Deste modo, identificaram-se 80 proteínas extracelulares e 162 intracelulares, um marco para a família *Botryosphaeriaceae* que contém apenas um membro com o proteoma caracterizado. Realizou-se também uma extensa análise comparativa dos géis 2D para evidenciar as proteínas expressas de forma diferenciada durante a mimetização de infeção. Foram ainda comparados os perfis proteicos de duas estirpes com diferentes graus de virulência.

Em suma, caracterizou-se pela primeira vez o secretoma e proteoma de *D. corticola*. Os resultados obtidos contribuiram ainda para a elucidação de alguns aspetos da biologia do fungo. A estirpe avirulenta contém um leque variado de proteínas que facilitam a adaptação a vários substratos, e as proteínas identificadas sugerem que este fungo degrada os tecidos dos hospedeiros recorrendo a reações de Fenton. Além disso, constatou-se que esta estirpe metaboliza ácido aminobutírico, uma molécula que poderá ser o factor desencadeante da transição do estado latente para patogénico. Por fim, o secretoma inclui potenciais factores de patogenicidade como a deuterolisina (peptidase M35) e a cerato-platanina, proteínas que poderão desempenhar um papel activo no modo de vida fitopatogénico do fungo. De forma geral, os resultados sugerem que *D. corticola* tem um estilo de vida hemibiotrófico, transitando de uma interacção biotrófica para necrotrófica após a ocorrência de distúrbios fisiológicos da planta. Esta percepção é essencial para o futuro desenvolvimento de medidas efectivas de protecção das plantas.

Keywords *Diplodia corticola*, *Botryosphaeriaceae*, cork oak decline, proteome, secretome, *de novo* sequencing

Abstract

Diplodia corticola is regarded as the most virulent fungus involved in cork oak decline, being able to infect not only *Quercus* species (mainly *Q. suber* and *Q. ilex*), but also grapevines (*Vitis vinifera*) and eucalypts (*Eucalyptus* sp.). This endophytic fungus is also a pathogen whose virulence usually manifests with the onset of plant stress. Considering that the infection normally culminates in host death, there is a growing ecologic and socio-economic concern about *D. corticola* propagation. The molecular mechanisms of infection are hitherto largely unknown.

Accordingly, the aim of this study was to unveil potential virulence effectors implicated in *D. corticola* infection. This knowledge is fundamental to outline the molecular framework that permits the fungal invasion and proliferation in plant hosts, causing disease. Since the effectors deployed are mostly proteins, we adopted a proteomic approach.

We performed *in planta* pathogenicity tests to select two *D. corticola* strains with distinct virulence degrees for our studies.

Like other filamentous fungi *D. corticola* secretes protein at low concentrations *in vitro* in the presence of high levels of polysaccharides, two characteristics that hamper the fungal secretome analysis. Therefore, we first compared several methods of extracellular protein extraction to assess their performance and compatibility with 1D and 2D electrophoretic separation. TCA-Acetone and TCA-phenol protein precipitation were the most efficient methods and the former was adopted for further studies.

The proteins were extracted and separated by 2D-PAGE, proteins were digested with trypsin and the resulting peptides were further analysed by MS/MS. Their identification was performed by *de novo* sequencing and/or MASCOT search. We were able to identify 80 extracellular and 162 intracellular proteins, a milestone for the *Botryosphaeriaceae* family that contains only one member with the proteome characterized. We also performed an extensive comparative 2D gel analysis to highlight the differentially expressed proteins during the host mimicry. Moreover, we compared the protein profiles of the two strains with different degrees of virulence.

In short, we characterized for the first time the secretome and proteome of *D. corticola.* The obtained results contribute to the elucidation of some aspects of the biology of the fungus. The avirulent strain contains an assortment of proteins that facilitate the adaptation to diverse substrates and the identified proteins suggest that the fungus degrades the host tissues through Fenton reactions. On the other hand, the virulent strain seems to have adapted its secretome to the host characteristics. Furthermore, the results indicate that this strain metabolizes aminobutyric acid, a molecule that might be the triggering factor of the transition from a latent to a pathogenic state. Lastly, the secretome includes potential pathogenicity effectors, such as deuterolysin (peptidase M35) and cerato-platanin, proteins that might play an active role in the phytopathogenic lifestyle of the fungus. Overall, our results suggest that *D. corticola* has a hemibiotrophic lifestyle, switching from a biotrophic to a necrotrophic interaction after plant physiologic disturbances.This understanding is essential for further development of effective plant protection measures.

Trefwoorden

Diplodia corticola, *Botryosphaeriaceae*, achteruitgang van de kurk eik, proteoom, secretoom, *de novo* sequencing

Samenvatting

Diplodia corticola behoort tot de meest virulente plantenpathogene schimmels en wordt verantwoordelijk geacht voor de achteruitgang van de kurkeik populatie. Ze infecteert niet alleen *Quercus* soorten (voornamelijk *Q. suber* en *Q. ilex*), maar ook wijnstokken (*Vitis vinifera*) en eucalyptus (*Eucalyptus* sp.). Deze endofytische schimmel is een pathogeen waarvan de virulentie zich meestal manifesteert wanneer de plant een stress ervaart, bijvoorbeeld bij droogte. Gelet op het feit dat de infectie meestal fataal is voor de gastheerplant, is er een groeiende ecologische en sociaal-economische bezorgdheid over *D. corticola*. De moleculaire mechanismen vande infectie zijn tot nu toe echter grotendeels onbekend.

Het doel van deze studie was dan ook om potentiële virulentie effectoren betrokken bij *D. corticola* infectie te ontdekken, wat ons een fundamentele kennis moet opleveren over het moleculaire arsenaal waarmee de schimmel invasie en proliferatie kan uitvoeren in plantgastheren. Aangezien dergelijke effectoren meestal eiwitten zijn, kozen we voor proteoomanalyse als benadering van de problematiek.

Wij zijn gestart met het testen van *in planta* pathogeniciteit testen van verschillende stammen op basis waarvan twee *D. corticola* stammen met verschillende virulentiegraadwerden geselecteerd voor verdere studies.

Zoals andere filamenteuze schimmelssecreteert *D. corticola in vitro* relatief lage gehalten van eiwittenin aanwezigheid van grote hoeveelheden polysacchariden, wat de analyse van het secretoom bemoeilijkt. Daarom, vergeleken we eerst verschillende methoden voor de extractie van extracellulaire eiwitten op basis van hun performantie en compatibiliteit met 1D en 2D elektroforetische scheiding. Eiwitprecipitatie met TCA-aceton en TCA-fenol bleken de meest efficiënte methoden, de eerste methode werd uitgekozen voor de verdere analysen.

Eiwitten werden vervolgens geëxtraheerd en gescheiden via 2D-PAGE, en de peptiden werden verder geanalyseerd met MS/MS. De eiwitten werden geïdentificeerd door *de novo* sequentiebepaling en/of MASCOT als zoekroutine. Wij konden op deze manier 80 extracellulaire eiwitten en 162 intracellulaire identificeren, een mijlpaal voor de studies binnen de *Botryosphaeriaceae* familie waarvan tot nu toe van slechts drie leden het proteoom werd gekarakteriseerd. Dit werd gekoppeld aan een vergelijkende 2D-PAGE analyse om differentieel geproduceerde proteïnen betrokken bij host-pathogeen interactie te identificeren. Bovendien werden de eiwitprofielen van de twee stammen met verschillende virulentievergeleken.

Kortom, voor het eerst werd het secretoom en proteoom van D. corticolain kaart gebracht. De verkregen resultaten kunnen bijdragen tot de opheldering van de biologie van de schimmel. De avirulente stam bevat een assortiment van proteïnen toe dat het organisme toelaat om zich gemakkelijk aan te passen aan diverse omstandigheden en de geïdentificeerde eiwitten suggereren dat de schimmel weefsels van de aangetaste plantdoor Fenton reacties degradeert. Aan de andere kant, lijkt de virulente stam zijn secretoom veel beter aan de gastheerkenmerken te hebben aangepast. Bovendien blijkt uit de resultaten dat deze stam aminoboterzuur kan metaboliseren, een molecule die misschien wel de activerende factor van de overgang van een latente naar een pathogene toestand is.Tenslotte werden eiwitten geïdentificeerd, zoals deuterolysin (dipeptidylpeptidase M35) en cerato-platanin, die een actieve rol in de plantpathogene levensstijl van de schimmel kunnen hebben.Onze resultaten suggereren dat *D. corticola* een hemibiotrophic levensstijl onderhoudt, waarbij het overschakelt van een biotrofe naar een necrotrofe interactie ten gevolge van plantenfysiologische verstoringen. Deze kennis is van essentieel belang voor de verdere ontwikkeling van effectieve bestrijdingsmiddelen.

CONTENTS

RESUMO **13**

ABSTRACT **15**

SAMENVATTING **17**

CONTENTS **19**

LIST OF FIGURES **21**

LIST OF TABLES **22**

ABBREVIATIONS **23**

CHAPTER 1 - INTRODUCTION **27**

CORK OAK DECLINE 29

DIPLODIA CORTICOLA AS A PHYTOPATHOGENIC FUNGI 32

PLANT-FUNGAL INTERACTIONS 34

PROTEOMICS OF PHYTOPATHOGENIC FUNGI 38

AIMS OF THE WORK 40

REFERENCES 40

CHAPTER 2 - SECRETOME ANALYSIS IDENTIFIES POTENTIAL VIRULENCE FACTORS OF *DIPLODIA CORTICOLA*, A FUNGAL PATHOGEN INVOLVED IN CORK OAK (*QUERCUS SUBER*) DECLINE **49**

INTRODUCTION 51

MATERIAL AND METHODS 52

Microorganisms and culture conditions 52

Extracellular protein extraction methods 52

Protein concentration determination 53

1D- and 2D-electrophoresis 53

Mass spectrometry 54

RESULTS AND DISCUSSION 55

REFERENCES 62

CHAPTER 3 - PROTEOMIC PROFILE OF *DIPLODIA CORTICOLA* STRAINS WITH DISTINCT VIRULENCE DEGREES **67**

INTRODUCTION 69

MATERIAL AND METHODS 70

Qualitative pathogenicity tests 70

Fungal strains and plant seedlings *70*
In planta inoculations *70*
Secretome and proteome analysis 70
Culture conditions *70*
Extracellular protein extraction *71*
Intracellular protein extraction *72*
Protein quantification *72*
1D and 2D electrophoresis *72*
In-gel digestion and mass spectrometry *73*
Protein identification *74*
Gel image analysis *74*
RESULTS AND DISCUSSION 75
Qualitative pathogenicity tests 75
Secretome analysis 77
1D evaluation of protein extracts *77*
Control vs. infection-like secretomes of strains with different agressiveness *78*
Proteome analysis 98
1D evaluation of protein extracts *98*
Control vs. infection-like proteomes of strains with different agressiveness *98*
REFERENCES 122

CHAPTER 4 - CONCLUDING REMARKS AND FUTURE PERPECTIVES 131

MAJOR CONCLUSIONS 133
FUTURE PERSPECTIVES 134
REFERENCES 135

APPENDIX I 139

CAA 008 EXT CONTROL VS. CAA 499 EXT CONTROL 141
CAA 008 EXT INFECTION-LIKE VS. CAA 499 EXT INFECTION-LIKE 148
CAA 008 INT CONTROL VS. CAA 499 INT CONTROL 155

APPENDIX II 167

PUBLICATIONS 169
POSTER AND ORAL COMMUNICATIONS 177

LIST OF FIGURES

FIGURE 1 | DEVELOPMENT PATTERN OF CORK OAK DECLINE SYMPTOMATOLOGY 30
FIGURE 2 | CONCEPTUAL ZIZ-ZAG MODEL OF PLANT IMMUNE SYSTEM. 35
FIGURE 3 | CONCEPTUAL INVASION MODEL OF AN ATTEMPTED PLANT-INVADER SYMBIOSIS. 37
FIGURE 4 | SDS-PAGE OF SECRETOME PROTEINS FROM *D. CORTICOLA* EXTRACTED BY SEVERAL METHODS 56
FIGURE 5 | 2-DE OF PROTEINS EXTRACTED WITH TCA-ACETONE, TCA-PHENOL AND ULTRAFILTRATION 57
FIGURE 6 | NUMBER OF SPOTS DETECTED BY 2-DE OF PROTEINS EXTRACTED WITH THE VARIOUS METHODS USED 58
FIGURE 7 | *QUERCUS SUBER* DISEASE SEVERITY INDUCED BY *D. CORTICOLA* THROUGHOUT 30 DAYS AFTER INOCULATION 75
FIGURE 8 | *QUERCUS SUBER* DECLINING SYMPTOMS CAUSED BY ARTIFICIAL *D. CORTICOLA* STEM INFECTION 76
FIGURE 9 | SDS-PAGE OF *D. CORTICOLA* EXTRACELLULAR PROTEINS 77
FIGURE 10 | 2D AVERAGE GELS OF CONTROL AND INFECTION-LIKE SECRETOMES OF THE *D. CORTICOLA* AVIRULENT STRAIN. 87
FIGURE 11 | 2D AVERAGE GELS OF CONTROL AND INFECTION-LIKE SECRETOMES OF THE *D. CORTICOLA* VIRULENT STRAIN 92
FIGURE 12 | SDS-PAGE OF *D. CORTICOLA* INTRACELLULAR PROTEINS..... 98
FIGURE 13 | SUBCELLULAR LOCALIZATION DISTRIBUTION OF THE *D. CORTICOLA* INTRACELLULAR PROTEINS 99
FIGURE 14 | 2D AVERAGE GELS OF CONTROL AND INFECTION-LIKE PROTEOMES OF THE *D. CORTICOLA* AVIRULENT STRAIN 103
FIGURE 15 | 2D AVERAGE GELS OF CONTROL AND INFECTION-LIKE PROTEOMES OF THE *D. CORTICOLA* VIRULENT STRAIN ... 113
FIGURE 16 | 2D AVERAGE GELS OF *D. CORTICOLA* CONTROL SECRETOMES OF THE AVIRULENT AND VIRULENT STRAINS..... 141
FIGURE 17 | 2D AVERAGE GELS OF *D. CORTICOLA* INFECTION-LIKE SECRETOMES OF THE AVIRULENT AND VIRULENT STRAINS.... 148
FIGURE 18 | 2D AVERAGE GELS OF *D. CORTICOLA* CONTROL PROTEOMES OF THE AVIRULENT AND VIRULENT STRAINS..... 155

LIST OF TABLES

TABLE 1 | SUMMARY OF THE PROTOCOLS USED TO EXTRACT THE SECRETOME OF *D. CORTICOLA*..... 55

TABLE 2 | SUMMARY OF PROTEINS IDENTIFIED BY *DE NOVO* SEQUENCING..... 59

TABLE 3 | NUMBER OF EXTRACELLULAR PROTEINS IDENTIFIED IN *D. CORTICOLA* STRAINS CAA 008 AND CAA 499. 80

TABLE 4 | SUMMARY OF THE EXTRACELLULAR PROTEINS IDENTIFIED IN CAA 008 EXT CONTROL AND CAA 008 EXT INFECTION-LIKE BY *DE NOVO* SEQUENCING AND/OR MASCOT SEARCH..... 88

TABLE 5 | SUMMARY OF THE EXTRACELLULAR PROTEINS IDENTIFIED IN CAA 499 EXT CONTROL AND CAA 499 EXT INFECTION-LIKE BY *DE NOVO* SEQUENCING AND/OR MASCOT SEARCH. 93

TABLE 6 | NUMBER OF INTRACELLULAR PROTEINS IDENTIFIED IN BOTH CAA 008 AND CAA 499 *D. CORTICOLA* STRAINS..... 99

TABLE 7 | SUMMARY OF THE INTRACELLULAR PROTEINS IDENTIFIED IN CAA 008 INT CONTROL AND CAA 008 INT INFECTION-LIKE BY *DE NOVO* SEQUENCING AND/OR MASCOT SEARCH..... 104

TABLE 8 | SUMMARY OF THE INTRACELLULAR PROTEINS IDENTIFIED IN CAA 499 INT CONTROL AND CAA 499 INT INFECTION-LIKE BY *DE NOVO* SEQUENCING AND/OR MASCOT SEARCH..... 114

TABLE 9 | SUMMARY OF THE EXTRACELLULAR PROTEINS IDENTIFIED IN CAA 008 EXT CONTROL AND CAA 499 EXT CONTROL BY *DE NOVO* SEQUENCING AND/OR MASCOT SEARCH. 142

TABLE 10 | SUMMARY OF THE EXTRACELLULAR PROTEINS IDENTIFIED IN CAA 008 EXT INFECTION-LIKE AND CAA 499 EXT INFECTION-LIKE BY *DE NOVO* SEQUENCING AND/OR MASCOT SEARCH..... 149

TABLE 11 | SUMMARY OF THE INTRACELLULAR PROTEINS IDENTIFIED IN CAA 008 INT CONTROL AND CAA 499 INT CONTROL BY *DE NOVO* SEQUENCING AND/OR MASCOT SEARCH..... 156

ABBREVIATIONS

1D - 1-dimensional electrophoresis

2D - 2-dimensional electrophoresis

ACN - Acetonitrile

Avg - Average intensity of a spot in all gel images of a group

CAA - Acronym for Artur Alves Culture Colection

CAZy - Carbohydrate-active enzymes database

CBB - Coomassie Brilliant Blue G-250

CBS - Centraalbureau voor Schimmelcultures (Utrecht, Netherlands) accession number of strain culture

CHAPS - 3-[(3-cholamidopropyl) dimethyl-ammonio]-1-propanesulfonate (zwitterionic detergent)

CHCA - α-cyano-4-hydroxycinnamic acid

CWDE - Cell-wall degrading enzymes

Da - Dalton

DAMPs - Damage-associated molecular patterns

DTT - Dithiothreitol

EDTA - Ethylenediamine-tetraacetic acid

ETI - Effector-triggered immunity

ETS - Effector-triggered susceptibility

FASTS - Sequence alignment algorithm that compares unordered peptides to a protein sequence database

***g* -** Gravitational acceleration

GABA - γ-aminobutyric acid

GH - Glycoside hydrolase

GPS - Global Protein Server Explorer™

HR - Hypersensitive cell death response

IEF - Isoelectric focusing

INF-IND - Infection induced

IP - Invasion pattern

IPG - Immobilized pH gradient

IPR - Invasion pattern receptor

IPTR - Invasion pattern triggered response

L - Linear

MALDI - Matrix-assisted laser desorption/ ionization

MAMPs - Microbial-associated molecular patterns

MASCOT - Search engine software that uses mass spectrometry data to identify proteins from primary sequence databases

MS - Mass spectrometry (or spectra)

MS/MS - Tandem mass spectrometry (or spectra)

MW - Molecular weight

MWCO - Molecular-weight cutoff

NB-LRR - Nucleotide-binding site leucine-rich repeat class of proteins

NCBI - National Center for Biotechnology Information

NL - Nonlinear

NN - Neural network score of SecretomeP non-classical protein secretion predictor

p - *p*-value (significance level of a statistical test)

PAM - Point Accepted Mutation (amino acid substitution matrix)

PAMPs - Pathogen-associated molecular patterns

PDA - Potato dextrose agar

PDB - Potato dextrose broth

PEAKS - Mass spectrometry data analysis software

pI - Isoelectric point

PMF - Peptide mass fingerprint

PRRs - Pattern recognition receptors

PTI - PAMP-triggered immunity

PTM - Post-translational modification

R - Rapid

ROS - Reactive oxygen species

RT - Room temperature (± 25 ºC)

SD - Standard deviation

SDS - Sodium dodecyl sulfate

SDS-PAGE - Sodium dodecyl sulfate polyacrylamide gel electrophoresis

TCA - Trichloroacetic acid

TFA - Trifluoroacetic acid

TOF - Time of flight

Tris - 2-Amino-2-hydroxymethyl-propane-1,3-diol

CHAPTER 1

INTRODUCTION

CORK OAK DECLINE

Cork oak (*Quercus suber* L.) is an evergreen tree that naturally occurs in the Western Mediterranean region, namely in the Iberian Peninsula, which occupies around 61% of the total worldwide cork oak forests (APCOR, 2014d; Pereira et al., 2008). Due to its high longevity (250-300 years), cork oak forests are a biodiversity hotspot of fauna and flora, that coexist with an agro-silvo-pastoral system (APCOR, 2014b; Camilo-Alves, 2014; Pereira et al., 2008). Notwithstanding their ecological and social value, cork oak forests' relevance becomes even more prominent from an economic perspective due to its renewable bark, the cork. This natural product, distinguished by its thickness and high levels of suberin, is periodically harvested (every 9-12 years), without significant health consequences for the trees (Costa et al., 2015; Oliveira & Costa, 2012; Pereira et al., 2008). The traditional transformation of cork in stoppers is the major economic use of the tree, absorbing 68% of the cork production (APCOR, 2014d), but its properties such as acoustical and thermal insulation, water impermeability and energy absorbance are guiding to new applications in industries as diverse as aeronautic, construction and footwear (APCOR, 2014a, 2014c; Duarte & Bordado, 2015; Gil, 2015; Silva, 2005). In this context, Portugal stands as the worldwide leading country of cork production (49.6%), transformation and exportation (64.7%), representing about 2% of the total Portuguese exports (713.3 million euros in 2012) (APCOR, 2014d), being therefore an added-value to the Portuguese economy.

However, early in the XXth century the first reports appeared of an abnormal cork oak mortality in the Mediterranean basin, and since 1980s severe outbreaks triggered a growing ecologic and economic concern around the tree's health (Moreira & Martins, 2005; Sousa et al., 2007). The disease, called cork oak decline due to a general loss of vigour, is characterized by symptoms like branch dieback, foliar chlorosis, wilting and vascular necrosis. Still, the symptomatology may vary according to the pattern of disease development between a chronic or sudden decline. The first syndrome, most common, develops slowly during several years, presenting a gradual loss of foliage that starts on the top of the tree and progressively affects the whole crown or, instead, only some peripheric branches (Figure 1 B) (Camilo-Alves et al., 2013; Sousa et al., 2007). On the other hand, the sudden decline is characterized by a quick foliar drying of the crown (2 to 4 weeks), with the particularity that the leaves remain attached to the branches (Figure 1 A). This syndrome is notoriously more aggressive than the chronic decline and the only symptom visible is the generalized drying that culminates in cork oak death in one or two

seasons (Camilo-Alves et al., 2013; Sousa et al., 2007).

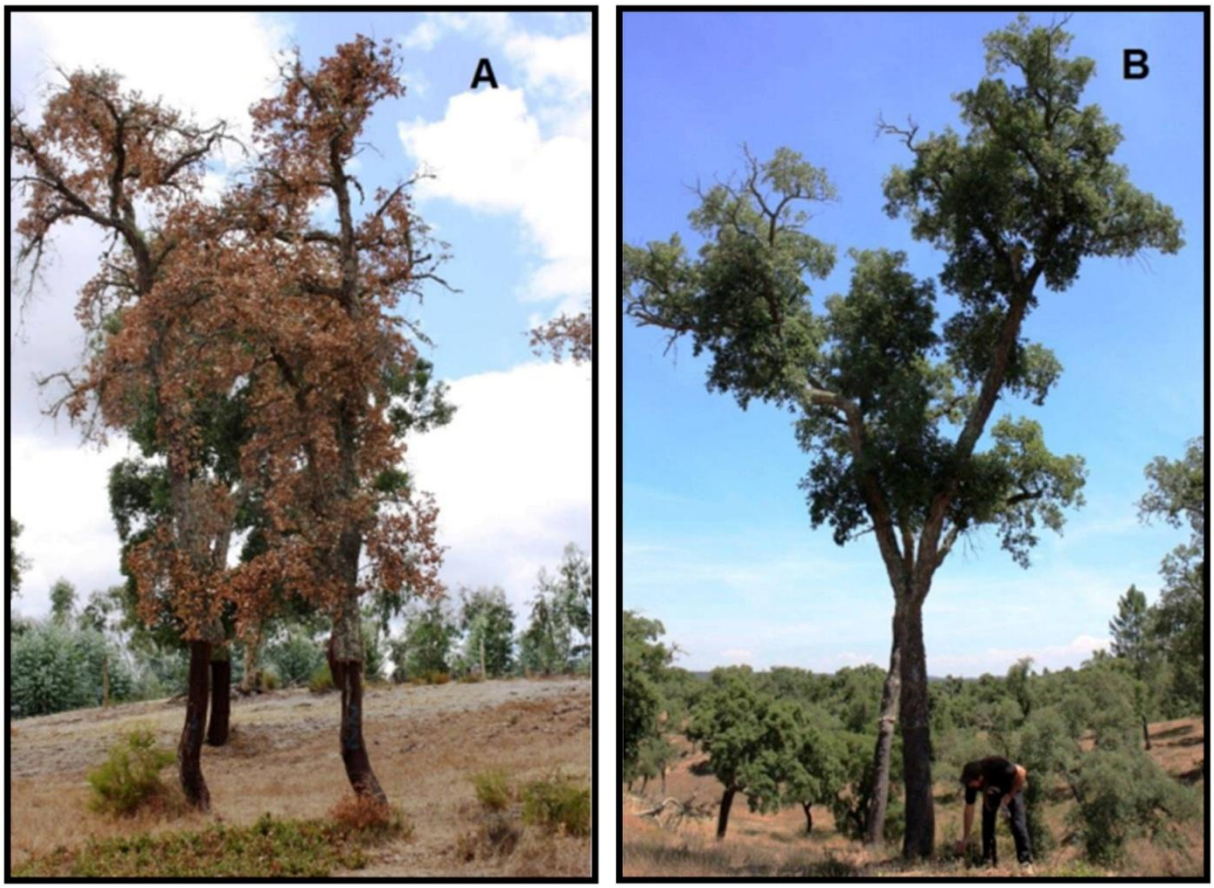

Figure 1 | Development pattern of cork oak decline symptomatology: A - sudden decline; B - chronic decline (Camilo-Alves, 2014).

Considered a complex multifactorial disease, cork oak decline results from the conjugation of adverse environmental and anthropogenic factors, such as drought and temperature stress, wildfires, soil erosion and alteration of traditional agricultural practices (Acácio, 2009; Bréda et al., 2006; Catry et al., 2012; Sousa et al., 2007). The recurrence of stressing episodes disturbs the tree physiologic status and consequently its resilience, becoming more vulnerable to opportunistic pathogens (Correia et al., 2014; Linaldeddu et al., 2011; Marçais & Bréda, 2006; Sousa et al., 2007; Wargo, 1996).

Among the biotic factors already associated to cork oak decline, the root pathogen *Phytophthora cinnamomi* Rands was regarded for a long time as the main fungal pathogen associated to the disease (Moreira & Martins, 2005; Sánchez et al., 2002; Scanu et al., 2013; Sousa et al., 2007). Extensively studied, it is currently known that *P. cinnamomi* pathogenicity induces root necrosis, decreases the net photosynthetic rate and reduces the physiologic water status of the trees (Robin et al., 2001; Sánchez et al., 2002; Sghaier-Hammami et al., 2013). Still, it was equally demonstrated that holm oaks (*Quercus ilex* subsp. *rotundifolia* L.) are more susceptible to

P. cinnamomi infection than cork oak seedlings, presenting symptoms more severe and a superior mortality rate (Camilo-Alves, 2014; Robin et al., 2001). These results reinforce the idea that *P. cinnamomi* contributes to cork oak decline, but might not be the most relevant biotic agent involved as previously believed. Besides, other fungi have consistently been recovered from declining sites, namely *Discula quercina* (Cooke) Sacc., *Biscogniauxia mediterranea* (De Not.) O. Kuntze and *Diplodia corticola* A.J.L. Philips, A. Alves et J. Luque (Alves et al., 2004; Linaldeddu et al., 2014, 2011; Luque et al., 2000; Moricca & Ragazzi, 2008; Sánchez et al., 2003), that together with *P. cinnamomi* are regarded as the main fungal pathogens provoking Mediterranean oak decline.

Discula quercina, for instance, occurs on the leaves and twigs of declining oaks, being the causal agent of oak anthracnose, a disease characterized by leaves displaying dark-brown spots with purplish margins (Linaldeddu et al., 2011; Moricca & Ragazzi, 2008). Nonetheless, its frequency is less reported on *Q. suber* (0.8-4.8%) than on *Quercus cerris* L. (≤ 18.6%) (Franceschini et al., 2005; Ragazzi et al., 1999), the most vulnerable oak to *D. quercina* infection (Moricca & Ragazzi, 2011). Conversely, *B. mediterranea* is a predominant fungus of the *Q. suber* endophytic community (16.5-63.7%), mainly in the aerial organs (Franceschini et al., 2005; Linaldeddu et al., 2011). Despite the infection of these fungi occurs throughout the year, their infective ability increases during the rainfall season (Franceschini et al., 2005), being equally responsive to host drought stress (Capretti & Battisti, 2007; Linaldeddu et al., 2011; Luque et al., 2000), switching from a latent to pathogenic form after a plant stress episode. Well known as the causal agent of charcoal canker, *B. mediterranea* locally colonizes the host xylem and bark tissues, inducing necrosis, which eventually accelerates the tree decline (Vannini & Valentini, 1994). Neverthless, this fungus continues to be regarded as a secondary weak invader that attacks only vulnerable cork oaks.

Although poorly studied, some pathogenicity assays identified *D. corticola* (family *Botryosphaeriaceae*) as the most virulent pathogen involved in cork oak decline (Linaldeddu et al., 2009; Luque et al., 2000), surpassing even the widely studied *P. cinnamomi*. After stem inoculation, Luque et al. (2000) demonstrated that the fungus virulence is equally high in healthy and water-stressed cork oak seedlings, causing extensive vascular necrosis that culminated mostly on host death. From the plant physiologic point of view, *D. corticola* spread on vascular tissues has a negative impact on gas exchange, unbalancing the host metabolic processes (Linaldeddu et al., 2009). Nevertheless, despite this fungus has been considered the dominant pathogen on oak declining cankers (Linaldeddu et al., 2014; Sánchez et al., 2003), not always requiring a stress event to become pathogenic (Luque et al., 2000), the knowledge about its infection strategy is still

limited.

DIPLODIA CORTICOLA AS A PHYTOPATHOGENIC FUNGI

Diplodia corticola infections have been successively reported worldwide not only in *Q. suber*, but also on different oak ecosystems (*Q. ilex*, *Q. agrifolia* Née, *Q. coccifera* L., *Q. chrysolepis* Liebm. or *Q. virginiana* Mill.), in grapevines (*Vitis vinifera* L.) or even in eucalypts (*Eucalyptus globulus* Labill.) (Alves et al., 2004; Barradas et al., 2015; Carlucci & Frisullo, 2009; Dreaden et al., 2011; Linaldeddu et al., 2014; Lynch et al., 2013; Tsopelas et al., 2010; Úrbez-Torres et al., 2010b; Varela et al., 2011). The pathogenicity tests carried out on different hosts demonstrated that the symptoms induced by the fungus are transversal, causing necrotic lesions around the infection point, bleedings, discoloration of the vascular tissues and dieback as well as the formation of pycnidia around the inoculation points (Linaldeddu et al., 2009; Lynch et al., 2013; Tsopelas et al., 2010; Varela et al., 2011). Another observation during infection assays is the fast decline of the seedlings, which usually die after 4-6 weeks of inoculation, a pattern already described on cork oak forests as sudden decline (Figure 1 A). Moreover, when compared with other species, *D. corticola* is consistently the most aggressive pathogen for the host (Linaldeddu et al., 2014; Lynch et al., 2013), which suggests the relevance of this fungus as a key player on oak decline.

Remarkably, the available information regarding its infection strategy is still scarce. Luque & Girbal (1989), for instance, noticed an increase of *D. corticola* pathogenicity after cork oak debarking. This correlation might be associated to a direct entry of the pathogen through accidental wounds made during cork stripping. On the other hand, cork removal represents a plant stress episode that may trigger the infection (Costa et al., 2004). Likewise, in grapevines the *Botryosphaeriaceae* infections occur primarily in recent pruning wounds made during the rainfall season, contemporaneous to the conidia release, that with rain splash dispersion may result in infection of the exposed xylem (Úrbez-Torres et al., 2010a; Úrbez-Torres & Gubler, 2011).

Conversely, a transition from latent to pathogenic lifestyle after debarking is equally plausible. Cork harvesting implies a direct water loss on the stripped surface through stem evaporation, which implies an additional effort of the trees to avoid trunk dehydration and to maintain the water homeostasis, usually scarce on soil during the harvesting season (Oliveira & Costa, 2012). Thus, debarking represents a stressing event for cork oaks, favoring the onset of *D. corticola* pathogenicity after cork removal. This is in agreement with the disease triangle postulated in plant pathology that justifies the onset of a plant disease with the conjugation of three factors: a susceptible plant, a virulent pathogen and a favorable environment (Herman & Williams, 2012).

Besides colonizing the stem, there are evidences of *D. corticola* root colonization of *Q. agrifolia* (Lynch et al., 2013), as well as leaf penetration in *Q. suber* and *Q. cerris* (Paoletti et al., 2007), although the consequent epidemiologic implications in the field oak decline requires further investigations.

Irrespective of how the fungus gains access to the plant or what triggers the onset of the disease, the pathogenicity of *D. corticola* is deeply associated with phytotoxins. Among the phytotoxic metabolites already purified from *D. corticola* culture filtrates are the diplofuranones A and B, diplopyrone, sapinofuranone B, sphaeropsidins A-C and the diplobifuranylones A and B (Evidente et al., 2007, 2006, 2003). These secondary metabolites allow the extension of the fungal action in distant places from the production site, where they reproduce the disease symptomatology (Andolfi et al., 2011; Möbius & Hertweck, 2009). This explains the fast disease spread observed in *D. corticola* pathogenicity tests performed *in planta*, in which it was not possible to re-isolate the fungus from affected tissues far from the inoculation point (Mullerin, 2013). Indeed, it is consensual that the foliar symptoms induced by *Botryosphaeriaceae* pathogens are caused by phytotoxic compounds produced by the fungi in the stem tissues (Abou-Mansour et al., 2015).

Considering the *D. corticola* negative impact on cork oak forests some attempts have already been made to control the fungus proliferation. Luque et al. (2008), for instance, selected a range of commercial fungicides to be used after cork debarking. Among them, carbendazim was the most effective in the field, decreasing about 75% of debarked surface affected by cankers, if applied in a time range of 4 hours after debarking. Similar results were obtained in the control of *Botryosphaeriaceae* infection in grapevines, even though the carbendazim field control effectiveness was lower in Pitt et al. (2012) (27-41%) than in Amponsah et al. (2012) (93%). Despite the protection efficiency observed, the fungicides tested are unspecific for *D. corticola*, which might produce downstream effects on the beneficial endophytic population of cork oak, or even in the surrounding soil microbial community. Carbendazim is a systemic fungicide that interferes in the fungal β-tubulin subunit assembly, affecting subsequently the fungal cytoskeleton and mitosis (Leroux et al., 2002; Yang et al., 2011). Therefore, it is reasonable that the growth of other fungi besides *D. corticola* might be compromised. Furthermore, the trees' treatment 4 hours after the cork removal, the time required to improve the permeation of the fungicide, is not feasible in the field as Luque et al. (2008) could notice.

From a biocontrol point of view, Linaldeddu et al. (2005) presented the first evidences of *D. corticola* antagonism by the endophytic community of *Quercus* spp., namely *Trichoderma asperellum* Samuels, Lieckf. et Nirenberg, *T. fertile* Bissett and *T. harzianum* Rifai. Later, Campanile

et al. (2007) demonstrated that *T. viride* Pers. also antagonize *D. corticola* micelium growth in *in vitro* dual cultures (reduction of 28.5% over control). However, in the antagonistic tests performed *in planta*, *T. viride* had moderate effects on *D. corticola* proliferation in *Q. cerris* and no effects at all in *Q. pubescens* Willdenow. Conversely, *Fusarium tricinctum* (Corda) Sacc., which presented the lowest inhibitory effect *in vitro* (4.2%), was the most competitive fungus tested in both seedlings, reducing significantly the *D. corticola* infection. Thus, the outcome of antagonistic fungal interactions should be regarded as a three-way-interaction, involving not only the pathogenic and antagonist fungi, but also the plant (Vinale et al., 2008), which obviously increases the complexity of such studies.

Notwithstanding the efforts already made to understand the *D. corticola* proliferation through their hosts, the molecular aspects of its pathogenicity still needs to be clarified, in order to understand how it suppresses the plant defense mechanism and establishes its parasitism. Moreover, this knowledge is fundamental to develop effective disease management strategies.

PLANT-FUNGAL INTERACTIONS

Although plants possess several chemical and physical barriers to shield them against biotic threats, phytopathogens can overcome them (Egan & Talbot, 2008; Łazniewska et al., 2012). As soon as the fungal spores land the plant surface they secrete adhesive molecules, such as polysaccharides or glycoproteins, to consolidate the adhesion to the host and to prevent their detachment by wind or rainfall (Ikeda et al., 2012; Newey et al., 2007; Tucker & Talbot, 2001; Zelinger et al., 2006). After germination, some fungi penetrate into the plants through natural openings or wounds, while others have the ability to mechanically pierce the plant cell wall, using a specialized germ tube called appressorium (Herman & Williams, 2012; Łazniewska et al., 2012; Mendgen et al., 1996; Ryder & Talbot, 2015). This structure employs high turgor pressure to breach the plant cell wall physical barrier, acting often in combination with secreted cell-wall degrading enzymes (CWDE) that simultaneously potentiate the wall disruption and suppress the plant defences (Horbach et al., 2011; Kleemann et al., 2012; Pryce-Jones et al., 1999; Tucker & Talbot, 2001). *Botryosphaeriaceae* entry through wounds was already demonstrated in grapevines (Úrbez-Torres & Gubler, 2011), and it is thus plausible that this also happens in *D. corticola* infection of *Q. suber.* Nevertheless, in a study that aimed to proof that O_3 exposure of leaves predisposes them to fungal attacks, Paoletti et al. (2007) reported for the first time that *D. corticola* is able to colonize *Q. suber* and *Q. cerris* leaves. Scanning microscopy observations clearly demonstrated the presence of *D. corticola* hyphae on symptomatic oak leaves after spore germination. Another remarkable finding is that hyphae were never observed entering into

stomata, neither growing toward these natural openings. Instead, *D. corticola* hyphae embedded into the epicuticular waxes or eroded a hollow, forming in the latter case a right-angle bend at the cuticle entrance point. In both forms of entry, it is reasonable to hypothesize that the fungus develops an appressorium. Concurrently, it should secrete a plethora of hydrolytic and oxidative enzymes to penetrate the plant cell wall and its protective cuticle, as it seems to happen in *Macrophomina phaseolina* (Tassi) Goid., a *Botryosphaeriaceae* fungus phylogenetically close to *D. corticola* (Crous et al., 2006; Islam et al., 2012). However, the proteins implicated in this process still need to be identified.

Once within the plant, the colonization is accomplished by invasive hyphae or by haustoria, a hypha morphologically specialized towards nutrient uptake. It is noteworthy that filamentous fungi such as *D. corticola* remain always extracellular to their hosts, even when they invade intracellular spaces (separated by host-derived membranes) (Faulkner & Robatzek, 2012). Although the primary function of these hyphae is to fulfil the fungal nutrient requirements, these structures also deliver virulence effectors, like appressoria do, to restrain or evade the host defence system (Catanzariti et al., 2006; Giraldo & Valent, 2013; Horbach et al., 2011; Irieda et al., 2014; Kleemann et al., 2012). In fact, the successful colonization of a phytopathogen greatly depends on its ability to circumvent the plant immune system.

Tipically, the complex plant defence mechanism relies in the autonomous response of each cell to the pathogen and on systemic signals emitted from the infection point (Gómez-Gómez, 2004). Accordingly, some conceptual models have been developed to synthesise the framework of molecular interactions involved. The so-called zig-zag model is currently the most accepted (Figure 2) (Jones & Dangl, 2006). The first of four phases of this paradigm occurs in the apoplast

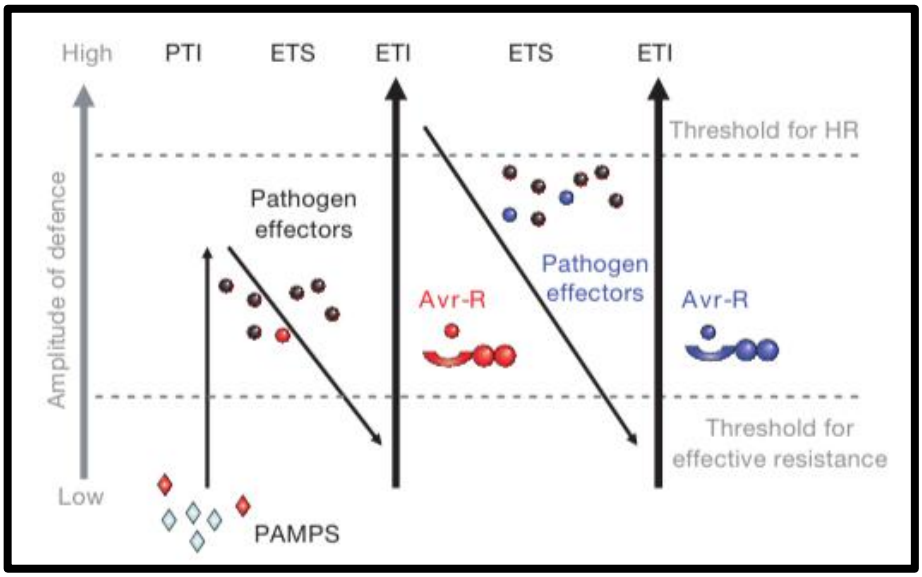

Figure 2 | Conceptual ziz-zag model of plant immune system (Jones & Dangl, 2006).

and is mediated by transmembrane pattern recognition receptors (PRRs) that in the presence of microbial- or pathogen-associated molecular patterns (MAMPS or PAMPs) elicit the PAMP-triggered immunity (PTI). Besides the microbial conserved structural molecules (PAMPS), it is currently accepted that transmembrane pattern recognition receptors may equally recognize endogenous molecules released during pathogen-induced cell damage (damage-associated molecular patterns, DAMPs) (Boller & Felix, 2009). This first line of defence is fast and usually quite efficient against non-adapted pathogen infections, comprising the concerted production of reactive oxygen species (ROS) and secretion of antimicrobial compounds, phytohormones, hydrolytic enzymes and inhibitors of microbial hydrolytic enzymes (Ahuja et al., 2012; Clérivet et al., 2000; El-Bebany et al., 2013; Herman & Williams, 2012; Luna et al., 2011; Pieterse et al., 2009; Torres, 2010). Still, successful pathogens evolved mechanisms to counterattack PAMP-triggered immunity response, both strengthening their effector production and subverting the host's immune response and surveillance (Herman & Williams, 2012; Jones & Dangl, 2006). The outcome is denominated by effector-triggered susceptibility (ETS), the second phase of zig-zag model. As a consequence, the plant activates its second line of defence, an exacerbated, faster and longer version of PAMP-triggered immunity called effector-triggered immunity (ETI, phase 3) (Tao et al., 2003). This response relies on both direct and indirect intracellular recognition of pathogen effectors by plant resistance proteins (most often nucleotide-binding site leucine-rich repeat class of proteins, NB-LRR) (Dangl & Jones, 2001; Gómez-Gómez, 2004; Jones & Dangl, 2006). In the case of indirect recognition, resistance proteins surveil the integrity of the endogenous effectors targets (not the pathogen effectors itself), triggering the downstream physiologic responses when signals of effector-induced cellular perturbation are detected (Gómez-Gómez, 2004). Generally, ETI culminates in a hypersensitive cell death response (HR), a programmed cell death of the proximal infection tissues induced by a localized ROS burst (Torres, 2010). The main purpose of this controlled plant death is to block the pathogen advance, preventing its spread through the plant. The fourth and final phase of the zig-zag model is justified by natural selection: pathogens resistant to ETI response survive and proliferate, eliciting a second outburst of plant immunity defences. However, PTI and ETI are pliable responses that frequently overlap to restrict the pathogens' propagation, not being possible to distinguish them. The plant resistance or susceptibility outcome is thus balanced by the formula (PTI + ETI) - ETS (Jones & Dangl, 2006).

While the zig-zag model is widely accepted, it still presents limitations. Recently an alternative paradigm called invasion model was proposed (Figure 3) (Cook et al., 2015). Briefly, this new model proposes that in an attempted plant-invader symbiosis the invasion patterns (IP, externally encoded or modified-self ligands) are recognized by plant IP receptors (IPR), prompting the

subsequent IP-triggered response (IPTR). A remarkable improvement of the invasion model is that, conversely to zig-zag model, the invasion patterns-triggered response not always culminates in plant immune response. Instead, the invasion patterns recognition might result in the end of symbiosis or in continued symbiosis, depending of the plant-invader interaction outcome. This interaction is commonly controlled by invader effectors, whereby in case of IPTR effector manipulation failure, the symbiosis cease. On the other hand, if the invader effectors successfully manipulate the plant IPTR, this response may be suppressed (biotrophic interactions) or used in benefit of invaders colonization (necrotrophic interactions), preserving in both cases the symbiosis. The continuity of symbiosis and effector deployment may then provoke host-perceivable IPs, sustaining the IPTR. Accordingly, the invasion model bridges some shortcomings of zig-zag model, namely the absence of a strict distinction between PTI and ETI and the omission of DAMPs as plant immunity elicitors (Cook et al., 2015).

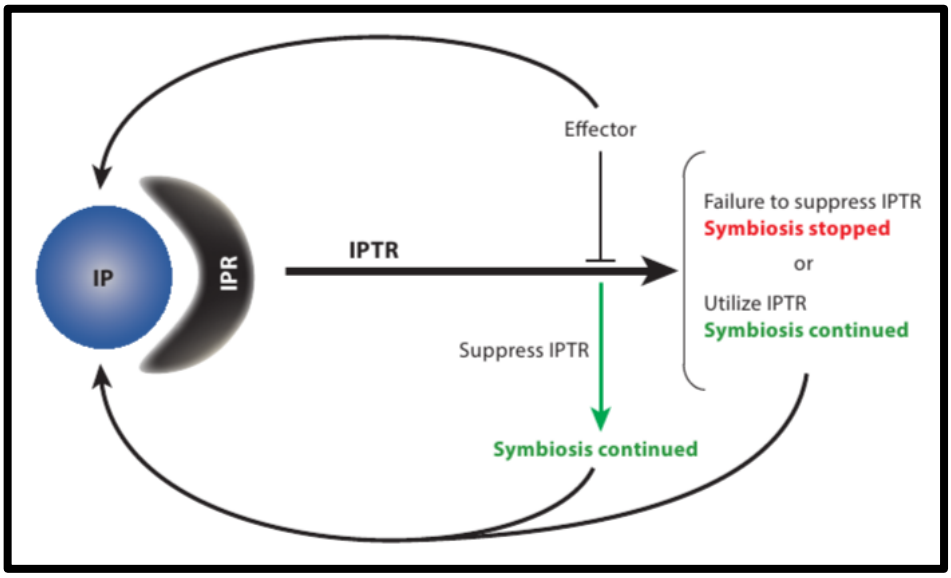

Figure 3 | Conceptual invasion model of an attempted plant-invader symbiosis (Cook et al., 2015).

Notwithstanding this background of plant-pathogen interactions, the molecular understanding of *Q. suber* immune response against biotic factors is substantially scarce. Coelho et al. (2011), for instance, demonstrated that the defence strategies deployed during the cork oak interaction with *P. cinnamomi* resemble the system used by other plants, such as the cowpea (*Vigna unguiculata* (L.) Walp.) against *Rhizoctonia solani* J.G. Kühn or the wheat (*Triticum aestivum* L.) against *Mycosphaerella graminicola* (Fuckel) J. Schröt. (Chandra et al., 2007; Ray et al., 2003). This study identified 7 genes, 4 of which were overexpressed in root cells during the first 24 h of infection. The authors suggested that the assigned proteins might play a role in the counterattack of *P. cinnamomi* invasion. According to the recently developed inducible plant immunity model, these proteins are probably IPRs able to perceive *P. cinnamomi* effectors, and proteins involved in the

activation of downstream IPTR responses like oxidative burst or plant cell wall reinforcement (lignin and suberin biosynthesis). Notwithstanding the authors have outlined a molecular mechanism of *Q. suber* defence against invaders, this model still requires further investigations to be consolidated.

From the invader perspective, the knowledge of *D. corticola* effectors remains almost nonexistent, even though research of *Botryosphaeriaceae* effectors is steadily growing (Abou-Mansour et al., 2015; Andolfi et al., 2011; Cobos et al., 2010; Evidente et al., 2003, 2012; Islam et al., 2012; Martos et al., 2008). Hence, it is demanding to study *D. corticola* effectors to highlight the molecular framework involved during its hosts' infections.

PROTEOMICS OF PHYTOPATHOGENIC FUNGI

Proteomic tools have proved essential for the analysis of the molecular biology of filamentous fungi. The recent growth of fungal proteomics' publications is intrinsically related with the technological developments of protein analysis and the concomitant release of genome sequences, although the difficulties around samples generation and mass spectrometry (MS) interpretation continues hampering such studies (Kim et al., 2007; Passel et al., 2013). This discipline has extensively been used to exploit the potential of fungi in biotechnological and medical applications (Kniemeyer, 2011; Oda et al., 2006; Oliveira & Graaff, 2011), having equally been employed to study the molecular biology of plant-fungal interactions (Bhadauria et al., 2010; González-Fernández & Jorrín-Novo, 2012). Proteomics of phytopathogenic fungi offer the possibility to study the total set of proteins present in a biological condition, highlighting at the same time functionally relevant proteins by comparative analysis. Accordingly, recurring to these technologies allows understanding how fungi respond to their environment and, as a consequence, to elucidate the molecular mechanisms subjacent to the infection establishment. Unfortunately, protein identification has been lagged by the reduced availability of genome sequences. Today this constraint has gradually been overcome with the introduction of computational algorithms to improve the *de novo* sequencing (Ma & Johnson, 2012; Muth et al., 2014; Zhang et al., 2012). This methodology derives the partial or complete amino acid peptide sequence directly from tandem mass spectra (MS/MS), using the mass differences of two adjacent fragment ions. Then, the obtained sequences are compared against protein sequence databases using homology searching algorithms such as BLAST or FASTA (Issac & Raghava, 2005; Ma & Johnson, 2012; Mackey et al., 2002; McGinnis & Madden, 2004; Paizs & Suhai, 2005). On the contrary, conventional peptide database searching, used for genome sequenced organisms,

relies on direct database queries to find the best theoretical peptide match for the experimental MS or MS/MS peptide (Liska & Shevchenko, 2003). Indeed, this methodology is known as peptide mass fingerprint (PMF), since it is based on the principle that every protein derives a unique set of peptide masses after enzymatic cleavage (Sickmann et al., 2003). Considered simpler and faster than *de novo* sequencing protein identification, this approach presents some accuracy and sensitivity weaknesses (Kapp et al., 2005). Nevertheless, these limitations are progressively diminishing in both methodologies due, in part, to the sensitivity improvement of mass spectrometers (Van Oudenhove & Devreese, 2013).

Nevertheless, successful protein identification is highly dependent on good sample preparation. Like plants, fungi are regarded as troublesome organisms for protein extraction purposes due to the robustness of their cell wall and, when extracellular proteins are targeted, to the presence of complex extracellular polysaccharide content in addition to a notorious low extracellular protein concentration (González-Fernández & Jorrín-Novo, 2013; Medina & Francisco, 2008; Pérez & Ribas, 2013). Therefore, the first step of a proteomic workflow, protein extraction, should be regarded carefully to avoid technical constraints. The subsequent protein separation step is primarily performed by two-dimensional electrophoresis (2D-PAGE), even though one-dimensional electrophoresis (1D-PAGE) is often used to assess preliminary results. Briefly, this powerful technique separates the proteins through two electrophoretic runs, isoelectric focusing (IEF) and SDS-PAGE that when combined are able to resolve thousands of proteins simultaneously (Görg et al., 2004). Isoelectric focusing, the first-dimension separation, resolves proteins according to their isoelectric point (pI). The proteins are then separated orthogonally by molecular weight (MW) in a SDS-PAGE. After separation, the distinct protein spots are detected with a suitable staining method, being then excised and enzymatically digested to produce peptide fragments for downstream MS analysis.

In short, 2D coupled with MS and followed by protein *de novo* sequencing is extensively used to study fungal phytopathogens, particularly the ones with unsequenced genomes (Cobos et al., 2010; González-Fernández et al., 2010; Meijer et al., 2014; Rogowska-Wrzesinska et al., 2013). These methodologies allow a comprehensive insight of the proteins expressed in a specific biologic state, greatly due to the high resolution, accuracy and separating capacity of 2D gels (Rogowska-Wrzesinska et al., 2013). 2D-PAGE enable thus to discriminate proteins that are differentially expressed between two biological conditions, to resolve isoforms and proteins with close pIs or MW, disclosing even hypothetical protein post-translational modifications (PTMs) (Jensen, 2006). Proteomics is therefore a vital discipline for plant-fungal interactions research, providing useful information about fungal pathogenicity and virulence effectors, an essential

knowledge to comprehend the intricate biology of infection.

AIMS OF THE WORK

The best approach to decide on strategies to successfully reduce the negative impact of a phytopathogen is trying to understand how it infects its hosts. Accordingly, the disclosure of the proteins involved in *D. corticola* pathogenesis may contribute to elucidate how this fungus colonizes cork oak trees, among other hosts, highlighting as well possible key protein targets for the development of effective disease management strategies.

Hence, the overall objective of this work is to contribute to the insight of the molecular mechanism of *D. corticola* infection. To achieve this purpose the following aims were drawn:

- Develop an efficient protocol for *D. corticola* extracellular proteins extraction;
- Evaluate the *D. corticola* strains virulence *in planta*;
- Characterize the basal and infection-like *D. corticola* secretome and cellular proteome;
- Compare the secretome and cellular proteomes of two strains with distinct virulence degrees.

REFERENCES

Abou-Mansour, E., Débieux, J.-L., Ramírez-Suero, M., Bénard-Gellon, M., Magnin-Robert, M., Spagnolo, A., Chong, J., Farine, S., Bertsch, C., L'Haridon, F., Serrano, M., Fontaine, F., Rego, C., Larignon, P. (2015). Phytotoxic metabolites from *Neofusicoccum parvum*, a pathogen of *Botryosphaeria* dieback of grapevine. *Phytochemistry*. **115** (**1**): 207–215.

Acácio, V. (2009). *The dynamics of cork oak systems in Portugal: the role of ecological and land use factors*. Wageningen University.

Ahuja, I., Kissen, R., Bones, A. (2012). Phytoalexins in defense against pathogens. *Trends in Plant Science*. **17** (**2**): 73–90.

Alves, A., Correia, A., Luque, J., Phillips, A. (2004). *Botryosphaeria corticola*, sp nov on *Quercus* species, with notes and description of *Botryosphaeria stevensii* and its anamorph, *Diplodia mutila*. *Mycologia*. **96** (**3**): 598–613.

Amponsah, N., Jones, E., Ridgway, H., Jaspers, M. (2012). Evaluation of fungicides for the management of *Botryosphaeria* dieback diseases of grapevines. *Pest Management Science*. **68** (**5**): 676–683.

Andolfi, A., Mugnai, L., Luque, J., Surico, G., Cimmino, A., Evidente, A. (2011). Phytotoxins produced by fungi associated with grapevine trunk diseases. *Toxins*. **3** (**12**): 1569–1605.

APCOR (2014a). *Construction and decoration materials*. Portuguese Cork Association.

APCOR (2014b). *Cork - Environmental importance*. Portuguese Cork Association.
APCOR (2014c). *Cork - Raw material*. Portuguese Cork Association.

APCOR (2014d). *Cork sector in numbers*. Portuguese Cork Association.

Barradas, C., Phillips, A., Correia, A., Diogo, E., Bragança, H., Alves, A. (2015). Diversity and potential impact of *Botryosphaeriaceae* species associated with *Eucalyptus globulus* plantations in Portugal. *Manuscript submitted for publication*.

Bhadauria, V., Banniza, S., Wang, L.-X., Wei, Y.-D., Peng, Y.-L. (2010). Proteomic studies of phytopathogenic fungi, oomycetes and their interactions with hosts. *European Journal of Plant Pathology*. **126** (**1**): 81–95.

Boller, T., Felix, G. (2009). A renaissance of elicitors: perception of microbe-associated molecular patterns and danger signals by pattern-recognition receptors. *Annual Review of Plant Biology*. **60** (**1**): 379–406.

Bréda, N., Huc, R., Granier, A., Dreyer, E. (2006). Temperate forest trees and stands under severe drought: a review of ecophysiological responses, adaptation processes and long-term consequences. *Annals of Forest Science*. **63** (**6**): 625–644.

Camilo-Alves, C. (2014). *Studies on cork oak decline: an integrated approach*. University of Évora.

Camilo-Alves, C., Clara, M., Ribeiro, N. (2013). Decline of Mediterranean oak trees and its association with *Phytophthora cinnamomi*: a review. *European Journal of Forest Research*. **132** (**3**): 411–432.

Campanile, G., Ruscelli, A., Luisi, N. (2007). Antagonistic activity of endophytic fungi towards *Diplodia corticola* assessed by *in vitro* and *in planta* tests. *European Journal of Plant Pathology*. **117** (**3**): 237–246.

Capretti, P., Battisti, A. (2007). Water stress and insect defoliation promote the colonization of *Quercus cerris* by the fungus *Biscogniauxia mediterranea*. *Forest Pathology*. **37** (**2**): 129–135.

Carlucci, A., Frisullo, S. (2009). First report of *Diplodia corticola* on grapevine in Italy. *Journal of Plant Pathology*. **91** (**1**): 231–240.

Catanzariti, A.-M., Dodds, P., Lawrence, G., Ayliffe, M., Ellis, J. (2006). Haustorially expressed secreted proteins from flax rust are highly enriched for avirulence elicitors. *The Plant Cell*. **18** (**1**): 243–256.

Catry, F., Moreira, F., Pausas, J., Fernandes, P., Rego, F., Cardillo, E., Curt, T. (2012). Cork oak vulnerability to fire: the role of bark harvesting, tree characteristics and abiotic factors. *PloS One*. **7** (**6**): e39810.

Chandra, A., Saxena, R., Dubey, A., Saxena, P. (2007). Change in phenylalanine ammonia lyase activity and isozyme patterns of polyphenol oxidase and peroxidase by salicylic acid leading to enhance resistance in cowpea against *Rhizoctonia solani*. *Acta Physiologiae Plantarum*. **29** (**4**): 361–367.

Clérivet, A., Déon, V., Alami, I., Lopez, F., Geiger, J.-P., Nicole, M. (2000). Tyloses and gels associated with cellulose accumulation in vessels are responses of plane tree seedlings (*Platanus* x *acerifolia*) to the vascular fungus *Ceratocystis fimbriata* f sp *platani*. *Trees*. **15** (**1**): 25–31.

Cobos, R., Barreiro, C., Mateos, R., Coque, J.-J. (2010). Cytoplasmic-and extracellular-proteome analysis of *Diplodia seriata*: a phytopathogenic fungus involved in grapevine decline. *Proteome Science*. **8** (**46**): 1–16.

Coelho, A., Horta, M., Ebadzad, G., Cravador, A. (2011). *Quercus suber* - *Phytophtora cinnamomi* interaction: a hypothetical molecular mechanism model. *New Zealand Journal of Forestry Science*. **41S** (**2011**): S143–S157.

Cook, D., Mesarich, C., Thomma, B. (2015). Understanding plant immunity as a surveillance system to detect invasion. *Annual Review of Phytopathology*. **53** (**25**): 1–23.

Correia, B., Rodriguez, J., Valledor, L., Almeida, T., Santos, C., Cañal, M., Pinto, G. (2014). Analysis of the

expression of putative heat-stress related genes in relation to thermotolerance of cork oak. *Journal of Plant Physiology*. **171** (**6**): 399–406.

Costa, A., Nunes, L., Spiecker, H., Graça, J. (2015). Insights into the responsiveness of cork oak (*Quercus suber* L) to bark harvesting. *Economic Botany*. **69** (**2**): 1–14.

Costa, A., Pereira, H., Oliveira, A. (2004). The effect of cork-stripping damage on diameter growth of *Quercus suber* L. *Forestry*. **77** (**1**): 1–8.

Crous, P., Slippers, B., Wingfield, M., Rheeder, J., Marasas, W., Philips, A., Alves, A., Burgess, T., Barber, P., Groenewald, J. (2006). Phylogenetic lineages in the *Botryosphaeriaceae*. *Studies in Mycology*. **55** (**1**): 235–253.

Dangl, J., Jones, J. (2001). Plant pathogens and integrated defence responses to infection. *Nature*. **411** (**6839**): 826–833.

Dreaden, T., Shin, K., Smith, J. (2011). First report of *Diplodia corticola* causing branch cankers on live oak (*Quercus virginiana*) in Florida. *ISME Journal*. **95** (**8**): 1027.

Duarte, A., Bordado, J. (2015). Cork - a renewable raw material: forecast of industrial potential and development priorities. *Frontiers in Materials*. **2** (**2**): 1–8.

Egan, M., Talbot, N. (2008). Genomes, free radicals and plant cell invasion: recent developments in plant pathogenic fungi. *Current Opinion in Plant Biology*. **11** (**4**): 367–372.

El-Bebany, A., Adam, L., Daayf, F. (2013). Differential accumulation of phenolic compounds in potato in response to weakly and highly aggressive isolates of *Verticillium dahliae*. *Canadian Journal of Plant Pathology*. **35** (**2**): 232–240.

Evidente, A., Andolfi, A., Fiore, M., Spanu, E., Franceschini, A., Maddau, L. (2007). Diplofuranones A and B, two further new 4-monosubstituted 2 (3H)-dihydrofuranones produced by *Diplodia corticola*, a fungus pathogen of cork oak. *ARKIVOC*. **7** (**VII**): 318–328.

Evidente, A., Andolfi, A., Fiore, M., Spanu, E., Maddau, L., Franceschini, A., Marras, F., Motta, A. (2006). Diplobifuranylones A and B, 5'-monosubstituted tetrahydro-2 H-bifuranyl-5-ones produced by *Diplodia corticola*, a fungus pathogen of cork oak. *Journal of Natural Products*. **69** (**4**): 671–674.

Evidente, A., Maddau, L., Spanu, E., Franceschini, A., Lazzaroni, S., Motta, A. (2003). Diplopyrone, a new phytotoxic tetrahydropyranpyran-2-one produced by *Diplodia mutila*, a fungus pathogen of cork oak. *Journal of Natural Products*. **66** (**2**): 313–315.

Evidente, A., Masi, M., Linaldeddu, B., Franceschini, A., Scanu, B., Cimmino, A., Andolfi, A., Motta, A., Maddau, L. (2012). Afritoxinones A and B, dihydrofuropyran-2-ones produced by *Diplodia africana* the causal agent of branch dieback on *Juniperus phoenicea*. *Phytochemistry*. **77** (**1**): 245–250.

Faulkner, C., Robatzek, S. (2012). Plants and pathogens: putting infection strategies and defence mechanisms on the map. *Current Opinion in Plant Biology*. **15** (**6**): 699–707.

Franceschini, A., Linaldeddu, B., Marras, F. (2005). Occurrence and distribution of fungal endophytes in declining cork oak forests in Sardinia (Italy). In: Villemant, V., Jamaa, M. (ed.). *IOBC WPRS BULLETIN*. IOBC/WPRS. pp. 67–74.

Gil, L. (2015). New Cork-Based Materials and Applications. *Materials*. **8** (**2**): 625–637.

Giraldo, M., Valent, B. (2013). Filamentous plant pathogen effectors in action. *Nature Reviews Microbiology*. **11** (**11**): 800–814.

Gómez-Gómez, L. (2004). Plant perception systems for pathogen recognition and defence. *Molecular immunology*. **41** (**11**): 1055–1062.

González-Fernández, R., Jorrín-Novo, J. (2012). Contribution of proteomics to the study of plant pathogenic fungi. *Journal of Proteome Research*. **11** (**1**): 3–16.

González-Fernández, R., Jorrín-Novo, J. (2013). Proteomic protocols for the study of filamentous fungi. In: Gupta, V., Tuohy, M., Ayyachamy, M., Turner, K., O'Donovan, A. (ed.). *Laboratory Protocols in Fungal Biology*. Springer. pp. 299–308.

González-Fernández, R., Prats, E., Jorrín-Novo, J. (2010). Proteomics of plant pathogenic fungi. *Journal of Biomedicine and Biotechnology*. **2010** (**1**): 1–36.

Görg, A., Weiss, W., Dunn, M. (2004). Current two-dimensional electrophoresis technology for proteomics. *Proteomics*. **4** (**12**): 3665–3685.

Herman, M., Williams, M. (2012). Fighting for their lives: plants and pathogens. *The Plant Cell*. **24** (**6**): 1–15.

Horbach, R., Navarro-Quesada, A., Knogge, W., Deising, H. (2011). When and how to kill a plant cell: infection strategies of plant pathogenic fungi. *Journal of Plant Physiology*. **168** (**1**): 51–62.

Ikeda, K., Kitagawa, H., Meguro, H., Inoue, K., Park, P., Shimoi, S. (2012). The role of the extracellular matrix (ECM) in phytopathogenic fungi: a potential target for disease control. In: Cumagun, C. (ed.). *Plant Pathology*. INTECH. pp. 131–150.

Irieda, H., Maeda, H., Akiyama, K., Hagiwara, A., Saitoh, H., Uemura, A., Terauchi, R., Takano, Y. (2014). *Colletotrichum orbiculare* secretes virulence effectors to a biotrophic interface at the primary hyphal neck via exocytosis coupled with SEC22-mediated traffic. *The Plant Cell*. **26** (**5**): 2265–2281.

Islam, S., Haque, S., Islam, M., Emdad, E., Halim, A., Hossen, Q., Hossain, Z., Ahmed, B., Rahim, S., Rahman, S., Alam, M., Hou, S., Wan, X., Saito, J., Alam, M. (2012). Tools to kill: genome of one of the most destructive plant pathogenic fungi *Macrophomina phaseolina*. *BMC Genomics*. **13** (**1**): 493–509.

Issac, B., Raghava, G. (2005). FASTA servers for sequence similarity search. In: Walker, J. (ed.). *The Proteomics Protocols Handbook*. Springer. pp. 503–525.

Jensen, O. (2006). Interpreting the protein language using proteomics. *Nature Reviews Molecular Cell Biology*. **7** (**6**): 391–403.

Jones, J., Dangl, J. (2006). The plant immune system. *Nature*. **444** (**7117**): 323–329.

Kapp, E., Schutz, F., Connolly, L., Chakel, J., Meza, J., Miller, C., Fenyo, D., Eng, J., Adkins, J., Omenn, G., Simpson, R. (2005). An evaluation, comparison, and accurate benchmarking of several publicly available MS/MS search algorithms: sensitivity and specificity analysis. *Proteomics*. **5** (**13**): 3475–3490.

Kim, Y., Nandakumar, M., Marten, M. (2007). Proteomics of filamentous fungi. *TRENDS in Biotechnology*. **25** (**9**): 395–400.

Kleemann, J., Rincon-Rivera, L., Takahara, H., Neumann, U., Themaat, E., Does, H., Hacquard, S., Stüber, K., Will, I., Schmalenbach, W., Schmelzer, E., O´Connell, R. (2012). Sequential delivery of host-induced virulence effectors by appressoria and intracellular hyphae of the phytopathogen *Colletotrichum higginsianum*. *PLoS Pathogens*. **8** (**4**): e1002643.

Kniemeyer, O. (2011). Proteomics of eukaryotic microorganisms: the medically and biotechnologically important fungal genus *Aspergillus*. *Proteomics*. **11** (**15**): 3232–3243.

Łazniewska, J., Macioszek, V., Kononowicz, A. (2012). Plant-fungus interface: the role of surface structures in plant resistance and susceptibility to pathogenic fungi. *Physiological and Molecular Plant Pathology*. **78** (**2012**): 24–30.

Leroux, P., Fritz, R., Debieu, D., Albertini, C., Lanen, C., Bach, J., Gredt, M., Chapeland, F. (2002). Mechanisms of resistance to fungicides in field strains of *Botrytis cinerea*. *Pest Management Science*. **58** (**9**): 876–888.

Linaldeddu, B., Maddau, L., Franceschini, A. (2005). Preliminary *in vitro* investigation on the interactions among endophytic fungi isolated from *Quercus* spp. In: Villemant, V., Jamaa, M. (ed.). *IOBC WPRS BULLETIN*. IOBC/WPRS. pp. 101–102.

Linaldeddu, B., Scanu, B., Maddau, L., Franceschini, A. (2014). *Diplodia corticola* and *Phytophthora cinnamomi*: the main pathogens involved in holm oak decline on Caprera Island (Italy). *Forest Pathology*. **44** (**3**): 191–200.

Linaldeddu, B., Sirca, C., Spano, D., Franceschini, A. (2009). Physiological responses of cork oak and holm oak to infection by fungal pathogens involved in oak decline. *Forest Pathology*. **39** (**4**): 232–238.

Linaldeddu, B., Sirca, C., Spano, D., Franceschini, A. (2011). Variation of endophytic cork oak-associated fungal communities in relation to plant health and water stress. *Forest Pathology*. **41** (**3**): 193–201.

Liska, A., Shevchenko, A. (2003). Combining mass spectrometry with database interrogation strategies in proteomics. *Trends in Analytical Chemistry*. **22** (**5**): 291–298.

Luna, E., Pastor, V., Robert, J., Flors, V., Mauch-Mani, B., Ton, J. (2011). Callose deposition: a multifaceted plant defense response. *Molecular Plant-Microbe Interactions*. **24** (**2**): 183–193.

Luque, J., Girbal, J. (1989). Dieback of cork oak (*Quercus suber*) in Catalonia (NE Spain) caused by *Botryosphaeria stevensii*. *European Journal of Forest Pathology*. **19** (**1**): 7–13.

Luque, J., Parladé, J., Pera, J. (2000). Pathogenicity of fungi isolated from *Quercus suber* in Catalonia (NE Spain). *Forest Pathology*. **30** (**5**): 247–263.

Luque, J., Pera, J., Parlade, J. (2008). Evaluation of fungicides for the control of *Botryosphaeria corticola* on cork oak in Catalonia (NE Spain). *Forest Pathology*. **38** (**3**): 147–155.

Lynch, S., Eskalen, A., Zambino, P., Mayorquin, J., Wang, D. (2013). Identification and pathogenicity of *Botryosphaeriaceae* species associated with coast live oak (*Quercus agrifolia*) decline in southern California. *Mycologia*. **105** (**1**): 125–140.

Ma, B., Johnson, R. (2012). *De novo* sequencing and homology searching. *Molecular & Cellular Proteomics*. **11** (**2**): 1–16.

Mackey, A., Haystead, T., Pearson, W. (2002). Getting more from less: algorithms for rapid protein identification with multiple short peptide sequences. *Molecular & Cellular Proteomics*. **1** (**2**): 139–147.

Marçais, B., Bréda, N. (2006). Role of an opportunistic pathogen in the decline of stressed oak trees. *Journal of Ecology*. **94** (**6**): 1214–1223.

Martos, S., Andolfi, A., Luque, J., Mugnai, L., Surico, G., Evidente, A. (2008). Production of phytotoxic metabolites by five species of *Botryosphaeriaceae* causing decline on grapevines, with special interest in the species *Neofusicoccum luteum* and *Neofusicoccum parvum*. *European Journal of Plant Pathology*. **121** (**4**): 451–461.

McGinnis, S., Madden, T. (2004). BLAST: at the core of a powerful and diverse set of sequence analysis tools.

Nucleic Acids Research. **32** (**2**): W20–W25.

Medina, M., Francisco, W. (2008). Isolation and enrichment of secreted proteins from filamentous fungi. In: Posch, A. (ed.). *2D PAGE: Sample Preparation and Fractionation*. Springer. pp. 275–285.

Meijer, H., Mancuso, F., Espadas, G., Seidl, M., Chiva, C., Govers, F., Sabidó, E. (2014). Profiling the secretome and extracellular proteome of the potato late blight pathogen *Phytophthora infestans*. *Molecular & Cellular Proteomics*. **13** (**8**): 2101–2113.

Mendgen, K., Hahn, M., Deising, H. (1996). Morphogenesis and mechanisms of penetration by plant pathogenic fungi. *Annual Review of Phytopathology*. **34** (**1**): 367–386.

Moreira, A., Martins, J. (2005). Influence of site factors on the impact of *Phytophthora cinnamomi* in cork oak stands in Portugal. *Forest Pathology*. **35** (**3**): 145–162.

Moricca, S., Ragazzi, A. (2008). Fungal endophytes in Mediterranean oak forests: a lesson from *Discula quercina*. *Phytopathology*. **98** (**4**): 380–386.

Moricca, S., Ragazzi, A. (2011). The holomorph *Apiognomonia quercina/Discula quercina* as a Pathogen/Endophyte in Oak. In: Pirttilä, A., Frank, A. (ed.). *Endophytes of Forest Trees: Biology and Applications*. Forestry Sciences. Springer . pp. 47–66.

Mullerin, S. (2013). *The pathogenicity of* Diplodia corticola *and* Diplodia quercivora *on oak species of the southeastern coastal plain: a host-range study*. University of Florida.

Muth, T., Weilnböck, L., Rapp, E., Huber, C., Martens, L., Vaudel, M., Barsnes, H. (2014). DeNovoGUI: an open source graphical user interface for *de novo* sequencing of tandem mass spectra. *Journal of Proteome Research*. (**13**): 1143–1146.

Möbius, N., Hertweck, C. (2009). Fungal phytotoxins as mediators of virulence. *Current opinion in plant biology*. **12** (**4**): 390–398.

Newey, L., Caten, C., Green, J. (2007). Rapid adhesion of *Stagonospora nodorum* spores to a hydrophobic surface requires pre-formed cell surface glycoproteins. *Mycological Research*. **111** (**11**): 1255–1267.

Oda, K., Kakizono, D., Yamada, O., Iefuji, H., Akita, O., Iwashita, K. (2006). Proteomic analysis of extracellular proteins from *Aspergillus oryzae* grown under submerged and solid-state culture conditions. *Applied and Environmental Microbiology*. **72** (**5**): 3448–3457.

Oliveira, G., Costa, A. (2012). How resilient is *Quercus suber* L to cork harvesting? A review and identification of knowledge gaps. *Forest Ecology and Management*. **270** (**1**): 257–272.

Oliveira, J., Graaff, L. (2011). Proteomics of industrial fungi: trends and insights for biotechnology. *Applied Microbiology and Biotechnology*. **89** (**2**): 225–237.

Van Oudenhove, L., Devreese, B. (2013). A review on recent developments in mass spectrometry instrumentation and quantitative tools advancing bacterial proteomics. *Applied Microbiology and Biotechnology*. **97** (**11**): 4749–4762.

Paizs, B., Suhai, S. (2005). Fragmentation pathways of protonated peptides. *Mass Spectrometry Reviews*. **24** (**4**): 508–548.

Paoletti, E., Anselmi, N., Franceschini, A. (2007). Pre-exposure to ozone predisposes oak leaves to attacks by *Diplodia corticola* and *Biscogniauxia mediterranea*. *The Scientific World Journal*. **7** (**S1**): 222–230.

Passel, M., Schaap, P., Graaff, L. (2013). Proteomics of filamentous fungi. In: Toldrá, F., Nollet, L. (ed.).

Proteomics in Foods. Springer. pp. 563–578.

Pereira, J., Bugalho, M., Caldeira, M. (2008). *From the cork oak to cork - a sustainable system*. Gonçalves, C. (ed.). APCOR - Portuguese Cork Association.

Pérez, P., Ribas, J. (2013). Fungal cell wall analysis. In: Gupta, V., Tuohy, M. (ed.). *Laboratory Protocols in Fungal Biology*. Springer. pp. 175–196.

Pieterse, C., Leon-Reyes, A., Ent, S., Wees, S. (2009). Networking by small-molecule hormones in plant immunity. *Nature Chemical Biology*. **5** (**5**): 308–316.

Pitt, W., Sosnowski, M., Huang, R., Qiu, Y., Steel, C., Savocchia, S. (2012). Evaluation of fungicides for the management of *Botryosphaeria* canker of grapevines. *Plant Disease*. **96** (**9**): 1303–1308.

Pryce-Jones, E., Carver, T., Gurr, S. (1999). The roles of cellulase enzymes and mechanical force in host penetration by *Erysiphe graminis* f sp *hordei*. *Physiological and Molecular Plant Pathology*. **55** (**3**): 175–182.

Ragazzi, A., Moricca, S., Capretti, P., Dellavalle, I. (1999). Endophytic presence of *Discula quercina* on declining *Quercus cerris*. *Journal of Phytopathology*. **147** (**7-8**): 437–440.

Ray, S., Anderson, J., Urmeev, F., Goodwin, S. (2003). Rapid induction of a protein disulfide isomerase and defense-related genes in wheat in response to the hemibiotrophic fungal pathogen *Mycosphaerella graminicola*. *Plant Molecular Biology*. **53** (**5**): 741–754.

Robin, C., Capron, G., Desprez-Loustau, M. (2001). Root infection by *Phytophthora cinnamomi* in seedlings of three oak species. *Plant Pathology*. **50** (**6**): 708–716.

Rogowska-Wrzesinska, A., Bihan, M.-C., Thaysen-Andersen, M., Roepstorff, P. (2013). 2D gels still have a niche in proteomics. *Journal of Proteomics*. **88** (**1**): 4–13.

Ryder, L., Talbot, N. (2015). Regulation of appressorium development in pathogenic fungi. *Current Opinion in Plant Biology*. **26** (**1**): 8–13.

Sánchez, M., Caetano, P., Ferraz, J., Trapero, A. (2002). *Phytophthora* disease of *Quercus ilex* in south-western Spain. *Forest Pathology*. **32** (**1**): 5–18.

Sánchez, M., Venegas, J., Romero, M., Phillips, A., Trapero, A. (2003). *Botryosphaeria* and related taxa causing oak canker in southwestern Spain. *Plant Disease*. **87** (**12**): 1515–1521.

Scanu, B., Linaldeddu, B., Franceschini, A., Anselmi, N., Vannini, A., Vettraino, A. (2013). Occurrence of *Phytophthora cinnamomi* in cork oak forests in Italy. *Forest Pathology*. **43** (**4**): 340–343.

Sghaier-Hammami, B., Valero-Galvàn, J., Romero-Rodríguez, M., Navarro-Cerrillo, R., Abdelly, C., Jorrín-Novo, J. (2013). Physiological and proteomics analyses of holm oak (*Quercus ilex* subsp *ballota* [Desf] Samp) responses to *Phytophthora cinnamomi*. *Plant Physiology and Biochemistry*. **71** (**1**): 191–202.

Sickmann, A., Mreyen, M., Meyer, H. (2003). Mass spectrometry - a key technology in proteome research. In: Hecker, M., Müllner, S., Cahill, D., Cash, P., Cordwell, S., Hecker, M., Meyer, H., Mreyen, M., Nordhoff, E., Nouwens, A., Schubert, W., Sickmann, A., Vanbogelen, R., Walsh, B. (ed.). *Advances in Biochemical Engineering/Biotechnology*. Springer. pp. 141–176.

Silva, S. (2005). Cork: properties, capabilities and applications. *International Materials Reviews*. **50** (**6**): 345–365.

Sousa, E., Santos, M., Varela, M., Henriques, J. (2007). *Perda de vigor dos montados de sobro e azinho:*

Análise da situação e perspectivas. Ministério da Agricultura, do Desenvolvimento e das Pescas.

Tao, Y., Xie, Z., Chen, W., Glazebrook, J., Chang, H.-S., Han, B., Zhu, T., Zou, G., Katagiri, F. (2003). Quantitative nature of *Arabidopsis* responses during compatible and incompatible interactions with the bacterial pathogen *Pseudomonas syringae*. *The Plant Cell*. **15** (**2**): 317–330.

Torres, M. (2010). ROS in biotic interactions. *Physiologia Plantarum*. **138** (**4**): 414–429.

Tsopelas, P., Slippers, B., Gonou-Zagou, Z., Wingfield, M. (2010). First report of *Diplodia corticola* in Greece on kermes oak (*Quercus coccifera*). *Plant Pathology*. **59** (**4**): 805–805.

Tucker, S., Talbot, N. (2001). Surface attachment and pre-penetration stage development by plant pathogenic fungi. *Annual Review of Phytopathology*. **39** (**1**): 385–417.

Úrbez-Torres, J., Battany, M., Bettiga, L., Gispert, C., McGourty, G., Roncoroni, J., Smith, R., Verdegaal, P., Gubler, W. (2010a). *Botryosphaeriaceae* species spore-trapping studies in California vineyards. *Plant Disease*. **94** (**6**): 717–724.

Úrbez-Torres, J., Gubler, W. (2011). Susceptibility of grapevine pruning wounds to infection by *Lasiodiplodia theobromae* and *Neofusicoccum parvum*. *Plant Pathology*. **60** (**2**): 261–270.

Úrbez-Torres, J., Peduto, F., Rooney-Latham, S., Gubler, W. (2010b). First report of *Diplodia corticola* causing grapevine (*Vitis vinifera*) cankers and trunk cankers and dieback of canyon live oak (*Quercus chrysolepis*) in California. *Plant Disease*. **94** (**6**): 785–785.

Vannini, A., Valentini, R. (1994). Influence of water relations on *Quercus cerris* - *Hypoxylon mediterraneum* interaction: a model of drought-induced susceptibility to a weakness parasite. *Tree Physiology*. **14** (**2**): 129–139.

Varela, C., Fernández, V., Casal, O., Vázquez, J. (2011). First report of cankers and dieback caused by *Neofusicoccum mediterraneum* and *Diplodia corticola* on grapevine in Spain. *Plant Disease*. **95** (**10**): 1315–1315.

Vinale, F., Sivasithamparam, K., Ghisalberti, E., Marra, R., Woo, S., Lorito, M. (2008). *Trichoderma*-plant-pathogen interactions. *Soil Biology and Biochemistry*. **40** (**1**): 1–10.

Wargo, P. (1996). Consequences of environmental stress on oak: predisposition to pathogens. *Annals of Forest Science*. **53** (**2-3**): 359–368.

Yang, C., Hamel, C., Vujanovic, V., Gan, Y. (2011). Fungicide: modes of action and possible impact on nontarget microorganisms. *International Scholarly Research Notices*. **2011** (**1**): 1–8.

Zelinger, E., Hawes, C., Gurr, S., Dewey, F. (2006). Attachment and adhesion of conidia of *Stagonospora nodorum* to natural and artificial surfaces. *Physiological and Molecular Plant Pathology*. **68** (**4**): 209–215.

Zhang, J., Xin, L., Shan, B., Chen, W., Xie, M., Yuen, D., Zhang, W., Zhang, Z., Lajoie, G., Ma, B. (2012). PEAKS DB: *de novo* sequencing assisted database search for sensitive and accurate peptide identification. *Molecular & Cellular Proteomics*. **11** (**4**): 1–8.

CHAPTER 2

SECRETOME ANALYSIS IDENTIFIES POTENTIAL VIRULENCE FACTORS OF *Diplodia corticola*, A FUNGAL PATHOGEN INVOLVED IN CORK OAK (*Quercus suber*) DECLINE

This chapter is based on the article "Secretome analysis identifies potential virulence factors of *Diplodia corticola*, a fungal pathogen involved in cork oak (*Quercus suber*) decline" published in the Canadian Journal of Microbiology (See Appendix II).

INTRODUCTION

The family *Botryosphaeriaceae* includes a diversity of fungi with a mostly endophytic lifestyle, commonly related to woody plant diseases (Alves et al., 2004; Damm et al., 2007; Marincowitz et al., 2008; Mehl et al., 2011; Úrbez-Torres & Gubler, 2009). Their virulence usually manifests with the onset of plant stress, accelerating the development of disease symptoms that eventually culminate in host dead (Slippers & Wingfield, 2007). Accordingly, their ecological and economic impact is considerable, particularly in profitable trees such as the cork oak. The involvement of a specific member of this family, the phytopathogen *Diplodia corticola* A.J.L. Phillips, A. Alves et J. Luque (*Botryosphaeriaceae*), in the decline of cork oak forests was already described (Alves et al., 2004; Linaldeddu et al., 2009). It causes symptoms like dieback, canker and vascular necrosis in oak trees. However, the exact mechanism of pathogenesis used by this fungus remains unknown.

In the last decade, proteomics of phytopathogenic fungi has been growingly used in an attempt to understand the molecular mechanisms behind plant-pathogen interactions (González-Fernández & Jorrín-Novo, 2012). More specifically, secretome characterization of such fungi may contribute to elucidate its pathogenesis mechanism, supplying information for the further development of disease management strategies. Indeed, fungi secrete proteins with relevant roles for nutrition and infection (Faulkner & Robatzek, 2012; Jonge et al., 2011). Remarkably, until now only one proteomic study was performed regarding organisms belonging to this family (Cobos et al., 2010), in which the sparse amount of sequenced genomes (Blanco-Ulate et al., 2013; Islam et al., 2012; Morales-Cruz et al., 2015; Nest et al., 2014) represents a limiting factor for protein identification. Nevertheless, 2D gel-based proteomics followed by *de novo* sequencing approach is particularly useful and reliable for protein identification of organisms with unsequenced genomes such as *D. corticola* (Rogowska-Wrzesinska et al., 2013; Tannu & Hemby, 2007). Still, the analysis of the secretome is hampered by difficulties related to the very low concentration of extracellular proteins, the high amount of polysaccharides, and the presence of low-molecular-weight metabolites also secreted by these organisms (Chevallet et al., 2007; Erjavec et al., 2012). These molecules interfere with protein extraction and protein separation methods, especially 2D-electrophoresis. The choice of an adequate extraction method is, therefore, a crucial step to obtain a good protein profile that can be subsequent and successfully analysed.

Hence, we aimed to optimize a protocol compatible with protein analysis by 1D and 2D electrophoresis, which allows collecting the secretome of *D. corticola* as well as other filamentous fungi and, concurrently, removing interfering substances from the medium. Moreover, we successfully identified the major extracellular proteins of *D. corticola* that may eventually be related to its pathogenicity.

MATERIAL AND METHODS

MICROORGANISMS AND CULTURE CONDITIONS

The strain used in this study was *D. corticola* CBS112548. Cultures were maintained on Potato Dextrose Agar (PDA) medium (Merck, Germany). For secretome extraction, a mycelium plug with 0.5 cm diameter from a 6-day-old PDA plate was inoculated into a 250 mL flask containing 50 mL of Potato Dextrose Broth (PDB), and incubated for 12 days at room temperature (± 25ºC). All assays were performed in triplicate. Culture supernatants were individually collected by filtration and stored at -20ºC until use. The dry-weight of mycelia was determined to evaluate the fungal biomass. For this, filtered mycelia were dried at 50ºC for 4 days before weighting. The extracellular protein fraction was then concentrated as described below.

EXTRACELLULAR PROTEIN EXTRACTION METHODS

Protocol 1 (Trichloroacetic acid (TCA)-acetone) was based on a previously described method (Cobos et al., 2010). After thawing, the culture supernatant (35mL) was centrifuged (48400×*g*, 1h at 4ºC) to discard precipitated polysaccharides. One volume of ice-cold TCA/acetone [20%/80% (w/v)] with 0.14% (w/v) DTT was added to the supernatant and incubated at -20ºC (1h). Precipitated proteins were recovered by centrifugation (15000×*g*, 20 min, 4ºC) and excess TCA was removed from the precipitate by washing with 10 mL of ice-cold acetone (2×), and 10 mL of ice-cold 80% acetone (v/v). Residual acetone was air-dried and the protein pellet was resuspended in 500 µL of lysis buffer (7 M urea, 2 M thiourea, 4% CHAPS, 30 mM Tris-base) and stored at -20ºC.

Protocol 2 (TCA-phenol) was adapted from a previously described method (Fernández-Acero et al., 2009). After thawing, the culture supernatant (35 mL) was centrifuged (48400×*g*, 1h at 4ºC) to discard precipitated polysaccharides. Proteins were precipitated by the addition of one volume of ice-cold TCA/acetone [20%/80% (w/v), 1h, -20ºC], and collected by centrifugation at 15000×*g* (20 min, 4ºC). The precipitate was successively washed with 10 mL of ice-cold TCA/acetone [20%/80% (w/v), twice], 10 mL of 20% TCA (w/v), and twice with 10 mL of ice-cold 80% acetone (v/v).

Residual acetone was air-dried and the protein pellet was resuspended in 5 mL of dense SDS buffer [30% (w/v) sucrose, 2% (w/v) SDS, 0.1 M Tris-HCl pH 8.0, 5% (v/v) 2-mercaptoethanol] adding then 5 mL of phenol equilibrated with 10 mM Tris-HCl, pH 8.0, 1 mM EDTA (Sigma-Aldrich, USA). The resulting solution was vigorously mixed and centrifuged at 15000×*g* (10 min, 4ºC). The phenol phase was transferred to a tube to which 5 volumes of cold 0.1 M ammonium acetate in methanol were added and incubated at -20ºC overnight to promote protein precipitation. Afterwards, proteins were recovered by centrifugation and washed twice with 10 mL of cold 0.1 M ammonium acetate in methanol, followed by two washes with 10 mL of ice-cold 80% acetone (v/v). The air-dried pellet was finally resuspended in 500 µL lysis buffer and stored at -20ºC.

Protocol 3 (ultrafiltration with protein cleaning): polysaccharides were separated as described for protocol 1 and the resultant supernatant was concentrated by ultrafiltration with Vivaspin concentrator (MWCO 3 kDa, Sartorious), at 4000 rpm (4 ºC). Retained proteins were purified with 2-D Clean-Up kit (GE Healthcare, USA; from now on mentioned as protein cleaning), according to the manufacturer's instructions. The proteins were solubilized in 500 µL of lysis buffer and stored at -20ºC.

Protocol 4 (ultrafiltration without protein cleaning): this method is identical to method 3 with the exception of the final cleaning step. Therefore, the proteins were immediately resuspended in 500 µL of lysis buffer and stored at -20ºC after their concentration.

Protocol 5 (ultrafiltration without polysaccharide precipitation): this method is similar to method 3 with the exception of the initial polysaccharide removal step. After protein cleaning, the resultant pellet was solubilized in 500 µL of lysis buffer and stored at -20ºC.

Protocol 6 (lyophilisation): culture supernatant (35mL) was concentrated by lyophilization (Snijders Scientific) for 24 h at -50ºC. Afterwards, proteins were cleaned as previously described, solubilized in 500 µL of lysis buffer and stored at -20ºC.

PROTEIN CONCENTRATION DETERMINATION

Protein concentration was determined with the 2-D Quant Kit (GE Healthcare, USA), according to the manufacturer's instructions.

1D- AND 2D-ELECTROPHORESIS

Proteins were separated by SDS-PAGE or by 2D. For SDS-PAGE, 30 µg of protein extract were diluted (1:1) in 8 M urea, 100 mM Tris, 100 mM bicine, 2% SDS, 2% 2-mercaptoethanol, and heated for 5 min at 100ºC. Proteins were separated by 12.5% SDS-PAGE gel electrophoresis, according to Laemmli's protocol (Laemmli, 1970), for 120 min at 120 V, in a Mini-PROTEAN 3 Cell

(Bio-Rad, USA).

For 2D, 240 µg of protein extract were loaded onto IPG strips (pH 3-5.6 NL or pH 3-11 NL, 13 cm, GE Healthcare) that were actively rehydrated (50 V, 10h) with 250 µL of rehydratation buffer (7 M urea, 2 M thiourea, 4% CHAPS, 30 mM Tris-base, 2% DTT, 2% IPG buffer pH 3-5.6 NL and bromophenol blue). IEF was performed on a Ettan IPGphor 3 system (GE Healthcare, Sweden) at 20ºC limited to 50 µA/strip according to the following parameters: 1h at 150 V, 2h at 500 V, 6h 500-1000 V, 3h 1000-8000 V and 8000 V until 20000 Vhr. Prior to second dimension, the IPG strips were reduced and alkylated for 15 min with 1% (w/v) DTT and afterwards with 2.5% (w/v) iodoacetamide in 5 mL equilibration buffer [50 mM Tris-HCl (pH 8.8), 6 M urea, 30% (w/v) glycerol, 2% SDS and traces of bromophenol blue], respectively. After equilibration, the strips were juxtaposed to 12.5% lab cast SDS-PAGE gels on a PROTEAN II xi Cell (Bio-Rad, USA) system. Proteins were separated initially at 2 W/gel (2h) and then at 6 W/gel (limited to 200 V) until the dye marker reached the end of the gel.

Proteins were visualized by Coomassie Brilliant Blue G-250 (CBB) staining. Each gel image was acquired using the GS-800 calibrated imaging densitometer (Bio-Rad, USA). CBB stained 2-DE gels were analysed with PDQuest software (Bio-Rad, USA) to determine the number of protein spots per gel.

MASS SPECTROMETRY

Randomly selected 2D spots were excised and successively guanidinated, digested with trypsin and N-terminal sulfonated to enhance the *de novo* sequencing (Sergeant et al., 2005). The tryptic peptides were then analyzed by tandem mass spectrometry on a 4800 Plus MALDI TOF/TOF Analyser system (AB Sciex, USA). As the standard settings MASCOT search (Matrix Science, UK) was unsuccessful, due to the lack of information on the non-redundant NCBI fungal database (Cobos et al., 2010; Standing, 2003), it was proceeded to PEAKS® *de novo* sequencing (PEAKS Studio 6.0, BSI, Canada) (Zhang et al., 2012). The PEAKS® search parameters encompassed fragment mass error tolerance of 0.3 Da, carbamidomethylation (57.02) and guanidination (42.02) as fixed modifications, and acetylation (N-terminus) (42.01), 4-sulfophenyl isothiocyanate (214.97) and methionine, histidine and tryptophan oxidation (15.99) as variable modifications. In addition, manual interpretation of the spectra was performed to confirm the previous results and the similarity of the identified peptide sequences was searched with FASTS algorithm (Mackey et al., 2002) (standard settings search (matrix PAM 120) against UniProtKB Fungi subset; $p<0.05$ scores were considered significant). The subcellular localization of identified proteins was predicted using BaCelLo predictor (Pierleoni et al., 2006) and the theoretical pI searched with

Compute pI/Mw tool available on ExPASy (Gasteiger et al., 2005).

RESULTS AND DISCUSSION

Secreted proteins from *D. corticola* grown on PDA were extracted by six different methods (Table 1). Comparison of SDS-PAGE performance of these extracts (Figure 4) showed that the protocols based on protein precipitation (protocols 1 and 2) were more efficient than the methods that excluded this step (Figure 4). In these protocols (1 and 2) the protein molecular weights ranged between 218 and 23 kDa, distributed over a mean of 12 bands after TCA-acetone extraction and 15 bands after TCA-phenol precipitation. Conversely, the maximum detected bands with methods 3-6 were 10 bands (protocol 5), distributed over a lower molecular weight range (113 – 25 kDa), which indicates loss of proteins and/or poor recovery after extraction. The resolution was also poorest in these methods, presenting faint bands (Figure 4).

Table 1 | Summary of the protocols used to extract the secretome of *D. corticola* and respective protein concentration average [determined by the 2-D Quant Kit (GE Healthcare, USA)]. The inclusion of a polysaccharide removal step or a protein cleaning step are indicated by + (included) or - (not included).

Extraction method	Polysaccharide removal	Protein cleaning with 2-D Clean-Up kit	Average protein concentration ($\mu g.ml^{-1}$) ± SD
1. TCA-acetone	+	-	1580.8 ± 916.5
2. TCA-phenol	+	-	3935.4 ± 930.8
3. Ultrafiltration	+	+	4414.7 ± 568.5
4. Ultrafiltration	+	-	1989.9 ± 105.7
5. Ultrafiltration	-	+	5217.5 ± 711.3
6. Lyophilization	+	+	456.7 ± 264.7

The results indicated thus a limited applicability of ultrafiltration to concentrate fungal secretomes, confirming previous noticed drawbacks such as rapid membrane clogging and the consequent adsorption (and loss) of proteins to the gelatinous material that was retained on the membrane (Chevallet et al., 2007; Fragner et al., 2009). In an attempt to avoid the rapid membrane clogging a polysaccharide removal step was added to protocols 3 and 4. However, this did not result in improved gel patterns (protocol 3 - 9 bands (MW – 103.4 - 31.7 kDa); protocol 4 - no bands). Still, the initial polysaccharide removal step can be considered as essential in protocols that involve protein precipitation such as protocols 1 and 2, since these sugars co-precipitate with proteins, not only distorting the protein quantification (Fragner et al., 2009), but also interfering in electrophoretic separation.

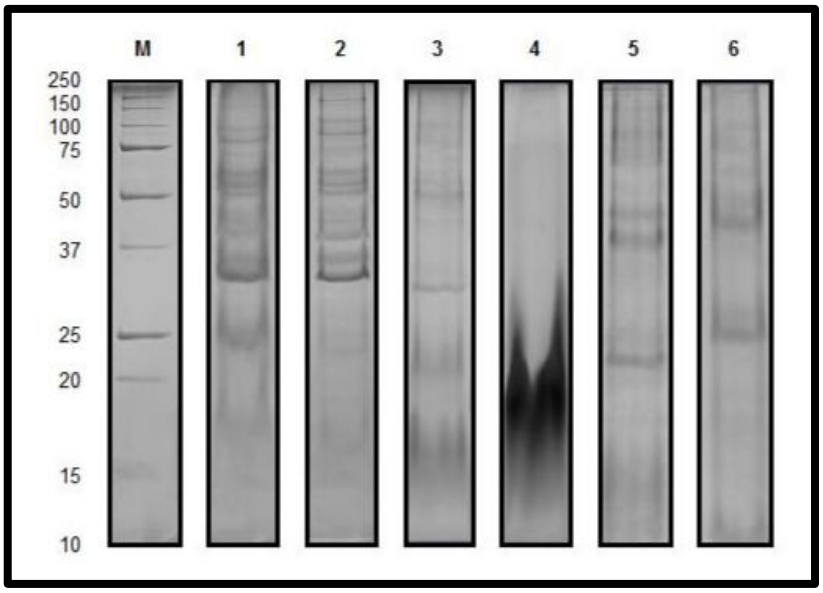

Figure 4 | SDS-PAGE of secretome proteins from *D. corticola* extracted by several methods. Three biological replicates were used for each protocol. M – Precision Plus Protein Unstained Standard (kDa) (Bio-Rad, USA).

Despite the unsatisfactory performance, protocol 4 highlighted the importance of protein cleaning (2-D Clean-Up kit) after concentration in methods that do not involve protein precipitation. Considering that precipitation protocols efficiently remove most protein contaminants (salts, detergents or phenolic compounds) (Medina & Francisco, 2008), it is necessary to combine ultrafiltration with a cleaning step to discard such interfering compounds. Comparison of protocols 4 and 5 (without and with a cleaning step after ultrafiltration, respectively), clearly demonstrates the improvement introduced by the cleaning step on electrophoresis separation (Figure 4). However, conversely to what was predicted, SDS-PAGE of protocol 5 was slightly better than protocol 3 (with polysaccharide removal and cleaning steps) (Figure 4), which probably is related to the performance of ultrafiltration methods. As we could experience, membrane clogging precludes the forecast of ultrafiltration behaviour, compromising therefore the protocol reproducibility. Although cheaper than any of the other methods that were tested, lyophilisation was the less efficient concentration method, leading to low protein recovery and poor electrophoresis performance. These pitfalls are most likely due to the difficult protein solubilisation in the lysis buffer, even after the protein cleaning step.

The most efficient methods were therefore TCA-acetone and TCA-phenol (Figure 4), overcoming the disadvantageous loss of proteins during precipitation and washing steps usually associated to these protocols (Carpentier et al., 2005). Indeed, like previously described, TCA-phenol extracts presented a better band pattern definition than TCA-acetone extracts (Figure 4) (Carpentier et al., 2005; Saravanan & Rose, 2004). Nevertheless, this slight improvement may not be sufficient to compensate for the risks associated to phenol and methanol toxicity (Faurobert et

al., 2007), as well as for the increased time-consumption when compared with the TCA-acetone protocol. Hence, we regard protocol 1 as the best method for *D.corticola* secretome extraction, considering its efficiency, safety and cost.

We additionally evaluated the methods by analysis of the extracted proteins using 2-D electrophoresis. The first approaches were performed with broad-range pH strips (pH 3-11 NL), but since *D. corticola* secretome is mainly located on the acidic region (Figure 5), as has been reported for other filamentous fungi (Callegari & Navarrete, 2012; Cobos et al., 2010; Fragner et al., 2009; Zorn et al., 2005), strips with a narrow acidic pH range were used to improve gel resolution.

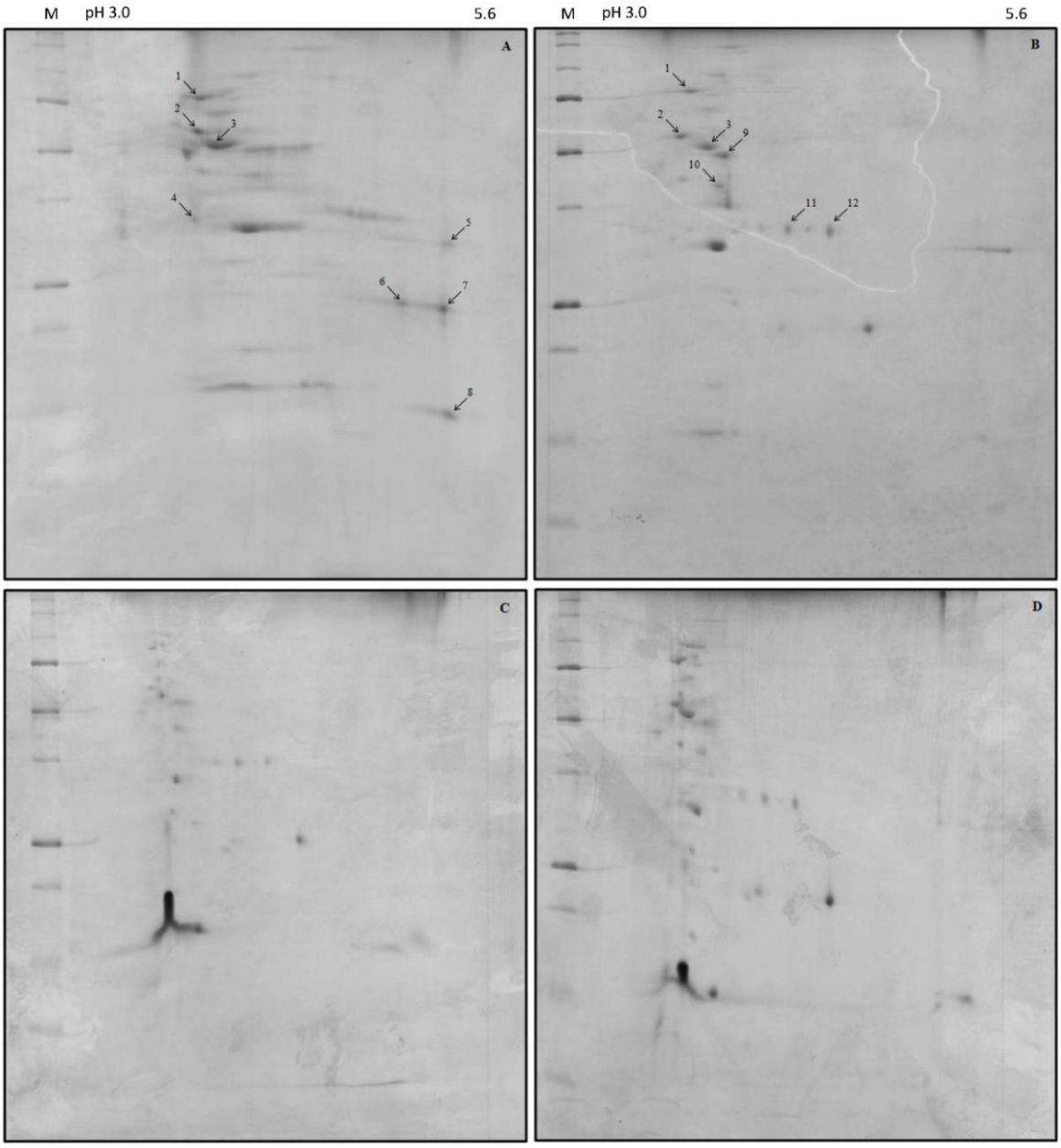

Figure 5 | 2-DE of proteins extracted with TCA-Acetone (A, protocol 1), TCA-Phenol (B, protocol 2) and ultrafiltration (C, protocol 3; D, protocol 5). M - Precision Plus Protein Standard (Bio-Rad, USA).

Curiously, in contrast to what we expected from the 1D profiles, where the band definition of protocols 3 and 5 were worse than in protocols 1 and 2, 2D gels presented a similar number of spots with comparable definitions (Figure 6). This may be explained by the presence of an interfering substance not removed during the protein cleaning step, which was not absorbed during the strip rehydration.

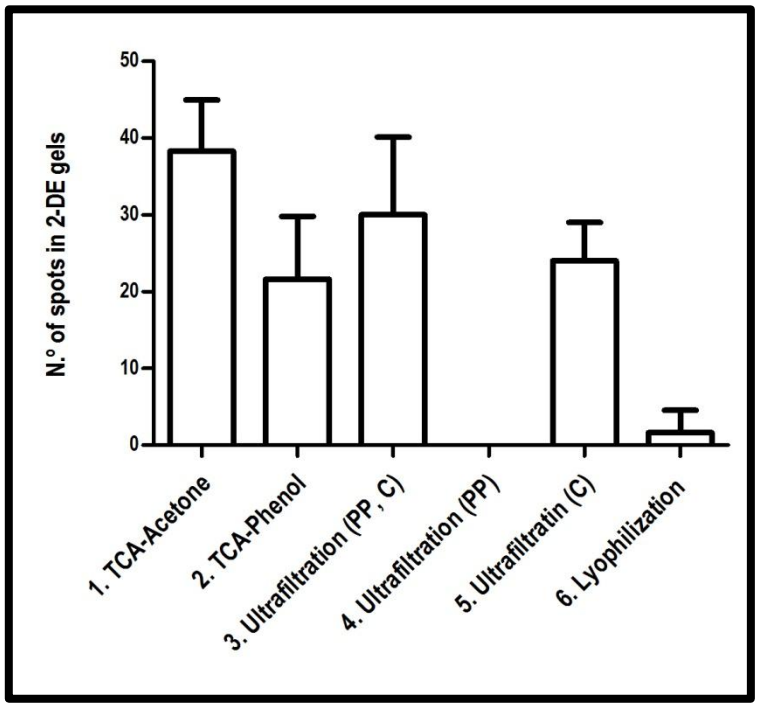

Figure 6 | Number of spots detected by 2-DE of proteins extracted with the various methods used. PP – polysaccharide precipitation, C – protein cleaning with 2-D Clean-Up Kit.

Nonetheless, based on 1D profiles, only spots obtained from extraction protocols TCA-acetone and TCA-phenol were randomly selected for identification. The overall identification rate was similar in both methods, having been identified 69 % of the spots obtained with protocol 1 (11 out of 16) and 58% of the spots obtained with protocol 2 (11 out of 19). Some of the spots were identified twice (replicates), in order to confirm protein identification. The spots were identified based on *de novo* sequenced peptides, whose similarity was searched with FASTS algorithm (Mackey et al., 2002) against UniProtKB Fungi subset (Table 2). Some proteins where identified in different spots with the same molecular weight, but with slightly different isoelectric points [spots 6, 7 (peptidase M35 deuterolysin) and spots 11, 12 (spherulation-specific family 4), Figure 5 A,B], indicative for possible post-translational modifications that need to be further investigated. In addition, BaCelLo fungi-specific predictor (Pierleoni et al., 2006) confirmed the extracellular localization of all identified proteins (Table 2).

Table 2 | Summary of proteins identified by *de novo* sequencing. Peptide similarity search was performed with FASTS algorithm (Mackey et al., 2002) ($p < 0.05$ scores were considered significant).

Spot	Protein	Accession number	Organism	Theoretical pI[1]	Subcellular localization[2]
1	Glucoamylase	K2S7L9	*Macrophomina phaseolina* (strain MS6)	5.37	Extracellular
2	Glycoside hydrolase family 71	K2R498	*Macrophomina phaseolina* (strain MS6)	4.84	Extracellular
3	Putative carboxypeptidase S1	R1GF60	*Neofusicoccum parvum* UCRNP2	4.45	Extracellular
4	Neuraminidase	K2SSW0	*Macrophomina phaseolina* (strain MS6)	4.27	Extracellular
5	Putative serine protease	R1GM11	*Neofusicoccum parvum* UCRNP2	6.07	Extracellular
6,7	Peptidase M35 deuterolysin	K2SDQ0	*Macrophomina phaseolina* (strain MS6)	5.34	Extracellular
8	Uncharacterized protein	K2RZ98	*Macrophomina phaseolina* (strain MS6)	5.59	Extracellular
9	Putative ferulic acid esterase	R1EDH3	*Neofusicoccum parvum* UCRNP2	4.79	Extracellular
10	Putative glucan-β-glucosidase	R1GIC9	*Neofusicoccum parvum* UCRNP2	4.73	Extracellular
11, 12	Spherulation-specific family 4	K2RK67	*Macrophomina phaseolina* (strain MS6)	4.04	Extracellular

[1] Compute pI/Mw, ExPASy (Gasteiger et al., 2005)

[2] BaCelLo (Pierleoni et al., 2006)

Still, the limited genomic data available on family *Botryophaeriaceae* fungi constrained protein identification, as reported before on a study of *D. seriata* proteome (Cobos et al., 2010). Nevertheless, most of the identified proteins display homology with the fungal pathogen *Macrophomina phaseolina* (Tassi) Goid., and in less extent with *Neofusicoccum parvum* (Pennycook & Samuels) Crous, Slippers et A.J.L. Phillips, both members of the *Botryosphaeriaceae* whose genomes were recently sequenced (Blanco-Ulate et al., 2013; Islam et al., 2012) and integrated into UniProtKB.

Functional distribution of the extracellular proteins of *D. corticola* is consonant to what was previously described to other filamentous fungi (Girard et al., 2013; Islam et al., 2012). The identified proteins mainly belong to hydrolases (glucoamylase, glycoside hydrolase 71, neuraminidase and putative glucan-β-glucosidase), and in less extent to proteases (putative carboxypeptidase S1, putative serine protease and M35 deuterolysin) (Table 2).

Although the basal function of the identified carbohydrate-degrading enzymes is to fulfil the nutritional needs of *D. corticola*, they possibly have an active involvement on its phytopathogenic lifestyle, degrading the lignocellulosic barrier of plant cell walls (Abbas et al., 2005; Jung et al., 2012; Wang et al., 2011). During infection, fungi secrete a plethora of hydrolytic enzymes to degrade the plant polysaccharides aiming to compromise its integrity. Notably, the hydrolases identified belong to the 3 classes known to work synergistically to degrade cellulose [(exo-glucanases, endo-glucanases and β-glucosidases (Horn et al., 2012), having already been described on the secretome of wood degrading fungi (Abbas et al., 2005; Phalip et al., 2005; Sato et al., 2007), as well as in phytopathogenic fungi (Fernández-Acero et al., 2010; Jung et al., 2012; Wang et al., 2011). The carbohydrate metabolism enzymes play thus an active role on the establishment of fungal infection, while sustaining its nutritional and energetic requirements from infected plant biomass (Faulkner & Robatzek, 2012; Pietro et al., 2009). Moreover, cellulose degrading enzymes concurrently require the assistance of carbohydrate esterases (Aspeborg et al., 2012) to deacetylate the substituted saccharides (esters or amides) of plant celluloses (Biely, 2012), such as the putative ferulic acid esterase identified in spot 9. Generally, these enzymes are known to release ferulic acid, one of the oligomeric building blocks of suberin (Graça & Santos, 2007), the main bark constituent of oak trees (Jové et al., 2011). Ferulic acid esterase may therefore be relevant for *D. corticola* pathogenesis establishment, contributing to compromise the suberin integrity. Likewise, the molecules released after ester bond cleavage can have a signaling function on infection (Pietro et al., 2009). Furthermore, neuraminidase (spot 4) is an exo-glycosidase that cleaves glycoconjugates, releasing the terminal sialic acid residues (Warwas et al., 2010). Although its role on fungal phytopathogenicity is not yet clear, it is plausible that this

enzyme can contribute to cell wall disruption, making the glycoproteins present on plant cell wall matrix (Lerouxel et al., 2006) more accessible to other fungal glycoside hydrolases.

The successful colonization of a pathogen benefits as well from the existence of proteases and peptidases to impair the plant proteins and to evade from plant defense mechanism, profiting simultaneously from the amino acids released to support its growth demands (Espino et al., 2010; Faulkner & Robatzek, 2012; Jung et al., 2012). Previous studies already demonstrated that filamentous fungi secrete more proteases in the presence of plant extracts (Espino et al., 2010; Phalip et al., 2005; Zorn et al., 2005), emphasizing their importance on fungal pathogenicity strategies. Besides proteases' function on basal metabolism, the peptidases found on *D. corticola* secretome (Table 2) can likewise be involved on host colonization. Their functional diversity (exo- and endo-proteases) reflects their synergistic interplay (Girard et al., 2013). Serine carboxypeptidase S1 (spot3) is an exoprotease that seems to efficiently work in an acidic environment (Figure 5 A), likewise the serine endopeptidade found in spot 5, a characteristic already described in other plant infection models (Billon-Grand et al., 2002; Li et al., 2012). Similarly, the Zn^{2+} metalloendopeptidase deuterolysin (spots 6 and 7) was described as a virulence factor not only in pathogenic fungi (Monod et al., 2002), but also in bacteria (Arnadottir et al., 2009).

In this study, we additionally identified a spherulation-specific family 4 protein (spots 11, 12) previously reported in *Magnaporthe oryzae* B.C. Couch secretome (Jung et al., 2012). Although its secretion may be a response to nutrient starvation, this protein can likewise be involved in sporulation which usually follows infection to spread the fungus through the host (Wilson & Talbot, 2009). More studies need to be performed to understand the function of this sporulation-inducing protein, which has 2 isoforms on *D. corticola* secretome (Figure 5).

To summarize, we presented a comparison of different secretome extraction protocols, concluding that methods involving protein precipitation are the most efficient to collect these low abundant proteins. Furthermore, TCA-acetone and TCA-phenol are similarly efficient, but considering the time-consumption and the associated toxicity of the last method, we opted for the former, with a previous polysaccharide removal step, to study the secretome of *D. corticola*. However, more efforts need to be done to increase the fungal annotated databases, particularly in *Botryosphaeriaceae* family to which *D. corticola* belongs, in an attempt to improve the homology search and protein identification rates. Nonetheless, we identified by *de novo* sequencing several fungal glycoside hydrolases and proteases that can be involved in *D. corticola* pathogenesis towards cork oak and other hosts. In addition, this work represents an advance on the characterization of the proteome of members of the family *Botryosphaeriaceae*.

REFERENCES

Abbas, A., Koc, H., Liu, F., Tien, M. (2005). Fungal degradation of wood: initial proteomic analysis of extracellular proteins of *Phanerochaete chrysosporium* grown on oak substrate. *Current Genetics*. **47** (**1**): 49–56.

Alves, A., Correia, A., Luque, J., Phillips, A. (2004). *Botryosphaeria corticola*, sp nov on *Quercus* species, with notes and description of *Botryosphaeria stevensii* and its anamorph, *Diplodia mutila*. *Mycologia*. **96** (**3**): 598–613.

Arnadottir, H., Hvanndal, I., Andresdottir, V., Burr, S., Frey, J., Gudmundsdottir, B. (2009). The AsaP1 peptidase of *Aeromonas salmonicida* subsp *achromogenes* is a highly conserved deuterolysin metalloprotease (family M35) and a major virulence factor. *Journal of Bacteriology*. **191** (**1**): 403–410.

Aspeborg, H., Coutinho, P., Wang, Y., Brumer, H., Henrissat, B. (2012). Evolution, substrate specificity and subfamily classification of glycoside hydrolase family 5 (GH5). *BMC Evolutionary Biology*. **12** (**1**): 186–202.

Biely, P. (2012). Microbial carbohydrate esterases deacetylating plant polysaccharides. *Biotechnology Advances*. **30** (**6**): 1575–1588.

Billon-Grand, G., Poussereau, N., Fèvre, M. (2002). The extracellular proteases secreted *in vitro* and *in planta* by the phytopathogenic fungus *Sclerotinia sclerotiorum*. *Journal of Phytopathology*. **150** (**8-9**): 507–511.

Blanco-Ulate, B., Rolshausen, P., Cantu, D. (2013). Draft genome sequence of *Neofusicoccum parvum* isolate UCR-NP2, a fungal vascular pathogen associated with grapevine cankers. *Genome Announcements*. **1** (**3**): e00339–13.

Callegari, E., Navarrete, M. (2012). The use of mass spectrometry for characterization of fungal secretomes. In: Prasain, J. (ed.). *Tandem Mass Spectrometry - Applications and Principles*. INTECH. pp. 221–234.

Carpentier, S., Witters, E., Laukens, K., Deckers, P., Swennen, R., Panis, B. (2005). Preparation of protein extracts from recalcitrant plant tissues: an evaluation of different methods for two-dimensional gel electrophoresis analysis. *Proteomics*. **5** (**10**): 2497–2507.

Chevallet, M., Diemer, H., Dorssealer, A., Villiers, C., Rabilloud, T. (2007). Toward a better analysis of secreted proteins: the example of the myeloid cells secretome. *Proteomics*. **7** (**11**): 1757–1770.

Cobos, R., Barreiro, C., Mateos, R., Coque, J.-J. (2010). Cytoplasmic-and extracellular-proteome analysis of *Diplodia seriata*: a phytopathogenic fungus involved in grapevine decline. *Proteome Science*. **8** (**46**): 1–16.

Damm, U., Crous, P., Fourie, P. (2007). *Botryosphaeriaceae* as potential pathogens of *Prunus* species in South Africa, with descriptions of *Diplodia africana* and *Lasiodiplodia plurivora* sp nov. *Mycologia*. **99** (**5**): 664–680.

Erjavec, J., Kos, J., Ravnikar, M., Dreo, T., Sabotic, J. (2012). Proteins of higher fungi - from forest to application. *Trends in Biotechnology*. **30** (**5**): 259–273.

Espino, J., Gutiérrez-Sánchez, G., Brito, N., Shah, P., Orlando, R., González, C. (2010). The *Botrytis cinerea* early secretome. *Proteomics*. **10** (**16**): 3020–3034.

Faulkner, C., Robatzek, S. (2012). Plants and pathogens: putting infection strategies and defence mechanisms on the map. *Current Opinion in Plant Biology*. **15** (**6**): 699–707.

Faurobert, M., Pelpoir, E., Chaïb, J. (2007). Phenol extraction of proteins for proteomic studies of recalcitrant plant tissues. In: Thiellement, H., Zivy, M., Damerval, C., Méchin, V. (ed.). *Plant Proteomics: Methods and Protocols*. Humana Press. pp. 9–14.

Fernández-Acero, F., Colby, T., Harzen, A., Cantoral, J., Schmidt, J. (2009). Proteomic analysis of the phytopathogenic fungus *Botrytis cinerea* during cellulose degradation. *Proteomics*. **9** (**10**): 2892–2902.

Fernández-Acero, F., Colby, T., Harzen, A., Carbú, M., Wieneke, U., Cantoral, J., Schmidt, J. (2010). 2-DE proteomic approach to the *Botrytis cinerea* secretome induced with different carbon sources and plant-based elicitors. *Proteomics*. **10** (**12**): 2270–2280.

Fragner, D., Zomorrodi, M., Kües, U., Majcherczyk, A. (2009). Optimized protocol for the 2-DE of extracellular proteins from higher basidiomycetes inhabiting lignocellulose. *Electrophoresis*. **30** (**14**): 2431–2441.

Gasteiger, E., Hoogland, C., Gattiker, A., Duvaud, S., Wilkins, M., Appel, R., Bairoch, A. (2005). Protein identification and analysis tools on the ExPASy server. In: Walker, J. (ed.). *The Proteomics Protocols Handbook*. Humana Press. pp. 571–607.

Girard, V., Dieryckx, C., Job, C., Job, D. (2013). Secretomes: the fungal strike force. *Proteomics*. **13** (**3-4**): 597–608.

González-Fernández, R., Jorrín-Novo, J. (2012). Contribution of proteomics to the study of plant pathogenic fungi. *Journal of Proteome Research*. **11** (**1**): 3–16.

Graça, J., Santos, S. (2007). Suberin: a biopolyester of plants' skin. *Macromolecular Bioscience*. **7** (**2**): 128–135.

Horn, S., Vaaje-Kolstad, G., Westereng, B., Eijsink, V.G. (2012). Novel enzymes for the degradation of cellulose. *Biotechnology for Biofuels*. **5** (**1**): 1–13.

Islam, S., Haque, S., Islam, M., Emdad, E., Halim, A., Hossen, Q., Hossain, Z., Ahmed, B., Rahim, S., Rahman, S., Alam, M., Hou, S., Wan, X., Saito, J., Alam, M. (2012). Tools to kill: genome of one of the most destructive plant pathogenic fungi *Macrophomina phaseolina*. *BMC Genomics*. **13** (**1**): 493–509.

Jonge, R., Bolton, M., Thomma, B. (2011). How filamentous pathogens co-opt plants: the ins and outs of fungal effectors. *Current Opinion in Plant Biology*. **14** (**4**): 400–406.

Jové, P., Olivella, M., Cano, L. (2011). Study of the variability in chemical composition of bark layers of *Quercus suber* L from different production areas. *BioResources*. **6** (**2**): 1806–1815.

Jung, Y.-H., Jeong, S.-H., Kim, S., Singh, R., Lee, J., Cho, Y.-S., Agrawal, G., Rakwal, R., Jwa, N.-S. (2012). Secretome analysis of *Magnaporthe oryzae* using *in vitro* systems. *Proteomics*. **12** (**6**): 878–900.

Laemmli, U. (1970). Cleavage of structural proteins during the assembly of the head of bacteriophage T4. *Nature*. **227** (**5259**): 680–685.

Lerouxel, O., Cavalier, D., Liepman, A., Keegstra, K. (2006). Biosynthesis of plant cell wall polysaccharides - a complex process. *Current Opinion in Plant Biology*. **9** (**6**): 621–630.

Li, B., Wang, W., Zong, Y., Qin, G., Tian, S. (2012). Exploring pathogenic mechanisms of *Botrytis cinerea* secretome under different ambient pH based on comparative proteomic analysis. *Journal of Proteome Research*. **11** (**8**): 4249–4260.

Linaldeddu, B., Sirca, C., Spano, D., Franceschini, A. (2009). Physiological responses of cork oak and holm oak to infection by fungal pathogens involved in oak decline. *Forest Pathology*. **39** (**4**): 232–238.

Mackey, A., Haystead, T., Pearson, W. (2002). Getting more from less: algorithms for rapid protein identification with multiple short peptide sequences. *Molecular & Cellular Proteomics*. **1** (**2**): 139–147.

Marincowitz, S., Groenewald, J., Wingfield, M., Crous, P. (2008). Species of *Botryosphaeriaceae* occurring on *Proteaceae*. *Persoonia: Molecular Phylogeny and Evolution of Fungi*. **21** (**1**): 111–118.

Medina, M., Francisco, W. (2008). Isolation and enrichment of secreted proteins from filamentous fungi. In: Posch, A. (ed.). *2D PAGE: Sample Preparation and Fractionation*. Springer. pp. 275–285.

Mehl, J., Slippers, B., Roux, J., Wingfield, M. (2011). *Botryosphaeriaceae* associated with *Pterocarpus angolensis* (kiaat) in South Africa. *Mycologia*. **103** (**3**): 534–553.

Monod, M., Capoccia, S., Léchenne, B., Zaugg, C., Holdom, M., Jousson, O. (2002). Secreted proteases from pathogenic fungi. *International Journal of Medical Microbiology*. **292** (**5**): 405–419.

Morales-Cruz, A., Amrine, K., Blanco-Ulate, B., Lawrence, D., Travadon, R., Rolshausen, P., Baumgartner, K., Cantu, D. (2015). Distinctive expansion of gene families associated with plant cell wall degradation, secondary metabolism, and nutrient uptake in the genomes of grapevine trunk pathogens. *BMC Genomics*. **16** (**1**): 469.

Nest, M., Bihon, W., Vos, L., Naidoo, K., Roodt, D., Rubagotti, E., Slippers, B., Steenkamp, E., Wilken, P., Wilson, A., Wingfield, M. (2014). Draft genome sequences of *Diplodia sapinea*, *Ceratocystis manginecans*, and *Ceratocystis moniliformis*. *IMA Fungus*. **5** (**1**): 135–140.

Phalip, V., Delalande, F., Carapito, C., Goubet, F., Hatsch, D., Leize-Wagner, E., Dupree, P., Dorsselaer, A., Jeltsch, J.-M. (2005). Diversity of the exoproteome of *Fusarium graminearum* grown on plant cell wall. *Current Genetics*. **48** (**6**): 366–379.

Pierleoni, A., Martelli, P., Fariselli, P., Casadio, R. (2006). BaCelLo: a balanced subcellular localization predictor. *Bioinformatics*. **22** (**14**): e408–e416.

Pietro, A., Roncero, M., Roldán, M. (2009). From tools of survival to weapons of destruction: the role of cell wall-degrading enzymes in plant infection. In: Deising, H. (ed.). *Plant Relationships*. Springer. pp. 181–200.

Rogowska-Wrzesinska, A., Bihan, M.-C., Thaysen-Andersen, M., Roepstorff, P. (2013). 2D gels still have a niche in proteomics. *Journal of Proteomics*. **88** (**1**): 4–13.

Saravanan, R., Rose, J. (2004). A critical evaluation of sample extraction techniques for enhanced proteomic analysis of recalcitrant plant tissues. *Proteomics*. **4** (**9**): 2522–2532.

Sato, S., Liu, F., Koc, H., Tien, M. (2007). Expression analysis of extracellular proteins from *Phanerochaete chrysosporium* grown on different liquid and solid substrates. *Microbiology*. **153** (**9**): 3023–3033.

Sergeant, K., Samyn, B., Debyser, G., Beeumen, J. (2005). *De novo* sequence analysis of N-terminal sulfonated peptides after in-gel guanidination. *Proteomics*. **5** (**9**): 2369–2380.

Slippers, B., Wingfield, M. (2007). *Botryosphaeriaceae* as endophytes and latent pathogens of woody plants: diversity, ecology and impact. *Fungal Biology Reviews*. **21** (**2**): 90–106.

Standing, K. (2003). Peptide and protein *de novo* sequencing by mass spectrometry. *Current Opinion in Structural Biology*. **13** (**5**): 595–601.

Tannu, N., Hemby, S. (2007). *De novo* protein sequence analysis of *Macaca mulatta*. *BMC Genomics*. **8** (**1**): 270–279.

Úrbez-Torres, J., Gubler, W. (2009). Pathogenicity of *Botryosphaeriaceae* species isolated from grapevine cankers in California. *Plant Disease*. **93** (**6**): 584–592.

Wang, Y., Wu, J., Park, Z., Kim, S., Rakwal, R., Agrawal, G., Kim, S., Kang, K. (2011). Comparative secretome investigation of *Magnaporthe oryzae* proteins responsive to nitrogen starvation. *Journal of Proteome Research*. **10** (**7**): 3136–3148.

Warwas, M., Yeung, J., Indurugalla, D., Mooers, A., Bennet, A., Moore, M. (2010). Cloning and characterization of a sialidase from the filamentous fungus, *Aspergillus fumigatus*. *Glycoconjugate Journal*. **27** (**5**): 533–548.

Wilson, R., Talbot, N. (2009). Under pressure: investigating the biology of plant infection by *Magnaporthe oryzae*. *Nature Reviews Microbiology*. **7** (**3**): 185–195.

Zhang, J., Xin, L., Shan, B., Chen, W., Xie, M., Yuen, D., Zhang, W., Zhang, Z., Lajoie, G., Ma, B. (2012). PEAKS DB: *de novo* sequencing assisted database search for sensitive and accurate peptide identification. *Molecular & Cellular Proteomics*. **11** (**4**): 1–8.

Zorn, H., Peters, T., Nimtz, M., Berger, R. (2005). The secretome of *Pleurotus sapidus*. *Proteomics*. **5** (**18**): 4832–4838.

CHAPTER 3

PROTEOMIC PROFILE OF *Diplodia corticola* STRAINS WITH DISTINCT VIRULENCE DEGREES

INTRODUCTION

Diplodia corticola A.J.L. Phillips, A. Alves et J. Luque (family *Botryosphaeriaceae*) is considered the most aggressive fungal pathogen involved in the Mediterranean cork oaks' decline (Alves et al., 2004; Linaldeddu et al., 2009; Luque et al., 2000). The decline is multifactorial and characterized by symptoms like branch dieback, foliar chlorosis and vascular necrosis. Besides *Quercus* species (mainly *Q. suber* L. and *Q. ilex* L.), *D. corticola* is also known to infect grapevines (*Vitis vinifera* L.) and eucalypts (*Eucalyptus globulus* Labill.) (Barradas et al., 2015; Carlucci & Frisullo, 2009; Varela et al., 2011), other economically profitable plants. This endophytic fungus is a pathogen, whose virulence usually manifests with the onset of plant stress, exacerbating the disease symptomatology (Slippers & Wingfield, 2007). Since *D. corticola* infection often culminates in plant death, its appearance increasingly entails considerable environmental and socio-economical negative repercussions. Nonetheless, the knowledge about its pathogenesis strategy is still scarce. Few attempts have already been made to understand how the fungus surpasses the natural barriers of their hosts to gain access to the vascular system or even how to control its proliferation (Campanile et al., 2007; Luque et al., 2008; Lynch et al., 2013; Paoletti et al., 2007). Therefore, the molecular network of fungal effectors involved in *D. corticola* infection remains largely unknown. This comprehension is fundamental to clarify how the fungus overcomes the plant immune defence and establishes the interaction with the plant. Understanding this is equally important to develop efficient disease management strategies to protect the cork oak forests.

Proteomic methodologies, such as 2D electrophoresis and *de novo* sequencing, have proved to be essential to investigate the molecular biology of plant-fungal interactions, particularly in organisms whose genome is poorly characterized (Escobar-Tovar et al., 2015; Girard et al., 2013; González-Fernández & Jorrín-Novo, 2012; Rogowska-Wrzesinska et al., 2013). Comparative proteomics offers the possibility to identify the proteins involved in a specific biological condition, highlighting concomitantly proteins that may act as virulence factors, the key elements of an infection process. Proteomics is therefore a crucial discipline to elucidate the molecular mechanisms subjacent to fungal pathogenicity, providing a comprehensive insight into the biology of infection.

Accordingly, the main objective of this study was to perform an extensive comparative analysis of both the secretome and the proteome of two *D. corticola* strains with distinct virulence degrees. Additionally, this work will also contribute for the characterization of a member of the family *Botryophaeriaceae*, a taxonomic group that comprises diverse wood fungal pathogens

(Slippers & Wingfield, 2007), which are poorly studied at both proteomic and genomic levels.

MATERIAL AND METHODS

QUALITATIVE PATHOGENICITY TESTS

Fungal strains and plant seedlings

The *D. corticola* strains used in this experiment were CAA 003 (CBS 112548), CAA 007-1 (CBS112550), CAA 008, CAA 009-1, CAA 009-2, CAA 010, CAA 499 and CAA 500. All cultures were routinely maintained in PDA medium plates (Merck, Germany) at room temperature (± 25 ºC, RT).

The 1-year-old *Q. suber* seedlings were weekly watered and kept at RT under natural light. For the infection assay, only seedlings without foliar symptoms were used.

In planta *inoculations*

The qualitative pathogenicity tests were conducted during 30 days (July 2012) to assess the major virulence differences of *D. corticola* strains. For this, groups of 4 cork oak seedlings were inoculated with one strain. The same number of plants was used as controls. The artificial stem wounds were made with a sterilized scalpel at ± 5-10 cm above the soil line and immediately inoculated with a 0.5 cm diameter mycelium plug from the leading edge of a 6-day-old PDA plate, mycelium facing the stem [adapted from (Linaldeddu et al., 2009)]. The controls were inoculated with a sterile PDA plug under the same experimental conditions and all inoculation points were covered with Parafilm® M (Sigma-Aldrich) to avoid dissecation. The seedlings were weekly watered and visually monitored for crown disease symptoms according to the following disease severity (DS) scale:

- 0 - no foliar symptoms;
- 1 - weak infection (≤ 25% of foliar dehydration and/or necrotic leaves);
- 2 - medium infection (25-50% of foliar dehydration and/or necrotic leaves);
- 3 - severe infection (50-75% of foliar dehydration and/or necrotic leaves);
- 4 - extreme infection (> 75% of foliar dehydration and/or necrotic leaves, or plant death).

SECRETOME AND PROTEOME ANALYSIS

Culture conditions

For the comparative secretome analysis 2 strains of *D. corticola* were used: the avirulent CAA

008 and the virulent CAA 499 (see results section). In both strains the control and infection-like secretomes were analysed. The cultures were routinely maintained in PDA medium plates (Merck, Germany) at room temperature (RT).

Two conditions were tested: control [fungi grown in optimal conditions of nutrients and temperature, as described in Fernandes et al. (2014)] and infection-like conditions (described below).

Briefly, a mycelium plug with 0.5 cm diameter from the leading edge of a 6-day-old PDA plate was inoculated into a 250 mL flask containing 50 mL of Potato Dextrose Broth (PDB), which was statically incubated for 12 days at RT.

For the infection-like secretome the procedure was similar, but a sterilized piece of cork oak stem (± 2g) was added to the PDB. All assays were performed in triplicate.

Culture supernatants were individually collected by filtration, the supernatant pH was measured (pH test strips) and stored at -20ºC until use. The dry-weight of mycelia was determined to evaluate the fungal biomass. For this, filtered mycelia were dried at 37ºC for 3 days before weighting.

The same procedure was repeated, substituting the cork oak piece added to the PDB in the infection-like secretome by 1% (w/v) of carboxymethylcellulose (CMC, Sigma-Aldrich). Liquid cultures were statically maintained at RT for 16 days.

The proteome of *D. corticola* strains CAA 008 and CAA 499 in control and infection-like conditions were analysed. For this, cultures were grown in PDA for 12 days at RT. To stimulate the infection-like proteome, the fungus grew in the presence of a sterilized piece of cork oak stem (± 2g). All assays were performed in triplicate. Mycelia were collected scraping the PDA surface with a sterilized scalpel, placing them immediately at 4ºC. Before storage at -80ºC the wet-weight of mycelia was determined to evaluate the fungal biomass.

Extracellular protein extraction

The extracellular proteins were extracted according to the TCA-Acetone protocol previously optimized (Fernandes et al., 2014), with slight alterations. Thus, after thawing, the culture supernatants were centrifuged at 48400×*g* (1h at 4ºC) to discard the precipitated polysaccharides. One volume of ice-cold TCA/acetone [20%/80% (w/v)] with 0.14% (w/v) DTT was added to the supernatant and incubated at -20ºC (1h). Precipitated proteins were recovered by centrifugation (15000×*g*, 20 min, 4ºC) and excess TCA was removed from the precipitate through successive washes with 2 mL of ice-cold acetone (3×) and 1 mL of ice-cold 80% acetone (v/v, 1×). Afterwards, the protein pellets were cleaned with 2-D Clean-Up kit (GE Healthcare, USA) according to the

manufacturer's instructions. The cleaned proteins were then resuspended in 500 µL of lysis buffer (7 M urea, 2 M thiourea, 4% CHAPS) and quantified before storage at -20ºC.

Intracellular protein extraction

Frozen mycelia were grinded in pre-cooled mortars in the presence of liquid nitrogen. The resulting powder was suspended in 10 mL of 10 mM potassium-phosphate buffer (K_2HPO_4-KH_2PO_4, pH 7.4) containing 0.07% DTT and cOmplete™ protease inhibitor cocktail (Roche, Germany). Samples were then sonicated on an ice bath, in a total of 3 min (cycles of 1s sonication and 2s pause) at 30% intensity (Branson Digital Sonifier), to dissociate the proteins from the cell wall debris. The homogenates were subsequently agitated at 4ºC for 2h and centrifuged at 15000×*g* during 30 min (at 4ºC). The proteins present in the supernatant were precipitated overnight with one volume of ice-cold TCA-acetone [20%/80% (w/v)] with 0.14% (w/v) DTT at -20ºC. The pellet collected by centrifugation (15000×*g*, 20 min at 4ºC) was successively washed with 2 mL of ice-cold acetone (3×) and 1 mL of ice-cold 80% acetone (v/v) (1×). The proteins were purified with 2-D Clean-Up kit (GE Healthcare, USA) according to the manufacturer's instructions, and solubilized in 500 µL of lysis buffer (7 M urea, 2 M thiourea, 4% CHAPS). At last, protein concentration was quantified and samples stored at -20ºC.

Protein quantification

Protein concentration was determined with the Coomassie Plus™ (Bradford) Assay Kit (Thermo Scientific, USA), according to the manufacturer's instructions (microplate protocol). Bovine serum albumin (2 mg/mL) was used as standard and lysis buffer as diluent of the standard dilutions. All assays were performed in triplicate.

1D and 2D electrophoresis

Proteins extracted were separated by SDS-PAGE separation and by 2D-electrophoresis.

For SDS-PAGE analysis, 30 µg of proteins were diluted (1:1) in Laemmli buffer [50 mM Tris-HCl (pH 6.8), 2% (w/v) SDS, 20% (v/v) glycerol, 8.7% β-mercaptoethanol and 0.005% bromophenol blue] and heated for 5 min at 100ºC. Proteins were separated by 12.5% SDS-PAGE gel electrophoresis, according to Laemmli's protocol (Laemmli, 1970), first at 80 V (15 min) and then at 120 V (± 60 min), in a Mini-PROTEAN 3 Cell (Bio-Rad, USA). Precision Plus Protein Unstained Standard (Bio-Rad, USA) was used as protein marker. Staining of secretome samples was performed with Pierce® Silver Stain for Mass Spectrometry (Thermo Scientific, USA) according to the manufacturer's instructions. Cellular proteome samples were fixed [50% (v/v) C_2H_5OH and 2%

(w/v) H_3PO_4] and stained with CBB-250 [34% (v/v) CH_3OH, 3% (w/v) H_3PO_4, 17% (w/v) $(NH_4)_2SO_4$ and 0.2% (w/v) CBB-G250]. The gels' background was removed with 30% (v/v) CH_3OH. Each gel image was acquired with GS-800 calibrated imaging densitometer (Bio-Rad, USA).

For 2D-PAGE, 17 cm IPG strips (pH 3-6 for secretome and pH 3-10 NL for cellular proteome samples, Biorad, USA) were passively rehydrated (16-18 h) with 300 µl of rehydration buffer [7 M urea, 2 M thiourea, 4% CHAPS, 2% DTT and 2% Bio-Lyte® 3/10 Ampholyte (BioRad, USA)] containing 80 µg (secretome) or 400 µg (cellular proteome) of proteins. IEF was performed on BioRad Protean® IEF System (USA) at 20ºC limited to 50 µA/strip according to the following parameters: 1h at 150 V (R), 2h at 500 V (R), 6h 1000 V (L), 3h 10000 V (L) and 10000 V (L) until 40000 Vhr (pH 3-6 strips) or 45000 Vhr (pH 3-10 NL strips). Prior to the second dimension, the IPG strips were reduced and alkylated for 15 min with 1% (w/v) DTT and afterwards with 2.5% (w/v) iodoacetamide in 2.5 mL equilibration buffer [50 mM Tris-HCl (pH 8.8), 6 M urea, 30% (w/v) glycerol and 2% SDS], respectively. After equilibration, the strips were applied to 12.5% lab cast SDS-PAGE gels [running buffer: 25 mM Tris, 192 mM glycine and 0.1% (w/v) SDS (BioRad, USA)] and sealed with 0.5% (w/v) agarose containing traces of bromophenol blue. Electrophoresis proceed on a PROTEAN II xi Cell system (Bio-Rad, USA), at 12 mA/gel (for 45 min) and then at 24 mA/gel until the bromophenol blue reached the bottom of the gel (± 7 h).

Proteins were stained with Pierce® Silver Stain for Mass Spectrometry (Thermo Scientific, USA), according to the manufacturer's instructions, or with CBB-G250. Each gel image was acquired with GS-800 calibrated imaging densitometer (Bio-Rad, USA).

In-gel digestion and mass spectrometry

Silver stained spots were manually excised and destained according to Pierce® Silver Stain for Mass Spectrometry (Thermo Scientific, USA) manufacturer's instructions. Conversely, CBB-G250 stained spots were destained with successive washes of 200 mM NH_4HCO_3/ 50% (v/v) ACN (2×) and 100% ACN (1×). Further, the proteins were enzymatically digested overnight at 37ºC with 0.1 µg/µL Sequencing Grade Modified Trypsin (stock solution, Promega, USA) diluted (1:50) in 50 mM NH_4HCO_3. The resultant tryptic peptides were extracted with 60% (v/v) ACN/ 0.1% (v/v) HCOOH, dried in SpeedVac and resolubilised in 0.1% (v/v) HCOOH. One µl of each peptide sample was applied on an Opti-TOF™ 384 MALDI plate and, once dried, covered with 0.5 mg/mL α-cyano-4-hydroxycinnamic acid (CHCA, Sigma-Aldrich) in 70% (v/v) ACN/ 0.1% TFA (v/v).

The MS spectra were acquired on a 4800 Plus MALDI TOF/TOF Analyser system (Darmstadt, Germany) operated with the 4000 Series Explorer™ software (version 3.5.3.) in reflector positive mode (λ_{laser}=355 nm). Before MS analysis the instrument was calibrated with 4700 Proteomics

Analyzer Mass Standards kit (ABSciex) according to the following peak matching parameters: minimum S/N - 50, mass tolerance - ± 0.5 m/z, minimum peaks to match - 4 and maximum outlier error - 3 ppm. The MS/MS calibration was based on fragments of Glu-fibrinopeptide B.

Protein identification

The peptides were *de novo* sequenced with a combination of two algorithms, PEAKS® 7.0 (Zhang et al., 2012) and DeNovoGUI (Muth et al., 2014). The search parameters included a precursor and fragment mass error tolerance of 0.1 Da (PEAKS) or 0.5 Da (DeNovoGUI), carbamidomethylation (57.02) as fixed modification, and acetylation (N-terminus) (42.01) and methionine, histidine and tryptophan oxidation (15.99) as variable modifications.

Peptide homology search used the FASTM/S algorithm (Mackey et al., 2002) (standard settings, matrix PAM 120) against the UniProtKB Knowledgebase and/or UniProtKB Fungi subset ($E_{value} \leq 0.05$ was considered significant). As soon as the *D. corticola* genome was sequenced (data not shown) the MS/MS spectra were re-searched with MASCOT (Matrix Science, UK), through Global Protein Server Explorer™ (GPS, v3.6, Applied Biosystems), against the protein database derived from the predicted *D. corticola* genes. The search parameters of this analysis included 2 trypsin missed cleavages, MS precursor mass error tolerance of 100 ppm, MS/MS fragment mass error tolerance of 0.25 Da, carbamidomethylation (57.02) as fixed modification, and acetylation (N-terminus) (42.01) and methionine, histidine and tryptophan oxidation (15.99) as variable modifications. The subcellular localization of the identified proteins was deduced using WoLF PSORT predictor (Horton et al., 2007) and the theoretical pI and MW determined with Compute pI/Mw tool available at ExPASy (Gasteiger et al., 2005). Proteins not predicted as extracellular in the secretome fraction were additionally analysed with SecretomeP 2.0 (Bendtsen et al., 2004) to assess their probability to be secreted through an unconventional pathway (proteins with NN score ≥ 0.5 were considered unconventionally secreted).

Gel image analysis

Silver and CBB-250 stained gels analysis was performed with Proteomweaver™ 2-D Analysis Software 4.0 (BioRad). First, the spots were detected using the detection parameter wizard, which adjusts the detection parameters to the intensity, contrast and radius of few selected spots of an average quality gel. Concurrently, the spots were automatically normalized using a pre-match normalization algorithm that sets the intensity of a reference spot to 1 and adjusts the remaining spots accordingly. After spot edition the gels were pair-matched (every gel image was matched to each other) and then multi-matched, extending the pair-match information to the whole

experiment in order to create the so-called superspots. Both matching steps were inspected and the mismatches manually edited. Finally, a precision pair-matched normalization algorithm was computed for further numerical analysis and the average gels were generated. To be included in these artificial representations the spots had to be present in 50% of the group gels. Protein spots that fulfilled the following requirements were considered differentially significant: minimal regulation factor of 2 (up-regulation) or 0.5 (down-regulation), minimal global frequency of 4 out of 6 gels, Student's t-test $p \leq 0.05$ and Mann-Whitney-Wilcoxon test $p=0$. To be considered absent or exclusive of one group condition, the group frequency of a spot should be 0% in one group and 100% in the other.

RESULTS AND DISCUSSION

QUALITATIVE PATHOGENICITY TESTS

Quercus suber disease symptoms induced by *D. corticola* strains were visually monitored for 30 days (July 2012) to qualitatively assess their virulence degrees (Figure 7). Control seedlings remained asymptomatic throughout the experiment (Figure 8 A), as happened in the seedlings inoculated with the strains CAA 008 (Figure 8 B) and CAA 009-2, considered for this reason avirulent. All other strains induced declining symptoms like foliar dehydration, discoloration and necrosis (Figure 8 C-F), even though with distinct magnitudes. The first symptoms caused by these virulent strains appeared few days after fungal inoculation, particularly in the most aggressive strains, CAA 499 and CAA 500 (Figure 7). After 23 days of infection two of the four seedlings

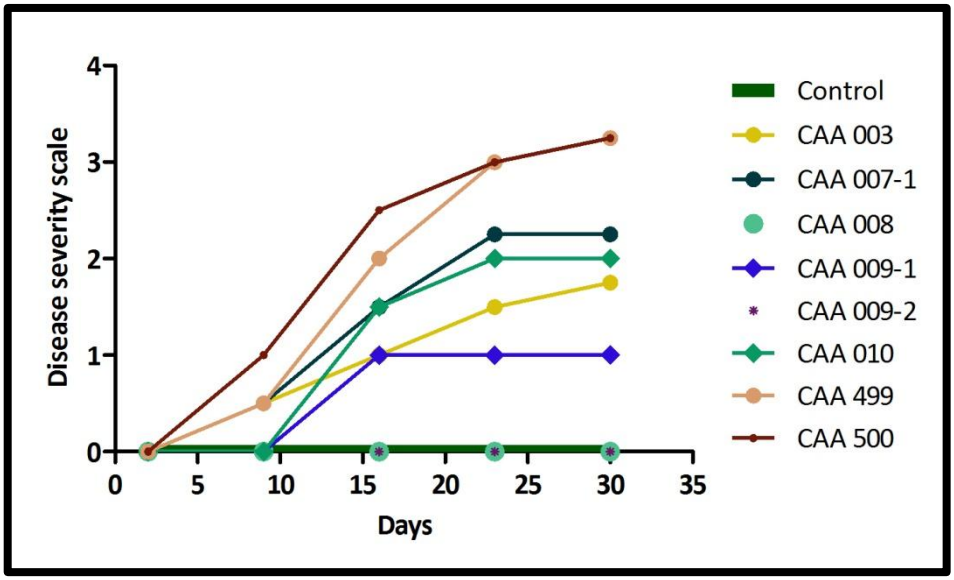

Figure 7 | *Quercus suber* disease severity induced by *D. corticola* throughout 30 days after inoculation. Four biological replicates were used per strain. DS scale: 0 - no foliar symptoms, 1 - weak infection, 2 - medium infection, 3 - severe infection and 4 - extreme infection.

inoculated with CAA 499 strain were dead. Moreover, in all symptomatologic seedlings the dried leaves stayed attached to the branches, even after plant death (Figure 8 G), a phenomenon characteristic of sudden cork oak decline described to occur in natural conditions (Camilo-Alves, 2014). Likewise, Lynch et al. (2013) observed that in *Q. agrifolia* Née *D. corticola* promoted the formation of epicormic shoots below the inoculation point. We also noticed that same phenomena in some seedlings of *Q. suber* (Figure 8 H). Pycnidia reproductive structures were equally visible after 3 weeks of infection (Figure 8 J,K), as previously noticed in similar

Figure 8 | *Quercus suber* declining symptoms caused by artificial *D. corticola* stem infection conducted during 30 days. A - Asymptomatic leaves of a negative control seedling (23 days), B - Asymptomatic leaves of a seedling inoculated with the avirulent strain CAA 008 (23 days), C - Foliar dehydration (CAA 007-1, 23 days), D - Foliar dehydration (CAA 500, 23 days), E - Foliar necrosis (CAA 499, 16 days), F - Foliar necrosis (CAA 003, 23 days), G - Dead seedling inoculated with an aggressive *D. corticola* strain, CAA 499, with the dried leaves attached to the branches (23 days), H - Epicormic shoots sprouting below the inoculation wound (CAA 010, 23 days), I - Sap exudation (CAA 009-1, 16 days), J - Pycnidia formation (CAA 007-1, 23 days), K - Pycnidia formation (CAA 009-1, 23 days).

pathogenicity tests (Linaldeddu et al., 2014, 2009; Luque et al., 2000; Lynch et al., 2013). In addition, one seedling inoculated with CAA 009-1, a mild-virulent strain (Figure 7), reacted to the fungal invasion secreting a sap exudation near the inoculation wound (Figure 8 I), a symptom already observed in the stem bark of some declining oaks (Gallego et al., 1999). Although qualitative, these results are in accordance with other pathogenicity tests performed in oaks, which stated *D. corticola* as an extremely virulent fungus for *Quercus* species (Linaldeddu et al., 2014, 2009; Luque et al., 1999; Lynch et al., 2013; Mullerin, 2013). Furthermore, it was demonstrated that virulence magnitude varies according to the *D. corticola* strain.

This experiment enabled to select strains with different virulence levels that were used in comparative proteomic studies: strain CAA 008 was selected as avirulent and strain CAA 499 as virulent strain.

SECRETOME ANALYSIS

1D evaluation of protein extracts

Proteins were separated by SDS-PAGE to assess the accuracy of protein quantification and to confirm the quality of the extraction (its suitability for 2D analysis). The protein profiles obtained show that the control secretome extraction was efficient (Figure 9 A, D), as happened in the secretome of *D. corticola* grown in the presence of cork oak stem (Figure 9 B, E). These results

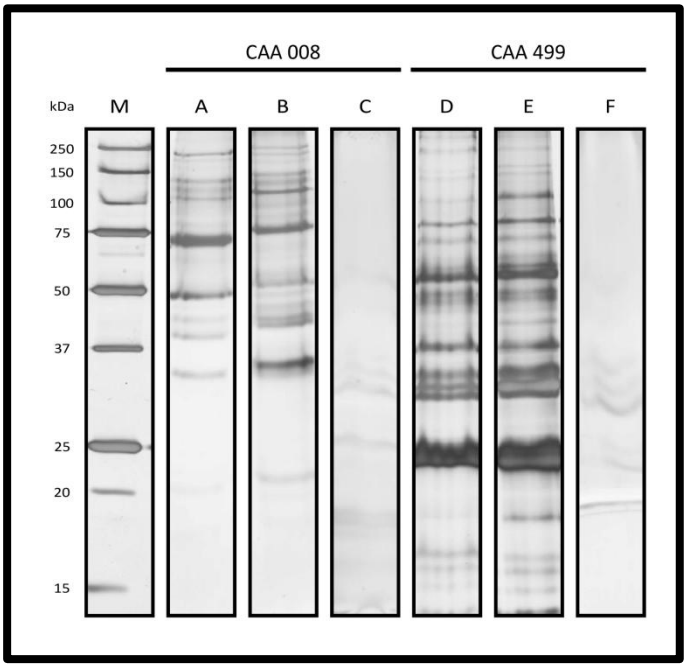

Figure 9 | SDS-PAGE of *D. corticola* extracellular proteins (30 µg). A - CAA 008 control, B - CAA 008 (cork oak stem), C - CAA 008 (CMC), D - CAA 499 control, E - CAA 499 (cork oak stem), F - CAA 499 (CMC), M - Precision Plus Protein Unstained Standard (Bio-Rad, USA). Gels were stained with Pierce® Silver Stain for Mass Spectrometry (Thermo Scientific, USA).

also demonstrate that the 1D protein profile of *D. corticola* avirulent and virulent strains are distinct (Figure 9 A, D). In addition, the electrophoretic separations show that *D. corticola* secretes more proteins in the presence of cork oak stem than CMC (Figure 9 B/C and E/F). This is concordant with the literature. Phalip et al. (2005) showed that *F. graminearum* grown in the presence of glucose secreted significantly less proteins than grown in the presence of hop plant cell wall. Fernández-Acero et al. (2010) studied the *Botrytis cinerea* Pers. response to several carbon sources. These authors demonstrated that the level of protein secretion is directly proportional to the supplement complexity. Fungi seems to secrete more proteins in the presence of complex substrates, such as cork oak stem, a behaviour probably justified by the requirement of a synergistic action of cell wall-degrading enzymes (CWDEs) to degrade the plant cell wall cellulose, hemicellulose, lignin, pectin and, in the case of cork oak, suberin (Jové et al., 2011; Plomion et al., 2001). Since enzyme secretion is an energetically expensive process, when supplemented with simpler carbon sources fungi secretes only the strictly necessary enzymes, adapting the protein secretion to their environment (Girard et al., 2013).

Moreover, CMC affects the viscosity of the protein extracts, which might have compromised the downstream steps of protein extraction, quantification and separation (Figure 9 C and F). Together, these results show that CMC is an ineffective plant mimicker to induce fungal protein secretion, which is in accordance with Cobos et al. (2010), who also evidenced the inefficiency of CMC to influence the *Diplodia seriata* De Not. proteome. Consequently, all comparative analysis performed in this work were based in the secretomes and cellular proteomes induced by cork oak stem.

Control vs. infection-like secretomes of strains with different agressiveness

Extracellular proteins are crucial for fungal plant infection. The identification of these proteins contribute to the discovery of plant-host interactions. In this study we used proteomic tools to characterize the secretome of *D. corticola*.

After protein separation by 2D and visualization with silver staining it was possible to assess the major dissimilarities between the control protein profile and the extracellular response to the cork oak stem added to the culture medium in both *D. corticola* strains studied. In total, we detected an average (± SD) of 116 ± 20 spots in the control secretome of the avirulent strain (Figure 10 A) and 137 ± 13 spots in the virulent strain (Figure 11 A), of which 29 were differentially expressed between CAA 008 and CAA 499 (Table 9). The number of detected spots in the infection-like secretomes increased slightly in both strains, with CAA 008 presenting an average of 145 ± 12 spots (Figure 10 B) and CAA 499 177 ± 13 spots (Figure 11 B). As expected, the

differences are more prominent in the virulent strain. These numbers are higher than the number of protein spots detected in the secretome of *D. seriata* (75 spots), the closest *Botryosphaeriaceae* whose proteome was studied (Cobos et al., 2010). In fact, low protein detection rates are usual among filamentous fungi secretomes (Abbas et al., 2005; Cao et al., 2009; Espino et al., 2010), a characteristic inherent to their behavior *in vitro*, namely the reduced protein secretion and the concomitant production of mucilaginous extracellular polysaccharides that hampers the separation (Girard et al., 2013). The efficiency of the extraction protocol and the sensitivity of the silver staining used in this work certainly contributed to the high amount of detected spots.

Despite all the constraints associated to protein identification in organisms with unsequenced genomes, we were able to identify the majority of extracellular proteins just with *de novo* sequencing (Table 4 and Table 5). This approach encompassed two algorithms, PEAKS® 7.0 (Zhang et al., 2012) and DeNovoGUI (Muth et al., 2014), a combination that greatly improved the overall rate of peptide sequencing. Together, they can bridge the sequencing shortcomings of each other, particularly in the MS/MS spectra with poorer quality, a process that nevertheless requires substantial manual interpretation, being for this reason extremely laborious and time-consuming. Further, as *D. corticola* genome was recently sequenced (data not shown) it was possible to re-search the MS/MS data against the protein database derived from the predicted fungus genes. The results obtained corroborated the identifications achieved before by *de novo* sequencing, contributing in some cases to the identification of spots undisclosed in the first approach (Table 4 and Table 5, spots 7, 10, 48, 49 and 58). Accordingly, we confirmed that MS/MS analysis may take advantage of the conjugation of various *de novo* sequencing, as well as database search algorithms, to improve and validate the obtained results. Actually, some authors had previously stated that due to the distinct characteristics of *de novo* sequencing and database search approaches, their results consonance confers *per se* a definite validation (Ma & Johnson, 2012; Sadygov et al., 2004).

Hence, considering the restricted genomic characterization of the *Botryosphaeriaceae* family, the extracellular protein identification rate was rather noteworthy (Table 3). We identified mainly hydrolases (56% in CAA 008 and 51% in CAA 499) and proteases (27% in CAA 008 and 31% in CAA 499), a functional distribution previously observed in Fernandes et al. (2014). Most of the identified proteins displayed homology with the fungi *Macrophomina phaseolina* (Tassi) Goid. and *Neofusicoccum parvum* (Pennycook & Samuels) Crous, Slippers et A.J.L. Phillips (Table 4 and Table 5), both taxonomically close to *D. corticola* (Liu et al., 2012), adding thus confidence to the identification results. Further, their theoretical pI ranged between 4.04 and 6.32, and the MW

betweeen 14.1 and 110.6 kDa (Table 4 and Table 5), which generally corresponded to the spot position on the gels (Figure 10 and Figure 11). Likewise in other fungi (Escobar-Tovar et al., 2015; Li et al., 2012), *D. corticola* has several spots identified as being the same protein, diverging in pI and/or MW. For instance, GH 31 was identified in 4 different spots (46, 47, 50 and 57), peptidase

Table 3 | Number of extracellular proteins identified in *D. corticola* strains CAA 008 and CAA 499.

	CAA 008	**CAA 499**
Hydrolases	42	41
Proteases	20	25
Oxidoreductases	2	2
Other funtions	10	11
Unknown	1	1
No. of proteins identified	75	80
No. of spots identified	67	72

A1 in 8 spots (18, 19, 21, 22, 35, 59, 137 and 148), peptidase M35 in 7 spots (3, 99, 104, 111, 112, 117, 126) and spherulation-specific family 4 in 3 spots (4, 6 and 71) (Figure 10 and Figure 11). This is usually an indicator of different protein isoforms or proteins altered by post-translational modifications (PTMs), such as glycosylation, acetylation, phosphorylation or even truncation (Rabilloud & Lelong, 2011; Rogers & Overall, 2013; Rogowska-Wrzesinska et al., 2013). The modified and unmodified proteins are predominantly distributed in juxtaposed horizontal series of spots along the 2D gels, as a consequence of the slight pI shifts induced by the modification addition or removal of electric charge (Rogowska-Wrzesinska et al., 2013). Conversely, vertical shifts like the existent between spots 18 and 59 (peptidase A1, Figure 10 and Figure 11) denote, for example, the existence of truncation, an irreversible proteolytic cleavage that produces shorter polypeptides with new or modified biological activities (Rogers & Overall, 2013). The vertical spot distribution might similarly demonstrate the ocurrence of protein degradation events in the secretome of *D. corticola* (Rogowska-Wrzesinska et al., 2013).

The extracellular localization of the proteins was confirmed with WoLF PSORT subcellular predictor (Horton et al., 2007), with the exception of β-1,3-glucanase protein (GH 64, spot 24), predicted as nuclear, alcohol dehydrogenase (spot 7), fumarylacetoacetase (spot 31) and cell wall protein (spot 127), predicted as cytoplasmic (ca. 4.5%, Table 4 and Table 5). In fact, the identification of intracellular proteins in the secretome fraction is recurrent among filamentous fungi studies (Adav et al., 2015; Cobos et al., 2010; Lu et al., 2010; Wartenberg et al., 2011), a pattern commonly justified by the occurrence of cell lysis during fungal growth or even during protein sample extraction. Nonetheless, the absence of housekeeping intracellular proteins in *D. corticola* secretome reinforces the contrary, the hypothesis that proteins lacking conventional

secretion signal motifs might also be secreted (Paper et al., 2007). A growing number of studies has actually confirmed the secretion of known intracellular fungal proteins without the classical N-terminal secretory signal peptides, though their extracellular functions or even their role in pathogenesis are not fully understood (Girard et al., 2013; Moore et al., 2002; Paper et al., 2007; Rolke et al., 2004; Wegener et al., 1999). Besides, several alternative secretion pathways were concurrently demonstrated in fungi (Shoji et al., 2014), namely the unconventional secretion of the *Ustilago maydis* (DC.) Corda endochitinase Cts1, a protein that does not contain a signal peptide and whose secretion is independent of both endoplasmic reticulum and Golgi apparatus, two organelles involved in the conventional secretory pathway (Shoji et al., 2014; Stock et al., 2012). In order to verify if the predicted intracellular proteins above mentioned are secreted through an unconventional secretory pathway we analysed their sequence with SecretomeP predictor (Bendtsen et al., 2004). The results obtained substantiate the high probability of β-1,3-glucanase protein (NN score=0.762), fumarylacetoacetase (NN score=0.519) and cell wall protein (NN score=0.561) contain a non-classical signal peptide that mediates their secretion through an alternative pathway. Conversely, Secretome P does not corroborate the secretion of the cytoplasmic alcohol dehydrogenase, although its NN score (0.473) is relatively close to the 0.5 threshold. According to Agrawal et al. (2010) the score outputs of such prediction programs should be regarded just as guidelines due to their data set limitations, whereby the protein might still be secreted. Alcohol dehydrogenase was equally identified in the secretome of *Aspergillus fumigatus* Fresen., wherein it was postulated as being a lignin degrading enzyme (Adav et al., 2015), a role also plausible in *D. corticola* since the protein is constitutively secreted in both strains (Table 9 and Table 10, Appendix I). Hence, these evidences support the presence of proteins hitherto known only by its intracellular functions in the *D. corticola* secretome. We can also suggest that their translocation to the extracellular space occurs presumably through unconventional secretory pathways.

Subsequently, we compared the protein profiles of the control and infection-like conditions to assess their differentially expressed proteins, a fundamental step to highlight the proteins that may behave as virulence factors during fungal pathogenesis. According to this analysis the spot 24, which includes the proteins neuraminidase and β-1,3-glucanase (GH 64, CAZy), is overexpressed in the avirulent infection-like secretome (4.9-fold up, p=0.0011) (Figure 10 and Table 4), while in the virulent strain the expression levels are not significantly different between control and infection-like profiles (Figure 11 and Table 5). Neuraminidase, found as well in spots 12 and 53 (Figure 10 and Figure 11), is a widespread exo-glycosidase that cleaves the sialic acid residues of glycoconjugates, which are probably used afterwards as a carbon source for fungal

growth (Monti et al., 2002; Warwas et al., 2010). Adding to the nutritional fulfilment, neuraminidase was ascertained to play a substantial role in viral and bacteria virulence (Burnaugh et al., 2008; Roy et al., 2011; Yondola et al., 2011), although this function has not yet been clarified in fungi. Still, the protein was recently identified in the secretomes of two other plant-pathogenic fungi, *Verticillium albo-atrum* Reinke et Berthold and *Mycosphaerella graminicola* (Fuckel) J. Schröt. (Amaral et al., 2012; Mandelc & Javornik, 2015), having also been sequenced in the genomes of the *Botryosphaeriaceae* fungi *M. phaseolina*, *N. parvum* and *D. seriata* (Blanco-Ulate et al., 2013; Islam et al., 2012; Morales-Cruz et al., 2015). Neuraminidase certainly assists the glycoside hydrolases of these phytopathogens to disrupt the plant cell wall during host invasion. On the other hand, the pathogenic ability of the fungal β-1,3-glucanase is better studied than in neuraminidase (Cao et al., 2009; Fu et al., 2013; Huser et al., 2009). β-glucanases are primarily recognized by the glucose mobilization for carbon and energy metabolism during fungal cell wall growth (Martin et al., 2007). Thus, considering the active role of neuraminidase and of β-1,3-glucanase (spot 24) in the lignocellulose hydrolysis, the gel analysis suggests that, conversely to the virulent strain, the avirulent strain increases its secretion levels to assimilate the nutrients from the supplemented cork oak stem.

Further, it was identified another β-1,3-glucanase (GH 55, CAZy) in the spots 39, 40, 42 and 43 (Figure 10 and Figure 11), which are more prevalent in the avirulent strain. The gels comparison demonstrated that in the control secretome 3 of the 4 spots were downregulated in the virulent strain (spot 39: 5.1-fold down, p=0.0102; spot 40: 5.2-fold down, p=0.0221; spot 43: 7.6-fold down, p=0.0213; Figure 16 and Table 9, Appendix I), occurring the same in the infection-like secretome (spot 39: 4.9-fold down, p=0.0348; spot 42: 5.2-fold down, p=0.0184; spot 43: 4.2-fold down, p=0.0202; Figure 17 and Table 10, Appendix I). Although the horizontal distribution indicates that the four GH 55 identified spots might be isoforms or post-translational modified proteins, the analysis confirmed that the overall expression of this hydrolase is lower in the virulent strain. Known by its exo- and endo-β-1,3-glucanase activity, this enzyme displays as well pectinolityc activity due to its pectin lyase domain, being therefore intrinsically associated to polysaccharide metabolism. However, since pectin is a minor compound of the cork cell wall (ca. 1.5%) in comparison with lignin (ca. 25%) or suberin (ca. 40%) (Pinto et al., 2009; Rocha et al., 2000), the virulent strain seems to have adapted the GH 55 enzyme expression to its host cell wall composition. On the contrary, the avirulent strain maintains a basal expression of the protein, probably increasing its levels if the pectin content of the substrate is higher than in cork oak.

Intriguingly, the pectate lyase detected (spot 113, Figure 11 and Table 5) follows a divergent trend. Although the differences between the average intensities (Avg) of the infection-like and

control secreted pectate lyase were not statistically significant, the virulent strain responds positively to the host mimicry ($Avg_{Control}$=0.305 and $Avg_{Infection\text{-}like}$=0.624), while the avirulent pectate lyase expression is, in general, lower than in the virulent strain (Figure 16 and Figure 17, Appendix I). Acting both on esterified polysaccharides, the dissimilarities of pectin and pectate lyase active sites have further implications in their substrate selection, with pectin lyases prefering highly methyl-esterified substrates and pectate lyases subtrates with lesser esterification degrees (Brink & Vries, 2011). Constituted by slightly branched polymers of arabinose residues (Rocha et al., 2000), the chemical composition of cork cell wall pectic polysaccharides might justify the presence of pectate lyase in the secretome of the virulent strain. In accordance, Biswal et al. (2014) demonstrated that even when pectin is a minor wood constituent, as happens in cork oak stem tissues, the aspen pectate lyase improves the lignocellulose saccharification yield, increasing then the solubility of the wood polysaccharides. Moreover, the upregulation of this enzyme in lethal isolates of *V. albo-atrum* compared to mild isolates was equally corroborated by Mandelc & Javornik (2015), having been implied its hypothetical contribution for the plant vascular system colonization. Therefore, these evidences suggest that the most agressive *D. corticola* strain has adjusted its set of extracellular proteins to the *Q. suber* cell wall characteristics, gaining advantage over the avirulent strain during the host colonization. Conversely, the latter seems to secrete a diverse set of proteins that allow the fungus to easily adapt to substrates with different chemical compositions.

Accordingly, the virulent strain should secrete other enzymes that enhance its capacity to deconstruct the cork tissues and/or pierce the host leaves. For example, proteins such as lipases are widely recognized as fungal pathogenicity factors due to their ability to hydrolize the lipids present in the host tissues into glycerol and free fatty acids (Blümke et al., 2014; Gaillardin, 2010; Subramoni et al., 2010; Voigt et al., 2005). Remarkably, the 2 spots identified as lipases (25 and 110) in *D. corticola* were found exclusively in the CAA 499 secretomes (Figure 16 and Figure 17, Appendix I). However, the relative steadiness of lipase spot intensities in response to cork oak stem (spot 110 $Avg_{Control}$=0.168 and $Avg_{Infection\text{-}like}$=0.192, Figure 11) suggests that the protein is constitutively secreted. Further, acting solely in water-insoluble esters bonds the lipases work in synergy with esterases, responsible for the cleavage of water-soluble ester bonds, being for this reason also regarded as fungal pathogenicity factors (Biely, 2012; Fojan et al., 2000). Together they contribute to the fulfilment of the fungal nutritional needs during host invasion, while they promote the adhesion and permeation of plant tissues (Pietro et al., 2009). Among the extracellular esterases identified in *D. corticola* are a carboxylesterase (spot 48), two ferulic acid esterases (spots 23 and 103) and three phosphoesterases (spots 28, 29 and 56) (Figure 10 and

Figure 11). In particular, ferulic acid esterases drew attention, since the suberized cork cell walls are structurally composed by ferulic acid, an hydroxycinnamic acid that represents ca. 9% of the total suberin monomers of *Q. suber* trees (Graça, 2010). However, contrary to what was expected, the CAA 499 ferulic acid esterase expression decreased in response to the host mimicry (spot 23: 2-fold down, p=0.0406; spot 103: 5-fold down, p=0.0202; Figure 11), being nevertheless higher than the CAA 008 infection-like expression (spot 23: 21.8-fold up, p=0.0015; spot 103: 5-fold up, p=0.0423; Figure 17, Appendix I). Such result indicates that the enzyme is constitutively secreted, but for unknown reasons its expression is slightly repressed when the virulent strain is exposed to cork oak stem.

Furthermore, fungal host colonization benefits of proteases' involvement, not only to protect the fungus against plant defenses, but also to mobilize nitrogen sources required for the hyphal growth (Faulkner & Robatzek, 2012; Fernandez et al., 2014; Girard et al., 2013; Pietro et al., 2009). Considering this, neutral protease 2 (peptidase M35, a Zn^{2+} metalloendopeptidase), also known as deuterolysin, was one of the proteases highlighted by the comparative gel analysis due to the substantial expression dissimilarities existent between the two strains. Among the spots identified in CAA 499 as being deuterolysin (3, 99, 104, 111, 112, 117, 126), only spot 3 was detected in CAA 008 (Figure 16 and Figure 17, Appendix I). In addition, spots 111 and 112 were absent in the CAA 499 infection-like secretome (Figure 11), which might then be proenzymes that become active in the presence of cork oak stem. Although previously detected in the secretome of other phytopathogenic fungi (Amaral et al., 2012; Collins, 2013; Espino et al., 2010; Li et al., 2012), this is the first time that an unbalanced distribution of peptidase M35 between two strains with distinct virulence degrees was demonstrated, highlighting it as a potential virulence factor of *D. corticola*. So far, only a bacterial member of the M35 family (AsaP1) was confirmed to be a virulence factor (Arnadottir et al., 2009), despite the numerous suggestions that proteins belonging to this metalloprotease family have an active role in fungal infections (Guyon et al., 2014; Li & Zhang, 2014; Monod et al., 2002). Consequently, the implications of the peptidase M35 prevalence in the *D. corticola* virulent strain should be further investigated to assess its effective contribution to fungal pathogenicity. In addition, the virulent strain secretes another Zn^{2+} metalloprotease (peptidase M43, spot 136) that is absent in the CAA 008 strain (Figure 17 and Table 10, Appendix I) and whose expression is up-regulated in the infection-like secretome (6.9-fold up, p=0.0053, Figure 11). Although there are few reports correlating the proteolytic activity of peptidase M43 family proteins with fungal virulence (Lu et al., 2009), in bacteria such association was already established. For instance, Hesami et al. (2011) indicated that the M43 cytophagalysin may be implicated in the *Flavobacterium psychrophilum* (Bernardet and Grimont 1989) Bernardet

et al. pathogenesis, causing host tissue necrosis. The results obtained in this work suggest that the peptidase M43 might be also relevant for *D. corticola* virulence, due to its uniqueness in the virulent strain and to the upregulation induced by the host mimicry.

Besides the lytic enzymes already mentioned, plant pathogenic fungi secrete other effectors that promote the host invasion, contributing for instance to fungal attachment, cell wall permeation or to the induction of disease symptoms. Cerato-platanin, found in spot 1 along with an extracellular guanyl-specific ribonuclease protein, raised especial attention because its expression in the virulent strain increased in response to the supplemented cork oak stem (2.2-fold up, p=0.0013, Figure 11 and Table 5), and also because there is growing evidence about the participation of this protein family in the fungal infection of plants (Baccelli, 2014; Pazzagli et al., 2014). Indeed, these small cysteine-rich non-proteolytic proteins have numerous roles in the infectious interface. For example, cerato-platanins are able to block the plant-fungus recognition, scavenging the chitin fragments or its N-acetylglucosamine monomers, which function as invasion patterns according to the recent invasion model of plant-microbe interactions (Barsottini et al., 2013; Cook et al., 2015; Frischmann et al., 2013; Pazzagli et al., 2014). On the other hand, there are indications that the cerato-platanins can be noticed as invasion patterns itself, eliciting plant defence events such as the generation of ROS and nitric oxide or the transcription of defense-related genes early after the plant recognition (Baccelli et al., 2014a, 2013; Frías et al., 2013; Lombardi et al., 2013; Pazzagli et al., 2014). Accordingly, Frías et al. (2014) reported that the *B. cinerea* cerato-platanin BcSpl1 cause cellular morphological alterations after the association to the plant plasma membrane, inducing subsequent macroscopic tissue necrotic lesions. Further, when localized on the fungal cell wall the expansin-like activity of cerato-platanins contribute to its remodelling and enlargement, ensuring the hyphal growth necessary for a successful host colonization (Baccelli, 2014; Gaderer et al., 2014). Nonetheless, the expansin-like activity of cerato-platanins might be even more important for the fungal virulence due to the ability to loosen the plant cellulose barrier, which facilitates the hyphal mechanical perforation during host colonization and the later fungal spread on dead plant tissues (Baccelli et al., 2014b; Baccelli, 2014; Barsottini et al., 2013). Therefore, the CAA 499 cerato-platanin upregulation registered *in vitro* in response to host exposition demonstrates that this protein may indeed act as a fungal effector during *D. corticola* infection, a role that should be validated in future *in planta* experiments.

Further, *D. corticola* secretome still contains another necrotic elicitor, the necrosis inducing protein (spot 7, Figure 10 and Figure 11), but we did not find significant differences between the control and infection-like profiles. Nevertheless, the average spot intensities imply a clear

prevalence of this protein in the secretome of the virulent strain (Control: $Avg_{CAA\ 008}$=0.107 and $Avg_{CAA\ 499}$=0.611, infection-like: $Avg_{CAA\ 008}$=0.127 and $Avg_{CAA\ 499}$=1.537, Figure 16 and Figure 17, Appendix I). The absence of statistical differences might be related to the spot intensity variability existent between the replicates of each group. Thus, similarly to cerato-platanin, the necrotic activity of this hypothetical *D. corticola* effector should be studied to assess its relevance for the fungal infectious process.

To summarize, we performed an extensive characterization of the secretome of two *D. corticola* strains with distinct virulence degrees and evaluated their response to the *in vitro* host mimicry. The resultant data suggests that the virulent strain has indeed adjusted its set of extracellular proteins to the host environment, making the fungus more competitive at the infectious interface than the avirulent strain. Nevertheless, the relevance of the proteins highlighted in this work should be further validated, in order to reveal their role in the molecular interactions of the *D. corticola* pathosystem. Moreover, we corroborated the usefulness of the comparative proteomic approach for the detection of potential virulence effectors, and demonstrated that the *de novo* sequencing still has a niche in the contemporary proteomics.

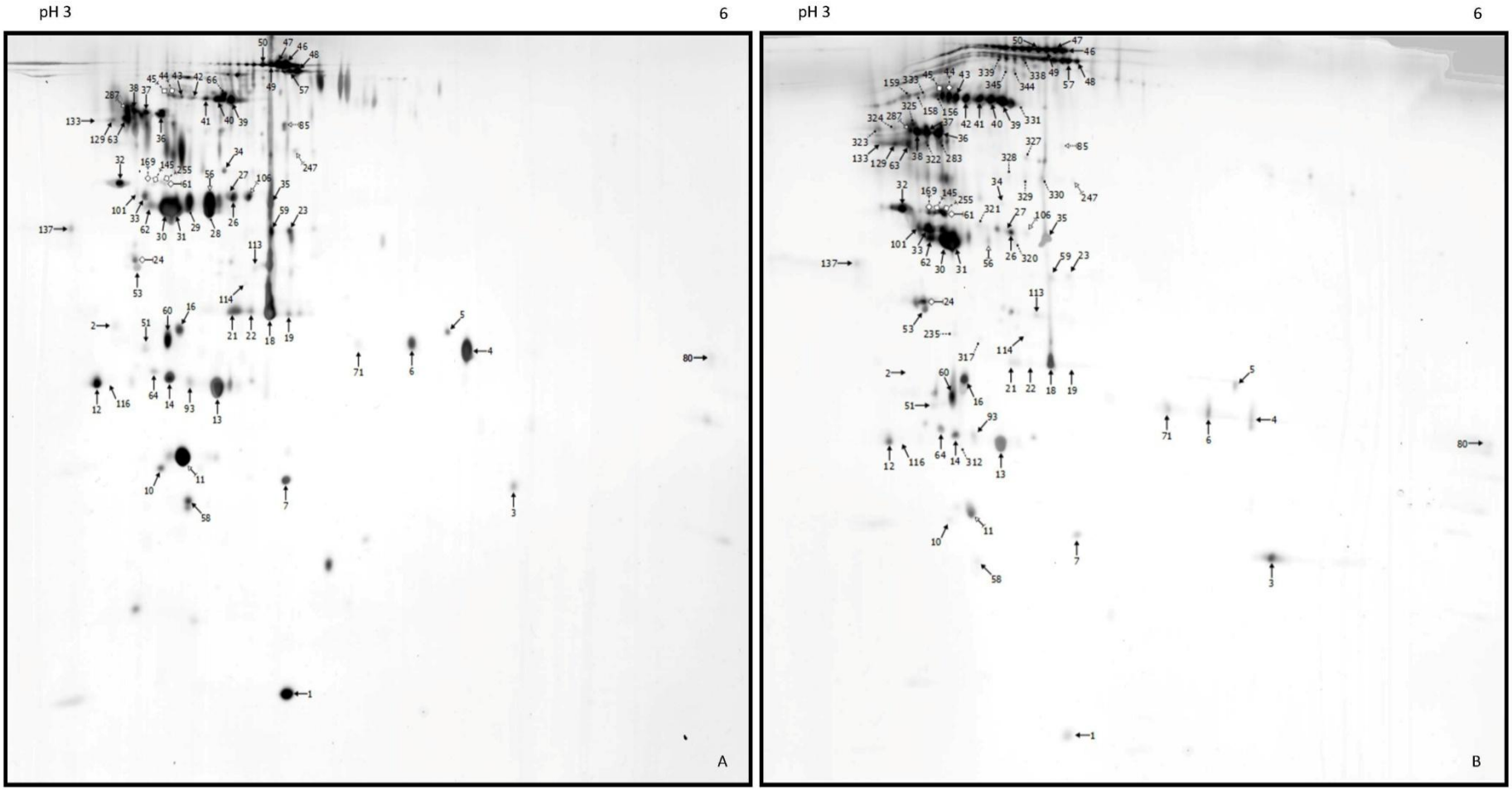

Legend:
- Spots common to both groups
- Up-regulated spots (identified)
- Up-regulated spots (non-identified)
- Down-regulated spots (identified)
- Down-regulated spots (non-identified)
- Spots exclusive of one of the groups (identified)
- Spots exclusive of one of the groups (non-identified)

Figure 10 | 2D average gels of control (A) and infection-like (B) secretomes of the *D. corticola* avirulent strain CAA 008. Three biological replicates were used for each condition. Gels were stained with Pierce® Silver Stain for Mass Spectrometry (Thermo Scientific, USA). Protein spots identified by *de novo* sequencing and/or MASCOT search are marked with filled arrow lines and the identifications are summarized in Table 4.

Table 4 | Summary of the extracellular proteins identified in CAA 008 EXT control and CAA 008 EXT infection-like by *de novo* sequencing (1) and/or MASCOT search (2). Theoretical pI and MW (3) were searched with Compute pI/Mw tool available at ExPASy (Gasteiger et al., 2005) and the subcellular localization (4) deduced with WoLF PSORT predictor (Horton et al., 2007).

Protein	Spot	Accession number	Organism	FASTM/S E_{value}[1]	MASCOT total Ion Score[2]	Theoretical pI[3]	Theoretical Mw[3] (Da)	Subcellular localization[4]
Spots exclusive of CAA 008 EXT control								
Hydrolases								
Phosphoesterase	28	K2RUW5	*Macrophomina phaseolina*	5.90E-29	485	4.64	43928.97	Extracellular
	29	K2RUW5	*Macrophomina phaseolina*	8.80E-03	151	4.64	43928.97	Extracellular
Proteases								
Peptidase S10 - Putative carboxypeptidase s1 protein	29	R1GF60	*Neofusicoccum parvum*	5.50E-16	80	4.45	52146.52	Extracellular
Spots down-regulated in CAA 008 EXT infection-like								
Hydrolases								
Phosphoesterase	56	K2RUW5	*Macrophomina phaseolina*	3.00E-15	—	4.64	43928.97	Extracellular
Oxidoreductases								
Putative ligninase lg6 protein (Peroxidase)	11	R1GJT0	*Neofusicoccum parvum*	5.30E-32	512	5.20	32232.20	Extracellular
Spots up-regulated in CAA 008 EXT infection-like								
Hydrolases								
GH 64 - Putative glucanase b protein (β-1,3-glucanase)	24	R1GK17	*Neofusicoccum parvum*	0.00E+00	327	5.82	42116.55	Nuclear
Neuraminidase (Sialidase)	24	K2RBR1	*Macrophomina phaseolina*	9.30E-11	—	4.32	40074.67	Extracellular
Unknown								
Uncharacterized protein	61	K2RWL4	*Macrophomina phaseolina*	6.80E-28	209	4.34	52231.60	Extracellular

Continued on next page

Protein	Spot	Accession number	Organism	FASTM/S E_{value}[1]	MASCOT total Ion Score[2]	Theoretical pI[3]	Theoretical Mw[3] (Da)	Subcellular localization[4]
Spots common to both control and infection-like								
Hydrolases								
Carboxylesterase family protein	48	DCO1_40s06646.t1	*Diplodia corticola*	—	76	4.68	61064.17	Extracellular
GH 13 - Putative α-amylase a type-1,2 protein	62	R1GPA2	*Neofusicoccum parvum*	0.00E+00	373	4.53	56053.14	Extracellular
	101	K2QLM3	*Macrophomina phaseolina*	4.00E-31	—	4.73	54649.73	Extracellular
GH 15 - Glucoamylase	63	C0NJV0	*Ajellomyces capsulatus*	0.00E+00	490	5.32	70492.86	Extracellular
	129	R1GLG1	*Neofusicoccum parvum*	1.60E-14	—	4.83	68531.74	Extracellular
	133	Q9C1V4	*Talaromyces emersonii*	3.00E-27	—	4.44	65429.22	Extracellular
GH 17 - Glycoside hydrolase family 17	13	K2STT8	*Macrophomina phaseolina*	0.00E+00	363	4.55	32022.55	Extracellular
	51	K2STT8	*Macrophomina phaseolina*	2.30E-07	64	4.55	32022.55	Extracellular
	53	K2STT8	*Macrophomina phaseolina*	2.30E-07	130	4.55	32022.55	Extracellular
	93	K2STT8	*Macrophomina phaseolina*	2.30E-07	—	4.55	32022.55	Extracellular
	114	K2STT8	*Macrophomina phaseolina*	5.20E-03	—	4.55	32022.55	Extracellular
GH 31 - Putative α-glucosidase protein	46	R1H1X1	*Neofusicoccum parvum*	0.00E+00	321	4.65	110578.06	Extracellular
	47	R1H1X1	*Neofusicoccum parvum*	0.00E+00	330	4.65	110578.06	Extracellular
	50	R1H1X1	*Neofusicoccum parvum*	2.40E-07	—	4.65	110578.06	Extracellular
	57	R1H1X1	*Neofusicoccum parvum*	0.00E+00	260	4.65	110578.06	Extracellular
GH 43 - Putative glycoside hydrolase family 43 protein	14	R1EDI8	*Neofusicoccum parvum*	5.70E-07	242	4.48	37269.32	Extracellular
	26	R1GE80	*Neofusicoccum parvum*	2.00E-09	169	5.73	48185.65	Extracellular
	27	R1GE80	*Neofusicoccum parvum*	1.30E-18	315	5.73	48185.65	Extracellular
	64	R1EDI8	*Neofusicoccum parvum*	3.60E-04	144	4.48	37269.32	Extracellular
GH 55 - Putative glycoside hydrolase family 55 protein	39	R1EP88	*Neofusicoccum parvum*	0.00E+00	529	4.52	84093.46	Extracellular
	40	R1EP88	*Neofusicoccum parvum*	0.00E+00	548	4.52	84093.46	Extracellular
	42	R1EP88	*Neofusicoccum parvum*	0.00E+00	529	4.52	84093.46	Extracellular
	43	R1EP88	*Neofusicoccum parvum*	1.90E-21	195	4.52	84093.46	Extracellular

Continued on next page

Protein	Spot	Accession number	Organism	FASTM/S E_{value}[1]	MASCOT total Ion Score[2]	Theoretical pI[3]	Theoretical Mw[3] (Da)	Subcellular localization[4]
GH 71 - Glycoside hydrolase family 71	32	K2R498	*Macrophomina phaseolina*	5.50E-17	250	4.84	49264.81	Extracellular
GH 93 - Putative glycoside hydrolase family 93 protein (Sialidase/ Neuraminidase)	12	R1GGQ9	*Neofusicoccum parvum*	1.40E-07	180	4.41	38051.25	Extracellular
	53	K2RBR1	*Macrophomina phaseolina*	0.00E+00	126	4.32	40074.67	Extracellular
Putative 5,3-nucleotidase protein	2	R1FUS1	*Neofusicoccum parvum*	3.70E-18	—	4.58	31154.86	Extracellular
Putative ferulic acid esterase protein	23	R1EDH3	*Neofusicoccum parvum*	1.50E-13	32	4.79	34891.92	Extracellular
Putative glutaminase protein	36	R1EUG4	*Neofusicoccum parvum*	6.40E-32	263	4.29	74937.86	Extracellular
	37	R1EUG4	*Neofusicoccum parvum*	0.00E+00	225	4.29	74937.86	Extracellular
	38	R1EUG4	*Neofusicoccum parvum*	0.00E+00	263	4.29	74937.86	Extracellular
	49	DCO1_62s08886.t1	*Diplodia corticola*	—	64	4.27	76639.88	Extracellular
Uncharacterized protein (fumarylacetoacetase)	31	A0A072PA62	*Exophiala aquamarina*	4.60E-26	—	5.84	46110.07	Cytoplasmic
Proteases								
Peptidase A1 - Putative a chain endothiapepsin	18	R1ESA5	*Neofusicoccum parvum*	0.00E+00	491	5.45	42563.05	Extracellular
	19	R1ESA5	*Neofusicoccum parvum*	4.20E-10	71	5.45	42563.05	Extracellular
	21	R1ESA5	*Neofusicoccum parvum*	0.00E+00	228	5.45	42563.05	Extracellular
	22	R1ESA5	*Neofusicoccum parvum*	1.90E-04	34	5.45	42563.05	Extracellular
	35	R1ESA5	*Neofusicoccum parvum*	0.00E+00	491	5.45	42563.05	Extracellular
	59	R1ESA5	*Neofusicoccum parvum*	4.30E-10	491	5.45	42563.05	Extracellular
	137	R1GM42	*Neofusicoccum parvum*	1.60E-08	—	4.27	41788.15	Extracellular
Peptidase M28 - Putative leucyl aminopeptidase protein	5	R1GBR8	*Neofusicoccum parvum*	1.20E-23	222	5.17	40706.16	Extracellular
Peptidase M35 - Neutral protease 2	3	K2SDQ0	*Macrophomina phaseolina*	1.20E-25	124	5.34	36981.99	Extracellular

Continued on next page

Protein	Spot	Accession number	Organism	FASTM/S E_{value}[1]	MASCOT total Ion Score[2]	Theoretical pI[3]	Theoretical Mw[3] (Da)	Subcellular localization[4]
Peptidase S10 - Putative carboxypeptidase s1 protein	30	R1GF60	*Neofusicoccum parvum*	0.00E+00	486	4.45	52146.52	Extracellular
	31	R1GF60	*Neofusicoccum parvum*	0.00E+00	668	4.45	52146.52	Extracellular
	34	R1GF60	*Neofusicoccum parvum*	0.00E+00	485	4.45	52146.52	Extracellular
	41	R1GF60	*Neofusicoccum parvum*	1.50E-14	112	4.45	52146.52	Extracellular
	62	R1GF60	*Neofusicoccum parvum*	4.40E-28	345	4.45	52146.52	Extracellular
	101	R1GF60	*Neofusicoccum parvum*	1.30E-32	—	4.45	52146.52	Extracellular
Peptidase S8 - Putative peptidase s8 s53 subtilisin kexin sedolisin protein	16	R1G6D0	*Neofusicoccum parvum*	0.00E+00	478	4.18	43069.94	Extracellular
	80	R1GM11	*Neofusicoccum parvum*	6.50E-11	—	6.07	39070.39	Extracellular
	116	R1EAW3	*Neofusicoccum parvum*	4.80E-02	—	4.73	40860.15	Extracellular
Oxidoreductases								
Alcohol dehydrogenase	7	DCO1_41s07359.t1	*Diplodia corticola*	—	50	6.32	40875.57	Cytoplasmic
Other functions								
Cell wall protein	10	DCO1_41s07341.t1	*Diplodia corticola*	—	173	4.48	21235.80	Extracellular
Cerato-platanin	1	E3QKQ8	*Colletotrichum graminicola*	6.90E-11	—	4.53	14119.72	Extracellular
Ferritin/ribonucleotide reductase-like protein	60	K2RIV9	*Macrophomina phaseolina*	0.00E+00	132	4.61	30766.62	Extracellular
Gamma-glutamyltransferase	58	DCO1_18s05278.t1	*Diplodia corticola*	—	170	4.48	22115.78	Extracellular
Necrosis inducing protein	7	T0JMK5	*Colletotrichum gloeosporioides*	2.20E-17	—	5.80	24934.67	Extracellular
Putative extracellular guanyl-specific ribonuclease protein	1	R1H1L9	*Neofusicoccum parvum*	3.30E-12	—	5.11	14564.95	Extracellular
Putative pectate lyase a protein (Lyase 1)	113	R1ED02	*Neofusicoccum parvum*	6.50E-08	—	4.88	33291.57	Extracellular
Spherulation-specific family 4	4	K2RK67	*Macrophomina phaseolina*	1.00E-25	502	4.04	30373.78	Extracellular
	6	K2RK67	*Macrophomina phaseolina*	2.20E-20	502	4.04	30373.78	Extracellular
	71	K2RK67	*Macrophomina phaseolina*	2.80E-10	—	4.04	30373.78	Extracellular

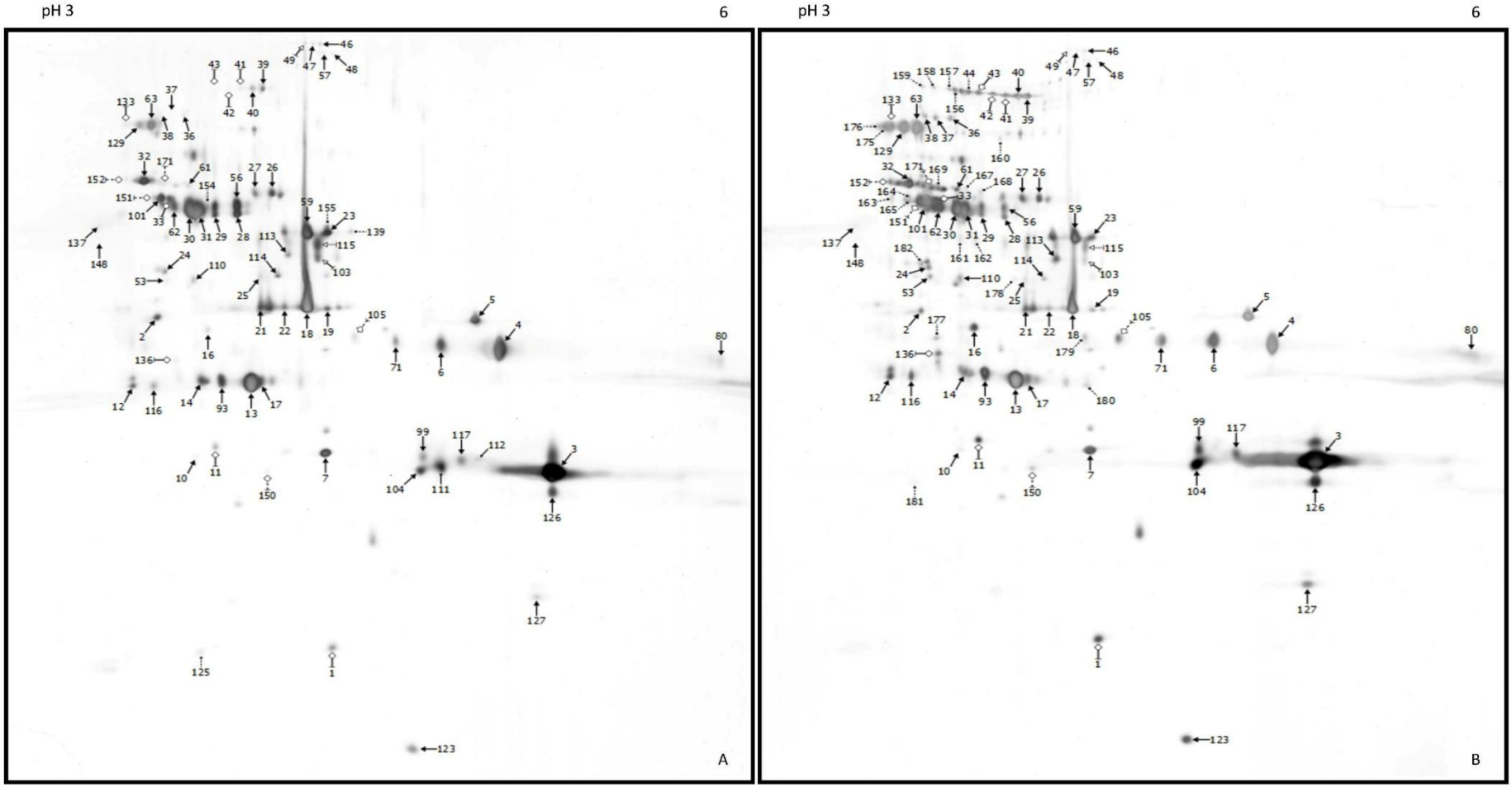

Legend:
- Spots common to both groups
- Up-regulated spots (identified)
- Up-regulated spots (non-identified)
- Down-regulated spots (identified)
- Down-regulated spots (non-identified)
- Spots exclusive of one of the groups (identified)
- Spots exclusive of one of the groups (non-identified)

Figure 11 | 2D average gels of control (A) and infection-like (B) secretomes of the *D. corticola* virulent strain CAA 499. Three biological replicates were used for each condition. Gels were stained with Pierce® Silver Stain for Mass Spectrometry (Thermo Scientific, USA). Protein spots identified by *de novo* sequencing and/or MASCOT search are marked with filled arrow lines and the identifications are described on Table 5.

Table 5 | Summary of the extracellular proteins identified in CAA 499 EXT control and CAA 499 EXT infection-like by *de novo* sequencing (1) and/or MASCOT search (2). Theoretical pI and MW (3) were searched with Compute pI/Mw tool available at ExPASy (Gasteiger et al., 2005) and the subcellular localization (4) deduced with WoLF PSORT predictor (Horton et al., 2007).

Protein	Spot	Accession number	Organism	FASTM/S E_{value}[1]	MASCOT total Ion Score[2]	Theoretical pI[3]	Theoretical Mw[3] (Da)	Subcellular localization[4]
Spots exclusive of CAA 499 EXT control								
Proteases								
Peptidase M35 - Neutral protease 2	111	K2SDQ0	*Macrophomina phaseolina*	4.20E-05	—	5.34	36981.99	Extracellular
	112	K2SDQ0	*Macrophomina phaseolina*	2.60E-03	—	5.34	36981.99	Extracellular
Spots down-regulated in CAA 499 EXT infection-like								
Hydrolases								
Glutaminase	49	DCO1_62s08886.t1	*Diplodia corticola*	—	64	4.27	76639.88	Extracellular
Putative ferulic acid esterase protein	23	R1EDH3	*Neofusicoccum parvum*	1.50E-13	32	4.79	34891.92	Extracellular
	103	R1EDH3	*Neofusicoccum parvum*	6.00E-14	—	4.79	34891.92	Extracellular
Spots up-regulated in CAA 499 EXT infection-like								
Hydrolases								
GH 15 - Glucoamylase	133	Q9C1V4	*Talaromyces emersonii*	3.00E-27	—	4.44	65429.22	Extracellular
GH 55 - Putative glycoside hydrolase family 55 protein	42	R1EP88	*Neofusicoccum parvum*	0.00E+00	529	4.52	84093.46	Extracellular
	43	R1EP88	*Neofusicoccum parvum*	1.90E-21	195	4.52	84093.46	Extracellular
Proteases								
Peptidase M43 - Putative metalloprotease 1 protein	136	R1GAQ6	*Neofusicoccum parvum*	5.10E-07	—	4.80	30491.66	Extracellular
Peptidase S10 - Putative carboxypeptidase s1 protein	41	R1GF60	*Neofusicoccum parvum*	1.50E-14	112	4.45	52146.52	Extracellular

Continued on next page

Protein	Spot	Accession number	Organism	FASTM/S E_{value}[1]	MASCOT total Ion Score[2]	Theoretical pI[3]	Theoretical Mw[3] (Da)	Subcellular localization[4]
Oxidoreductases								
Putative ligninase lg6 protein (Peroxidase)	11	R1GJT0	*Neofusicoccum parvum*	5.30E-32	512	5.20	32232.20	Extracellular
Other functions								
Cerato-platanin	1	E3QKQ8	*Colletotrichum graminicola*	6.90E-11	—	4.53	14119.72	Extracellular
Putative extracellular guanyl-specific ribonuclease protein	1	R1H1L9	*Neofusicoccum parvum*	3.30E-12	170	5.11	14564.95	Extracellular
Spots common to both control and infection-like								
Hydrolases								
Carboxylesterase family protein	48	DCO1_40s06646.t1	*Diplodia corticola*	—	76	4.68	61064.17	Extracellular
GH 13 - Putative α-amylase a type-1,2 protein	62	R1GPA2	*Neofusicoccum parvum*	0.00E+00	373	4.53	56053.14	Extracellular
	101	K2QLM3	*Macrophomina phaseolina*	4.00E-31	—	4.73	54649.73	Extracellular
GH 15 - Glucoamylase	63	C0NJV0	*Ajellomyces capsulatus*	0.00E+00	490	5.32	70492.86	Extracellular
	129	R1GLG1	*Neofusicoccum parvum*	1.60E-14	—	4.83	68531.74	Extracellular
GH 17 - Glycoside hydrolase family 17	13	K2STT8	*Macrophomina phaseolina*	0.00E+00	363	4.55	32022.55	Extracellular
	17	K2STT8	*Macrophomina phaseolina*	2.20E-07	112	4.55	32022.55	Extracellular
	53	K2STT8	*Macrophomina phaseolina*	2.30E-07	130	4.55	32022.55	Extracellular
	93	K2STT8	*Macrophomina phaseolina*	2.30E-07	—	4.55	32022.55	Extracellular
	114	K2STT8	*Macrophomina phaseolina*	5.20E-03	—	4.55	32022.55	Extracellular
GH 31 - Putative α-glucosidase protein	46	R1H1X1	*Neofusicoccum parvum*	0.00E+00	321	4.65	110578.06	Extracellular
	47	R1H1X1	*Neofusicoccum parvum*	0.00E+00	330	4.65	110578.06	Extracellular
	57	R1H1X1	*Neofusicoccum parvum*	0.00E+00	260	4.65	110578.06	Extracellular

Continued on next page

Protein	Spot	Accession number	Organism	FASTM/S E_{value}[1]	MASCOT total Ion Score[2]	Theoretical pI[3]	Theoretical Mw[3] (Da)	Subcellular localization[4]
GH 43 - Putative glycoside hydrolase family 43 protein	14	R1EDI8	*Neofusicoccum parvum*	5.70E-07	242	4.48	37269.32	Extracellular
	26	R1GE80	*Neofusicoccum parvum*	2.00E-09	169	5.73	48185.65	Extracellular
	27	R1GE80	*Neofusicoccum parvum*	1.30E-18	315	5.73	48185.65	Extracellular
GH 55 - Putative glycoside hydrolase family 55 protein	39	R1EP88	*Neofusicoccum parvum*	0.00E+00	529	4.52	84093.46	Extracellular
	40	R1EP88	*Neofusicoccum parvum*	0.00E+00	548	4.52	84093.46	Extracellular
GH 64 - Putative glucanase b protein (β-1,3-glucanase)	24	R1GK17	*Neofusicoccum parvum*	0.00E+00	327	5.82	42116.55	Nuclear
GH 71 - Glycoside hydrolase family 71	32	K2R498	*Macrophomina phaseolina*	5.50E-17	250	4.84	49264.81	Extracellular
GH 93 - Putative glycoside hydrolase family 93 protein (Sialidase/ Neuraminidase)	12	R1GGQ9	*Neofusicoccum parvum*	1.40E-07	180	4.41	38051.25	Extracellular
	24	K2RBR1	*Macrophomina phaseolina*	9.30E-11	—	4.32	40074.67	Extracellular
	53	K2RBR1	*Macrophomina phaseolina*	0.00E+00	126	4.32	40074.67	Extracellular
Lipase B (Uncharacterized protein)	25	K2R678	*Macrophomina phaseolina*	9.70E-08	113	5.43	48043.55	Extracellular
Lipase class 3	110	K2RK28	*Macrophomina phaseolina*	8.70E-20	—	5.09	30910.40	Extracellular
Phosphoesterase	28	K2RUW5	*Macrophomina phaseolina*	5.90E-29	485	4.64	43928.97	Extracellular
	29	K2RUW5	*Macrophomina phaseolina*	8.80E-03	151	4.64	43928.97	Extracellular
	56	K2RUW5	*Macrophomina phaseolina*	3.00E-15	—	4.64	43928.97	Extracellular
Putative 5,3-nucleotidase protein	2	R1FUS1	*Neofusicoccum parvum*	3.70E-18	—	4.58	31154.86	Extracellular
Putative glutaminase protein	36	R1EUG4	*Neofusicoccum parvum*	6.40E-32	263	4.29	74937.86	Extracellular
	37	R1EUG4	*Neofusicoccum parvum*	0.00E+00	225	4.29	74937.86	Extracellular
	38	R1EUG4	*Neofusicoccum parvum*	0.00E+00	263	4.29	74937.86	Extracellular
Uncharacterized protein (fumarylacetoacetase)	31	A0A072PA62	*Exophiala aquamarina*	4.60E-26	—	5.84	46110.07	Cytoplasmic

Continued on next page

Protein	Spot	Accession number	Organism	FASTM/S E_{value} [1]	MASCOT total Ion Score [2]	Theoretical pI [3]	Theoretical Mw [3] (Da)	Subcellular localization [4]
Proteases								
Peptidase A1 - Putative a chain endothiapepsin	18	R1ESA5	*Neofusicoccum parvum*	0.00E+00	491	5.45	42563.05	Extracellular
	19	R1ESA5	*Neofusicoccum parvum*	4.20E-10	71	5.45	42563.05	Extracellular
	21	R1ESA5	*Neofusicoccum parvum*	0.00E+00	228	5.45	42563.05	Extracellular
	22	R1ESA5	*Neofusicoccum parvum*	1.90E-04	34	5.45	42563.05	Extracellular
	59	R1ESA5	*Neofusicoccum parvum*	4.30E-10	491	5.45	42563.05	Extracellular
	137	R1GM42	*Neofusicoccum parvum*	1.60E-08	—	4.27	41788.15	Extracellular
	148	R1GM42	*Neofusicoccum parvum*	1.60E-08	—	4.27	41788.15	Extracellular
Peptidase M28 - Putative leucyl aminopeptidase protein	5	R1GBR8	*Neofusicoccum parvum*	1.20E-23	222	5.17	40706.16	Extracellular
Peptidase M35 - Neutral protease 2	3	K2SDQ0	*Macrophomina phaseolina*	1.20E-25	124	5.34	36981.99	Extracellular
	99	K2SDQ0	*Macrophomina phaseolina*	1.70E-19	—	5.34	36981.99	Extracellular
	104	K2SDQ0	*Macrophomina phaseolina*	1.20E-13	—	5.34	36981.99	Extracellular
	117	K2SDQ0	*Macrophomina phaseolina*	4.20E-05	—	5.34	36981.99	Extracellular
	126	K2SDQ0	*Macrophomina phaseolina*	1.00E-18	—	5.34	36981.99	Extracellular
Peptidase S10 - Putative carboxypeptidase s1 protein	29	R1GF60	*Neofusicoccum parvum*	5.50E-16	80	4.45	52146.52	Extracellular
	30	R1GF60	*Neofusicoccum parvum*	0.00E+00	486	4.45	52146.52	Extracellular
	31	R1GF60	*Neofusicoccum parvum*	0.00E+00	668	4.45	52146.52	Extracellular
	62	R1GF60	*Neofusicoccum parvum*	4.40E-28	345	4.45	52146.52	Extracellular
	101	R1GF60	*Neofusicoccum parvum*	1.30E-32	—	4.45	52146.52	Extracellular
Peptidase S8 - Putative peptidase s8 s53 subtilisin kexin sedolisin protein	16	R1G6D0	*Neofusicoccum parvum*	0.00E+00	478	4.18	43069.94	Extracellular
	80	R1GM11	*Neofusicoccum parvum*	6.50E-11	—	6.07	39070.39	Extracellular
	116	R1EAW3	*Neofusicoccum parvum*	4.80E-02	—	4.73	40860.15	Extracellular
Oxidoreductases								
Alcohol dehydrogenase	7	DCO1_41s07359.t1	*Diplodia corticola*	—	50	6.32	40875.57	Cytoplasmic

Continued on next page

Protein	Spot	Accession number	Organism	FASTM/S E_{value} [1]	MASCOT total Ion Score [2]	Theoretical pI [3]	Theoretical Mw [3] (Da)	Subcellular localization [4]
Other functions								
Cell wall protein (Cell outer membrane)	10	DCO1_41s07341.t1	*Diplodia corticola*	—	173	4.48	21235.80	Extracellular
	127	A0A017S003	*Aspergillus ruber*	1.40E-03	—	6.29	18838.42	Cytoplasmic
Necrosis inducing protein	7	T0JMK5	*Colletotrichum gloeosporioides*	2.20E-17	—	5.80	24934.67	Extracellular
Putative extracellular guanyl-specific ribonuclease protein	123	R1H1L9	*Neofusicoccum parvum*	2.70E-20	—	5.11	14564.95	Extracellular
Putative pectate lyase a protein (Lyase 1)	113	R1ED02	*Neofusicoccum parvum*	6.50E-08	—	4.88	33291.57	Extracellular
Spherulation-specific family 4	4	K2RK67	*Macrophomina phaseolina*	1.00E-25	502	4.04	30373.78	Extracellular
	6	K2RK67	*Macrophomina phaseolina*	2.20E-20	502	4.04	30373.78	Extracellular
	71	K2RK67	*Macrophomina phaseolina*	2.80E-10	—	4.04	30373.78	Extracellular
Unknown								
Uncharacterized protein	61	K2RWL4	*Macrophomina phaseolina*	6.80E-28	209	4.34	52231.60	Extracellular

PROTEOME ANALYSIS

1D evaluation of protein extracts

As performed for extracellular proteins, the intracellular proteins were first separated by 1D to evaluate the protein extract quality and the quantification accuracy. Figure 12 shows that the protocol employed was efficient to disrupt the recalcitrant fungal cell wall of *D. corticola*, producing extracts compatible with electrophoretic separation. Although the band patterns present less dissimilarities than the secretome between the avirulent and virulent strains, it is still possible distinguish the two protein profiles.

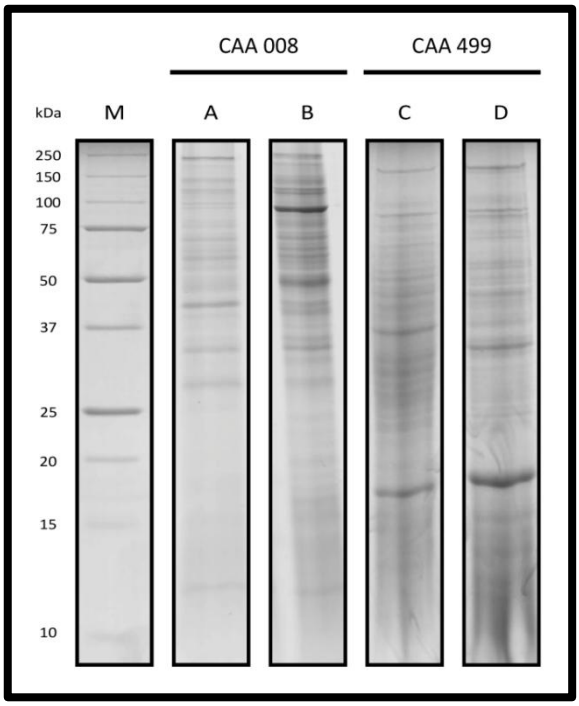

Figure 12 | SDS-PAGE of *D. corticola* intracellular proteins (30 µg). A - CAA 008 control, B - CAA 008 infection-like, C - CAA 499 control, D - CAA 499 infection-like, M - Precision Plus Protein Unstained Standard (Bio-Rad, USA). Gels were stained with CBB-G250.

Control vs. infection-like proteomes of strains with different agressiveness

The intracellular proteomic map of *D. corticola* was generated for the first time in this study. After protein separation by 2D and visualization with CBB-G250 it was possible to assess the main differences existent between the control and infection-like protein profiles of the two strains presenting distinct virulence degrees. Altogether, we detected an average (± SD) of 230 ± 48 spots in the control proteome of the avirulent strain (Figure 14 A) and 234 ± 38 spots in the virulent strain (Figure 15 A), of which 43 were differentially expressed between CAA 008 and CAA 499 (Table 11, Appendix I). In turn, we detected 264 ± 61 spots in the infection-like proteome of the

avirulent strain (Figure 14 B) and 215 ± 68 spots in the virulent strain (Figure 15 B). Similar as in the secretome analysis, the protein identification rate was rather remarkable (ca. 56% of the spots identified, Table 6) in comparison with other fungi, such as *D. seriata* (9.6%) or *Sclerotinia sclerotiorum* (Lib.) de Bary (45.5%) (Cobos et al., 2010; Yajima & Kav, 2006). We identified mainly oxidoreductases (29% in CAA 008 and 31% in CAA 499), followed by hydrolases (19% in CAA 008 and 16% in CAA 499), transferases (19% in CAA 008 and 17% in CAA 499) and proteases (17% in

Table 6 | Number of intracellular proteins identified in both CAA 008 and CAA 499 *D. corticola* strains.

	CAA 008	CAA 499
Hydrolases	31	26
Proteases	27	24
Oxidoreductases	47	51
Transferases	30	28
Phosphatases	2	3
Lyases	5	5
Hydratases	7	5
Isomerases	3	3
Other funtions	9	17
No. of proteins identified	161	162
No. of spots identified	138	128

CAA 008 and 15% in CAA 499). The theoretical pI of these proteins ranged between 4.18 and 9.13, and the MW between 12.1 and 122.7 kDa (Table 7 and Table 8). Further, the subcellular localization was analyzed with WoLF PSORT predictor (Horton et al., 2007), with most of the control proteins containing cytoplasmic (67%) and mitochondrial (15%) localization signals (Figure 13), which denotes experimental consistency. The extracellular proteins found in the cellular proteome (11%) are most probably proteins already targeted to be secreted at the time-point of mycelia harvesting.

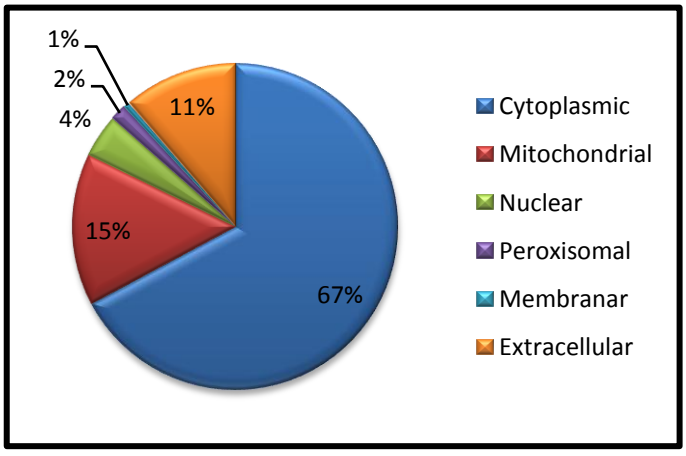

Figure 13 | Subcellular localization distribution of the *D. corticola* intracellular proteins (Horton et al., 2007).

Unlike the secretome, the comparative analysis of the intracellular proteomes revealed striking similarities between the control and infection-like profiles in each strain (Table 7 and Table 8). Nonetheless, the minor divergences may still give some insights about the biology of *D. corticola.* For instance, the 2-fold up-regulation of the 4-aminobutyrate aminotransferase (p=0.0132, spot 93, Table 8), registered in the infection-like proteome of the virulent strain, indicates that the fungus might actively metabolize γ-aminobutyric acid (GABA) during infection as happens with *Cladosporium fulvum* Cooke (Divon & Fluhr, 2007; Kumar & Punekar, 1997; Solomon & Oliver, 2002). Indeed, *C. fulvum* seems to take advantage of the plant defence mechanisms, using the GABA accumulated in the apoplast interface to fulfil its nitrogen requirements during infection (Divon & Fluhr, 2007; Solomon & Oliver, 2002, 2001). Further, Solomon & Oliver (2002) observed that this pathogen could likely manipulate the plant metabolism to maintain or even increase the apoplastic GABA concentration, sustaining a biotrophic interaction. Besides, the accumulation of GABA has been successively reported as a plant protection response to adverse environmental factors (Bae et al., 2009; Bouché et al., 2003; Kinnersley & Turano, 2000; Mazzucotelli et al., 2006), precisely one of the etiologic causes of cork oak decline (Acácio, 2009; Bréda et al., 2006; Sousa et al., 2007). In addition to these signaling/defence functions, Nabais et al. (2005) demonstrated that the GABA levels of *Q. ilex* xylem sap increase considerably during May, June and July as a consequence of the internal nitrogen remobilization required for the development of new shoots. Intriguingly, this GABA flux, that must occur as well in *Q. suber*, is contemporaneous of the cork debarking season, a period considered more susceptible to *D. corticola* infection (Costa et al., 2004; Luque & Girbal, 1989). Therefore, it is reasonable to hypothesize that there might exist a relationship between the host GABA pool and the *D. corticola* infection, a hypothesis that is reinforced by the up-regulation of the 4-aminobutyrate aminotransferase (spots 93) registered in this work. Moreover, the accumulation of GABA might be the triggering factor for the transition from a latent to a pathogenic lifestyle. Evidently, this line of reasoning should be studied afterwards.

On the other hand, the glucose-methanol-choline oxidoreductase (alcohol oxidase) up-regulation registered in the avirulent strain (spot 39: 18.9-fold up, p=0.0341; spot 41: 11.1-fold up, p=0.0103; spot 332: 11-fold up, p=0.0399; Figure 14 and Table 7) demonstrates that the exposure to cork oak stem stimulates the fungal methanol metabolism. A similar effect was previously described in the brown-rot fungus *Postia placenta* (Fr.) M.J. Larsen & Lombard when exposed to cellulose (Martinez et al., 2009). Still, the catabolism of methanol should have another reason for the fungus than its nutritional value. Most likely, the methanol derives from the lignin demethylation (Arantes et al., 2012; Filley et al., 2002; Yelle et al., 2008) and serves as a source of

hydrogen peroxide (H_2O_2) after its oxidation by the alcohol oxidase into formaldehyde and H_2O_2 (Klei et al., 2006; Zutphen et al., 2010). According to the subcellular localization of the identified proteins this reaction should occur in the hyphal cytoplasm or mitochondria (Table 7), conversely to yeasts that enclose such reactions in peroxisomes to protect the cells from the resultant hazardous molecules (Klei et al., 2006). Similarly, the alcohol oxidase of the wood-degrading *Gloeophyllum trabeum* (Pers.) Murrill was ultrastructurally localized in the periplasmic and extracellular spaces, but not in the peroxisomes (Daniel et al., 2007).

Further, if the fungus intended to detoxify the reactive H_2O_2 as happens in the methylotrophic yeasts (Klei et al., 2006; Zutphen et al., 2010), we would expect that the catalase expression increased in the same proportion as alcohol oxidase to respect the reaction stoichiometry. However, such pattern was not observed, despite the slight increment of catalase's spots intensity registered in the infection-like profile (spots, 53, 54, 55 and 115, Figure 14). This might be thus an indication that the fungus mobilizes the H_2O_2 for other purposes. The necrotrophic fungi, for instance, usually mobilize the intracellular produced ROS to the host interface, where it increases the oxidative burst (Heller & Tudzynski, 2011). Due to the lack of strain agressiveness and to the reaction to cork oak stem, we might hypothetize that the H_2O_2 is being mobilized to the extracellular space to assist the plant biomass degradation. Indeed, it is currently recognized that the brown-rotting fungi use highly reactive molecules to modify the plant cell wall in the initial stage of decay, enabling the subsequent infiltration of the large cell wall deconstructing enzymes (Arantes et al., 2012; Eastwood et al., 2011; Hammel et al., 2002). Accordingly, the H_2O_2 resultant of the methanol oxidation might be translocated to react with Fe^{2+} through the Fenton reaction ($Fe^{2+} + H_2O_2 + H^+ \rightarrow Fe^{3+} + \bullet OH + H_2O$), generating hydroxyl radicals (•OH) that disrupt the proximal wood biomass (Arantes et al., 2012; Hammel et al., 2002). The Fe^{2+} required for the reaction derives most likely from the insoluble iron oxides of plant tissues, whereby it needs to be locally solubilized and reduced to ferrous iron before the involvement in Fenton chemistry (Arantes et al., 2012). Although the mechanism of iron reduction in wood biodegradation is not completely understood (Arantes et al., 2012), *D. corticola* secretome reveals a noteworthy data. The fungus expresses a ferritin-ribonucleotide reductase-like protein (spot 60) that is found exclusively in the avirulent strain (Figure 10 and Figure 16, Appendix I). This protein gathers the dual functions required for the solubilization of plant iron, chelation and reductase activity. Thus, after the dissolution of wood iron oxides, promoted perhaps by the secretome acidity that weakens the Fe-O bonds (Arantes et al., 2012; Lee et al., 2006), the ferritin must concentrate the iron in the bioavailable ferric state (Theil, 2007; Torti & Torti, 2002). Later, when required to generate hydroxyl radicals the stored iron should be reduced and released as close as possible to

the wood cell wall to protect the fungal hyphae (Hammel et al., 2002). Hence, the results presented in this work strongly suggest that the avirulent strain, but not the virulent, resorts to a non-enzymatic wood degradation mechanism to improve the assimilation of the supplemented cork oak stem, a process that resembles the brown-rot decay. Naturally, further experiments need to be performed to corroborate this hypothesis.

In short, we accomplished for the first time a substantial characterization of the representative proteome of the phytopathogen *D. corticola*. Furthermore, the comparative analysis of the 2D gel image profiles indicated that the avirulent and virulent strains present minor intracellular proteomic dissimilarities, which nevertheless gave some insights about the biology of the fungus. First, the virulent strain ability to metabolize γ-aminobutyric acid coupled with the seasonal/stress variations of the host GABA pool suggest that this molecule might be somehow related with the onset of *D. corticola* infections. Indeed, this might explain or at least contribute to the understanding of why the fungus seems to change in some situations from a latent to a pathogenic lifestyle. On the other hand, the avirulent strain proteome evidenced the fungus aptitude to disrupt the recalcitrant wood cell walls through a non-enzymatic mechanism previously described in wood decay-related fungi. The findings reported in this work provide a useful basis for the design of further investigations to elucidate the molecular biology of its interaction with the plant hosts.

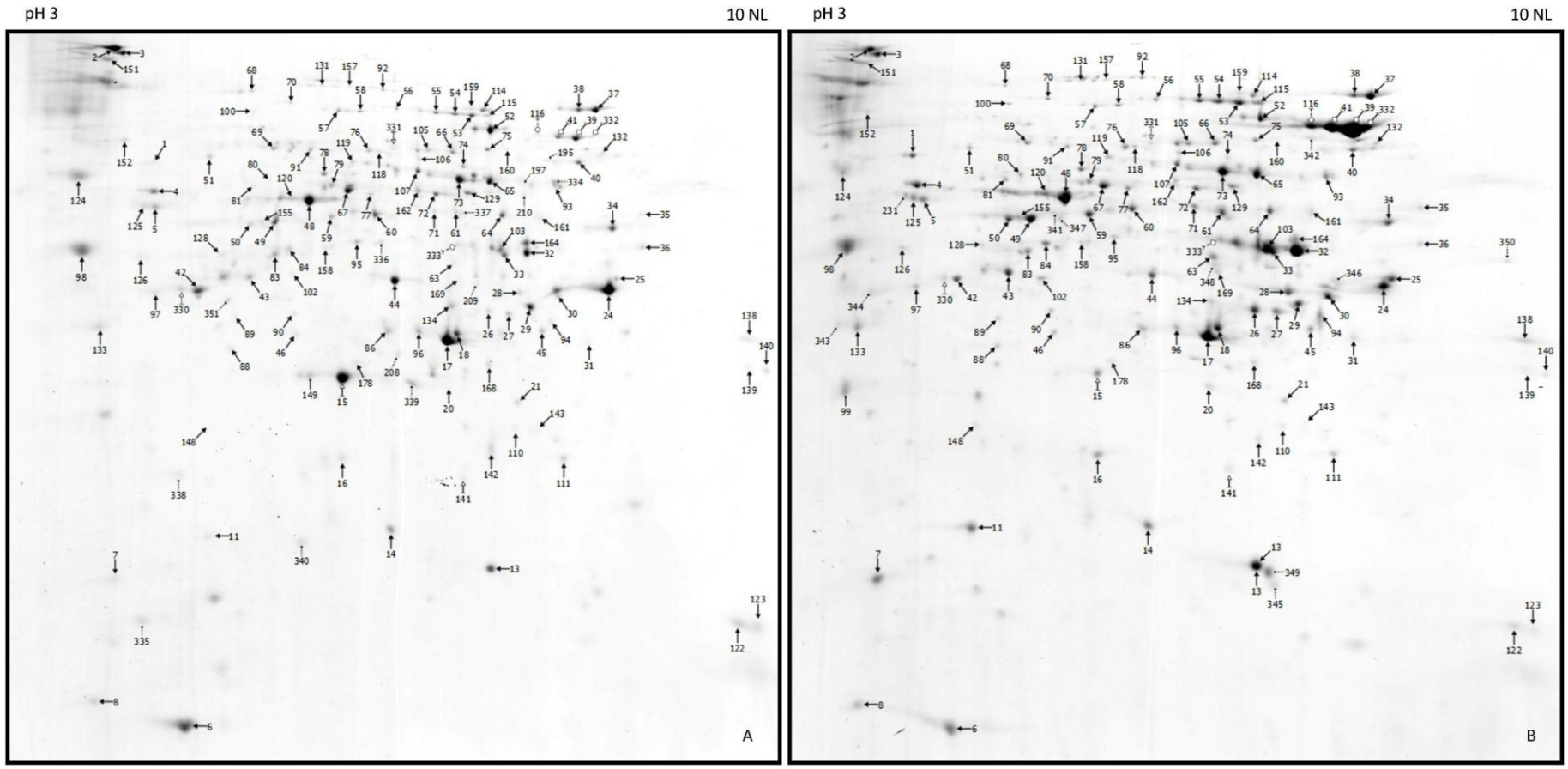

Legend:
- Spots common to both groups
- Up-regulated spots (identified)
- Up-regulated spots (non-identified)
- Down-regulated spots (identified)
- Down-regulated spots (non-identified)
- Spots exclusive of one of the groups (identified)
- Spots exclusive of one of the groups (non-identified)

Figure 14 | 2D average gels of control (A) and infection-like (B) proteomes of the *D. corticola* avirulent strain CAA 008. Three biological replicates were used for each condition. Gels were stained with CBB-250. Protein spots identified by *de novo* sequencing and/or MASCOT search are marked with filled arrow lines and the identifications are summarized in Table 7.

Table 7 | Summary of the intracellular proteins identified in CAA 008 INT control and CAA 008 INT infection-like by *de novo* sequencing (1) and/or MASCOT search (2). Theoretical pI and MW (3) were searched with Compute pI/Mw tool available at ExPASy (Gasteiger et al., 2005) and the subcellular localization (4) deduced with WoLF PSORT predictor (Horton et al., 2007).

Protein	Spot	Accession number	Organism	FASTM/S E_{value} [1]	MASCOT total Ion Score [2]	Theoretical pI [3]	Theoretical Mw [3] (Da)	Subcellular localization [4]
Spots exclusive of CAA 008 INT control								
Transferases								
Dj-1 family protein	149	L2FW83	*Colletotrichum gloeosporioides*	5.00E-08	153	5.41	26577.56	Cytoplasmic
Spots exclusive of CAA 008 INT infection-like								
Oxidoreductases								
Putative ligninase lg6 protein	99	R1GJT0	*Neofusicoccum parvum*	2.20E-31	512	5.20	32232.20	Extracellular
Spots down-regulated in CAA 008 INT infection-like								
Proteases								
Proteasome subunit β type (component pre 3)	141	R1GH44	*Neofusicoccum parvum*	0.00E+00	165	6.22	24813.98	Cytoplasmic
Transferases								
Dj-1 family protein	15	L2FW83	*Colletotrichum gloeosporioides*	1.50E-21	331	5.41	26577.56	Cytoplasmic
Spots up-regulated in CAA 008 INT infection-like								
Oxidoreductases								
Glucose-methanol-choline oxidoreductase (alcohol oxidase)	39	R1EEN8	*Neofusicoccum parvum*	0.00E+00	1319	6.44	74359.05	Cytoplasmic
	41	R1EEN8	*Neofusicoccum parvum*	0.00E+00	1217	6.44	74359.05	Cytoplasmic
	332	K2R576	*Macrophomina phaseolina*	7.80E-18	187	6.93	68179.13	Mitochondrial

Continued on next page

Protein	Spot	Accession number	Organism	FASTM/S E_{value}[1]	MASCOT total Ion Score[2]	Theoretical pI[3]	Theoretical Mw[3] (Da)	Subcellular localization[4]
Spots common to both control and infection-like								
Hydrolases								
αβ hydrolase	46	DCO1_9s03329.t1	*Diplodia corticola*	—	65	5.51	32613.91	Mitochondrial
	61	R1EXW5	*Neofusicoccum parvum*	4.50E-35	331	5.88	49829.51	Mitochondrial
	71	R1EXW5	*Neofusicoccum parvum*	0.00E+00	429	5.88	49829.51	Mitochondrial
	77	K2R5Z4	*Macrophomina phaseolina*	9.90E-32	223	5.34	47708.07	Cytoplasmic
	128	DCO1_87s10149.t1	*Diplodia corticola*	—	128	5.14	37876.66	Cytoplasmic
αβ hydrolase - Putative dienelactone hydrolase family protein	26	R1G7F4	*Neofusicoccum parvum*	0.00E+00	646	5.99	29496.62	Cytoplasmic
Acetamidase/Formamidase	79	K2RFA7	*Macrophomina phaseolina*	0.00E+00	345	5.55	45023.14	Cytoplasmic
Acetyl-CoA hydrolase/transferase	75	K2SBN2	*Macrophomina phaseolina*	0.00E+00	358	6.36	58269.36	Mitochondrial
Adenosylhomocysteinase	60	K2R5D9	*Macrophomina phaseolina*	0.00E+00	300	5.75	48793.22	Cytoplasmic
	95	R1G6V6	*Neofusicoccum parvum*	0.00E+00	209	5.84	48855.29	Cytoplasmic
Fumarylacetoacetase	81	V9DKH3	*Cladophialophora carrionii*	7.00E-26	375	5.45	45889.97	Cytoplasmic
GH 17 - Glycoside hydrolase family 17	133	K2STT8	*Macrophomina phaseolina*	3.80E-12	103	4.55	32022.55	Extracellular
GH 31 - Putative α-glucosidase protein	2	R1H1X1	*Neofusicoccum parvum*	0.00E+00	353	4.65	110578.06	Extracellular
	3	R1H1X1	*Neofusicoccum parvum*	0.00E+00	365	4.65	110578.06	Extracellular
	151	R1H1X1	*Neofusicoccum parvum*	0.00E+00	373	4.65	110578.06	Extracellular
	169	R1H1X1	*Neofusicoccum parvum*	1.60E-29	125	4.65	110578.06	Extracellular
GH 38 - α-mannosidase	31	K2RHM5	*Macrophomina phaseolina*	2.20E-03	49	5.97	122716.44	Cytoplasmic
	132	K2RHM5	*Macrophomina phaseolina*	6.30E-23	154	5.97	122716.44	Cytoplasmic
Putative acetyl-hydrolase protein	160	R1E7A7	*Neofusicoccum parvum*	0.00E+00	528	6.17	58163.23	Mitochondrial
Putative amidohydrolase family protein	158	R1E8S2	*Neofusicoccum parvum*	0.00E+00	69	5.93	40377.03	Cytoplasmic

Continued on next page

Protein	Spot	Accession number	Organism	FASTM/S E_{value} [1]	MASCOT total Ion Score [2]	Theoretical pI [3]	Theoretical Mw [3] (Da)	Subcellular localization [4]
Putative esterase (s-formylglutathione hydrolase)	96	K2S3K9	*Macrophomina phaseolina*	0.00E+00	318	6.07	31988.10	Mitochondrial
Putative β-lactamase family protein	49	R1G5K7	*Neofusicoccum parvum*	0.00E+00	930	5.34	44700.99	Cytoplasmic
	50	R1G5K7	*Neofusicoccum parvum*	9.00E-31	729	5.34	44700.99	Cytoplasmic
	59	R1GFI9	*Neofusicoccum parvum*	0.00E+00	691	5.52	39665.40	Cytoplasmic
	83	DCO1_1s00126.t1	*Diplodia corticola*	—	318	5.50	44772.36	Peroxisomal
	84	H1V6J2	*Colletotrichum higginsianum*	1.30E-04	242	5.10	41333.09	Cytoplasmic
	155	R1G5K7	*Neofusicoccum parvum*	0.00E+00	934	5.34	44700.99	Cytoplasmic
	161	DCO1_75s09589.t1	*Diplodia corticola*	—	80	5.27	40613.76	Cytoplasmic
Proteases								
Peptidase A1 - Putative aspartic endopeptidase pep2 protein	1	K2R7K4	*Macrophomina phaseolina*	3.80E-05	77	4.74	47347.32	Mitochondrial
	98	R1GUW7	*Neofusicoccum parvum*	0.00E+00	214	4.73	43261.72	Extracellular
Peptidase M1 - Peptidase M1 alanine aminopeptidase/leukotriene A4 hydrolase	56	K2SDN2	*Macrophomina phaseolina*	0.00E+00	370	5.44	99068.10	Cytoplasmic
	92	R1EX72	*Neofusicoccum parvum*	9.70E-15	50	5.80	98026.88	Cytoplasmic
	157	K2SDN2	*Macrophomina phaseolina*	5.80E-09	135	5.44	99068.10	Cytoplasmic
Peptidase M20 - Putative glutamate carboxypeptidase protein	78	R1GM30	*Neofusicoccum parvum*	0.00E+00	245	5.53	52763.15	Cytoplasmic
Peptidase M24 - Putative xaa-pro dipeptidase protein (Creatinase)	80	R1EB48	*Neofusicoccum parvum*	8.70E-23	158	5.89	85915.06	Mitochondrial
	100	R1EG89	*Neofusicoccum parvum*	9.80E-06	—	5.34	64557.62	Cytoplasmic
Peptidase M3 - Peptidase M3A/M3B	58	R1G7D2	*Neofusicoccum parvum*	9.10E-17	189	5.75	87524.39	Cytoplasmic
Peptidase M49 - Peptidase M49 dipeptidyl-peptidase III	57	K2RA25	*Macrophomina phaseolina*	3.30E-26	274	5.53	79140.74	Cytoplasmic
Peptidase S10 - Putative carboxypeptidase s1 protein	5	R1G0M1	*Neofusicoccum parvum*	0.00E+00	518	4.89	60702.13	Extracellular
	125	R1G0M1	*Neofusicoccum parvum*	0.00E+00	493	4.89	60702.13	Extracellular

Continued on next page

Protein	Spot	Accession number	Organism	FASTM/S E_{value}[1]	MASCOT total Ion Score[2]	Theoretical pI[3]	Theoretical Mw[3] (Da)	Subcellular localization[4]
Peptidase S8 - Putative autophagic serine protease alp2 protein	14	K2RXV9	*Macrophomina phaseolina*	0.00E+00	389	5.62	57279.71	Cytoplasmic
	45	K2RXV9	*Macrophomina phaseolina*	1.30E-34	147	5.62	57279.71	Cytoplasmic
	98	R1G6D0	*Neofusicoccum parvum*	1.40E-15	146	4.18	43069.94	Extracellular
	124	R1GMY2	*Neofusicoccum parvum*	6.80E-14	—	4.50	62019.98	Cytoplasmic
	138	R1GM11	*Neofusicoccum parvum*	1.60E-35	708	6.07	39070.39	Extracellular
Peptidase S9 -Putative oligopeptidase family protein	126	R1GWK1	*Neofusicoccum parvum*	1.80E-07	134	4.64	79701.64	Extracellular
Peptidase T1A - Proteasome subunit α type	46	R1GIL3	*Neofusicoccum parvum*	0.00E+00	352	5.59	27780.56	Cytoplasmic
	88	R1GFI6	*Neofusicoccum parvum*	6.00E-36	146	5.34	30083.11	Cytoplasmic
	90	R1G2P7	*Neofusicoccum parvum*	3.40E-21	54	5.72	31950.79	Cytoplasmic
	178	R1GT64	*Neofusicoccum parvum*	3.70E-34	196	5.80	28563.18	Mitochondrial
Proteasome subunit β type-2	110	DCO1_38s06588.t1	*Diplodia corticola*	—	164	6.96	21059.17	Mitochondrial
Putative proteasome component c5 protein (β type)	21	R1ECI6	*Neofusicoccum parvum*	0.00E+00	390	6.45	28968.64	Mitochondrial
	34	DCO1_19s02494.t1	*Diplodia corticola*	—	48	6.71	28986.62	Mitochondrial
Oxidoreductases								
6-phosphogluconate dehydrogenase, decarboxylating	67	K2S8M9	*Macrophomina phaseolina*	0.00E+00	675	5.99	54283.81	Cytoplasmic
	77	K2S8M9	*Macrophomina phaseolina*	3.30E-21	106	5.99	54283.81	Cytoplasmic
Catalase-peroxidase	53	K2QZ33	*Macrophomina phaseolina*	0.00E+00	667	5.82	80922.69	Cytoplasmic
	54	K2QZ33	*Macrophomina phaseolina*	0.00E+00	677	5.82	80922.69	Cytoplasmic
	55	K2QZ33	*Macrophomina phaseolina*	1.80E-16	229	5.82	80922.69	Cytoplasmic
	115	K2QZ33	*Macrophomina phaseolina*	0.00E+00	639	5.82	80922.69	Cytoplasmic
Dihydrolipoyl dehydrogenase	72	R1EKH2	*Neofusicoccum parvum*	0.00E+00	1237	6.94	54773.98	Mitochondrial
	107	R1EKH2	*Neofusicoccum parvum*	6.30E-28	59	6.94	54773.98	Mitochondrial
	162	K2RSR2	*Macrophomina phaseolina*	0.00E+00	472	7.22	54346.46	Mitochondrial
FAD dependent oxidoreductase	84	K2QPD2	*Macrophomina phaseolina*	0.00E+00	241	5.67	47900.98	Cytoplasmic
Glutamate dehydrogenase	64	K2SZ80	*Macrophomina phaseolina*	0.00E+00	360	6.43	48930.19	Cytoplasmic

Continued on next page

Protein	Spot	Accession number	Organism	FASTM/S E_{value} [1]	MASCOT total Ion Score [2]	Theoretical pI [3]	Theoretical Mw [3] (Da)	Subcellular localization [4]
Glyceraldehyde-3-phosphate dehydrogenase	24	K2SSH4	*Macrophomina phaseolina*	0.00E+00	761	6.92	36273.12	Cytoplasmic
	30	K2SSH4	*Macrophomina phaseolina*	0.00E+00	—	6.92	36273.12	Cytoplasmic
Malate dehydrogenase	28	S8AYZ5	*Penicillium oxalicum*	9.80E-09	87	7.71	35885.01	Mitochondrial
	29	K2SB76	*Macrophomina phaseolina*	0.00E+00	1005	8.86	35859.95	Mitochondrial
NADH:flavin oxidoreductase/NADH oxidase family protein	63	R1H0X2	*Neofusicoccum parvum*	0.00E+00	237	6.19	53783.33	Cytoplasmic
	161	R1EHB0	*Neofusicoccum parvum*	4.00E-19	369	5.82	43385.05	Cytoplasmic
Putative alcohol dehydrogenase domain protein	25	DCO1_11s03839.t1	*Diplodia corticola*	—	114	6.99	37098.88	Cytoplasmic
	84	R1EH70	*Neofusicoccum parvum*	0.00E+00	521	5.73	36414.20	Cytoplasmic
Glucose-methanol-choline oxidoreductase (alcohol oxidase)	33	R1EEN8	*Neofusicoccum parvum*	5.40E-03	—	6.44	74359.05	Cytoplasmic
Putative aldehyde dehydrogenase protein	63	R1H0X2	*Neofusicoccum parvum*	0.00E+00	237	6.19	53783.33	Cytoplasmic
	65	R1H0X2	*Neofusicoccum parvum*	0.00E+00	869	6.19	53783.33	Cytoplasmic
	73	R1H0X2	*Neofusicoccum parvum*	0.00E+00	1099	6.19	53783.33	Cytoplasmic
	164	R1H0X2	*Neofusicoccum parvum*	2.30E-06	66	6.19	53783.33	Cytoplasmic
	169	R1H0X2	*Neofusicoccum parvum*	1.70E-06	—	6.19	53783.33	Cytoplasmic
Putative choline oxidase protein	118	R1EJS8	*Neofusicoccum parvum*	0.00E+00	341	6.30	60138.57	Cytoplasmic
Putative fad binding domain-containing protein	152	R1EYD9	*Neofusicoccum parvum*	8.50E-03	387	4.71	57220.33	Extracellular
Putative formate dehydrogenase protein	32	R1G468	*Neofusicoccum parvum*	0.00E+00	611	6.29	40298.87	Cytoplasmic
	33	R1G468	*Neofusicoccum parvum*	4.20E-05	56	6.29	40298.87	Cytoplasmic
	103	R1G468	*Neofusicoccum parvum*	0.00E+00	690	6.29	40298.87	Cytoplasmic
Putative homogentisate-dioxygenase protein	129	R1EVN8	*Neofusicoccum parvum*	1.30E-06	—	6.06	58733.01	Cytoplasmic
Putative minor allergen alt a 7 protein	142	R1ENB8	*Neofusicoccum parvum*	1.30E-18	557	5.72	22135.00	Cytoplasmic
Putative nadh-ubiquinone oxidoreductase 78 kDa subunit protein	70	R1E5C6	*Neofusicoccum parvum*	8.00E-13	128	5.94	81566.38	Mitochondrial

Continued on next page

Protein	Spot	Accession number	Organism	FASTM/S E_{value}[1]	MASCOT total Ion Score[2]	Theoretical pI[3]	Theoretical Mw[3] (Da)	Subcellular localization[4]
Saccharopine dehydrogenase / Homospermidine synthase	162	K2RNB4	*Macrophomina phaseolina*	0.00E+00	663	5.86	50151.34	Cytoplasmic
Short-chain dehydrogenase/ reductase sdr	102	DCO1_1s00458.t1	*Diplodia corticola*	—	44	5.50	34373.20	Cytoplasmic
Short-chain dehydrogenase/ reductase SDR (l-xylulose reductase)	17	K2S1F3	*Macrophomina phaseolina*	0.00E+00	313	6.13	31597.72	Cytoplasmic
Short-chain dehydrogenase/ reductase SDR (Versicolorin reductase)	20	K2RCX3	*Macrophomina phaseolina*	1.20E-35	272	5.90	31170.57	Cytoplasmic
Superoxide dismutase [Mn/Fe]	111	R1GPF7	*Neofusicoccum parvum*	0.00E+00	211	9.13	25360.53	Mitochondrial
Superoxide dismutase [Cu-Zn]	13	R1GTN9	*Neofusicoccum parvum*	0.00E+00	589	6.03	15726.24	Cytoplasmic
Thioredoxin reductase	8	DCO1_53s07515.t1	*Diplodia corticola*	—	32	6.37	33319.94	Cytoplasmic
	27	M2QTA7	*Cochliobolus sativus*	5.60E-15	445	6.60	33646.58	Cytoplasmic
	28	M2QTA7	*Cochliobolus sativus*	0.00E+00	793	6.60	33646.58	Cytoplasmic
	30	M2QTA7	*Cochliobolus sativus*	0.00E+00	985	6.60	33646.58	Cytoplasmic
	94	M2QTA7	*Cochliobolus sativus*	3.70E-10	405	6.60	33646.58	Cytoplasmic
Transferases								
α-1,4 glucan phosphorylase	131	R1EPV1	*Neofusicoccum parvum*	0.00E+00	211	5.81	99659.87	Nuclear
α-D-phosphohexomutase superfamily	74	K2S027	*Macrophomina phaseolina*	5.60E-34	254	5.76	60123.07	Cytoplasmic
	106	DCO1_2s00877.t1	*Diplodia corticola*	—	71	—	60112.60	—
	119	K2S027	*Macrophomina phaseolina*	2.50E-26	139	5.76	60123.07	Cytoplasmic
4-aminobutyrate aminotransferase eukaryotic	93	K2SB97	*Macrophomina phaseolina*	0.00E+00	481	7.75	56383.98	Mitochondrial
Aminotransferase class V/Cysteine desulfurase	32	K2SAF5	*Macrophomina phaseolina*	1.90E-05	129	7.15	41599.64	Cytoplasmic
	164	K2SAF5	*Macrophomina phaseolina*	0.00E+00	129	7.15	41599.64	Cytoplasmic
Aspartate aminotransferase	36	K2R4A1	*Macrophomina phaseolina*	0.00E+00	387	7.19	46341.63	Peroxisomal

Continued on next page

Protein	Spot	Accession number	Organism	FASTM/S E_{value}[1]	MASCOT total Ion Score[2]	Theoretical pI[3]	Theoretical Mw[3] (Da)	Subcellular localization[4]
Citrate synthase	34	K2REF5	*Macrophomina phaseolina*	0.00E+00	395	8.77	51667.15	Mitochondrial
Galactokinase	69	K2RCE8	*Macrophomina phaseolina*	4.30E-28	—	5.55	57200.17	Cytoplasmic
Methionine synthase vitamin-B12 independent	37	K2RD18	*Macrophomina phaseolina*	0.00E+00	871	6.43	86349.70	Cytoplasmic
	38	K2RD18	*Macrophomina phaseolina*	0.00E+00	921	6.43	86349.70	Cytoplasmic
	125	K2RD18	*Macrophomina phaseolina*	3.80E-06	69	6.43	86349.70	Cytoplasmic
Methylcitrate synthase precursor	35	DCO1_18s05215.t1	*Diplodia corticola*	—	32	8.84	52449.18	Mitochondrial
Nucleoside diphosphate kinase	122	K2S9J1	*Macrophomina phaseolina*	0.00E+00	397	8.69	16744.19	Cytoplasmic
	123	K2S9J1	*Macrophomina phaseolina*	1.80E-30	94	8.69	16744.19	Cytoplasmic
Putative adenosine kinase protein	83	R1EV77	*Neofusicoccum parvum*	0.00E+00	367	5.37	38168.47	Cytoplasmic
Putative fggy-family carbohydrate kinase protein	69	R1GNA2	*Neofusicoccum parvum*	3.60E-34	476	5.18	65434.09	Cytoplasmic
Putative glutathione s-transferase protein	110	R1E9W5	*Neofusicoccum parvum*	6.80E-15	111	5.92	25351.88	Nuclear
	143	R1E9W5	*Neofusicoccum parvum*	1.20E-23	190	5.92	25351.88	Nuclear
Putative l-ornithine aminotransferase protein	61	R1EP24	*Neofusicoccum parvum*	1.80E-21	136	6,07	50244.43	Cytoplasmic
Putative phosphoenolpyruvate carboxykinase protein	66	R1EI04	*Neofusicoccum parvum*	0.00E+00	769	5.60	61566.52	Cytoplasmic
	105	R1EI04	*Neofusicoccum parvum*	0.00E+00	661	5.60	61566.52	Cytoplasmic
Spermidine synthase	89	K2RG56	*Macrophomina phaseolina*	0.00E+00	404	5.26	33118.81	Cytoplasmic
Transaldolase	42	R1GMD5	*Neofusicoccum parvum*	0.00E+00	634	5.19	35619.57	Cytoplasmic
Transketolase	52	K2RZI6	*Macrophomina phaseolina*	0.00E+00	950	5.87	74975.89	Cytoplasmic
	115	K2RZI6	*Macrophomina phaseolina*	1.40E-07	—	5.87	74975.89	Cytoplasmic
	168	K2RZI6	*Macrophomina phaseolina*	8.70E-07	76	5.87	74975.89	Cytoplasmic
Phosphatases								
Putative inorganic pyrophosphatase protein	43	R1EI42	*Neofusicoccum parvum*	0.00E+00	744	5.32	33476.03	Cytoplasmic

Continued on next page

Protein	Spot	Accession number	Organism	FASTM/S E_{value}[1]	MASCOT total Ion Score[2]	Theoretical pI[3]	Theoretical Mw[3] (Da)	Subcellular localization[4]
Putative-bisphosphoglycerate-independent phosphoglycerate mutase protein	91	R1EYX5	*Neofusicoccum parvum*	0.00E+00	420	5.40	57095.83	Cytoplasmic
Lyases								
Isocitrate lyase	40	R1EDG7	*Neofusicoccum parvum*	0.00E+00	367	6.93	60923.22	Cytoplasmic
Ketose-bisphosphate aldolase class-2	44	K2RZT2	*Macrophomina phaseolina*	0.00E+00	1111	5.72	39741.04	Cytoplasmic
Putative oxalate protein (Bicupin oxalate deCO2ase/Oxase)	124	R1E9V1	*Neofusicoccum parvum*	0.00E+00	391	4.57	48901.21	Extracellular
Putative phosphoketolase protein (aldehyde-lyase)	114	R1EPJ0	*Neofusicoccum parvum*	4.70E-05	—	5.88	90822.04	Cytoplasmic
	159	R1EPJ0	*Neofusicoccum parvum*	1.00E-03	125	5.88	90822.04	Cytoplasmic
Hydratases								
Aconitase A/isopropylmalate dehydratase small subunit swivel	76	K2QLG1	*Macrophomina phaseolina*	0.00E+00	372	6.21	84207.49	Mitochondrial
	114	K2QLG1	*Macrophomina phaseolina*	0.00E+00	898	6.21	84207.49	Mitochondrial
Enolase	48	K2SCR2	*Macrophomina phaseolina*	0.00E+00	958	5.29	47075.26	Cytoplasmic
	50	K2SCR2	*Macrophomina phaseolina*	4.40E-09	—	5.29	47075.26	Cytoplasmic
	84	K2SCR2	*Macrophomina phaseolina*	0.00E+00	306	5.29	47075.26	Cytoplasmic
	120	K2SCR2	*Macrophomina phaseolina*	2.00E-24	346	5.29	47075.26	Cytoplasmic
Putative 2-methylcitrate dehydratase protein	129	R1ED63	*Neofusicoccum parvum*	0.00E+00	387	6.15	55194.95	Cytoplasmic
Isomerases								
Aldose 1-epimerase	124	K2RLW1	*Macrophomina phaseolina*	2.90E-18	153	4.66	43895.67	Extracellular
Glucose-6-phosphate isomerase	107	R1GRZ3	*Neofusicoccum parvum*	0.00E+00	340	5.74	61861.97	Cytoplasmic
NAD-dependent epimerase/dehydratase	95	K2QUU1	*Macrophomina phaseolina*	6.50E-03	34	5.96	41017.65	Cytoplasmic

Continued on next page

Protein	Spot	Accession number	Organism	FASTM/S E_{value}[1]	MASCOT total Ion Score[2]	Theoretical pI[3]	Theoretical Mw[3] (Da)	Subcellular localization[4]
Other functions								
14-3-3 protein	97	K2SCW4	*Macrophomina phaseolina*	0.00E+00	239	4.92	30320.81	Nuclear
ATP synthase subunit beta	4	K2R9P7	*Macrophomina phaseolina*	0.00E+00	1543	5.41	55499.44	Mitochondrial
Cerato-platanin (Protein SnodProt1)	7	W3WKH2	*Pestalotiopsis fici* W106-1	1.20E-07	—	4.37	13993.65	Extracellular
Cupin RmlC-type	16	K2RCC3	*Macrophomina phaseolina*	1.00E-31	354	5.18	19078.40	Cytoplasmic
Heat shock protein 60 (Chaperonin Cpn60)	51	R1GDI3	*Neofusicoccum parvum*	0.00E+00	1138	5.52	61593.33	Mitochondrial
Heat shock protein Hsp70	68	K2RVT5	*Macrophomina phaseolina*	2.90E-03	—	5.12	79970.70	Cytoplasmic
Outer membrane β-barrel	11	A0A017S003	*Aspergillus ruber*	2.40E-13	703	6.29	18838.42	Cytoplasmic
	122	DCO1_53s07485.t1	*Diplodia corticola*	—	203	5.29	18733.37	Cytoplasmic
	129	DCO1_53s07485.t1	*Diplodia corticola*	—	38	5.29	18733.37	Cytoplasmic
	148	A0A017S003	*Aspergillus ruber*	6.70E-08	468	6.29	18838.42	Cytoplasmic
Porin eukaryotic type (outer mitochondrial membrane protein porin)	139	K2S952	*Macrophomina phaseolina*	1.60E-14	—	8.99	29738.39	Extracellular
	140	K2S952	*Macrophomina phaseolina*	2.40E-23	225	8.99	29738.39	Extracellular
Putative cyanovirin-n family protein	6	R1GQI8	*Neofusicoccum parvum*	1.50E-19	83	4.73	12102.21	Cytoplasmic
Putative g-protein complex beta subunit protein	94	R1GU67	*Neofusicoccum parvum*	4.80E-11	—	6.75	35070.56	Nuclear
Putative nmra-like family protein (pyridoxal-phosphate dependent enzyme)	18	R1G4S7	*Neofusicoccum parvum*	4.70E-12	312	5.79	34755.99	Cytoplasmic
	86	R1G4S7	*Neofusicoccum parvum*	0.00E+00	1009	5.79	34755.99	Cytoplasmic
	134	R1G4S7	*Neofusicoccum parvum*	6.50E-18	230	5.79	34755.99	Cytoplasmic

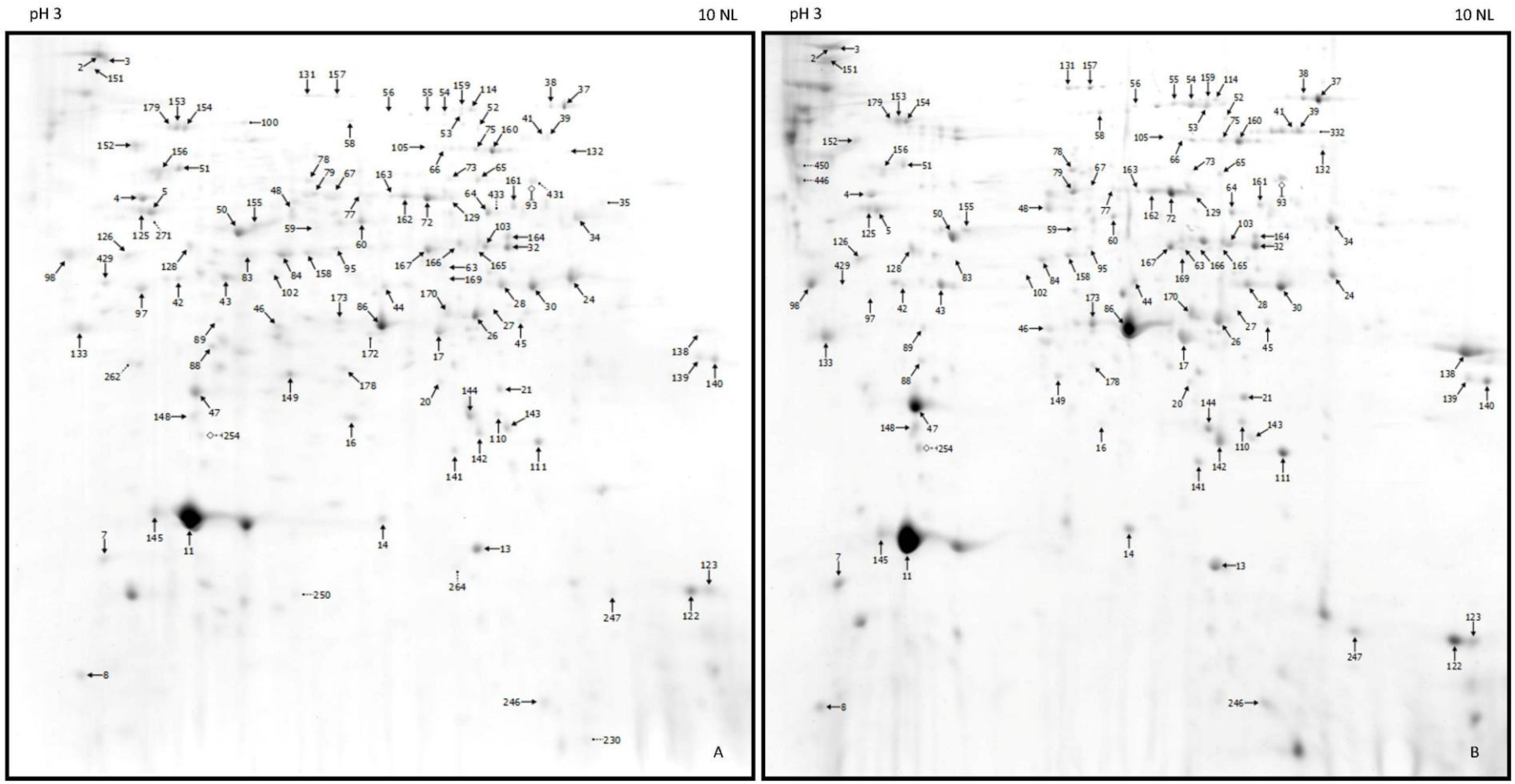

Figure 15 | 2D average gels of control (A) and infection-like (B) proteomes of the *D. corticola* virulent strain CAA 499. Three biological replicates were used for each condition. Gels were stained with CBB-250. Protein spots identified by *de novo* sequencing and/or MASCOT search are marked with filled arrow lines and the identifications are summarized in Table 8.

Table 8 | Summary of the intracellular proteins identified in CAA 499 INT control and CAA 499 INT infection-like by *de novo* sequencing (1) and/or MASCOT search (2). Theoretical pI and MW were searched with Compute pI/Mw tool (3) available at ExPASy (Gasteiger et al., 2005) and the subcellular localization (4) deduced with WoLF PSORT predictor (Horton et al., 2007).

Protein	Spot	Accession number	Organism	FASTM/S E_{value} [1]	MASCOT total Ion Score [2]	Theoretical pI [3]	Theoretical Mw [3] (Da)	Subcellular localization [4]
Spots exclusive of CAA 499 INT control								
Proteases								
Peptidase M24 - Putative xaa-pro dipeptidase protein (Creatinase)	100	R1EG89	*Neofusicoccum parvum*	9.80E-06	—	5.34	64557.62	Cytoplasmic
Transferases								
Methylcitrate synthase precursor	35	DCO1_18s05215.t1	*Diplodia corticola*	—	32	8.84	52449.18	Mitochondrial
S-methyl-5'-thioadenosine phosphorylase	172	R1GFT7	*Neofusicoccum parvum*	3.30E-30	112	5.85	33729.16	Cytoplasmic
Spots exclusive of CAA 499 INT infection-like								
Oxidoreductases								
Glucose-methanol-choline oxidoreductase (alcohol oxidase)	332	K2R576	*Macrophomina phaseolina*	7.80E-18	187	6.93	68179.13	Mitochondrial
Spots up-regulated in CAA 499 INT infection-like								
Oxidoreductases								
4-aminobutyrate aminotransferase eukaryotic	93	K2SB97	*Macrophomina phaseolina*	0.00E+00	481	7.75	56383.98	Mitochondrial

Continued on next page

Protein	Spot	Accession number	Organism	FASTM/S E_{value}[1]	MASCOT total Ion Score[2]	Theoretical pI[3]	Theoretical Mw[3] (Da)	Subcellular localization[4]
Spots common to both control and infection-like								
Hydrolases								
αβ hydrolase	46	DCO1_9s03329.t1	*Diplodia corticola*	—	65	5.51	32613.91	Mitochondrial
	77	K2R5Z4	*Macrophomina phaseolina*	9.90E-32	223	5.34	47708.07	Cytoplasmic
	128	DCO1_87s10149.t1	*Diplodia corticola*	—	128	5.14	37876.66	Cytoplasmic
αβ hydrolase - Putative dienelactone hydrolase family protein	26	R1G7F4	*Neofusicoccum parvum*	0.00E+00	646	5.99	29496.62	Cytoplasmic
	170	R1G7F4	*Neofusicoccum parvum*	0.00E+00	336	5.99	29496.62	Cytoplasmic
Acetamidase/Formamidase	79	K2RFA7	*Macrophomina phaseolina*	0.00E+00	345	5.55	45023.14	Cytoplasmic
Acetyl-CoA hydrolase/transferase	75	K2SBN2	*Macrophomina phaseolina*	0.00E+00	358	6.36	58269.36	Mitochondrial
Adenosylhomocysteinase	60	K2R5D9	*Macrophomina phaseolina*	0.00E+00	300	5.75	48793.22	Cytoplasmic
	95	R1G6V6	*Neofusicoccum parvum*	0.00E+00	209	5.84	48855.29	Cytoplasmic
GH 17 - Glycoside hydrolase family 17	133	K2STT8	*Macrophomina phaseolina*	3.80E-12	103	4.55	32022.55	Extracellular
GH 31 - Putative α-glucosidase protein	2	R1H1X1	*Neofusicoccum parvum*	0.00E+00	353	4.65	110578.06	Extracellular
	3	R1H1X1	*Neofusicoccum parvum*	0.00E+00	365	4.65	110578.06	Extracellular
	151	R1H1X1	*Neofusicoccum parvum*	0.00E+00	373	4.65	110578.06	Extracellular
	169	R1H1X1	*Neofusicoccum parvum*	1.60E-29	125	4.65	110578.06	Extracellular
GH 38 - α-mannosidase	132	K2RHM5	*Macrophomina phaseolina*	6.30E-23	154	5.97	122716.44	Cytoplasmic
Putative acetyl-hydrolase protein	160	R1E7A7	*Neofusicoccum parvum*	0.00E+00	528	6.17	58163.23	Mitochondrial
Putative amidohydrolase family protein	158	R1E8S2	*Neofusicoccum parvum*	0.00E+00	69	5.93	40377.03	Cytoplasmic
	163	R1GCN6	*Neofusicoccum parvum*	7.80E-30	412	5.90	53044.60	Cytoplasmic
Putative β-lactamase family protein	50	R1G5K7	*Neofusicoccum parvum*	9.00E-31	729	5.34	44700.99	Cytoplasmic
	59	R1GFI9	*Neofusicoccum parvum*	0.00E+00	691	5.52	39665.40	Cytoplasmic
	83	DCO1_1s00126.t1	*Diplodia corticola*	—	318	5.50	44772.36	Peroxisomal
	84	H1V6J2	*Colletotrichum higginsianum*	1.30E-04	242	5.10	41333.09	Cytoplasmic
	155	R1G5K7	*Neofusicoccum parvum*	0.00E+00	934	5.34	44700.99	Cytoplasmic
	161	DCO1_75s09589.t1	*Diplodia corticola*	—	80	5.27	40613.76	Cytoplasmic

Continued on next page

Protein	Spot	Accession number	Organism	FASTM/S E_{value}[1]	MASCOT total Ion Score[2]	Theoretical pI[3]	Theoretical Mw[3] (Da)	Subcellular localization[4]
Proteases								
Peptidase A1 - Putative aspartic endopeptidase pep2 protein	98	R1GUW7	*Neofusicoccum parvum*	0.00E+00	214	4.73	43261.72	Extracellular
Peptidase M1 - Peptidase M1 alanine aminopeptidase/leukotriene A4 hydrolase	56	K2SDN2	*Macrophomina phaseolina*	0.00E+00	370	5.44	99068.10	Cytoplasmic
	157	K2SDN2	*Macrophomina phaseolina*	5.80E-09	135	5.44	99068.10	Cytoplasmic
Peptidase M20 - Putative glutamate carboxypeptidase protein	78	R1GM30	*Neofusicoccum parvum*	0.00E+00	245	5.53	52763.15	Cytoplasmic
Peptidase M3 - Peptidase M3A/M3B	58	R1G7D2	*Neofusicoccum parvum*	9.10E-17	189	5.75	87524.39	Cytoplasmic
Peptidase M35 - Neutral protease 2	47	K2SDQ0	*Macrophomina phaseolina*	1.30E-22	195	5.34	36981.99	Extracellular
Peptidase S10 - Putative carboxypeptidase s1 protein	5	R1G0M1	*Neofusicoccum parvum*	0.00E+00	518	4.89	60702.13	Extracellular
	125	R1G0M1	*Neofusicoccum parvum*	0.00E+00	493	4.89	60702.13	Extracellular
Peptidase S8 - Putative autophagic serine protease alp2 protein	14	K2RXV9	*Macrophomina phaseolina*	0.00E+00	389	5.62	57279.71	Cytoplasmic
	45	K2RXV9	*Macrophomina phaseolina*	1.30E-34	147	5.62	57279.71	Cytoplasmic
	98	R1G6D0	*Neofusicoccum parvum*	1.40E-15	146	4.18	43069.94	Extracellular
	124	R1GMY2	*Neofusicoccum parvum*	6.80E-14	—	4.50	62019.98	Cytoplasmic
	138	R1GM11	*Neofusicoccum parvum*	1.60E-35	708	6.07	39070.39	Extracellular
Peptidase S9 -Putative oligopeptidase family protein	126	R1GWK1	*Neofusicoccum parvum*	1.80E-07	134	4.64	79701.64	Extracellular
Peptidase T1A - Proteasome subunit α type	46	R1GIL3	*Neofusicoccum parvum*	0.00E+00	352	5.59	27780.56	Cytoplasmic
	88	R1GFI6	*Neofusicoccum parvum*	6.00E-36	146	5.34	30083.11	Cytoplasmic
	178	R1GT64	*Neofusicoccum parvum*	3.70E-34	196	5.80	28563.18	Mitochondrial
Proteasome subunit β type-2	110	DCO1_38s06588.t1	*Diplodia corticola*	—	164	6.96	21059.17	Mitochondrial
	141	R1GH44	*Neofusicoccum parvum*	0.00E+00	165	6.22	24813.98	Cytoplasmic
Putative proteasome component c5 protein (β type)	21	R1ECI6	*Neofusicoccum parvum*	0.00E+00	390	6.45	28968.64	Mitochondrial
	34	DCO1_19s02494.t1	*Diplodia corticola*	—	48	6.71	28896.62	Mitochondrial

Continued on next page

Protein	Spot	Accession number	Organism	FASTM/S E_{value}[1]	MASCOT total Ion Score[2]	Theoretical pI[3]	Theoretical Mw[3] (Da)	Subcellular localization[4]
Oxidoreductases								
6-phosphogluconate dehydrogenase, decarboxylating	67	K2S8M9	*Macrophomina phaseolina*	0.00E+00	675	5.99	54283.81	Cytoplasmic
	77	K2S8M9	*Macrophomina phaseolina*	3.30E-21	106	5.99	54283.81	Cytoplasmic
Catalase-peroxidase	53	K2QZ33	*Macrophomina phaseolina*	0.00E+00	667	5.82	80922.69	Cytoplasmic
	54	K2QZ33	*Macrophomina phaseolina*	0.00E+00	677	5.82	80922.69	Cytoplasmic
	55	K2QZ33	*Macrophomina phaseolina*	1.80E-16	229	5.82	80922.69	Cytoplasmic
Choline dehydrogenase	153	I8A444	*Aspergillus oryzae*	9.00E-08	637	4.91	67679.52	Extracellular
	154	I8A444	*Aspergillus oryzae*	1.00E-09	540	4.91	67679.52	Extracellular
	179	DCO1_53s07484.t1	*Diplodia corticola*	—	148	4.93	67662.73	Extracellular
Dihydrolipoyl dehydrogenase	72	R1EKH2	*Neofusicoccum parvum*	0.00E+00	1237	6.94	54773.98	Mitochondrial
	162	K2RSR2	*Macrophomina phaseolina*	0.00E+00	472	7.22	54346.46	Mitochondrial
FAD dependent oxidoreductase	84	K2QPD2	*Macrophomina phaseolina*	0.00E+00	241	5.67	47900.98	Cytoplasmic
Glutamate dehydrogenase	64	K2SZ80	*Macrophomina phaseolina*	0.00E+00	360	6.43	48930.19	Cytoplasmic
Glyceraldehyde-3-phosphate dehydrogenase	24	K2SSH4	*Macrophomina phaseolina*	0.00E+00	761	6.92	36273.12	Cytoplasmic
	30	K2SSH4	*Macrophomina phaseolina*	0.00E+00	—	6.92	36273.12	Cytoplasmic
Malate dehydrogenase	28	S8AYZ5	*Penicillium oxalicum*	9.80E-09	87	7.71	35885.01	Mitochondrial
NADH:flavin oxidoreductase/NADH oxidase family protein	63	R1H0X2	*Neofusicoccum parvum*	0.00E+00	237	6.19	53783.33	Cytoplasmic
	161	R1EHB0	*Neofusicoccum parvum*	4.00E-19	369	5.82	43385.05	Cytoplasmic
	167	R1EE14	*Neofusicoccum parvum*	0.00E+00	1477	5.97	41452.60	Mitochondrial
Putative alcohol dehydrogenase domain protein	84	R1EH70	*Neofusicoccum parvum*	0.00E+00	521	5.73	36414.20	Cytoplasmic
Glucose-methanol-choline oxidoreductase (alcohol oxidase)	39	R1EEN8	*Neofusicoccum parvum*	0.00E+00	1319	6.44	74359.05	Cytoplasmic
	41	R1EEN8	*Neofusicoccum parvum*	0.00E+00	1217	6.44	74359.05	Cytoplasmic
Putative aldehyde dehydrogenase protein	63	R1H0X2	*Neofusicoccum parvum*	0.00E+00	237	6.19	53783.33	Cytoplasmic
	65	R1H0X2	*Neofusicoccum parvum*	0.00E+00	869	6.19	53783.33	Cytoplasmic
	73	R1H0X2	*Neofusicoccum parvum*	0.00E+00	1099	6.19	53783.33	Cytoplasmic
	164	R1H0X2	*Neofusicoccum parvum*	2.30E-06	66	6.19	53783.33	Cytoplasmic
	169	R1H0X2	*Neofusicoccum parvum*	1.70E-06	—	6.19	53783.33	Cytoplasmic

Continued on next page

Protein	Spot	Accession number	Organism	FASTM/S E_{value}[1]	MASCOT total Ion Score[2]	Theoretical pI[3]	Theoretical Mw[3] (Da)	Subcellular localization[4]
Putative fad binding domain-containing protein	152	R1EYD9	*Neofusicoccum parvum*	8.50E-03	387	4.71	57220.33	Extracellular
	156	R1EYD9	*Neofusicoccum parvum*	8.40E-03	749	4.71	57220.33	Extracellular
Putative formate dehydrogenase protein	32	R1G468	*Neofusicoccum parvum*	0.00E+00	611	6.29	40298.87	Cytoplasmic
	103	R1G468	*Neofusicoccum parvum*	0.00E+00	690	6.29	40298.87	Cytoplasmic
	165	R1G468	*Neofusicoccum parvum*	0.00E+00	169	6.29	40298.87	Cytoplasmic
Putative homogentisate-dioxygenase protein	129	R1EVN8	*Neofusicoccum parvum*	1.30E-06	—	6.06	58733.01	Cytoplasmic
Putative minor allergen alt a 7 protein	142	R1ENB8	*Neofusicoccum parvum*	1.30E-18	557	5.72	22135.00	Cytoplasmic
Putative s-glutathione dehydrogenase protein	165	R1GWD9	*Neofusicoccum parvum*	1.30E-33	121	6.46	40901.83	Cytoplasmic
Saccharopine dehydrogenase / Homospermidine synthase	162	K2RNB4	*Macrophomina phaseolina*	0.00E+00	663	5.86	50151.34	Mitochondrial
Short-chain dehydrogenase/ reductase sdr	102	DCO1_1s00458.t1	*Diplodia corticola*	—	44	5.50	34373.20	Cytoplasmic
Short-chain dehydrogenase/ reductase SDR (l-xylulose reductase)	17	K2S1F3	*Macrophomina phaseolina*	0.00E+00	313	6.13	31597.72	Cytoplasmic
Short-chain dehydrogenase/ reductase SDR (Versicolorin reductase)	20	K2RCX3	*Macrophomina phaseolina*	1.20E-35	272	5.90	31170.57	Cytoplasmic
Superoxide dismutase [Mn/Fe]	111	R1GPF7	*Neofusicoccum parvum*	0.00E+00	211	9.13	25360.53	Mitochondrial
	144	K2RKY9	*Macrophomina phaseolina*	2.80E-04	120	8.89	33373.71	Membranar
Superoxide dismutase [Cu-Zn]	13	R1GTN9	*Neofusicoccum parvum*	0.00E+00	589	6.03	15726.24	Cytoplasmic
Thioredoxin reductase	8	DCO1_53s07515.t1	*Diplodia corticola*	—	32	6.37	33319.94	Cytoplasmic
	27	M2QTA7	*Cochliobolus sativus*	5.60E-15	445	6.60	33646.58	Cytoplasmic
	28	M2QTA7	*Cochliobolus sativus*	0.00E+00	793	6.60	33646.58	Cytoplasmic
	30	M2QTA7	*Cochliobolus sativus*	0.00E+00	985	6.60	33646.58	Cytoplasmic

Continued on next page

Protein	Spot	Accession number	Organism	FASTM/S E_{value}[1]	MASCOT total Ion Score[2]	Theoretical pI[3]	Theoretical Mw[3] (Da)	Subcellular localization[4]
Transferases								
α-1,4 glucan phosphorylase	131	R1EPV1	*Neofusicoccum parvum*	0.00E+00	211	5.81	99659.87	Nuclear
Aminotransferase class V/Cysteine desulfurase	32	K2SAF5	*Macrophomina phaseolina*	1.90E-05	129	7.15	41599.64	Cytoplasmic
	164	K2SAF5	*Macrophomina phaseolina*	0.00E+00	129	7.15	41599.64	Cytoplasmic
Citrate synthase	34	K2REF5	*Macrophomina phaseolina*	0.00E+00	395	8.77	51667.15	Mitochondrial
Dj-1 family protein	149	L2FW83	*Colletotrichum gloeosporioides*	5.00E-08	153	5.41	26577.56	Cytoplasmic
Methionine synthase vitamin-B12 independent	37	K2RD18	*Macrophomina phaseolina*	0.00E+00	871	6.43	86349.70	Cytoplasmic
	38	K2RD18	*Macrophomina phaseolina*	0.00E+00	921	6.43	86349.70	Cytoplasmic
	125	K2RD18	*Macrophomina phaseolina*	3.80E-06	69	6.43	86349.70	Cytoplasmic
Nucleoside diphosphate kinase	122	K2S9J1	*Macrophomina phaseolina*	0.00E+00	397	8.69	16744.19	Cytoplasmic
	123	K2S9J1	*Macrophomina phaseolina*	1.80E-30	94	8.69	16744.19	Cytoplasmic
Putative adenosine kinase protein	83	R1EV77	*Neofusicoccum parvum*	0.00E+00	367	5.37	38168.47	Cytoplasmic
Putative glutathione s-transferase protein	110	R1E9W5	*Neofusicoccum parvum*	6.80E-15	111	5.92	25351.88	Nuclear
	143	R1E9W5	*Neofusicoccum parvum*	1.20E-23	190	5.92	25351.88	Nuclear
	144	R1E9W5	*Neofusicoccum parvum*	0.00E+00	111	5.92	25351.88	Nuclear
	246	R1E9W5	*Neofusicoccum parvum*	9.70E-03	153	5.92	25351.88	Nuclear
	247	M3B7C6	*Sphaerulina musiva*	7.90E-07	127	6.71	25966.87	Cytoplasmic
Putative phosphoenolpyruvate carboxykinase protein	66	R1EI04	*Neofusicoccum parvum*	0.00E+00	769	5.60	61566.52	Cytoplasmic
	105	R1EI04	*Neofusicoccum parvum*	0.00E+00	661	5.60	61566.52	Cytoplasmic
Spermidine synthase	89	K2RG56	*Macrophomina phaseolina*	0.00E+00	404	5.26	33118.81	Cytoplasmic
Transaldolase	42	R1GMD5	*Neofusicoccum parvum*	0.00E+00	634	5.19	35619.57	Cytoplasmic
Transketolase	52	K2RZI6	*Macrophomina phaseolina*	0.00E+00	950	5.87	74975.89	Cytoplasmic
Phosphatases								
Putative histidine acid phosphatase protein	166	R1EVB6	*Neofusicoccum parvum*	0.00E+00	194	7.57	57788.33	Mitochondrial
Putative inorganic pyrophosphatase protein	43	R1EI42	*Neofusicoccum parvum*	0.00E+00	744	5.32	33476.03	Cytoplasmic

Continued on next page

Protein	Spot	Accession number	Organism	FASTM/S E_{value}[1]	MASCOT total Ion Score[2]	Theoretical pI[3]	Theoretical Mw[3] (Da)	Subcellular localization[4]
Lyases								
Ketose-bisphosphate aldolase class-2	44	K2RZT2	*Macrophomina phaseolina*	0.00E+00	1111	5.72	39741.04	Cytoplasmic
Putative oxalate protein (Bicupin oxalate deCO2ase/Oxase)	124	R1E9V1	*Neofusicoccum parvum*	0.00E+00	391	4.57	48901.21	Extracellular
Putative phosphoketolase protein (aldehyde-lyase)	114	R1EPJ0	*Neofusicoccum parvum*	4.70E-05	—	5.88	90822.04	Cytoplasmic
	159	R1EPJ0	*Neofusicoccum parvum*	1.00E-03	125	5.88	90822.04	Cytoplasmic
Hydratases								
Aconitase A/isopropylmalate dehydratase small subunit swivel	114	K2QLG1	*Macrophomina phaseolina*	0.00E+00	898	6.21	84207.49	Mitochondrial
Enolase	48	K2SCR2	*Macrophomina phaseolina*	0.00E+00	958	5.29	47075.26	Cytoplasmic
	50	K2SCR2	*Macrophomina phaseolina*	4.40E-09	—	5.29	47075.26	Cytoplasmic
	84	K2SCR2	*Macrophomina phaseolina*	0.00E+00	306	5.29	47075.26	Cytoplasmic
Putative 2-methylcitrate dehydratase protein	129	R1ED63	*Neofusicoccum parvum*	0.00E+00	387	6.15	55194.95	Cytoplasmic
Isomerases								
Aldose 1-epimerase	124	K2RLW1	*Macrophomina phaseolina*	2.90E-18	153	4.66	43895.67	Extracellular
NAD-dependent epimerase/dehydratase	95	K2QUU1	*Macrophomina phaseolina*	6.50E-03	34	5.96	41017.65	Cytoplasmic
Other functions								
14-3-3 protein	97	K2SCW4	*Macrophomina phaseolina*	0.00E+00	239	4.92	30320.81	Nuclear
ATP synthase subunit beta	4	K2R9P7	*Macrophomina phaseolina*	0.00E+00	1543	5.41	55499.44	Mitochondrial
Cerato-platanin (Protein SnodProt1)	7	W3WKH2	*Pestalotiopsis fici* W106-1	1.20E-07	—	4.37	13993.65	Extracellular
Cupin RmlC-type	16	K2RCC3	*Macrophomina phaseolina*	1.00E-31	354	5.18	19078.40	Cytoplasmic
Heat shock protein 60 (Chaperonin Cpn60)	51	R1GDI3	*Neofusicoccum parvum*	0.00E+00	1138	5.52	61593.33	Mitochondrial

Continued on next page

Protein	Spot	Accession number	Organism	FASTM/S E_{value}[1]	MASCOT total Ion Score[2]	Theoretical pI[3]	Theoretical Mw[3] (Da)	Subcellular localization[4]
Outer membrane β-barrel	11	A0A017S003	*Aspergillus ruber*	2.40E-13	703	6.29	18838.42	Cytoplasmic
	122	DCO1_53s07485.t1	*Diplodia corticola*	—	203	5.29	18733.37	Cytoplasmic
	129	DCO1_53s07485.t1	*Diplodia corticola*	—	38	5.29	18733.37	Cytoplasmic
	145	A0A017S003	*Aspergillus ruber*	6.60E-08	752	6.29	18838.42	Cytoplasmic
	148	A0A017S003	*Aspergillus ruber*	6.70E-08	468	6.29	18838.42	Cytoplasmic
	153	DCO1_53s07485.t1	*Diplodia corticola*	—	98	5.29	18733.37	Cytoplasmic
Porin eukaryotic type (outer mitochondrial membrane protein porin)	139	K2S952	*Macrophomina phaseolina*	1.60E-14	—	8.99	29738.39	Cytoplasmic
	140	K2S952	*Macrophomina phaseolina*	2.40E-23	225	8.99	29738.39	Cytoplasmic
	429	A0A0C4FE13	*Puccinia triticina*	2.80E-09	—	4.55	25487.62	Cytoplasmic and nuclear
Putative nmra-like family protein (pyridoxal-phosphate dependent enzyme)	86	R1G4S7	*Neofusicoccum parvum*	0.00E+00	1009	5.79	34755.99	Cytoplasmic
	173	R1G4S7	*Neofusicoccum parvum*	0.00E+00	604	5.79	34755.99	Cytoplasmic

REFERENCES

Abbas, A., Koc, H., Liu, F., Tien, M. (2005). Fungal degradation of wood: initial proteomic analysis of extracellular proteins of *Phanerochaete chrysosporium* grown on oak substrate. *Current Genetics*. **47** (**1**): 49–56.

Acácio, V. (2009). *The dynamics of cork oak systems in Portugal: the role of ecological and land use factors*. Wageningen University.

Adav, S., Ravindran, A., Sze, S. (2015). Quantitative proteomic study of *Aspergillus fumigatus* secretome revealed deamidation of secretory enzymes. *Journal of Proteomics*. **119** (**1**): 154–168.

Agrawal, G., Jwa, N.-S., Lebrun, M.-H., Job, D., Rakwal, R. (2010). Plant secretome: unlocking secrets of the secreted proteins. *Proteomics*. **10** (**4**): 799–827.

Alves, A., Correia, A., Luque, J., Phillips, A. (2004). *Botryosphaeria corticola*, sp nov on *Quercus* species, with notes and description of *Botryosphaeria stevensii* and its anamorph, *Diplodia mutila*. *Mycologia*. **96** (**3**): 598–613.

Amaral, A., Antoniw, J., Rudd, J., Hammond-Kosack, K. (2012). Defining the predicted protein secretome of the fungal wheat leaf pathogen *Mycosphaerella graminicola*. *PloS One*. **7** (**12**): e49904.

Arantes, V., Jellison, J., Goodell, B. (2012). Peculiarities of brown-rot fungi and biochemical Fenton reaction with regard to their potential as a model for bioprocessing biomass. *Applied Microbiology and Biotechnology*. **94** (**2**): 323–338.

Arnadottir, H., Hvanndal, I., Andresdottir, V., Burr, S., Frey, J., Gudmundsdottir, B. (2009). The AsaP1 peptidase of *Aeromonas salmonicida* subsp *achromogenes* is a highly conserved deuterolysin metalloprotease (family M35) and a major virulence factor. *Journal of Bacteriology*. **191** (**1**): 403–410.

Baccelli, I. (2014). Cerato-platanin family proteins: one function for multiple biological roles? *Frontiers in Plant Science*. **5** (**1**): 769–772.

Baccelli, I., Lombardi, L., Luti, S., Bernardi, R., Picciarelli, P., Scala, A., Pazzagli, L. (2014a). Cerato-platanin induces resistance in *Arabidopsis* leaves through stomatal perception, overexpression of salicylic acid- and ethylene-signalling genes and camalexin biosynthesis. *PloS One*. **9** (**6**): e100959.

Baccelli, I., Luti, S., Bernardi, R., Scala, A., Pazzagli, L. (2014b). Cerato-platanin shows expansin-like activity on cellulosic materials. *Applied Microbiology and Biotechnology*. **98** (**1**): 175–184.

Baccelli, I., Scala, A., Pazzagli, L., Bernardi, R. (2013). Early transcription of defence-related genes in *Platanus* × *acerifolia* leaves following treatment with cerato-platanin. *Biologia Plantarum*. **57** (**3**): 571–575.

Bae, H., Sicher, R., Kim, M., Kim, S.-H., Strem, M., Melnick, R., Bailey, B. (2009). The beneficial endophyte *Trichoderma hamatum* isolate DIS 219b promotes growth and delays the onset of the drought response in *Theobroma cacao*. *Journal of Experimental Botany*. **60** (**11**): 3279–3295.

Barradas, C., Phillips, A., Correia, A., Diogo, E., Bragança, H., Alves, A. (2015). Diversity and potential impact of *Botryosphaeriaceae* species associated with *Eucalyptus globulus* plantations in Portugal. *Manuscript submitted for publication*.

Barsottini, M., Oliveira, J., Adamoski, D., Teixeira, P., Prado, P., Tiezzi, H., Sforça, M., Cassago, A., Portugal, R., Oliveira, P., Zeri, A., Dias, S., Pereira, G., Ambrosio, A. (2013). Functional diversification of cerato-

platanins in *Moniliophthora perniciosa* as seen by differential expression and protein function specialization. *Molecular Plant-Microbe Interactions*. **26** (**11**): 1281–1293.

Bendtsen, J., Jensen, L., Blom, N., Heijne, G., Brunak, S. (2004). Feature-based prediction of non-classical and leaderless protein secretion. *Protein Engineering, Design & Selection*. **17** (**4**): 349–356.

Biely, P. (2012). Microbial carbohydrate esterases deacetylating plant polysaccharides. *Biotechnology Advances*. **30** (**6**): 1575–1588.

Biswal, A., Soeno, K., Gandla, M., Immerzeel, P., Pattathil, S., Lucenius, J., Serimaa, R., Hahn, M., Moritz, T., Jönsson, L., Israelsson-Nordström, M., Mellerowicz, E. (2014). Aspen pectate lyase PtxtPL1-27 mobilizes matrix polysaccharides from woody tissues and improves saccharification yield. *Biotechnology for Biofuels*. **7** (**1**): 11–23.

Blanco-Ulate, B., Rolshausen, P., Cantu, D. (2013). Draft genome sequence of *Neofusicoccum parvum* isolate UCR-NP2, a fungal vascular pathogen associated with grapevine cankers. *Genome Announcements*. **1** (**3**): e00339–13.

Blümke, A., Falter, C., Herrfurth, C., Sode, B., Bode, R., Schäfer, W., Feussner, I., Voigt, C. (2014). Secreted fungal effector lipase releases free fatty acids to inhibit innate immunity-related callose formation during wheat head infection. *Plant Physiology*. **165** (**1**): 346–358.

Bouché, N., Fait, A., Bouchez, D., Møller, S., Fromm, H. (2003). Mitochondrial succinic-semialdehyde dehydrogenase of the γ-aminobutyrate shunt is required to restrict levels of reactive oxygen intermediates in plants. *Proceedings of the National Academy of Sciences*. **100** (**11**): 6843–6848.

Bréda, N., Huc, R., Granier, A., Dreyer, E. (2006). Temperate forest trees and stands under severe drought: a review of ecophysiological responses, adaptation processes and long-term consequences. *Annals of Forest Science*. **63** (**6**): 625–644.

Brink, J., Vries, R. (2011). Fungal enzyme sets for plant polysaccharide degradation. *Applied Microbiology and Biotechnology*. **91** (**6**): 1477–1492.

Burnaugh, A., Frantz, L., King, S. (2008). Growth of *Streptococcus pneumoniae* on human glycoconjugates is dependent upon the sequential activity of bacterial exoglycosidases. *Journal of Bacteriology*. **190** (**1**): 221–230.

Camilo-Alves, C. (2014). *Studies on cork oak decline: an integrated approach*. University of Évora.

Campanile, G., Ruscelli, A., Luisi, N. (2007). Antagonistic activity of endophytic fungi towards *Diplodia corticola* assessed by *in vitro* and *in planta* tests. *European Journal of Plant Pathology*. **117** (**3**): 237–246.

Cao, T., Kim, Y., Kav, N., Strelkov, S. (2009). A proteomic evaluation of *Pyrenophora tritici-repentis*, causal agent of tan spot of wheat, reveals major differences between virulent and avirulent isolates. *Proteomics*. **9** (**5**): 1177–1196.

Carlucci, A., Frisullo, S. (2009). First report of *Diplodia corticola* on grapevine in Italy. *Journal of Plant Pathology*. **91** (**1**): 231–240.

Cobos, R., Barreiro, C., Mateos, R., Coque, J.-J. (2010). Cytoplasmic-and extracellular-proteome analysis of *Diplodia seriata*: a phytopathogenic fungus involved in grapevine decline. *Proteome Science*. **8** (**46**): 1–16.

Collins, C. (2013). *A Genomic and Proteomic Investigation of the Plant Pathogen* Armillaria mellea*: Buried Treasure or Hidden Threat?* National University of Ireland Maynooth.

Cook, D., Mesarich, C., Thomma, B. (2015). Understanding plant immunity as a surveillance system to detect invasion. *Annual Review of Phytopathology*. **53** (**25**): 1–23.

Costa, A., Pereira, H., Oliveira, A. (2004). The effect of cork-stripping damage on diameter growth of *Quercus suber* L. *Forestry*. **77** (**1**): 1–8.

Daniel, G., Volc, J., Filonova, L., Plíhal, O., Kubátová, E., Halada, P. (2007). Characteristics of *Gloeophyllum trabeum* alcohol oxidase, an extracellular source of H2O2 in brown rot decay of wood. *Applied and Environmental Microbiology*. **73** (**19**): 6241–6253.

Divon, H., Fluhr, R. (2007). Nutrition acquisition strategies during fungal infection of plants. *FEMS Microbiology Letters*. **266** (**1**): 65–74.

Eastwood, D., Floudas, D., Binder, M., Majcherczyk, A., Schneider, P., Aerts, A., Asiegbu, F., Baker, S., Barry, K., Bendiksby, M., Blumentritt, M., Coutinho, P., Cullen, D., Vries, R., Gathman, A., Goodell, B., Henrissat, B., Ihrmark, K., Kauserud, H., Kohler, A., LaButti, K., Lapidus, A., Lavin, J., Lee, Y.-H., Lindquist, E., Lilly, W., Lucas, S., Morin, E., Murat, C., Oguiza, J., Park, J., Pisabarro, A., Riley, R., Rosling, A., Salamov, A., Schmidt, O., Schmutz, J., Skrede, I., Stenli, J., Wiebenga, A., Xie, X., Kües, U., Hibbett, D., Hoffmeister, D., Högberg, N., Martin, F., Grigoriev, I., Watkinson, S. (2011). The plant cell wall-decomposing machinery underlies the functional diversity of forest fungi. *Science*. **333** (**6043**): 762–765.

Escobar-Tovar, L., Guzmán-Quesada, M., Sandoval-Fernández, J., Gómez-Lim, M. (2015). Comparative analysis of the *in vitro* and *in planta* secretomes from *Mycosphaerella fijiensis* isolates. *Fungal Biology*. **119** (**6**): 447–470.

Espino, J., Gutiérrez-Sánchez, G., Brito, N., Shah, P., Orlando, R., González, C. (2010). The *Botrytis cinerea* early secretome. *Proteomics*. **10** (**16**): 3020–3034.

Faulkner, C., Robatzek, S. (2012). Plants and pathogens: putting infection strategies and defence mechanisms on the map. *Current Opinion in Plant Biology*. **15** (**6**): 699–707.

Fernandes, I., Alves, A., Correia, A., Devreese, B., Esteves, A.C. (2014). Secretome analysis identifies potential virulence factors of *Diplodia corticola*, a fungal pathogen involved in cork oak (*Quercus suber*) decline. *Fungal Biology*. **118** (**5**): 516–523.

Fernandez, J., Marroquin-Guzman, M., Wilson, R. (2014). Mechanisms of nutrient acquisition and utilization during fungal infections of leaves. *Annual Review of Phytopathology*. **52** (**1**): 155–174.

Fernández-Acero, F., Colby, T., Harzen, A., Carbú, M., Wieneke, U., Cantoral, J., Schmidt, J. (2010). 2-DE proteomic approach to the *Botrytis cinerea* secretome induced with different carbon sources and plant-based elicitors. *Proteomics*. **10** (**12**): 2270–2280.

Filley, T., Cody, G., Goodell, B., Jellison, J., Noser, C., Ostrofsky, A. (2002). Lignin demethylation and polysaccharide decomposition in spruce sapwood degraded by brown rot fungi. *Organic Geochemistry*. **33** (**2**): 111–124.

Fojan, P., Jonson, P., Petersen, M., Petersen, S. (2000). What distinguishes an esterase from a lipase: a novel structural approach. *Biochimie*. **82** (**11**): 1033–1041.

Frías, M., Brito, N., González, C. (2013). The *Botrytis cinerea* cerato-platanin BcSpl1 is a potent inducer of systemic acquired resistance (SAR) in tobacco and generates a wave of salicylic acid expanding from the site of application. *Molecular Plant Pathology*. **14** (**2**): 191–196.

Frías, M., Brito, N., González, M., González, C. (2014). The phytotoxic activity of the cerato-platanin BcSpl1 resides in a two-peptide motif on the protein surface. *Molecular Plant Pathology*. **15** (**4**): 342–351.

Frischmann, A., Neudl, S., Gaderer, R., Bonazza, K., Zach, S., Gruber, S., Spadiut, O., Friedbacher, G., Grothe, H., Seidl-Seiboth, V. (2013). Self-assembly at air/water interfaces and carbohydrate binding properties of the small secreted protein EPL1 from the fungus *Trichoderma atroviride*. *Journal of Biological Chemistry*. **288** (**6**): 4278–4287.

Fu, H., Feng, J., Aboukhaddour, R., Cao, T., Hwang, S.-F., Strelkov, S. (2013). An exo-1,3-β-glucanase GLU1 contributes to the virulence of the wheat tan spot pathogen *Pyrenophora tritici-repentis*. *Fungal Biology*. **117** (**10**): 673–681.

Gaderer, R., Bonazza, K., Seidl-Seiboth, V. (2014). Cerato-platanins: a fungal protein family with intriguing properties and application potential. *Applied Microbiology and Biotechnology*. **98** (**11**): 4795–4803.

Gaillardin, C. (2010). Lipases as pathogenicity factors of fungi. In: Timmis, K. (ed.). *Handbook of Hydrocarbon and Lipid Microbiology*. Springer. pp. 3259–3268.

Gallego, F., Algaba, A.P., Fernandez-Escobar, R. (1999). Etiology of oak decline in Spain. *European Journal of Forest Pathology*. **29** (**1**): 17–27.

Gasteiger, E., Hoogland, C., Gattiker, A., Duvaud, S., Wilkins, M., Appel, R., Bairoch, A. (2005). Protein identification and analysis tools on the ExPASy server. In: Walker, J. (ed.). *The Proteomics Protocols Handbook*. Humana Press. pp. 571–607.

Girard, V., Dieryckx, C., Job, C., Job, D. (2013). Secretomes: the fungal strike force. *Proteomics*. **13** (**3-4**): 597–608.

González-Fernández, R., Jorrín-Novo, J. (2012). Contribution of proteomics to the study of plant pathogenic fungi. *Journal of Proteome Research*. **11** (**1**): 3–16.

Graça, J. (2010). Hydroxycinnamates in suberin formation. *Phytochemistry Reviews*. **9** (**1**): 85–91.

Guyon, K., Balagué, C., Roby, D., Raffaele, S. (2014). Secretome analysis reveals effector candidates associated with broad host range necrotrophy in the fungal plant pathogen *Sclerotinia sclerotiorum*. *BMC Genomics*. **15** (**1**): 336– 353.

Hammel, K., Kapich, A., Jensen, K., Ryan, Z. (2002). Reactive oxygen species as agents of wood decay by fungi. *Enzyme and Microbial Technology*. **30** (**4**): 445–453.

Heller, J., Tudzynski, P. (2011). Reactive oxygen species in phytopathogenic fungi: signaling, development, and disease. *Annual Review of Phytopathology*. **49** (**1**): 369–390.

Hesami, S., Metcalf, D., Lumsden, J., Macinnes, J. (2011). Identification of cold-temperature-regulated genes in *Flavobacterium psychrophilum*. *Applied and Environmental Microbiology*. **77** (**5**): 1593–1600.

Horton, P., Park, K.-J., Obayashi, T., Fujita, N., Harada, H., Adams-Collier, C., Nakai, K. (2007). WoLF PSORT: protein localization predictor. *Nucleic Acids Research*. **35** (**2**): W585–W587.

Huser, A., Takahara, H., Schmalenbach, W., O'Connell, R. (2009). Discovery of pathogenicity genes in the crucifer anthracnose fungus *Colletotrichum higginsianum*, using random insertional mutagenesis. *Molecular Plant-Microbe Interactions*. **22** (**2**): 143–156.

Islam, S., Haque, S., Islam, M., Emdad, E., Halim, A., Hossen, Q., Hossain, Z., Ahmed, B., Rahim, S., Rahman, S., Alam, M., Hou, S., Wan, X., Saito, J., Alam, M. (2012). Tools to kill: genome of one of the most destructive plant pathogenic fungi *Macrophomina phaseolina*. *BMC Genomics*. **13** (**1**): 493–509.

Jové, P., Olivella, M., Cano, L. (2011). Study of the variability in chemical composition of bark layers of *Quercus suber* L from different production areas. *BioResources*. **6** (**2**): 1806–1815.

Kinnersley, A., Turano, F. (2000). Gamma aminobutyric acid (GABA) and plant responses to stress. *Critical Reviews in Plant Sciences*. **19** (**6**): 479–509.

Klei, I., Yurimoto, H., Sakai, Y., Veenhuis, M. (2006). The significance of peroxisomes in methanol metabolism in methylotrophic yeast. *Biochimica et Biophysica Acta*. **1763** (**12**): 1453–1462.

Kumar, S., Punekar, N. (1997). The metabolism of 4-aminobutyrate (GABA) in fungi. *Mycological Research*. **101** (**04**): 403–409.

Laemmli, U. (1970). Cleavage of structural proteins during the assembly of the head of bacteriophage T4. *Nature*. **227** (**5259**): 680–685.

Lee, S., Tran, T., Park, Y., Kim, S., Kim, M. (2006). Study on the kinetics of iron oxide leaching by oxalic acid. *International Journal of Mineral Processing*. **80** (**2**): 144–152.

Li, B., Wang, W., Zong, Y., Qin, G., Tian, S. (2012). Exploring pathogenic mechanisms of *Botrytis cinerea* secretome under different ambient pH based on comparative proteomic analysis. *Journal of Proteome Research*. **11** (**8**): 4249–4260.

Li, J., Zhang, K.-Q. (2014). Independent expansion of zincin metalloproteinases in *Onygenales* fungi may be associated with their pathogenicity. *PloS One*. **9** (**2**): e90225.

Linaldeddu, B., Scanu, B., Maddau, L., Franceschini, A. (2014). *Diplodia corticola* and *Phytophthora cinnamomi*: the main pathogens involved in holm oak decline on Caprera Island (Italy). *Forest Pathology*. **44** (**3**): 191–200.

Linaldeddu, B., Sirca, C., Spano, D., Franceschini, A. (2009). Physiological responses of cork oak and holm oak to infection by fungal pathogens involved in oak decline. *Forest Pathology*. **39** (**4**): 232–238.

Liu, J.-K., Phookamsak, R., Doilom, M., Wikee, S., Li, Y.-M., Ariyawansha, H., Boonmee, S., Chomnunti, P., Dai, D.-Q., Bhat, J.D., others (2012). Towards a natural classification of *Botryosphaeriales*. *Fungal Diversity*. **57** (**1**): 149–210.

Lombardi, L., Faoro, F., Luti, S., Baccelli, I., Martellini, F., Bernardi, R., Picciarelli, P., Scala, A., Pazzagli, L. (2013). Differential timing of defense-related responses induced by cerato-platanin and cerato-populin, two non-catalytic fungal elicitors. *Physiologia Plantarum*. **149** (**3**): 408–421.

Lu, G., Wolf, H., Shang, Y., Filippi, C., Bhattarai, K., Li, D., Ebbole, D. (2009). Developing resources for analysis of secreted proteins from *Magnaporthe oryzae*. In: Xiaofan, Wang and Valent, Barbara (ed.). *Advances in Genetics, Genomics and Control of Rice Blast Disease*. Springer. pp. 113–124.

Lu, X., Sun, J., Nimtz, M., Wissing, J., Zeng, A.-P., Rinas, U. (2010). The intra- and extracellular proteome of *Aspergillus niger* growing on defined medium with xylose or maltose as carbon substrate. *Microbial Cell Factories*. **9** (**1**): 23–35.

Luque, J., Cohen, M., Savé, R., Biel, C., Álvarez, I. (1999). Effects of three fungal pathogens on water relations, chlorophyll fluorescence and growth of *Quercus suber* L. *Annals of Forest Science*. **56** (**1**): 19–26.

Luque, J., Girbal, J. (1989). Dieback of cork oak (*Quercus suber*) in Catalonia (NE Spain) caused by *Botryosphaeria stevensii*. *European Journal of Forest Pathology*. **19** (**1**): 7–13.

Luque, J., Parladé, J., Pera, J. (2000). Pathogenicity of fungi isolated from *Quercus suber* in Catalonia (NE Spain). *Forest Pathology*. **30** (**5**): 247–263.

Luque, J., Pera, J., Parlade, J. (2008). Evaluation of fungicides for the control of *Botryosphaeria corticola* on cork oak in Catalonia (NE Spain). *Forest Pathology*. **38** (**3**): 147–155.

Lynch, S., Eskalen, A., Zambino, P., Mayorquin, J., Wang, D. (2013). Identification and pathogenicity of *Botryosphaeriaceae* species associated with coast live oak (*Quercus agrifolia*) decline in southern California. *Mycologia*. **105** (**1**): 125–140.

Ma, B., Johnson, R. (2012). *De novo* sequencing and homology searching. *Molecular & Cellular Proteomics*. **11** (**2**): 1–16.

Mackey, A., Haystead, T., Pearson, W. (2002). Getting more from less: algorithms for rapid protein identification with multiple short peptide sequences. *Molecular & Cellular Proteomics*. **1** (**2**): 139–147.

Mandelc, S., Javornik, B. (2015). The secretome of vascular wilt pathogen *Verticillium albo-atrum* in simulated xylem fluid. *Proteomics*. **15** (**1**): 787–797.

Martin, K., McDougall, B., McIlroy, S., Chen, J., Seviour, R. (2007). Biochemistry and molecular biology of exocellular fungal β-(1,3)-and β-(1,6)-glucanases. *FEMS Microbiology Reviews*. **31** (**2**): 168–192.

Martinez, D., Challacombe, J., Morgenstern, I., Hibbett, D., Schmoll, M., Kubicek, C., Ferreira, P., Ruiz-Duenas, F., Martinez, A., Kersten, P., Hammel, K., Wymelenberg, A., Gaskell, J., Lindquist, E., Sabat, G., Bondurant, S., Larrondo, L., Canessa, P., Vicuna, R., Yadav, J., Doddapaneni, H., Subramanian, V., Pisabarro, A., Lavín, J., Oguiza, J., Master, E., Henrissat, B., Coutinho, P., Harris, P., Magnuson, J., Baker, S., Bruno, K., Kenealy, W., Hoegger, P., Kües, U., Ramaya, P., Lucas, S., Salamov, A., Shapiro, H., Tu, H., Chee, C., Misra, M., Xie, G., Teter, S., Yaver, D., James, T., Mokrejs, M., Pospisek, M., Grigoriev, I., Brettin, T., Rokhsar, D., Berka, R., Cullen, D. (2009). Genome, transcriptome, and secretome analysis of wood decay fungus *Postia placenta* supports unique mechanisms of lignocellulose conversion. *Proceedings of the National Academy of Sciences*. **106** (**6**): 1954–1959.

Mazzucotelli, E., Tartari, A., Cattivelli, L., Forlani, G. (2006). Metabolism of γ-aminobutyric acid during cold acclimation and freezing and its relationship to frost tolerance in barley and wheat. *Journal of Experimental Botany*. **57** (**14**): 3755–3766.

Monod, M., Capoccia, S., Léchenne, B., Zaugg, C., Holdom, M., Jousson, O. (2002). Secreted proteases from pathogenic fungi. *International Journal of Medical Microbiology*. **292** (**5**): 405–419.

Monti, E., Preti, A., Venerando, B., Borsani, G. (2002). Recent development in mammalian sialidase molecular biology. *Neurochemical Research*. **27** (**7-8**): 649–663.

Moore, S., Vries, O., Tudzynski, P. (2002). The major Cu,Zn SOD of the phytopathogen *Claviceps purpurea* is not essential for pathogenicity. *Molecular Plant Pathology*. **3** (**1**): 9–22.

Morales-Cruz, A., Amrine, K., Blanco-Ulate, B., Lawrence, D., Travadon, R., Rolshausen, P., Baumgartner, K., Cantu, D. (2015). Distinctive expansion of gene families associated with plant cell wall degradation, secondary metabolism, and nutrient uptake in the genomes of grapevine trunk pathogens. *BMC Genomics*. **16** (**1**): 469.

Mullerin, S. (2013). *The pathogenicity of* Diplodia corticola *and* Diplodia quercivora *on oak species of the southeastern coastal plain: a host-range study*. University of Florida.

Muth, T., Weilnböck, L., Rapp, E., Huber, C., Martens, L., Vaudel, M., Barsnes, H. (2014). DeNovoGUI: an open source graphical user interface for *de novo* sequencing of tandem mass spectra. *Journal of Proteome Research*. (**13**): 1143–1146.

Nabais, C., Hagemeyer, J., Freitas, H. (2005). Nitrogen transport in the xylem sap of *Quercus ilex*: the role of ornithine. *Journal of Plant Physiology*. **162** (**5**): 603–606.

Paoletti, E., Anselmi, N., Franceschini, A. (2007). Pre-exposure to ozone predisposes oak leaves to attacks by *Diplodia corticola* and *Biscogniauxia mediterranea*. *The Scientific World Journal*. **7** (**S1**): 222–230.

Paper, J., Scott-Craig, J., Adhikari, N., Cuomo, C., Walton, J. (2007). Comparative proteomics of extracellular proteins *in vitro* and *in planta* from the pathogenic fungus *Fusarium graminearum*. *Proteomics*. **7** (**17**): 3171–3183.

Pazzagli, L., Seidl-Seiboth, V., Barsottini, M., Vargas, W., Scala, A., Mukherjee, P. (2014). Cerato-platanins: elicitors and effectors. *Plant Science*. **228** (**1**): 79–87.

Phalip, V., Delalande, F., Carapito, C., Goubet, F., Hatsch, D., Leize-Wagner, E., Dupree, P., Dorsselaer, A., Jeltsch, J.-M. (2005). Diversity of the exoproteome of *Fusarium graminearum* grown on plant cell wall. *Current Genetics*. **48** (**6**): 366–379.

Pietro, A., Roncero, M., Roldán, M. (2009). From tools of survival to weapons of destruction: the role of cell wall-degrading enzymes in plant infection. In: Deising, H. (ed.). *Plant Relationships*. Springer. pp. 181–200.

Pinto, P., Sousa, A., Silvestre, A., Neto, C., Gandini, A., Eckerman, C., Holmbom, B. (2009). *Quercus suber* and *Betula pendula* outer barks as renewable sources of oleochemicals: a comparative study. *Industrial Crops and Products*. **29** (**1**): 126–132.

Plomion, C., Leprovost, G., Stokes, A. (2001). Wood formation in trees. *Plant physiology*. **127** (**4**): 1513–1523.

Rabilloud, T., Lelong, C. (2011). Two-dimensional gel electrophoresis in proteomics: a tutorial. *Journal of Proteomics*. **74** (**10**): 1829–1841.

Rocha, S., Coimbra, M., Delgadillo, I. (2000). Demonstration of pectic polysaccharides in cork cell wall from *Quercus suber* L. *Journal of Agricultural and Food Chemistry*. **48** (**6**): 2003–2007.

Rogers, L., Overall, C. (2013). Proteolytic post-translational modification of proteins: proteomic tools and methodology. *Molecular & Cellular Proteomics*. **12** (**12**): 3532–3542.

Rogowska-Wrzesinska, A., Bihan, M.-C., Thaysen-Andersen, M., Roepstorff, P. (2013). 2D gels still have a niche in proteomics. *Journal of Proteomics*. **88** (**1**): 4–13.

Rolke, Y., Liu, S., Quidde, T., Williamson, B., Schouten, A., Weltring, K.-M., Siewers, V., Tenberge, K., Tudzynski, B., Tudzynski, P. (2004). Functional analysis of H2O2-generating systems in *Botrytis cinerea*: the major Cu-Zn-superoxide dismutase (BCSOD1) contributes to virulence on French bean, whereas a glucose oxidase (BCGOD1) is dispensable. *Molecular Plant Pathology*. **5** (**1**): 17–27.

Roy, S., Honma, K., Douglas, C., Sharma, A., Stafford, G. (2011). Role of sialidase in glycoprotein utilization by *Tannerella forsythia*. *Microbiology*. **157** (**11**): 3195–3202.

Sadygov, R., Cociorva, D., Yates, J. (2004). Large-scale database searching using tandem mass spectra: looking up the answer in the back of the book. *Nature Methods*. **1** (**3**): 195–202.

Shoji, J., Kikuma, T., Kitamoto, K. (2014). Vesicle trafficking, organelle functions, and unconventional secretion in fungal physiology and pathogenicity. *Current Opinion in Microbiology*. **20** (**1**): 1–9.

Slippers, B., Wingfield, M. (2007). *Botryosphaeriaceae* as endophytes and latent pathogens of woody plants: diversity, ecology and impact. *Fungal Biology Reviews*. **21** (**2**): 90–106.

Solomon, P., Oliver, R. (2002). Evidence that γ-aminobutyric acid is a major nitrogen source during *Cladosporium fulvum* infection of tomato. *Planta*. **214** (**3**): 414–420.

Solomon, P., Oliver, R. (2001). The nitrogen content of the tomato leaf apoplast increases during infection by *Cladosporium fulvum*. *Planta*. **213** (**2**): 241–249.

Sousa, E., Santos, M., Varela, M., Henriques, J. (2007). *Perda de vigor dos montados de sobro e azinho: Análise da situação e perspectivas*. Ministério da Agricultura, do Desenvolvimento e das Pescas.

Stock, J., Sarkari, P., Kreibich, S., Brefort, T., Feldbrügge, M., Schipper, K. (2012). Applying unconventional secretion of the endochitinase Cts1 to export heterologous proteins in *Ustilago maydis*. *Journal of Biotechnology*. **161** (**2**): 80–91.

Subramoni, S., Suárez-Moreno, Z., Venturi, V. (2010). Lipases as pathogenicity factors of plant pathogens. In: Timmis, K. (ed.). *Handbook of hydrocarbon and lipid microbiology*. 2010 Springer. pp. 3269–3277.

Theil, E. (2007). The ferritin protein nanocage and biomineral, from single Fe atoms to FeO nanoparticles: Starting with EXAFS. *X-Ray Absorption Fine Structure*. **882** (**1**): 15–18.

Torti, F., Torti, S. (2002). Regulation of ferritin genes and protein. *Blood*. **99** (**10**): 3505–3516.

Varela, C., Fernández, V., Casal, O., Vázquez, J. (2011). First report of cankers and dieback caused by *Neofusicoccum mediterraneum* and *Diplodia corticola* on grapevine in Spain. *Plant Disease*. **95** (**10**): 1315–1315.

Voigt, C., Schäfer, W., Salomon, S. (2005). A secreted lipase of *Fusarium graminearum* is a virulence factor required for infection of cereals. *The Plant Journal*. **42** (**3**): 364–375.

Wartenberg, D., Lapp, K., Jacobsen, I., Dahse, H.-M., Kniemeyer, O., Heinekamp, T., Brakhage, A. (2011). Secretome analysis of *Aspergillus fumigatus* reveals Asp-hemolysin as a major secreted protein. *International Journal of Medical Microbiology*. **301** (**7**): 602–611.

Warwas, M., Yeung, J., Indurugalla, D., Mooers, A., Bennet, A., Moore, M. (2010). Cloning and characterization of a sialidase from the filamentous fungus, *Aspergillus fumigatus*. *Glycoconjugate Journal*. **27** (**5**): 533–548.

Wegener, S., Ransom, R., Walton, J. (1999). A unique eukaryotic beta-xylosidase gene from the phytopathogenic fungus *Cochliobolus carbonum*. *Microbiology* . **145** (**5**): 1089–1095.

Yajima, W., Kav, N. (2006). The proteome of the phytopathogenic fungus *Sclerotinia sclerotiorum*. *Proteomics*. **6** (**22**): 5995–6007.

Yelle, D., Ralph, J., Lu, F., Hammel, K. (2008). Evidence for cleavage of lignin by a brown rot basidiomycete. *Environmental Microbiology*. **10** (**7**): 1844–1849.

Yondola, M., Fernandes, F., Belicha-Villanueva, A., Uccelini, M., Gao, Q., Carter, C., Palese, P. (2011). Budding capability of the influenza virus neuraminidase can be modulated by tetherin. *Journal of Virology*. **85** (**6**): 2480–2491.

Zhang, J., Xin, L., Shan, B., Chen, W., Xie, M., Yuen, D., Zhang, W., Zhang, Z., Lajoie, G., Ma, B. (2012). PEAKS DB: *de novo* sequencing assisted database search for sensitive and accurate peptide identification. *Molecular & Cellular Proteomics*. **11** (**4**): 1–8.

Zutphen, T., Baerends, R., Susanna, K., Jong, A., Kuipers, O., Veenhuis, M., Klei, I. (2010). Adaptation of *Hansenula polymorpha* to methanol: a transcriptome analysis. *BMC Genomics*. **11** (**1**): 1–12.

CHAPTER 4

CONCLUDING REMARKS AND FUTURE PERPECTIVES

MAJOR CONCLUSIONS

Diplodia corticola has been associated with declining diseases, with particular incidence in *Quercus* species (Linaldeddu et al., 2009; Lynch et al., 2013; Úrbez-Torres et al., 2010). Since most of known affected hosts are agriculturally exploited, its frequent occurrence raises a natural ecological, social and economic concern. From a biologic point of view, the best approach to counteract this decline is to obtain a comprehensive understanding of the molecular biology of the plant-fungal interaction. Accordingly, we proposed to characterize the set of proteins expressed by this phytophatogen, comparing it with an infection-like profile to describe which changes were induced by the host mimicry.

Due to the characteristics of *D. corticola*, we optimized protocols for extracellular and intracellular proteins' extraction compatible with 1D and 2D electrophoretic separations. As such, after 2D gel separation and MS/MS *de novo* sequencing, we identified for the first time the secretome and proteome of this phytopathogen. Subsequently, we compared the control and infection-like protein profiles of two strains with divergent virulence degrees, an analysis that gave important insights about the biology of the fungus.

We concluded that the avirulent strain secretome contains an assortment of proteins that facilitates the adaptation to substrates with distinct chemical compositions. Further, proteome analysis brought some insights about the mechanism used by this fungus to disrupt the plant cell walls. Similarly to the brown-rot fungi, the avirulent strain of *D. corticola* seems to resort to highly reactive molecules to degrade non-enzimatically the plant tissues, a strategy that creates space for the pervasion of the cell wall deconstructing enzymes. On the other hand, the extracellular proteins of the virulent strain suggest that the fungus has adjusted its secretome to the host cell wall chemical properties, which represents an advantage during the infection.

Besides, we unveiled some proteins that might be directly involved in the pathogenicity of *D. corticola*. Peptidase M35 (deuterolysin), for example, was previously disclosed in the secretomes of other phytopathogenic fungi (Collins, 2013; Espino et al., 2010; Li et al., 2012), but we demonstrated for the first time in this work that the enzyme is more prevalent in the virulent strain. Likewise, we noticed an up-regulation of cerato-platanin when the strain was exposed to cork oak, an observation that is in agreement with other fungal pathosystems. This is actually the first time that such result was described in *Botryosphaeriaceae* fungi. Prior studies confirmed that cerato-platanin is responsible for the induction of plant necrotic lesions (Frías et al., 2014). It facilitates as well the hyphae's mechanical perforation of the plant cellulose barrier due to its

expansin-like activity (Baccelli et al., 2014; Baccelli, 2014; Barsottini et al., 2013). Another remarkable finding involves the intracellular enzyme 4-aminobutyrate aminotransferase. Its up-regulation in the virulent infection-like proteome indicates that the fungus increases the metabolism of γ-aminobutyric acid (GABA) during infection. One of the plant defences against biotic and environmental adverse factors is precisely the accumulation of GABA (Bae et al., 2009; Kinnersley & Turano, 2000; Solomon & Oliver, 2001). In addition, this molecule (most probably) accumulates during the debarking season due to the nitrogen remobilization required for the formation of new shoots (Nabais et al., 2005). Since the onset of *D. corticola* infections usually occurs after trees' exposition to adverse abiotic factors and/or cork removal (Costa et al., 2004; Linaldeddu et al., 2011; Luque & Girbal, 1989; Marçais & Bréda, 2006; Sousa et al., 2007), we hypothesized that the plant GABA pool might be a triggering factor for the transition from latent to pathogenic lifestyle.

The data gathered suggest that *D. corticola* has a hemibiotrophic lifestyle, switching from a biotrophic to a necrotrophic interaction after plants' stressing episodes. This conclusion is corroborated by the fact that the fungus colonizes living plant tissues, secreting concomitantly proteins such as cerato-platanin and necrosis inducing factor, a strategy that characterizes the hemibiotrophic fungi (Dou & Zhou, 2012; Horbach et al., 2011).

In short, this work contributed largely to the protein characterization of *D. corticola* and subsequently for the *Botryosphaeriaceae* family. Further, we could infer about the molecular biology of the fungus, highlighting concomitantly some proteins that might play a crucial role during infection. Such information will be particularly valuable for the development of subsequent studies.

FUTURE PERSPECTIVES

This investigation raised some interesting questions that must be answered to improve the knowledge of the *D. corticola* molecular biology during infection. We believe, for instance, that the lipases found solely in the virulent strain might be determinant for the perforation of the *Quercus* sp. aerial tissues, a point of entry described by Paoletti et al. (2007). The quantification of the fungal lipolytic activity exposed to different substrates, including *Quercus* leaves, would be of great interest to evaluate the involvement of such proteins in the fungal colonization strategy. Similarly, the implications of the peptidase M35 prevalence in the virulent strain should be investigated to substantiate its role in the fungal pathogenicity. The relevance of each individual spot identified as peptidase M35 must equally be studied to confirm if the spots are indeed

modified proteins.

The up-regulation of cerato-platanin in response to the host mimicry indicates that this small-cysteine-rich protein might play a role in the virulent strain host colonization. However, there are, to our knowledge, no studies concerning the function of this protein in fungi belonging to the *Botryosphaeriaceae* family. First, it is necessary to verify the extracellular location of the protein. Previous studies demonstrated that regardless of the constant identification of cerato-platanin in the extracellular medium, the protein is primarily bound to the fungal cell wall (Boddi et al., 2004; Frías et al., 2014). The weak nature of the bond that links the protein to the cell wall is responsible for the identification of the protein in the extracellular medium (Frías et al., 2014). Second, it is important to study the significance of the expansin-like activity in the plant-fungal interaction. Finally, it should be determined if cerato-platanin functions as a scanvenger of fungal molecules susceptible to be recognized by the plant surveillance mechanism, or instead if works as a plant defence elicitor to amplify the oxidative burst that culminates in necrotic lesions (Baccelli et al., 2013; Barsottini et al., 2013; Frías et al., 2014; Frischmann et al., 2013; Lombardi et al., 2013).

In addition, the ability to metabolize γ-aminobutyric acid, particularly during infection, must be validated, confirming as well the presumed relationship of plant's GABA accumulation and the onset/ intensification of *D. corticola* infection.

On the other hand, the data gathered in this work strongly suggests that the avirulent strain resorts to a non-enzymatic mechanism widely used by brown-rot fungi to degrade the cork oak stem. The first approach to corroborate such hypothesis must comprise the quantification of the reactive molecules present in the extracellular medium during the degradation of diverse substrates. Further, the ocurrence of Fenton reactions to generate these radicals should be inferred and, if confirmed, establish the involvement of the ferritin-ribonucleotide reductase-like protein in the iron bioavailability.

Briefly, the questions raised in this work require a multidisciplinary approach to be answered, but surely will benefit the current understanding of the molecular biology of *D. corticola.*

REFERENCES

Baccelli, I. (2014). Cerato-platanin family proteins: one function for multiple biological roles? *Frontiers in Plant Science*. **5** (**1**): 769–772.

Baccelli, I., Luti, S., Bernardi, R., Scala, A., Pazzagli, L. (2014). Cerato-platanin shows expansin-like activity on cellulosic materials. *Applied Microbiology and Biotechnology*. **98** (**1**): 175–184.

Baccelli, I., Scala, A., Pazzagli, L., Bernardi, R. (2013). Early transcription of defence-related genes in *Platanus* × *acerifolia* leaves following treatment with cerato-platanin. *Biologia Plantarum*. **57** (**3**): 571–575.

Bae, H., Sicher, R., Kim, M., Kim, S.-H., Strem, M., Melnick, R., Bailey, B. (2009). The beneficial endophyte *Trichoderma hamatum* isolate DIS 219b promotes growth and delays the onset of the drought response in *Theobroma cacao*. *Journal of Experimental Botany*. **60** (**11**): 3279–3295.

Barsottini, M., Oliveira, J., Adamoski, D., Teixeira, P., Prado, P., Tiezzi, H., Sforça, M., Cassago, A., Portugal, R., Oliveira, P., Zeri, A., Dias, S., Pereira, G., Ambrosio, A. (2013). Functional diversification of cerato-platanins in *Moniliophthora perniciosa* as seen by differential expression and protein function specialization. *Molecular Plant-Microbe Interactions*. **26** (**11**): 1281–1293.

Boddi, S., Comparini, C., Calamassi, R., Pazzagli, L., Cappugi, G., Scala, A. (2004). Cerato-platanin protein is located in the cell walls of ascospores, conidia and hyphae of *Ceratocystis fimbriata* f sp *platani*. *FEMS Microbiology Letters*. **233** (**2**): 341–346.

Collins, C. (2013). *A Genomic and Proteomic Investigation of the Plant Pathogen* Armillaria mellea*: Buried Treasure or Hidden Threat?* National University of Ireland Maynooth.

Costa, A., Pereira, H., Oliveira, A. (2004). The effect of cork-stripping damage on diameter growth of *Quercus suber* L. *Forestry*. **77** (**1**): 1–8.

Dou, D., Zhou, J.-M. (2012). Phytopathogen effectors subverting host immunity: different foes, similar battleground. *Cell Host & Microbe*. **12** (**4**): 484–495.

Espino, J., Gutiérrez-Sánchez, G., Brito, N., Shah, P., Orlando, R., González, C. (2010). The *Botrytis cinerea* early secretome. *Proteomics*. **10** (**16**): 3020–3034.

Frías, M., Brito, N., González, M., González, C. (2014). The phytotoxic activity of the cerato-platanin BcSpl1 resides in a two-peptide motif on the protein surface. *Molecular Plant Pathology*. **15** (**4**): 342–351.

Frischmann, A., Neudl, S., Gaderer, R., Bonazza, K., Zach, S., Gruber, S., Spadiut, O., Friedbacher, G., Grothe, H., Seidl-Seiboth, V. (2013). Self-assembly at air/water interfaces and carbohydrate binding properties of the small secreted protein EPL1 from the fungus *Trichoderma atroviride*. *Journal of Biological Chemistry*. **288** (**6**): 4278–4287.

Horbach, R., Navarro-Quesada, A., Knogge, W., Deising, H. (2011). When and how to kill a plant cell: infection strategies of plant pathogenic fungi. *Journal of Plant Physiology*. **168** (**1**): 51–62.

Kinnersley, A., Turano, F. (2000). Gamma aminobutyric acid (GABA) and plant responses to stress. *Critical Reviews in Plant Sciences*. **19** (**6**): 479–509.

Li, B., Wang, W., Zong, Y., Qin, G., Tian, S. (2012). Exploring pathogenic mechanisms of *Botrytis cinerea* secretome under different ambient pH based on comparative proteomic analysis. *Journal of Proteome Research*. **11** (**8**): 4249–4260.

Linaldeddu, B., Sirca, C., Spano, D., Franceschini, A. (2009). Physiological responses of cork oak and holm oak to infection by fungal pathogens involved in oak decline. *Forest Pathology*. **39** (**4**): 232–238.

Linaldeddu, B., Sirca, C., Spano, D., Franceschini, A. (2011). Variation of endophytic cork oak-associated fungal communities in relation to plant health and water stress. *Forest Pathology*. **41** (**3**): 193–201.

Lombardi, L., Faoro, F., Luti, S., Baccelli, I., Martellini, F., Bernardi, R., Picciarelli, P., Scala, A., Pazzagli, L. (2013). Differential timing of defense-related responses induced by cerato-platanin and cerato-populin, two non-catalytic fungal elicitors. *Physiologia Plantarum*. **149** (**3**): 408–421.

Luque, J., Girbal, J. (1989). Dieback of cork oak (*Quercus suber*) in Catalonia (NE Spain) caused by *Botryosphaeria stevensii*. *European Journal of Forest Pathology*. **19** (**1**): 7–13.

Lynch, S., Eskalen, A., Zambino, P., Mayorquin, J., Wang, D. (2013). Identification and pathogenicity of *Botryosphaeriaceae* species associated with coast live oak (*Quercus agrifolia*) decline in southern California. *Mycologia*. **105** (**1**): 125–140.

Marçais, B., Bréda, N. (2006). Role of an opportunistic pathogen in the decline of stressed oak trees. *Journal of Ecology*. **94** (**6**): 1214–1223.

Nabais, C., Hagemeyer, J., Freitas, H. (2005). Nitrogen transport in the xylem sap of *Quercus ilex*: the role of ornithine. *Journal of Plant Physiology*. **162** (**5**): 603–606.

Paoletti, E., Anselmi, N., Franceschini, A. (2007). Pre-exposure to ozone predisposes oak leaves to attacks by *Diplodia corticola* and *Biscogniauxia mediterranea*. *The Scientific World Journal*. **7** (**S1**): 222–230.

Solomon, P., Oliver, R. (2001). The nitrogen content of the tomato leaf apoplast increases during infection by *Cladosporium fulvum*. *Planta*. **213** (**2**): 241–249.

Sousa, E., Santos, M., Varela, M., Henriques, J. (2007). *Perda de vigor dos montados de sobro e azinho: Análise da situação e perspectivas*. Ministério da Agricultura, do Desenvolvimento e das Pescas.

Úrbez-Torres, J., Peduto, F., Rooney-Latham, S., Gubler, W. (2010). First report of *Diplodia corticola* causing grapevine (*Vitis vinifera*) cankers and trunk cankers and dieback of canyon live oak (*Quercus chrysolepis*) in California. *Plant Disease*. **94** (**6**): 785–785.

APPENDIX I

CAA 008 EXT CONTROL VS. CAA 499 EXT CONTROL

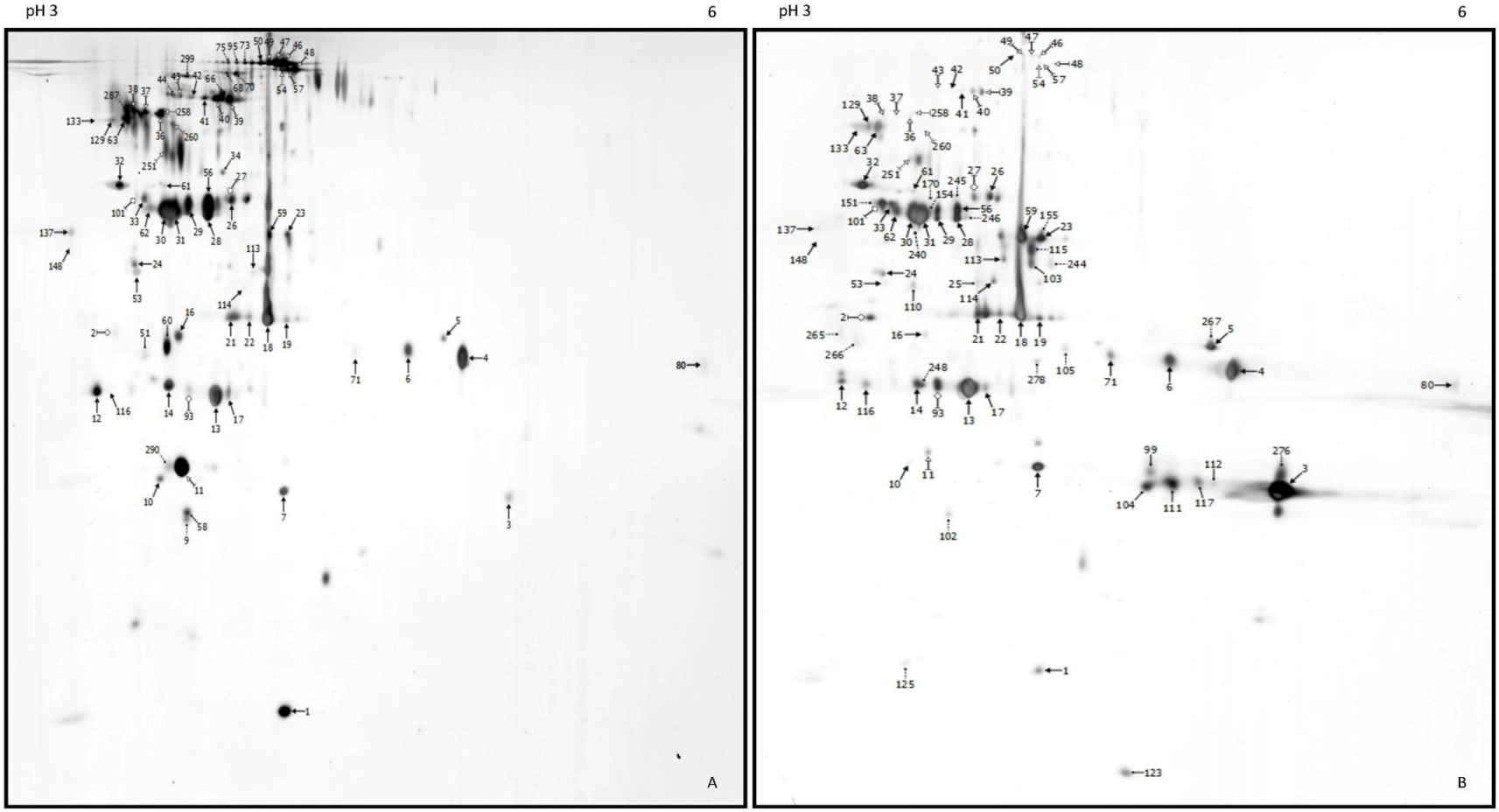

Legend:
- Spots common to both groups
- Up-regulated spots (identified)
- Up-regulated spots (non-identified)
- Down-regulated spots (identified)
- Down-regulated spots (non-identified)
- Spots exclusive of one of the groups (identified)
- Spots exclusive of one of the groups (non-identified)

Figure 16 | 2D average gels of *D. corticola* control secretomes of the avirulent (CAA 008, A) and virulent (CAA 499, B) strains. Three biological replicates were used for each condition. Gels were stained with Pierce® Silver Stain for Mass Spectrometry (Thermo Scientific, USA). Protein spots identified by *de novo* sequencing and/or MASCOT search are marked with filled arrow lines and the identifications are described on Table 9.

Table 9 | Summary of the extracellular proteins identified in CAA 008 EXT control and CAA 499 EXT control by *de novo* sequencing (1) and/or MASCOT search (2). Theoretical pI and MW (3) were searched with Compute pI/Mw tool available at ExPASy (Gasteiger et al., 2005) and the subcellular localization (4) deduced with WoLF PSORT predictor (Horton et al., 2007).

Protein	Spot	Accession number	Organism	FASTM/S E_{value}[1]	MASCOT total Ion Score[2]	Theoretical pI[3]	Theoretical Mw[3] (Da)	Subcellular localization[4]
Spots exclusive of CAA 008 EXT control								
Hydrolases								
GH 17 - Glycoside hydrolase family 17	51	K2STT8	*Macrophomina phaseolina*	2.30E-07	64	4.55	32022.55	Extracellular
Proteases								
Peptidase S10 - Putative carboxypeptidase s1 protein	34	R1GF60	*Neofusicoccum parvum*	0.00E+00	485	4.45	52146.52	Extracellular
Other functions								
Ferritin/ribonucleotide reductase-like protein	60	K2RIV9	*Macrophomina phaseolina*	0.00E+00	132	4.61	30766.62	Extracellular
Gamma-glutamyltransferase	58	DCO1_18s05278.t1	*Diplodia corticola*	—	170	4.48	22115.78	Extracellular
Spots exclusive of CAA 499 EXT control								
Hydrolases								
Lipase B (Uncharacterized protein)	25	K2R678	*Macrophomina phaseolina*	9.70E-08	113	5.43	48043.55	Extracellular
Lipase class 3	110	K2RK28	*Macrophomina phaseolina*	8.70E-20	—	5.09	30910.40	Extracellular
Putative ferulic acid esterase protein	103	R1EDH3	*Neofusicoccum parvum*	6.00E-14	—	4.79	34891.92	Extracellular

Continued on next page

Protein	Spot	Accession number	Organism	FASTM/S E_{value}[1]	MASCOT total Ion Score[2]	Theoretical pI[3]	Theoretical Mw[3] (Da)	Subcellular localization[4]
Proteases								
Peptidase M35 - Neutral protease 2	99	K2SDQ0	*Macrophomina phaseolina*	1.70E-19	—	5.34	36981.99	Extracellular
	104	K2SDQ0	*Macrophomina phaseolina*	1.20E-13	—	5.34	36981.99	Extracellular
	111	K2SDQ0	*Macrophomina phaseolina*	4.20E-05	—	5.34	36981.99	Extracellular
	112	K2SDQ0	*Macrophomina phaseolina*	2.60E-03	—	5.34	36981.99	Extracellular
	117	K2SDQ0	*Macrophomina phaseolina*	4.20E-05	—	5.34	36981.99	Extracellular
Other functions								
Putative extracellular guanyl-specific ribonuclease protein	123	R1H1L9	*Neofusicoccum parvum*	2.70E-20	—	5.11	14564.95	Extracellular
Spots down-regulated in CAA 499 EXT control								
Hydrolases								
Carboxylesterase family protein	48	DCO1_40s06646.t1	*Diplodia corticola*	—	76	4.68	61064.17	Extracellular
GH 31 - Putative α-glucosidase protein	46	R1H1X1	*Neofusicoccum parvum*	0.00E+00	321	4.65	110578.06	Extracellular
	47	R1H1X1	*Neofusicoccum parvum*	0.00E+00	330	4.65	110578.06	Extracellular
	57	R1H1X1	*Neofusicoccum parvum*	0.00E+00	260	4.65	110578.06	Extracellular
GH 55 - Putative glycoside hydrolase family 55 protein	39	R1EP88	*Neofusicoccum parvum*	0.00E+00	529	4.52	84093.46	Extracellular
	40	R1EP88	*Neofusicoccum parvum*	0.00E+00	548	4.52	84093.46	Extracellular
	43	R1EP88	*Neofusicoccum parvum*	1.90E-21	195	4.52	84093.46	Extracellular
Putative glutaminase protein	36	R1EUG4	*Neofusicoccum parvum*	6.40E-32	263	4.29	74937.86	Extracellular
	37	R1EUG4	*Neofusicoccum parvum*	0.00E+00	225	4.29	74937.86	Extracellular
	38	R1EUG4	*Neofusicoccum parvum*	0.00E+00	263	4.29	74937.86	Extracellular
	49	DCO1_62s08886.t1	*Diplodia corticola*	—	64	4.27	76639.88	Extracellular

Continued on next page

Protein	Spot	Accession number	Organism	FASTM/S E_{value}[1]	MASCOT total Ion Score[2]	Theoretical pI[3]	Theoretical Mw[3] (Da)	Subcellular localization[4]
Oxidoreductases								
Putative ligninase lg6 protein (Peroxidase)	11	R1GJT0	*Neofusicoccum parvum*	5.30E-32	512	5.20	32232.20	Extracellular
Spots up-regulated in CAA 499 EXT control								
Hydrolases								
GH 13 - Putative α-amylase a type-1,2 protein	101	K2QLM3	*Macrophomina phaseolina*	4.00E-31	—	4.73	54649.73	Extracellular
GH 17 - Glycoside hydrolase family 17	93	K2STT8	*Macrophomina phaseolina*	2.30E-07	—	4.55	32022.55	Extracellular
GH 43 - Putative glycoside hydrolase family 43 protein	27	R1GE80	*Neofusicoccum parvum*	1.30E-18	315	5.73	48185.65	Extracellular
Putative 5,3-nucleotidase protein	2	R1FUS1	*Neofusicoccum parvum*	3.70E-18	—	4.58	31154.86	Extracellular
Proteases								
Peptidase S10 - Putative carboxypeptidase s1 protein	101	R1GF60	*Neofusicoccum parvum*	1.30E-32	—	4.45	52146.52	Extracellular
Spots common to both control and infection-like								
Hydrolases								
GH 13 - Putative α-amylase a type-1,2 protein	62	R1GPA2	*Neofusicoccum parvum*	0.00E+00	373	4.53	56053.14	Extracellular
GH 15 - Glucoamylase	63	C0NJV0	*Ajellomyces capsulatus*	0.00E+00	490	5.32	70492.86	Extracellular
	129	R1GLG1	*Neofusicoccum parvum*	1.60E-14	—	4.83	68531.74	Extracellular
	133	Q9C1V4	*Talaromyces emersonii*	3.00E-27	—	4.44	65429.22	Extracellular

Continued on next page

Protein	Spot	Accession number	Organism	FASTM/S E_{value}[1]	MASCOT total Ion Score[2]	Theoretical pI[3]	Theoretical Mw[3] (Da)	Subcellular localization[4]
GH 17 - Glycoside hydrolase family 17	13	K2STT8	*Macrophomina phaseolina*	0.00E+00	363	4.55	32022.55	Extracellular
	17	K2STT8	*Macrophomina phaseolina*	2.20E-07	112	4.55	32022.55	Extracellular
	53	K2STT8	*Macrophomina phaseolina*	2.30E-07	130	4.55	32022.55	Extracellular
	114	K2STT8	*Macrophomina phaseolina*	5.20E-03	—	4.55	32022.55	Extracellular
GH 31 - Putative α-glucosidase protein	50	R1H1X1	*Neofusicoccum parvum*	2.40E-07	—	4.65	110578.06	Extracellular
GH 43 - Putative glycoside hydrolase family 43 protein	14	R1EDI8	*Neofusicoccum parvum*	5.70E-07	242	4.48	37269.32	Extracellular
	26	R1GE80	*Neofusicoccum parvum*	2.00E-09	169	5.73	48185.65	Extracellular
GH 55 - Putative glycoside hydrolase family 55 protein	42	R1EP88	*Neofusicoccum parvum*	0.00E+00	529	4.52	84093.46	Extracellular
GH 64 - Putative glucanase b protein (β-1,3-glucanase)	24	R1GK17	*Neofusicoccum parvum*	0.00E+00	327	5.82	42116.55	Nuclear
GH 71 - Glycoside hydrolase family 71	32	K2R498	*Macrophomina phaseolina*	5.50E-17	250	4.84	49264.81	Extracellular
	33	R1GD52	Neofusicoccum parvum	1.50E-09	134	4.21	43378.40	Extracellular
GH 93 - Putative glycoside hydrolase family 93 protein (Sialidase/ Neuraminidase)	12	R1GGQ9	*Neofusicoccum parvum*	1.40E-07	180	4.41	38051.25	Extracellular
	24	K2RBR1	*Macrophomina phaseolina*	9.30E-11	—	4.32	40074.67	Extracellular
	53	K2RBR1	*Macrophomina phaseolina*	0.00E+00	126	4.32	40074.67	Extracellular
Phosphoesterase	28	K2RUW5	*Macrophomina phaseolina*	5.90E-29	485	4.64	43928.97	Extracellular
	29	K2RUW5	*Macrophomina phaseolina*	8.80E-03	151	4.64	43928.97	Extracellular
	56	K2RUW5	*Macrophomina phaseolina*	3.00E-15	—	4.64	43928.97	Extracellular
Putative ferulic acid esterase protein	23	R1EDH3	*Neofusicoccum parvum*	1.50E-13	32	4.79	34891.92	Extracellular
Uncharacterized protein (fumarylacetoacetase)	31	A0A072PA62	*Exophiala aquamarina*	4.60E-26	—	5.84	46110.07	Cytoplasmic

Continued on next page

Protein	Spot	Accession number	Organism	FASTM/S E_{value}[1]	MASCOT total Ion Score[2]	Theoretical pI[3]	Theoretical Mw[3] (Da)	Subcellular localization[4]
Proteases								
Peptidase A1 - Putative a chain endothiapepsin	18	R1ESA5	*Neofusicoccum parvum*	0.00E+00	491	5.45	42563.05	Extracellular
	19	R1ESA5	*Neofusicoccum parvum*	4.20E-10	71	5.45	42563.05	Extracellular
	21	R1ESA5	*Neofusicoccum parvum*	0.00E+00	228	5.45	42563.05	Extracellular
	22	R1ESA5	*Neofusicoccum parvum*	1.90E-04	34	5.45	42563.05	Extracellular
	59	R1ESA5	*Neofusicoccum parvum*	4.30E-10	491	5.45	42563.05	Extracellular
	137	R1GM42	*Neofusicoccum parvum*	1.60E-08	—	4.27	41788.15	Extracellular
	148	R1GM42	*Neofusicoccum parvum*	1.60E-08	—	4.27	41788.15	Extracellular
Peptidase M28 - Putative leucyl aminopeptidase protein	5	R1GBR8	*Neofusicoccum parvum*	1.20E-23	222	5.17	40706.16	Extracellular
Peptidase M35 - Neutral protease 2	3	K2SDQ0	*Macrophomina phaseolina*	1.20E-25	124	5.34	36981.99	Extracellular
Peptidase S10 - Putative carboxypeptidase s1 protein	29	R1GF60	*Neofusicoccum parvum*	5.50E-16	80	4.45	52146.52	Extracellular
	30	R1GF60	*Neofusicoccum parvum*	0.00E+00	486	4.45	52146.52	Extracellular
	31	R1GF60	*Neofusicoccum parvum*	0.00E+00	668	4.45	52146.52	Extracellular
	41	R1GF60	*Neofusicoccum parvum*	1.50E-14	112	4.45	52146.52	Extracellular
	62	R1GF60	*Neofusicoccum parvum*	4.40E-28	345	4.45	52146.52	Extracellular
Peptidase S8 - Putative peptidase s8 s53 subtilisin kexin sedolisin protein	16	R1G6D0	*Neofusicoccum parvum*	0.00E+00	478	4.18	43069.94	Extracellular
	80	R1GM11	*Neofusicoccum parvum*	6.50E-11	—	6.07	39070.39	Extracellular
	116	R1EAW3	*Neofusicoccum parvum*	4.80E-02	—	4.73	40860.15	Extracellular
Oxidoreductases								
Alcohol dehydrogenase	7	DCO1_41s07359.t1	*Diplodia corticola*	—	50	6.32	40875.17	Cytoplasmic
Other functions								
Cell wall protein	10	DCO1_41s07341.t1	*Diplodia corticola*	—	173	4.48	21235.80	Extracellular
Cerato-platanin	1	E3QKQ8	*Colletotrichum graminicola*	6.90E-11	—	4.53	14119.72	Extracellular
Necrosis inducing protein	7	T0JMK5	*Colletotrichum gloeosporioides*	2.20E-17	—	5.80	24934.67	Extracellular

Continued on next page

Protein	Spot	Accession number	Organism	FASTM/S E_{value}[1]	MASCOT total Ion Score[2]	Theoretical pI[3]	Theoretical Mw[3] (Da)	Subcellular localization[4]
Putative extracellular guanyl-specific ribonuclease protein	1	R1H1L9	*Neofusicoccum parvum*	3.30E-12	—	5.11	14564.95	Extracellular
Putative pectate lyase a protein (Lyase 1)	113	R1ED02	*Neofusicoccum parvum*	6.50E-08	—	4.88	33291.57	Extracellular
Spherulation-specific family 4	4	K2RK67	*Macrophomina phaseolina*	1.00E-25	502	4.04	30373.78	Extracellular
	6	K2RK67	*Macrophomina phaseolina*	2.20E-20	502	4.04	30373.78	Extracellular
	71	K2RK67	*Macrophomina phaseolina*	2.80E-10	—	4.04	30373.78	Extracellular
Unknown								
Uncharacterized protein	61	K2RWL4	*Macrophomina phaseolina*	6.80E-28	209	4.34	52231.60	Extracellular

CAA 008 EXT INFECTION-LIKE VS. CAA 499 EXT INFECTION-LIKE

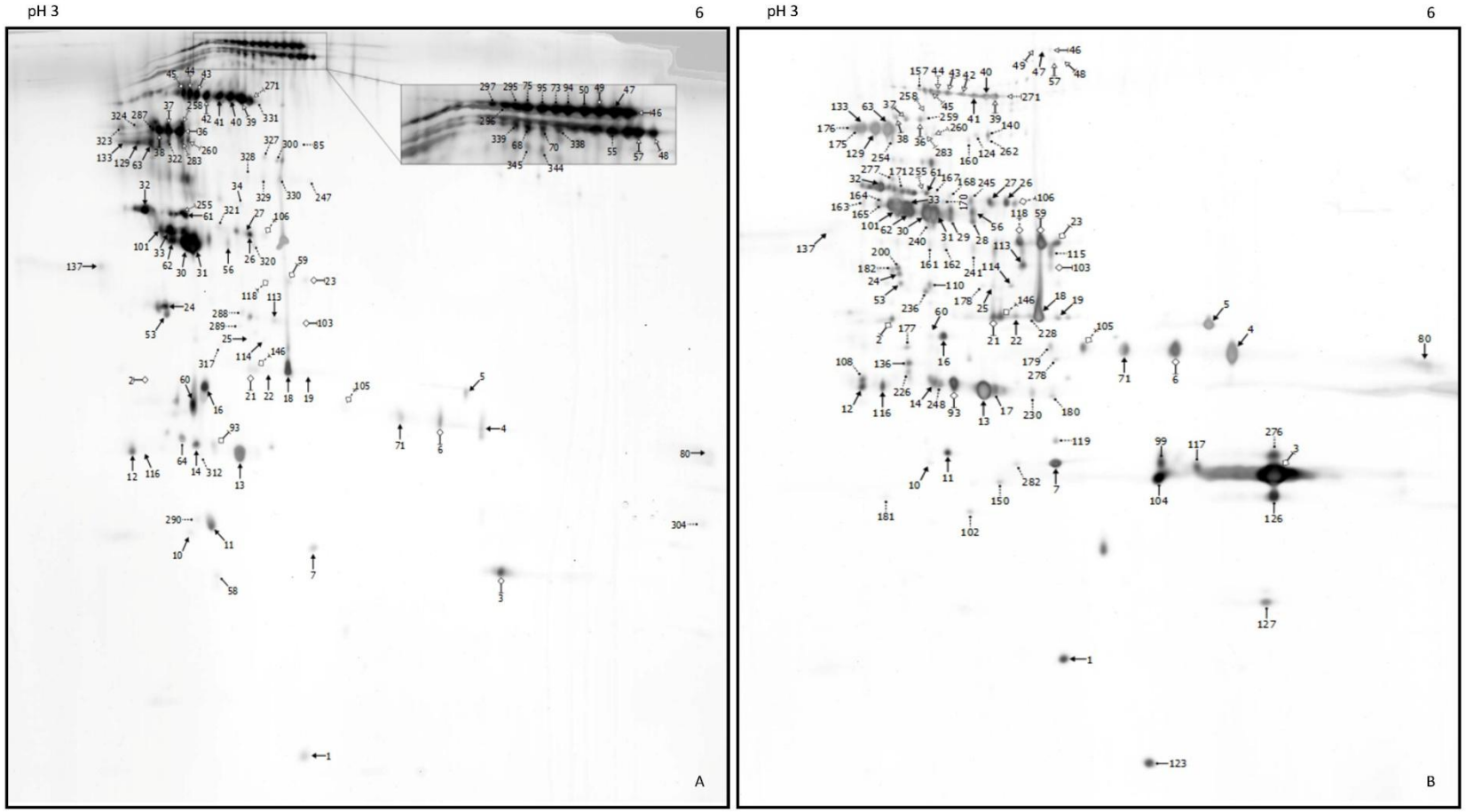

Legend:
- Spots common to both groups
- Up-regulated spots (identified)
- Up-regulated spots (non-identified)
- Down-regulated spots (identified)
- Down-regulated spots (non-identified)
- Spots exclusive of one of the groups (identified)
- Spots exclusive of one of the groups (non-identified)

Figure 17 | 2D average gels of *D. corticola* infection-like secretomes of the avirulent (CAA 008, A) and virulent (CAA 499, B) strains. Three biological replicates were used for each condition. Gels were stained with Pierce® Silver Stain for Mass Spectrometry (Thermo Scientific, USA). Protein spots identified by *de novo* sequencing and/or MASCOT search are marked with filled arrow lines and the identifications are described on Table 10.

Table 10 | Summary of the extracellular proteins identified in CAA 008 EXT infection-like and CAA 499 EXT infection-like by *de novo* sequencing (1) and/or MASCOT search (2). Theoretical pI and MW (3) were searched with Compute pI/Mw tool available at ExPASy (Gasteiger et al., 2005) and the subcellular localization (4) deduced with WoLF PSORT predictor (Horton et al., 2007).

Protein	Spot	Accession number	Organism	FASTM/S E_{value}[1]	MASCOT total Ion Score[2]	Theoretical pI[3]	Theoretical Mw[3] (Da)	Subcellular localization[4]
Spots exclusive of CAA 008 EXT infection-like								
Hydrolases								
GH 31 - Putative α-glucosidase protein	50	R1H1X1	*Neofusicoccum parvum*	2.40E-07	—	4.65	110578.06	Extracellular
GH 43 - Putative glycoside hydrolase family 43 protein	64	R1EDI8	*Neofusicoccum parvum*	3.60E-04	144	4.48	37269.32	Extracellular
Proteases								
Peptidase S10 - Putative carboxypeptidase s1 protein	34	R1GF60	*Neofusicoccum parvum*	0.00E+00	485	4.45	52146.52	Extracellular
Other functions								
Gamma-glutamyltransferase	58	DCO1_18s05278.t1	*Diplodia corticola*	—	170	4.48	22115.78	Extracellular
Spots exclusive of CAA 499 EXT infection-like								
Hydrolases								
GH 17 - Glycoside hydrolase family 17	17	K2STT8	*Macrophomina phaseolina*	2.20E-07	112	4.55	32022.55	Extracellular
Lipase class 3	110	K2RK28	*Macrophomina phaseolina*	8.70E-20	—	5.09	30910.40	Extracellular
Phosphoesterase	28	K2RUW5	*Macrophomina phaseolina*	5.90E-29	485	4.64	43928.97	Extracellular
	29	K2RUW5	*Macrophomina phaseolina*	8.80E-03	151	4.64	43928.97	Extracellular

Continued on next page

Protein	Spot	Accession number	Organism	FASTM/S E_{value}[1]	MASCOT total Ion Score[2]	Theoretical pI[3]	Theoretical Mw[3] (Da)	Subcellular localization[4]
Proteases								
Peptidase M35 - Neutral protease 2	99	K2SDQ0	*Macrophomina phaseolina*	1.70E-19	—	5.34	36981.99	Extracellular
	104	K2SDQ0	*Macrophomina phaseolina*	1.20E-13	—	5.34	36981.99	Extracellular
	117	K2SDQ0	*Macrophomina phaseolina*	4.20E-05	—	5.34	36981.99	Extracellular
	126	K2SDQ0	*Macrophomina phaseolina*	1.00E-18	—	5.34	36981.99	Extracellular
Peptidase M43 - Putative metalloprotease 1 protein	136	R1GAQ6	*Neofusicoccum parvum*	5.10E-07	—	4.80	30491.66	Extracellular
Peptidase S10 - Putative carboxypeptidase s1 protein	29	R1GF60	*Neofusicoccum parvum*	5.50E-16	80	4.45	52146.52	Extracellular
Other functions								
Putative extracellular guanyl-specific ribonuclease protein	123	R1H1L9	*Neofusicoccum parvum*	2.70E-20	—	5.11	14564.95	Extracellular
Uncharacterized protein (Cell outer membrane)	127	A0A017S003	*Aspergillus ruber*	1.40E-03		6.29	18838.42	Extracellular
Spots down-regulated in CAA 499 EXT infection-like								
Hydrolases								
Carboxylesterase family protein	48	DCO1_40s06646.t1	*Diplodia corticola*	—	76	4.68	61064.17	Extracellular
GH 31 - Putative α-glucosidase protein	46	R1H1X1	*Neofusicoccum parvum*	0.00E+00	321	4.65	110578.06	Extracellular
	57	R1H1X1	*Neofusicoccum parvum*	0.00E+00	260	4.65	110578.06	Extracellular
GH 55 - Putative glycoside hydrolase family 55 protein	39	R1EP88	*Neofusicoccum parvum*	0.00E+00	529	4.52	84093.46	Extracellular
	42	R1EP88	*Neofusicoccum parvum*	0.00E+00	529	4.52	84093.46	Extracellular
	43	R1EP88	*Neofusicoccum parvum*	1.90E-21	195	4.52	84093.46	Extracellular

Continued on next page

Protein	Spot	Accession number	Organism	FASTM/S E_{value}[1]	MASCOT total Ion Score[2]	Theoretical pI[3]	Theoretical Mw[3] (Da)	Subcellular localization[4]
Putative glutaminase protein	36	R1EUG4	*Neofusicoccum parvum*	6.40E-32	263	4.29	74937.86	Extracellular
	37	R1EUG4	*Neofusicoccum parvum*	0.00E+00	225	4.29	74937.86	Extracellular
	38	R1EUG4	*Neofusicoccum parvum*	0.00E+00	263	4.29	74937.86	Extracellular
	49	DCO1_62s08886.t1	*Diplodia corticola*	—	64	4.27	76639.88	Extracellular
Spots up-regulated in CAA 499 EXT infection-like								
Hydrolases								
GH 17 - Glycoside hydrolase family 17	93	K2STT8	*Macrophomina phaseolina*	2.30E-07	—	4.55	32022.55	Extracellular
Putative 5,3-nucleotidase protein	2	R1FUS1	*Neofusicoccum parvum*	3.70E-18	—	4.58	31154.86	Extracellular
Putative ferulic acid esterase protein	23	R1EDH3	*Neofusicoccum parvum*	1.50E-13	32	4.79	34891.92	Extracellular
	103	R1EDH3	*Neofusicoccum parvum*	6.00E-14	—	4.79	34891.92	Extracellular
Proteases								
Peptidase A1 - Putative a chain endothiapepsin	21	R1ESA5	*Neofusicoccum parvum*	0.00E+00	228	5.45	42563.05	Extracellular
	59	R1ESA5	*Neofusicoccum parvum*	4.30E-10	491	5.45	42563.05	Extracellular
Peptidase M35 - Neutral protease 2	3	K2SDQ0	*Macrophomina phaseolina*	1.20E-25	124	5.34	36981.99	Extracellular
Spots common to both control and infection-like								
Hydrolases								
GH 13 - Putative α-amylase a type-1,2 protein	62	R1GPA2	*Neofusicoccum parvum*	0.00E+00	373	4.53	56053.14	Extracellular
	101	K2QLM3	*Macrophomina phaseolina*	4.00E-31	—	4.73	54649.73	Extracellular
GH 15 - Glucoamylase	63	C0NJV0	*Ajellomyces capsulatus*	0.00E+00	490	5.32	70492.86	Extracellular
	129	R1GLG1	*Neofusicoccum parvum*	1.60E-14	—	4.83	68531.74	Extracellular
	133	Q9C1V4	*Talaromyces emersonii*	3.00E-27	—	4.44	65429.22	Extracellular

Continued on next page

Protein	Spot	Accession number	Organism	FASTM/S E_{value}[1]	MASCOT total Ion Score[2]	Theoretical pI[3]	Theoretical Mw[3] (Da)	Subcellular localization[4]
GH 17 - Glycoside hydrolase family 17	13	K2STT8	*Macrophomina phaseolina*	0.00E+00	363	4.55	32022.55	Extracellular
	53	K2STT8	*Macrophomina phaseolina*	2.30E-07	130	4.55	32022.55	Extracellular
	114	K2STT8	*Macrophomina phaseolina*	5.20E-03	—	4.55	32022.55	Extracellular
GH 31 - Putative α-glucosidase protein	47	R1H1X1	*Neofusicoccum parvum*	0.00E+00	330	4.65	110578.06	Extracellular
GH 43 - Putative glycoside hydrolase family 43 protein	14	R1EDI8	*Neofusicoccum parvum*	5.70E-07	242	4.48	37269.32	Extracellular
	26	R1GE80	*Neofusicoccum parvum*	2.00E-09	169	5.73	48185.65	Extracellular
	27	R1GE80	*Neofusicoccum parvum*	1.30E-18	315	5.73	48185.65	Extracellular
GH 55 - Putative glycoside hydrolase family 55 protein	40	R1EP88	*Neofusicoccum parvum*	0.00E+00	548	4.52	84093.46	Extracellular
GH 64 - Putative glucanase b protein (β-1,3-glucanase)	24	R1GK17	*Neofusicoccum parvum*	0.00E+00	327	5.82	42116.55	Nuclear
GH 71 - Glycoside hydrolase family 71	32	K2R498	*Macrophomina phaseolina*	5.50E-17	250	4.84	49264.81	Extracellular
	33	R1GD52	Neofusicoccum parvum	1.50E-09	134	4.21	43378.40	Extracellular
GH 93 - Putative glycoside hydrolase family 93 protein (Sialidase/ Neuraminidase)	12	R1GGQ9	*Neofusicoccum parvum*	1.40E-07	180	4.41	38051.25	Extracellular
	24	K2RBR1	*Macrophomina phaseolina*	9.30E-11	—	4.32	40074.67	Extracellular
	53	K2RBR1	*Macrophomina phaseolina*	0.00E+00	126	4.32	40074.67	Extracellular
Lipase B (Uncharacterized protein)	25	K2R678	*Macrophomina phaseolina*	9.70E-08	113	5.43	48043.55	Extracellular
Phosphoesterase	56	K2RUW5	*Macrophomina phaseolina*	3.00E-15	—	4.64	43928.97	Extracellular
Uncharacterized protein (fumarylacetoacetase)	31	A0A072PA62	*Exophiala aquamarina*	4.60E-26	—	5.84	46110.07	Cytoplasmic
Proteases								
Peptidase A1 - Putative a chain endothiapepsin	18	R1ESA5	*Neofusicoccum parvum*	0.00E+00	491	5.45	42563.05	Extracellular
	19	R1ESA5	*Neofusicoccum parvum*	4.20E-10	71	5.45	42563.05	Extracellular
	22	R1ESA5	*Neofusicoccum parvum*	1.90E-04	34	5.45	42563.05	Extracellular
	137	R1GM42	*Neofusicoccum parvum*	1.60E-08	—	4.27	41788.15	Extracellular

Continued on next page

Protein	Spot	Accession number	Organism	FASTM/S E_{value}[1]	MASCOT total Ion Score[2]	Theoretical pI[3]	Theoretical Mw[3] (Da)	Subcellular localization[4]
Peptidase M28 - Putative leucyl aminopeptidase protein	5	R1GBR8	*Neofusicoccum parvum*	1.20E-23	222	5.17	40706.16	Extracellular
Peptidase S10 - Putative carboxypeptidase s1 protein	30	R1GF60	*Neofusicoccum parvum*	0.00E+00	486	4.45	52146.52	Extracellular
	31	R1GF60	*Neofusicoccum parvum*	0.00E+00	668	4.45	52146.52	Extracellular
	41	R1GF60	*Neofusicoccum parvum*	1.50E-14	112	4.45	52146.52	Extracellular
	62	R1GF60	*Neofusicoccum parvum*	4.40E-28	345	4.45	52146.52	Extracellular
	101	R1GF60	*Neofusicoccum parvum*	1.30E-32	—	4.45	52146.52	Extracellular
Peptidase S8 - Putative peptidase s8 s53 subtilisin kexin sedolisin protein	16	R1G6D0	*Neofusicoccum parvum*	0.00E+00	478	4.18	43069.94	Extracellular
	80	R1GM11	*Neofusicoccum parvum*	6.50E-11	—	6.07	39070.39	Extracellular
	116	R1EAW3	*Neofusicoccum parvum*	4.80E-02	—	4.73	40860.15	Extracellular
Oxidoreductases								
Alcohol dehydrogenase	7	DCO1_41s07359.t1	*Diplodia corticola*	—	50	6.32	40875.57	Cytoplasmic
Putative ligninase lg6 protein (Peroxidase)	11	R1GJT0	*Neofusicoccum parvum*	5.30E-32	512	5.20	32232.20	Extracellular
Other functions								
Cell wall protein	10	DCO1_41s07341.t1	*Diplodia corticola*	—	173	4.48	21235.80	Extracellular
Cerato-platanin	1	E3QKQ8	*Colletotrichum graminicola*	6.90E-11	—	4.53	14119.72	Extracellular
Ferritin/ribonucleotide reductase-like protein	60	K2RIV9	*Macrophomina phaseolina*	0.00E+00	132	4.61	30766.62	Extracellular
Necrosis inducing protein	7	T0JMK5	*Colletotrichum gloeosporioides*	2.20E-17	—	5.80	24934.67	Extracellular
Putative extracellular guanyl-specific ribonuclease protein	1	R1H1L9	*Neofusicoccum parvum*	3.30E-12	—	5.11	14564.95	Extracellular

Continued on next page

Protein	Spot	Accession number	Organism	FASTM/S E_{value}[1]	MASCOT total Ion Score[2]	Theoretical pI[3]	Theoretical Mw[3] (Da)	Subcellular localization[4]
Putative pectate lyase a protein (Lyase 1)	113	R1ED02	*Neofusicoccum parvum*	6.50E-08	—	4.88	33291.57	Extracellular
Spherulation-specific family 4	4	K2RK67	*Macrophomina phaseolina*	1.00E-25	502	4.04	30373.78	Extracellular
	71	K2RK67	*Macrophomina phaseolina*	2.80E-10	—	4.04	30373.78	Extracellular
Unknown								
Uncharacterized protein	61	K2RWL4	*Macrophomina phaseolina*	6.80E-28	209	4.34	52231.60	Extracellular

CAA 008 INT CONTROL VS. CAA 499 INT CONTROL

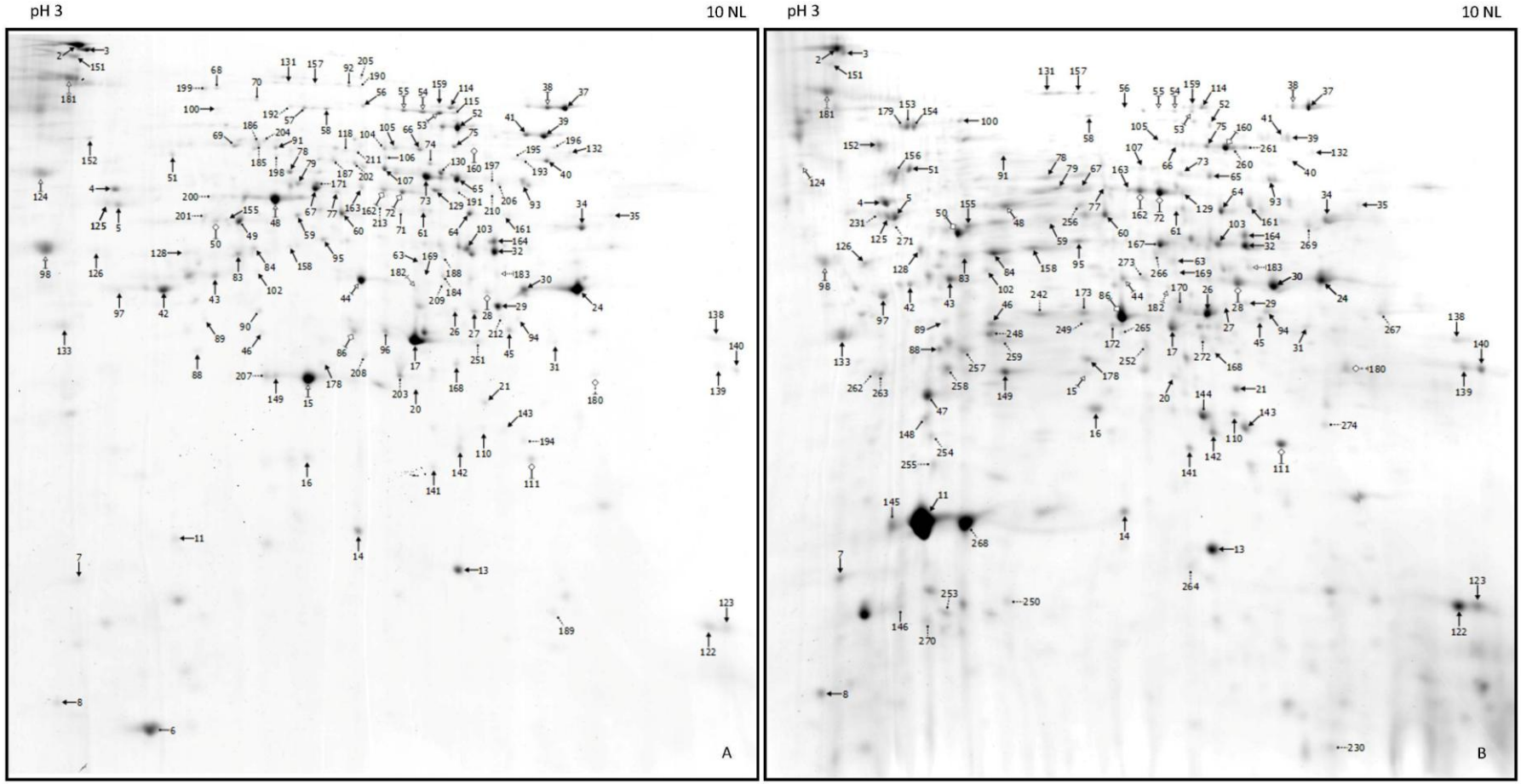

Figure 18 | 2D average gels of *D. corticola* control proteomes of the avirulent (CAA 008, A) and virulent (CAA 499, B) strains. Three biological replicates were used for each condition. Gels were stained with CBB-250. Protein spots identified by *de novo* sequencing and/or MASCOT search are marked with filled arrow lines and the identifications are described on Table 11.

Table 11 | Summary of the intracellular proteins identified in CAA 008 INT control and CAA 499 INT control by *de novo* sequencing (1) and/or MASCOT search (2). Theoretical pI and MW (3) were searched with Compute pI/Mw tool available at ExPASy (Gasteiger et al., 2005) and the subcellular localization (4) deduced with WoLF PSORT predictor (Horton et al., 2007).

Protein	Spot	Accession number	Organism	FASTM/S E_{value} [1]	MASCOT total Ion Score [2]	Theoretical pI [3]	Theoretical Mw [3] (Da)	Subcellular localization [4]
Spots exclusive of CAA 008 INT control								
Hydrolases								
αβ hydrolase	71	R1EXW5	*Neofusicoccum parvum*	0.00E+00	429	5.88	49829.51	Mitochondrial
Putative esterase (s-formylglutathione hydrolase)	96	K2S3K9	*Macrophomina phaseolina*	0.00E+00	318	6.07	31988.10	Mitochondrial
Putative β-lactamase family protein	49	R1G5K7	*Neofusicoccum parvum*	0.00E+00	930	5.34	44700.99	Cytoplasmic
Proteases								
Peptidase M1 - Peptidase M1 alanine aminopeptidase/ leukotriene A4 hydrolase	92	R1EX72	*Neofusicoccum parvum*	9.70E-15	50	5.80	98026.88	Cytoplasmic
Peptidase M49 - Peptidase M49 dipeptidyl-peptidase III	57	K2RA25	*Macrophomina phaseolina*	3.30E-26	274	5.53	79140.74	Cytoplasmic
Peptidase T1A - Proteasome subunit α type	90	R1G2P7	*Neofusicoccum parvum*	3.40E-21	54	5.72	31950.79	Cytoplasmic
Oxidoreductases								
Catalase-peroxidase	115	K2QZ33	*Macrophomina phaseolina*	0.00E+00	639	5.82	80922.69	Cytoplasmic
Galactokinase	69	K2RCE8	*Macrophomina phaseolina*	4.30E-28	—	5.55	57200.17	Cytoplasmic
Putative choline oxidase protein	118	R1EJS8	*Neofusicoccum parvum*	0.00E+00	341	6.30	60138.57	Cytoplasmic
Putative fggy-family carbohydrate kinase protein	69	R1GNA2	*Neofusicoccum parvum*	3.60E-34	476	5.18	65434.09	Cytoplasmic

Continued on next page

Protein	Spot	Accession number	Organism	FASTM/S E_{value} [1]	MASCOT total Ion Score [2]	Theoretical pI [3]	Theoretical Mw [3] (Da)	Subcellular localization [4]
Putative nadh-ubiquinone oxidoreductase 78 kDa subunit protein	70	R1E5C6	*Neofusicoccum parvum*	8.00E-13	128	5.94	81566.38	Mitochondrial
Transferases								
α-D-phosphohexomutase superfamily	74	K2S027	*Macrophomina phaseolina*	5.60E-34	254	5.76	60123.07	Cytoplasmic
	106	DCO1_2s00877.t1	*Diplodia corticola*	—	71	6.00	59921.85	Cytoplasmic
Transketolase	115	K2RZI6	*Macrophomina phaseolina*	1.40E-07	—	5.87	74975.89	Cytoplasmic
Other functions								
Heat shock protein Hsp70	68	K2RVT5	*Macrophomina phaseolina*	2.90E-03	—	5.12	79970.70	Cytoplasmic
Putative cyanovirin-n family protein	6	R1GQI8	*Neofusicoccum parvum*	1.50E-19	83	4.73	12102.21	Cytoplasmic
<u>Spots exclusive of CAA 499 INT control</u>								
Hydrolases								
αβ hydrolase - Putative dienelactone hydrolase family protein	170	R1G7F4	*Neofusicoccum parvum*	0.00E+00	336	5.99	29496.62	Cytoplasmic
β-lactamase family protein	146	DCO1_1s00126.t1	*Diplodia corticola*	—	43	5.50	44772.36	Peroxisomal
Proteases								
Peptidase M35 - Neutral protease 2	47	K2SDQ0	*Macrophomina phaseolina*	1.30E-22	195	5.34	36981.99	Extracellular
Oxidoreductases								
Choline dehydrogenase	153	I8A444	*Aspergillus oryzae*	9.00E-08	637	4.91	67679.52	Extracellular
	154	I8A444	*Aspergillus oryzae*	1.00E-09	540	4.91	67679.52	Extracellular
	179	DCO1_53s07484.t1	*Diplodia corticola*	—	148	4.93	67662.73	Extracellular
Putative fad binding domain-containing protein	156	R1EYD9	*Neofusicoccum parvum*	8.40E-03	749	4.71	57220.33	Extracellular

Continued on next page

Protein	Spot	Accession number	Organism	FASTM/S E_{value}[1]	MASCOT total Ion Score[2]	Theoretical pI[3]	Theoretical Mw[3] (Da)	Subcellular localization[4]
NADH:flavin oxidoreductase/NADH oxidase family protein	167	R1EE14	*Neofusicoccum parvum*	0.00E+00	1477	5.97	41452.60	Mitochondrial
Superoxide dismutase [Mn/Fe]	144	K2RKY9	*Macrophomina phaseolina*	2.80E-04	120	8.89	33373.71	Membranar
Transferases								
Putative glutathione s-transferase protein	144	R1E9W5	*Neofusicoccum parvum*	0.00E+00	111	5.92	25351.88	Nuclear
S-methyl-5'-thioadenosine phosphorylase	172	R1GFT7	*Neofusicoccum parvum*	3.30E-30	112	5.85	33729.16	Cytoplasmic
Other functions								
Outer membrane β-barrel	145	A0A017S003	*Aspergillus ruber*	6.60E-08	752	6.29	18838.42	Cytoplasmic
	148	A0A017S003	*Aspergillus ruber*	6.70E-08	468	6.29	18838.42	Cytoplasmic
	153	DCO1_53s07485.t1	*Diplodia corticola*	—	98	5.29	18733.37	Cytoplasmic
Putative nmra-like family protein (pyridoxal-phosphate dependent enzyme)	173	R1G4S7	*Neofusicoccum parvum*	0.00E+00	604	5.79	34755.99	Cytoplasmic
Unknown								
Uncharacterized protein	146	K2S8R4	*Macrophomina phaseolina*	1.80E-11	—	5.20	14512.76	Nuclear
<u>Spots down-regulated in CAA 499 INT control</u>								
Proteases								
Peptidase A1 - Putative aspartic endopeptidase pep2 protein	98	R1GUW7	*Neofusicoccum parvum*	0.00E+00	214	4.73	43261.72	Extracellular
Peptidase S8 - Putative autophagic serine protease alp2 protein	98	R1G6D0	*Neofusicoccum parvum*	1.40E-15	146	4.18	43069.94	Cytoplasmic
	124	R1GMY2	*Neofusicoccum parvum*	6.80E-14	—	4.50	62019.98	Extracellular

Continued on next page

Protein	Spot	Accession number	Organism	FASTM/S E_{value} [1]	MASCOT total Ion Score [2]	Theoretical pI [3]	Theoretical Mw [3] (Da)	Subcellular localization [4]
Oxidoreductases								
Catalase-peroxidase	53	K2QZ33	*Macrophomina phaseolina*	0.00E+00	667	5.82	80922.69	Cytoplasmic
	54	K2QZ33	*Macrophomina phaseolina*	0.00E+00	677	5.82	80922.69	Cytoplasmic
	55	K2QZ33	*Macrophomina phaseolina*	1.80E-16	229	5.82	80922.69	Cytoplasmic
Transferases								
Dj-1 family protein	15	L2FW83	*Colletotrichum gloeosporioides*	1.50E-21	331	5.41	26577.56	Cytoplasmic
Methionine synthase vitamin-B12 independent	38	K2RD18	*Macrophomina phaseolina*	0.00E+00	921	6.43	86349.70	Cytoplasmic
Lyases								
Ketose-bisphosphate aldolase class-2	44	K2RZT2	*Macrophomina phaseolina*	0.00E+00	1111	5.72	39741.04	Cytoplasmic
Putative oxalate protein (Bicupin oxalate deCO2ase/Oxase)	124	R1E9V1	*Neofusicoccum parvum*	0.00E+00	391	4.57	48901.21	Extracellular
Hydratases								
Enolase	48	K2SCR2	*Macrophomina phaseolina*	0.00E+00	958	5.29	47075.26	Cytoplasmic
Isomerases								
Aldose 1-epimerase	124	K2RLW1	*Macrophomina phaseolina*	2.90E-18	153	4.66	43895.67	Extracellular
Spots up-regulated in CAA 499 INT control								
Hydrolases								
Putative acetyl-hydrolase protein	160	R1E7A7	*Neofusicoccum parvum*	0.00E+00	528	6.17	58163.23	Mitochondrial
Putative β-lactamase family protein	50	R1G5K7	*Neofusicoccum parvum*	9.00E-31	729	5.34	44700.99	Cytoplasmic
Oxidoreductases								
Malate dehydrogenase	28	S8AYZ5	*Penicillium oxalicum*	9.80E-09	87	7.71	35885.01	Mitochondrial
Dihydrolipoyl dehydrogenase	72	R1EKH2	*Neofusicoccum parvum*	0.00E+00	1237	6.94	54773.98	Mitochondrial
	162	K2RSR2	*Macrophomina phaseolina*	0.00E+00	472	7.22	54346.46	Mitochondrial

Continued on next page

Protein	Spot	Accession number	Organism	FASTM/S E_{value} [1]	MASCOT total Ion Score [2]	Theoretical pI [3]	Theoretical Mw [3] (Da)	Subcellular localization [4]
Saccharopine dehydrogenase / Homospermidine synthase	162	K2RNB4	*Macrophomina phaseolina*	0.00E+00	663	5.86	50151.34	Cytoplasmic
Superoxide dismutase [Mn/Fe]	111	R1GPF7	*Neofusicoccum parvum*	0.00E+00	211	9.13	25360.53	Mitochondrial
Thioredoxin reductase	28	M2QTA7	*Cochliobolus sativus*	0.00E+00	793	6.60	33646.58	Cytoplasmic
Hydratases								
Enolase	50	K2SCR2	*Macrophomina phaseolina*	4.40E-09	—	5.29	47075.26	Cytoplasmic
Other functions								
Putative nmra-like family protein (pyridoxal-phosphate dependent enzyme)	86	R1G4S7	*Neofusicoccum parvum*	0.00E+00	1009	5.79	34755.99	Cytoplasmic
Spots common to both control and infection-like								
Hydrolases								
αβ hydrolase	46	DCO1_9s03329.t1	*Diplodia corticola*	—	65	5.51	32613.91	Mitochondrial
	61	R1EXW5	*Neofusicoccum parvum*	4.50E-35	331	5.88	49829.51	Mitochondrial
	77	K2R5Z4	*Macrophomina phaseolina*	9.90E-32	223	5.34	47708.07	Cytoplasmic
	128	DCO1_87s10149.t1	*Diplodia corticola*	—	128	5.14	37876.66	Cytoplasmic
αβ hydrolase - Putative dienelactone hydrolase family protein	26	R1G7F4	*Neofusicoccum parvum*	0.00E+00	646	5.99	29496.62	Cytoplasmic
Acetamidase/Formamidase	79	K2RFA7	*Macrophomina phaseolina*	0.00E+00	345	5.55	45023.14	Cytoplasmic
Acetyl-CoA hydrolase/transferase	75	K2SBN2	*Macrophomina phaseolina*	0.00E+00	358	6.36	58269.36	Mitochondrial
Adenosylhomocysteinase	60	K2R5D9	*Macrophomina phaseolina*	0.00E+00	300	5.75	48793.22	Cytoplasmic
	95	R1G6V6	*Neofusicoccum parvum*	0.00E+00	209	5.84	48855.29	Cytoplasmic
GH 17 - Glycoside hydrolase family 17	133	K2STT8	*Macrophomina phaseolina*	3.80E-12	103	4.55	32022.55	Extracellular

Continued on next page

Protein	Spot	Accession number	Organism	FASTM/S E_{value}[1]	MASCOT total Ion Score[2]	Theoretical pI[3]	Theoretical Mw[3] (Da)	Subcellular localization[4]
GH 31 - Putative α-glucosidase protein	2	R1H1X1	*Neofusicoccum parvum*	0.00E+00	353	4.65	110578.06	Extracellular
	3	R1H1X1	*Neofusicoccum parvum*	0.00E+00	365	4.65	110578.06	Extracellular
	151	R1H1X1	*Neofusicoccum parvum*	0.00E+00	373	4.65	110578.06	Extracellular
	169	R1H1X1	*Neofusicoccum parvum*	1.60E-29	125	4.65	110578.06	Extracellular
GH 38 - α-mannosidase	31	K2RHM5	*Macrophomina phaseolina*	2.20E-03	49	5.97	122716.44	Cytoplasmic
	132	K2RHM5	*Macrophomina phaseolina*	6.30E-23	154	5.97	122716.44	Cytoplasmic
Putative amidohydrolase family protein	158	R1E8S2	*Neofusicoccum parvum*	0.00E+00	69	5.93	40377.03	Cytoplasmic
	163	R1GCN6	*Neofusicoccum parvum*	7.80E-30	412	5.90	53044.60	Cytoplasmic
Putative β-lactamase family protein	59	R1GFI9	*Neofusicoccum parvum*	0.00E+00	691	5.52	39665.40	Cytoplasmic
	83	DCO1_1s00126.t1	*Diplodia corticola*	—	318	5.50	44772.36	Peroxisomal
	84	H1V6J2	*Colletotrichum higginsianum*	1.30E-04	242	5.10	41333.09	Cytoplasmic
	155	R1G5K7	*Neofusicoccum parvum*	0.00E+00	934	5.34	44700.99	Cytoplasmic
	161	DCO1_75s09589.t1	*Diplodia corticola*	—	80	5.27	40613.76	Cytoplasmic
Proteases								
Peptidase M1 - Peptidase M1 alanine aminopeptidase/ leukotriene A4 hydrolase	56	K2SDN2	*Macrophomina phaseolina*	0.00E+00	370	5.44	99068.10	Cytoplasmic
	157	K2SDN2	*Macrophomina phaseolina*	5.80E-09	135	5.44	99068.10	Cytoplasmic
Peptidase M20 - Putative glutamate carboxypeptidase protein	78	R1GM30	*Neofusicoccum parvum*	0.00E+00	245	5.53	52763.15	Cytoplasmic
Peptidase M24 - Putative xaa-pro dipeptidase protein (Creatinase)	100	R1EG89	*Neofusicoccum parvum*	9.80E-06	—	5.34	64557.62	Cytoplasmic
Peptidase M3 - Peptidase M3A/M3B	58	R1G7D2	*Neofusicoccum parvum*	9.10E-17	189	5.75	87524.39	Cytoplasmic
Peptidase S10 - Putative carboxypeptidase s1 protein	5	R1G0M1	*Neofusicoccum parvum*	0.00E+00	518	4.89	60702.13	Extracellular
	125	R1G0M1	*Neofusicoccum parvum*	0.00E+00	493	4.89	60702.13	Extracellular

Continued on next page

Protein	Spot	Accession number	Organism	FASTM/S E_{value}[1]	MASCOT total Ion Score[2]	Theoretical pI[3]	Theoretical Mw[3] (Da)	Subcellular localization[4]
Peptidase S8 - Putative autophagic serine protease alp2 protein	14	K2RXV9	*Macrophomina phaseolina*	0.00E+00	389	5.62	57279.71	Extracellular
	45	K2RXV9	*Macrophomina phaseolina*	1.30E-34	147	5.62	57279.71	Extracellular
	138	R1GM11	*Neofusicoccum parvum*	1.60E-35	708	6.07	39070.39	Extracellular
Peptidase S9 -Putative oligopeptidase family protein	126	R1GWK1	*Neofusicoccum parvum*	1.80E-07	134	4.64	79701.64	Extracellular
Peptidase T1A - Proteasome subunit α type	46	R1GIL3	*Neofusicoccum parvum*	0.00E+00	352	5.59	27780.56	Cytoplasmic
	88	R1GFI6	*Neofusicoccum parvum*	6.00E-36	146	5.34	30083.11	Cytoplasmic
	178	R1GT64	*Neofusicoccum parvum*	3.70E-34	196	5.80	28563.18	Mitochondrial
Proteasome subunit β type-2	110	DCO1_38s06588.t1	*Diplodia corticola*	—	164	6.96	21059.17	Mitochondrial
	141	R1GH44	*Neofusicoccum parvum*	0.00E+00	165	6.22	24813.98	Cytoplasmic
Putative proteasome component c5 protein (β type)	21	R1ECI6	*Neofusicoccum parvum*	0.00E+00	390	6.45	28968.64	Mitochondrial
	34	DCO1_19s02494.t1	*Diplodia corticola*	—	48	6.71	28986.62	Mitochondrial
Oxidoreductases								
6-phosphogluconate dehydrogenase, decarboxylating	67	K2S8M9	*Macrophomina phaseolina*	0.00E+00	675	5.99	54283.81	Cytoplasmic
	77	K2S8M9	*Macrophomina phaseolina*	3.30E-21	106	5.99	54283.81	Cytoplasmic
Dihydrolipoyl dehydrogenase	107	R1EKH2	*Neofusicoccum parvum*	6.30E-28	59	6.94	54773.98	Mitochondrial
FAD dependent oxidoreductase	84	K2QPD2	*Macrophomina phaseolina*	0.00E+00	241	5.67	47900.98	Cytoplasmic
Glutamate dehydrogenase	64	K2SZ80	*Macrophomina phaseolina*	0.00E+00	360	6.43	48930.19	Cytoplasmic
Glyceraldehyde-3-phosphate dehydrogenase	24	K2SSH4	*Macrophomina phaseolina*	0.00E+00	761	6.92	36273.12	Cytoplasmic
	30	K2SSH4	*Macrophomina phaseolina*	0.00E+00	—	6.92	36273.12	Cytoplasmic
Malate dehydrogenase	29	K2SB76	*Macrophomina phaseolina*	0.00E+00	1005	8.86	35859.95	Mitochondrial
NADH:flavin oxidoreductase/NADH oxidase family protein	63	R1H0X2	*Neofusicoccum parvum*	0.00E+00	237	6.19	53783.33	Cytoplasmic
	161	R1EHB0	*Neofusicoccum parvum*	4.00E-19	369	5.82	43385.05	Cytoplasmic
Putative alcohol dehydrogenase domain protein	84	R1EH70	*Neofusicoccum parvum*	0.00E+00	521	5.73	36414.20	Cytoplasmic
Glucose-methanol-choline oxidoreductase (alcohol oxidase)	39	R1EEN8	*Neofusicoccum parvum*	0.00E+00	1319	6.44	74359.05	Cytoplasmic
	41	R1EEN8	*Neofusicoccum parvum*	0.00E+00	1217	6.44	74359.05	Cytoplasmic

Continued on next page

Protein	Spot	Accession number	Organism	FASTM/S E_{value}[1]	MASCOT total Ion Score[2]	Theoretical pI[3]	Theoretical Mw[3] (Da)	Subcellular localization[4]
Putative aldehyde dehydrogenase protein	63	R1H0X2	*Neofusicoccum parvum*	0.00E+00	237	6.19	53783.33	Cytoplasmic
	65	R1H0X2	*Neofusicoccum parvum*	0.00E+00	869	6.19	53783.33	Cytoplasmic
	73	R1H0X2	*Neofusicoccum parvum*	0.00E+00	1099	6.19	53783.33	Cytoplasmic
	164	R1H0X2	*Neofusicoccum parvum*	2.30E-06	66	6.19	53783.33	Cytoplasmic
	169	R1H0X2	*Neofusicoccum parvum*	1.70E-06	—	6.19	53783.33	Cytoplasmic
Putative fad binding domain-containing protein	152	R1EYD9	*Neofusicoccum parvum*	8.50E-03	387	4.71	57220.33	Extracellular
Putative formate dehydrogenase protein	32	R1G468	*Neofusicoccum parvum*	0.00E+00	611	6.29	40298.87	Cytoplasmic
	103	R1G468	*Neofusicoccum parvum*	0.00E+00	690	6.29	40298.87	Cytoplasmic
Putative homogentisate-dioxygenase protein	129	R1EVN8	*Neofusicoccum parvum*	1.30E-06	—	6.06	58733.01	Cytoplasmic
Putative minor allergen alt a 7 protein	142	R1ENB8	*Neofusicoccum parvum*	1.30E-18	557	5.72	22135.00	Cytoplasmic
Short-chain dehydrogenase/ reductase sdr	102	DCO1_1s00458.t1	*Diplodia corticola*	—	44	5.50	34373.20	Cytoplasmic
Short-chain dehydrogenase/ reductase SDR (l-xylulose reductase)	17	K2S1F3	*Macrophomina phaseolina*	0.00E+00	313	6.13	31597.72	Cytoplasmic
Short-chain dehydrogenase/ reductase SDR (Versicolorin reductase)	20	K2RCX3	*Macrophomina phaseolina*	1.20E-35	272	5.90	31170.57	Cytoplasmic
Superoxide dismutase [Cu-Zn]	13	R1GTN9	*Neofusicoccum parvum*	0.00E+00	589	6.03	15726.24	Cytoplasmic
Thioredoxin reductase	8	DCO1_53s07515.t1	*Diplodia corticola*	—	32	6.37	33319.94	Cytoplasmic
	27	M2QTA7	*Cochliobolus sativus*	5.60E-15	445	6.60	33646.58	Cytoplasmic
	30	M2QTA7	*Cochliobolus sativus*	0.00E+00	985	6.60	33646.58	Cytoplasmic
	94	M2QTA7	*Cochliobolus sativus*	3.70E-10	405	6.60	33646.58	Cytoplasmic
Transferases								
α-1,4 glucan phosphorylase	131	R1EPV1	*Neofusicoccum parvum*	0.00E+00	211	5.81	99659.87	Nuclear

Continued on next page

Protein	Spot	Accession number	Organism	FASTM/S E_{value}[1]	MASCOT total Ion Score[2]	Theoretical pI[3]	Theoretical Mw[3] (Da)	Subcellular localization[4]
Aminotransferase class V/Cysteine desulfurase	32	K2SAF5	*Macrophomina phaseolina*	1.90E-05	129	7.15	41599.64	Cytoplasmic
	164	K2SAF5	*Macrophomina phaseolina*	0.00E+00	129	7.15	41599.64	Cytoplasmic
4-aminobutyrate aminotransferase eukaryotic	93	K2SB97	*Macrophomina phaseolina*	0.00E+00	481	7.75	56383.98	Mitochondrial
Citrate synthase	34	K2REF5	*Macrophomina phaseolina*	0.00E+00	395	8.77	51667.15	Mitochondrial
Dj-1 family protein	149	L2FW83	*Colletotrichum gloeosporioides*	5.00E-08	153	5.41	26577.56	Cytoplasmic
Methionine synthase vitamin-B12 independent	37	K2RD18	*Macrophomina phaseolina*	0.00E+00	871	6.43	86349.70	Cytoplasmic
	125	K2RD18	*Macrophomina phaseolina*	3.80E-06	69	6.43	86349.70	Cytoplasmic
Methylcitrate synthase precursor	35	DCO1_18s05215.t1	*Diplodia corticola*	—	32	8.84	52449.18	Mitochondrial
Nucleoside diphosphate kinase	122	K2S9J1	*Macrophomina phaseolina*	0.00E+00	397	8.69	16744.19	Cytoplasmic
	123	K2S9J1	*Macrophomina phaseolina*	1.80E-30	94	8.69	16744.19	Cytoplasmic
Putative adenosine kinase protein	83	R1EV77	*Neofusicoccum parvum*	0.00E+00	367	5.37	38168.47	Cytoplasmic
Putative glutathione s-transferase protein	110	R1E9W5	*Neofusicoccum parvum*	6.80E-15	111	5.92	25351.88	Nuclear
	143	R1E9W5	*Neofusicoccum parvum*	1.20E-23	190	5.92	25351.88	Nuclear
Putative l-ornithine aminotransferase protein	61	R1EP24	*Neofusicoccum parvum*	1.80E-21	136	6,07	50244.43	Cytoplasmic
Putative phosphoenolpyruvate carboxykinase protein	66	R1EI04	*Neofusicoccum parvum*	0.00E+00	769	5.60	61566.52	Cytoplasmic
	105	R1EI04	*Neofusicoccum parvum*	0.00E+00	661	5.60	61566.52	Cytoplasmic
Spermidine synthase	89	K2RG56	*Macrophomina phaseolina*	0.00E+00	404	5.26	33118.81	Cytoplasmic
Transaldolase	42	R1GMD5	*Neofusicoccum parvum*	0.00E+00	634	5.19	35619.57	Cytoplasmic
Transketolase	52	K2RZI6	*Macrophomina phaseolina*	0.00E+00	950	5.87	74975.89	Cytoplasmic
	168	K2RZI6	*Macrophomina phaseolina*	8.70E-07	76	5.87	74975.89	Cytoplasmic
Phosphatases								
Putative inorganic pyrophosphatase protein	43	R1EI42	*Neofusicoccum parvum*	0.00E+00	744	5.32	33476.03	Cytoplasmic

Continued on next page

Protein	Spot	Accession number	Organism	FASTM/S E_{value}[1]	MASCOT total Ion Score[2]	Theoretical pI[3]	Theoretical Mw[3] (Da)	Subcellular localization[4]
Putative-bisphosphoglycerate-independent phosphoglycerate mutase protein	91	R1EYX5	*Neofusicoccum parvum*	0.00E+00	420	5.40	57095.83	Extracellular
Lyases								
Isocitrate lyase	40	R1EDG7	*Neofusicoccum parvum*	0.00E+00	367	6.93	60923.22	Cytoplasmic
Putative phosphoketolase protein (aldehyde-lyase)	114	R1EPJ0	*Neofusicoccum parvum*	4.70E-05	—	5.88	90822.04	Cytoplasmic
	159	R1EPJ0	*Neofusicoccum parvum*	1.00E-03	125	5.88	90822.04	Cytoplasmic
Hydratases								
Aconitase A/isopropylmalate dehydratase small subunit swivel	114	K2QLG1	*Macrophomina phaseolina*	0.00E+00	898	6.21	84207.49	Mitochondrial
Enolase	84	K2SCR2	*Macrophomina phaseolina*	0.00E+00	306	5.29	47075.26	Cytoplasmic
Putative 2-methylcitrate dehydratase protein	129	R1ED63	*Neofusicoccum parvum*	0.00E+00	387	6.15	55194.95	Cytoplasmic
Isomerases								
Glucose-6-phosphate isomerase	107	R1GRZ3	*Neofusicoccum parvum*	0.00E+00	340	5.74	61861.97	Cytoplasmic
NAD-dependent epimerase/dehydratase	95	K2QUU1	*Macrophomina phaseolina*	6.50E-03	34	5.96	41017.65	Cytoplasmic
Other functions								
14-3-3 protein	97	K2SCW4	*Macrophomina phaseolina*	0.00E+00	239	4.92	30320.81	Nuclear
ATP synthase subunit beta	4	K2R9P7	*Macrophomina phaseolina*	0.00E+00	1543	5.41	55499.44	Mitochondrial
Cerato-platanin (Protein SnodProt1)	7	W3WKH2	*Pestalotiopsis fici* W106-1	1.20E-07	—	4.37	13993.65	Extracellular
Cupin RmlC-type	16	K2RCC3	*Macrophomina phaseolina*	1.00E-31	354	5.18	19078.40	Cytoplasmic
Heat shock protein 60 (Chaperonin Cpn60)	51	R1GDI3	*Neofusicoccum parvum*	0.00E+00	1138	5.52	61593.33	Mitochondrial

Continued on next page

Protein	Spot	Accession number	Organism	FASTM/S E_{value}[1]	MASCOT total Ion Score[2]	Theoretical pI[3]	Theoretical Mw[3] (Da)	Subcellular localization[4]
Outer membrane β-barrel	11	A0A017S003	*Aspergillus ruber*	2.40E-13	703	6.29	18838.42	Cytoplasmic
	122	DCO1_53s07485.t1	*Diplodia corticola*	—	203	5.29	18733.37	Cytoplasmic
	129	DCO1_53s07485.t1	*Diplodia corticola*	—	38	5.29	18733.37	Cytoplasmic
Porin eukaryotic type (outer mitochondrial membrane protein porin)	139	K2S952	*Macrophomina phaseolina*	1.60E-14	—	8.99	29738.39	Cytoplasmic
	140	K2S952	*Macrophomina phaseolina*	2.40E-23	225	8.99	29738.39	Cytoplasmic
Putative g-protein complex beta subunit protein	94	R1GU67	*Neofusicoccum parvum*	4.80E-11	—	6.75	35070.56	Nuclear

APPENDIX II

PUBLICATIONS

FUNGAL BIOLOGY 118 (2014) 516–523

ELSEVIER

British Mycological Society promoting fungal science

journal homepage: www.elsevier.com/locate/funbio

Secretome analysis identifies potential virulence factors of *Diplodia corticola*, a fungal pathogen involved in cork oak (*Quercus suber*) decline

Isabel FERNANDES[a,b], *Artur ALVES*[a], *António CORREIA*[a], *Bart DEVREESE*[b], *Ana Cristina ESTEVES*[a,*]

[a]*Department of Biology, CESAM, Aveiro University, Campus Universitário de Santiago, 3810-193 Aveiro, Portugal*
[b]*Department of Biochemistry, Physiology and Microbiology, Laboratory of Protein Biochemistry and Protein Engineering, Ghent University, K.L. Ledeganckstraat 35, 9000 Ghent, Belgium*

ARTICLE INFO

Article history:
Received 7 January 2014
Received in revised form
16 March 2014
Accepted 9 April 2014
Available online 18 April 2014
Corresponding Editor:
Steven Bates

Keywords:
2D-electrophoresis
Botryosphaeriaceae
Filamentous fungi
Plant pathogen
Quercus suber

ABSTRACT

The characterisation of the secretome of phytopathogenic fungi may contribute to elucidate the molecular mechanisms of pathogenesis. This is particularly relevant for *Diplodia corticola*, a fungal plant pathogen belonging to the family *Botryosphaeriaceae*, whose genome remains unsequenced. This phytopathogenic fungus is recognised as one of the most important pathogens of cork oak, being related to the decline of cork oak forests in the Iberian Peninsula.

Unfortunately, secretome analysis of filamentous fungi is limited by the low protein concentration and by the presence of many interfering substances, such as polysaccharides, which affect the separation and analysis by 1D and 2D gel electrophoresis. We compared six protein extraction protocols concerning their suitability for further application with proteomic workflows. The protocols involving protein precipitation were the most efficient, with emphasis on TCA–acetone protocol, allowing us to identify the most abundant proteins on the secretome of this plant pathogen. Approximately 60 % of the spots detected were identified, all corresponding to extracellular proteins. Most proteins identified were carbohydrate degrading enzymes and proteases that may be related to *D. corticola* pathogenicity.

Although the secretome was assessed in a noninfection environment, potential virulence factors such as the putative glucan-β-glucosidase, neuraminidase, and the putative ferulic acid esterase were identified.

The data obtained forms a useful basis for a deeper understanding of the pathogenicity and infection biology of *D. corticola*. Moreover, it will contribute to the development of proteomics studies on other members of the *Botryosphaeriaceae*.

Introduction

Fungi from the family *Botryosphaeriaceae* can infect plants causing diseases and often death (Alves *et al.* 2004; Damm *et al.* 2007; Marincowitz *et al.* 2008; Mehl *et al.* 2011; Úrbez-Torres & Gubler 2009). Their ecological and economic impact is considerable – particularly when they infect profitable trees such as cork oak. The involvement of *Diplodia corticola* (a member of the

* *Corresponding author*. Tel.: +351 234 370 774; fax: +351 234 372 587.
E-mail address: acesteves@ua.pt (A. C. Esteves).
1878-6146/$ – see front matter
http://dx.doi.org/10.1016/j.funbio.2014.04.006

Botryosphaeriaceae) on the decline of cork oak forests is well known (Alves *et al.* 2004; Linaldeddu *et al.* 2009). It causes symptoms like dieback, canker, and vascular necrosis in oak trees, but the mechanism of pathogenesis is unknown.

In the last decade, proteomics of phytopathogenic fungi has been increasingly applied to study plant–pathogen interactions (Gonzalez-Fernandez & Jorrín-Novo 2012). More specifically, secretome characterisation of phytopathogenic fungi may contribute to elucidate the infection mechanism and provide information for the development of disease management strategies.

Remarkably, only Cobos *et al.* (2010) used proteomics to characterise a member of the *Botryosphaeriaceae* family. This gap is due to the low number of sequenced genomes of that family making protein identification difficult. Nevertheless, 2-D gel-based proteomics followed by *de novo* sequencing allows identifying proteins from organisms with unsequenced genomes, such as *D. corticola* (Rogowska-Wrzesinska *et al.* 2013; Tannu & Hemby 2007). Another possible reason for the low number of proteomics studies of the *Botryosphaeriaceae* family is that the analysis of the secretome is constrained by the low concentration of extracellular proteins, the high amount of polysaccharides, and the presence of low-molecular-weight metabolites also secreted by fungi (Chevallet *et al.* 2007; Erjavec *et al.* 2012). These molecules interfere with protein extraction and separation methods, making the choice of an adequate extraction method crucial for proteomics (Lemos *et al.* 2010).

We aimed to optimize an extraction protocol suitable for secretome analysis by 1D and 2D electrophoresis and to identify the major extracellular proteins of *D. corticola*. This is the first report describing the secretome of *D. corticola*, providing a first view on the machinery this organism could exploit in plant infection.

Material and methods

Microorganisms and culture conditions

The strain used in this study was *Diplodia corticola* CBS112548. Cultures were maintained on Potato Dextrose Agar (PDA) medium (Merck, Germany). For secretome extraction, a mycelium plug with 0.5 cm diameter from a 6-d-old PDA plate was inoculated into a 250 mL flask containing 50 mL of Potato Dextrose Broth (PDB), and statically incubated for 12 d at room temperature (±25 °C). All assays were performed in triplicate. Culture supernatants were individually collected by gravitational filtration through filter paper and stored at −20 °C until use. The dry-weight of mycelia was determined to evaluate the fungal biomass. For this, filtered mycelia were dried at 50 °C for 4 d before weighting. The extracellular protein fraction was then concentrated as described below.

Extracellular protein extraction protocols

Protocol 1 (Trichloroacetic acid (TCA)–acetone) was based on a previously described method (Cobos *et al.* 2010). After thawing, the culture supernatant (35 mL) was centrifuged (48 400×*g*, 1 h at 4 °C) to discard precipitated polysaccharides. One volume of ice-cold TCA/acetone [20 %/80 % (w/v)] with 0.14 % (w/v) DTT was added to the supernatant and incubated at −20 °C (1 h). Precipitated proteins were recovered by centrifugation (15 000×*g*, 20 min, 4 °C) and excess TCA was removed from the precipitate by washing with 10 mL of ice-cold acetone (2×) and 10 mL of ice-cold 80 % acetone (v/v). Residual acetone was air-dried and the protein pellet was resuspended in 500 µL of lysis buffer (7 M urea, 2 M thiourea, 4 % CHAPS, 30 mM Tris-base) and stored at −20 °C.

Protocol 2 (TCA–phenol) was adapted from a previously described method (Fernández-Acero *et al.* 2009). After thawing, the culture supernatant (35 mL) was centrifuged (48 400×*g*, 1 h at 4 °C) to discard precipitated polysaccharides. Proteins were precipitated by the addition of one volume of ice-cold TCA/acetone [20 %/80 % (w/v), 1 h, −20 °C], and collected by centrifugation at 15 000×*g* (20 min, 4 °C). The precipitate was successively washed with 10 mL of ice-cold TCA/acetone [20 %/80 % (w/v), twice], 10 mL of 20 % TCA (w/v), and twice with 10 mL of ice-cold 80 % acetone (v/v). Residual acetone was air-dried and the protein pellet was resuspended in 5 mL of dense Sodium dodecyl sulfate (SDS) buffer [30 % (w/v) sucrose, 2 % (w/v) SDS, 0.1 M Tris–HCl pH 8.0, 5 % (v/v) 2-mercaptoethanol] adding then 5 mL of phenol equilibrated with 10 mM Tris–HCl, pH 8.0, 1 mM Ethylenediaminetetraacetic acid (EDTA) (Sigma–Aldrich, USA). The resulting solution was vigorously mixed and centrifuged at 15 000×*g* (10 min, 4 °C). The phenol phase was transferred to a tube to which five volumes of cold 0.1 M ammonium acetate in methanol were added and incubated at −20 °C overnight to promote protein precipitation. Afterwards, proteins were recovered by centrifugation and washed twice with 10 mL of cold 0.1 M ammonium acetate in methanol, followed by two washes with 10 mL of ice-cold 80 % acetone (v/v). The air-dried pellet was finally resuspended in 500 µL lysis buffer and stored at −20 °C.

Protocol 3 (ultrafiltration with protein cleaning): polysaccharides were separated as described for method 1 and the resultant supernatant was concentrated by ultrafiltration with Vivaspin concentrator (MWCO 3 kDa, Sartorious), at 4000 rpm (4 °C). Retained proteins were purified with 2-D Clean-Up kit (GE Healthcare, USA; from now on mentioned as protein cleaning), according to the manufacturer's instructions. The proteins were solubilized in 500 µL of lysis buffer and stored at −20 °C.

Protocol 4 (ultrafiltration without protein cleaning): this method is identical to method 3 with the exception of the final cleaning step. Therefore, the proteins were immediately resuspended in 500 µL of lysis buffer and stored at −20 °C after their concentration.

Method 5 (ultrafiltration without polysaccharide precipitation): this method is similar to method 3 with the exception of the initial polysaccharide removal step. After protein cleaning, the resultant pellet was solubilized in 500 µL of lysis buffer and stored at −20 °C.

Protocol 6 (lyophilisation): culture supernatant (35 mL) was concentrated by lyophilisation (Snijders Scientific) for 24 h at −50 °C. Afterwards, proteins were cleaned as previously described, solubilized in 500 µL of lysis buffer and stored at −20 °C.

Protein concentration determination

Protein concentration was determined with the 2-D Quant Kit (GE Healthcare, USA), according to the manufacturer's instructions.

1D- and 2D-electrophoresis

Proteins were separated by SDS-PAGE or by 2D-electrophoresis. For SDS-PAGE, 30 μg of protein extract were diluted (1:1) in 8 M urea, 100 mM Tris, 100 mM bicine, 2 % SDS, 2 % 2-mercaptoethanol, and heated for 5 min at 100 °C. Proteins were separated by 12.5 % SDS-PAGE gel electrophoresis, according to Laemmli (Laemmli 1970), for 120 min at 120 V, in a Mini-PROTEAN 3 Cell (Bio-Rad, USA).

For 2D-electrophoresis, 240 μg of protein extract were loaded onto Immobilized pH gradient (IPG) strips (pH 3–5.6 NL or pH 3–11 NL, 13 cm, GE Healthcare) that were actively rehydrated (50 V, 10 h) with 250 μL of rehydration buffer (7 M urea, 2 M thiourea, 4 % CHAPS, 30 mM Tris-base, 2 % Dithiothreitol (DTT), 2 % IPG buffer pH 3–5.6 NL and bromophenol blue). Isoelectric focusing (IEF) was performed on a Ettan IPGphor 3 system (GE Healthcare, Sweden) at 20 °C limited to 50 μA/strip according to the following parameters: 1 h at 150 V, 2 h at 500 V, 6 h 500–1000 V, 3 h 1000–8000 V and 8000 V until 20 000 Vhr. Prior to second dimension, the IPG strips were reduced and alkylated for 15 min with 1 % (w/v) DTT and afterwards with 2.5 % (w/v) iodoacetamide in 5 mL equilibration buffer [50 mM Tris–HCl (pH 8.8), 6 M Urea, 30 % (w/v) glycerol, 2 % SDS, and traces of bromophenol blue], respectively. After equilibration, the strips were juxtaposed to 12.5 % lab cast SDS-PAGE gels on a PROTEAN II xi Cell (Bio-Rad, USA) system. Proteins were separated initially at 2 W/gel (2 h) and then at 6 W/gel (limited to 200 V) until the dye marker reached the end of the gel.

Proteins were visualized by Coomassie Brilliant Blue G-250 (CBB) staining. Each gel image was acquired using the GS-800 calibrated imaging densitometer (Bio-Rad, USA). CBB stained 2-DE gels were analysed with PDQuest software (Bio-Rad, USA) to determine the number of protein spots per gel.

Mass spectrometry

Randomly selected 2-D spots were excised and successively guanidinated, digested with trypsin and N-terminal sulfonated to enhance the *de novo* sequencing (Sergeant et al. 2005). The tryptic peptides were then analysed by tandem mass spectrometry on a 4800 Plus MALDI TOF/TOF Analyser system (AB Sciex, USA). As the standard settings MASCOT search (Matrix Science, UK) was unsuccessful, due to the lack of information on the nonredundant NCBI fungal database (Cobos et al. 2010; Standing 2003), it was proceeded to PEAKS *de novo* sequencing (PEAKS Studio 6.0, BSI, Canada) (Zhang et al. 2012). The PEAKS search parameters encompassed fragment mass error tolerance of 0.3 Da, carbamidomethylation (57.02) and guanidination (42.02) as fixed modifications, and acetylation (N-terminus) (42.01), 4-sulfophenyl isothiocyanate (214.97) and methionine, histidine and tryptophan oxidation (15.99) as variable modifications. In addition, manual interpretation of the spectra was performed to confirm the previous results and the similarity of the identified peptide sequences was searched with FASTS algorithm (Mackey et al. 2001) (standard settings search (matrix PAM 120) against UniProtKB Fungi subset; $p < 0.05$ scores were considered significant). The subcellular localization of identified proteins was predicted using BaCelLo predictor (Pierleoni et al. 2006) and the theoretical pI searched with Compute pI/Mw tool available on ExPASy (Gasteiger et al. 2005).

Results and discussion

Secreted proteins from *Diplodia corticola* were extracted by six methods (Table 1). Analysis by SDS-PAGE (Fig 1) showed that the protocols based on protein precipitation (methods 1 and 2) were the most efficient (Fig 1): protocols 1 and 2 yielded an average of 12–15 bands (with molecular weights ranging between 218 and 23 kDa) and protocols 3–6 yielded a maximum of ten bands (distributed over a molecular weight range of 113–25 kDa) indicating proteins loss and/or poor protein recovery.

Based on 1-D profiles, 2D spots obtained from protocols TCA–acetone and TCA–phenol were randomly selected for identification (Fig 2). Three biological replicates per strain were analysed by 2-DE in the 3–5.6 pH range, since most proteins were found in this range. Similar acidic profiles were found for other filamentous fungi secretomes (Gonzalez-Fernandez et al. 2014). The overall identification rate was similar in both methods: 69 % (11 out of 16) of the spots obtained with methods 1 and 58 % (11 out of 19) of the spots with protocol 2. Some of the spots were identified twice in order to confirm protein identification. Cobos et al. (2010), that characterised the secretome of *Diplodia seriata*, were able to identify a similar number (16) of proteins, from which only 12 were extracellular.

Most of the proteins identified display homology with the fungal pathogen *Macrophomina phaseolina*, and in less extent with *Neofusicoccum parvum*, both members of the family *Botryosphaeriaceae* whose genomes were recently sequenced (Blanco-Ulate et al. 2013; Islam et al. 2012) and integrated

Table 1 – Summary of the protocols used to extract the secretome of *D. corticola* and respective protein concentration average [determined by the 2-D Quant Kit (GE Healthcare, USA)]. The inclusion of a polysaccharide removal step or a protein cleaning step are indicated by + (included) or – (not included).

Extraction protocol	Polysaccharide removal	Protein cleaning with 2-D Clean-Up kit (GE Healthcare, USA)	Average protein concentration (μg ml^{-1}) ± SD
1. TCA–acetone	+	–	1580.8 ± 916.5
2. TCA–phenol	+	–	3935.4 ± 930.8
3. Ultrafiltration	+	+	4414.7 ± 568.5
4. Ultrafiltration	+	–	1989.9 ± 105.7
5. Ultrafiltration	–	+	5217.4 ± 711.3
6. Lyophilisation	+	+	456.7 ± 264.7

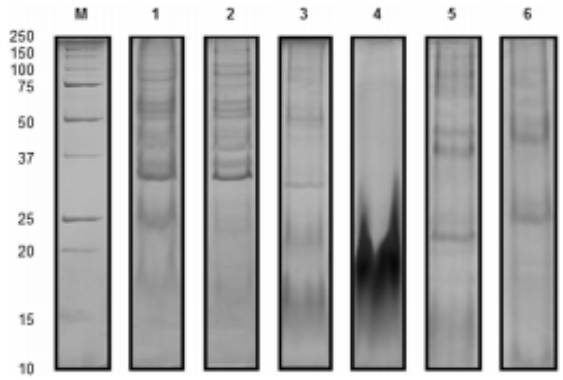

Fig 1 – SDS-PAGE of secretome proteins from *D. corticola* extracted by several methods. Three biological replicates were used for each protocol. M – Precision Plus Protein Unstained Standard (kDa) (Bio-Rad, USA).

into UniProtKB. The limited genomic data available of fungi from the family *Botryosphaeriaceae* significantly limited protein identification, as reported before for *D. seriata* (Cobos et al. 2010) and for other fungi, such as *Aspergillus flavus* [22 proteins identified (Medina et al. 2004)], *Trichoderma harzianum* [1 protein identified and sequenced (Suarez et al. 2005)], *Sclerotinia sclerotiorum* [18 proteins identified (Yajima & Kav 2006)]. We identified the secretome proteins based on *de novo* sequenced peptides, whose similarity was searched with FASTS algorithm (Mackey et al. 2001) against UniProtKB Fungi subset. All proteins identified were extracellular (Table 2) as confirmed by BaCelLo, a fungi-specific predictor (Pierleoni et al. 2006). The lack of intracellular proteins in the secretome of *D. corticola* reflects the suitability of the protein extraction methods used. In fact, the identification of intracellular proteins in the secretome of fungi is commonly considered an unavoidable consequence of sample preparation.

Additionally to the lack of genomic data, the absence of protein sequences from *Botryosphaeriaceae* fungi greatly constrained the identification of secreted proteins from these organisms. The low number of protein identified may also reflect a low homology with other fungi. In fact, the proteins of *D. corticola* secretome do not resemble that of *D. seriata* (Cobos et al. 2010), a close relative: with the exception of a glucosidase and a peptidase, no other proteins were found in both secretomes. Although both fungi are phytopathogenic, these differences on the secretome may reflect different infection strategies or adaptation to different hosts [*D. corticola* mainly infects *Quercus* sp. and in lower extension grapevines, while *D. seriata* is a plurivorous pathogen with a wide host range, including fruit trees and grapevines (Niekerk et al. 2006; Slippers et al. 2007)].

We identified the same protein in different spots – with the same molecular weight, but with slightly different isoelectric points (peptidase M35 deuterolysin, spots 6, 7 and spherulation-specific family 4, spots 11, 12) – indicating the presence of posttranslational modifications.

In order to get a better characterisation of the secretome, the putative biological functions of the proteins are discussed. The functional distribution of extracellular proteins of *D. corticola* is consonant to what was described for other filamentous fungi (Girard et al. 2013; Islam et al. 2012). The proteins are mainly hydrolases (glucoamylase, glycoside hydrolase 71, neuraminidase, and putative glucan-β-glucosidase) and proteases (putative carboxypeptidase S1, putative serine protease and M35 deuterolysin; Table 2) potentially involved in pathogenesis.

The putative glucan-β-glucosidase (spot 10) has been identified as a virulence factor in other microorganisms: it is directly involved in the virulence of the phytopathogenic *Pyrenophora tritici-repentis* (anamorph: *Drechslera tritici-repentis*), the necrotrophic fungus responsible for tan spot (Fu et al. 2013). Reuveni and colleagues (2007) also related fungus virulence of the phytopathogen *Alternaria alternata* to the expression of glucanases. Also, Huser et al. (2009) found that a β-1,3(4)-glucanase was involved in the virulence of the crucifer anthracnose fungus *Colletotrichum higginsianum*. It is plausible that such an enzyme, able to cleave glucose residues from the nonreducing terminus of a β-glucan chain, widely present in plant cell walls (Martin et al. 2007) can function in the penetration of the plant cell wall or in remodelling fungal cell-wall glucans during infection. The putative glucan-β-glucosidase (spot 10) closest relative (from *Neofusicoccum parvum* UCRNP2, EOD48046.1) shares 63 % identity (data not shown) with the *Pyrenophora tritici-repentis* GLU1 (EDU47467.1) and the same domain composition – signal peptide and glycosyl hydrolase family 5 domain – suggesting that similar functions may be shared (Letunic et al. 2012). Furthermore, the presence of the putative glucan-β-glucosidase in the secretome of *D. corticola* is in agreement with the prediction by Fu et al. (2013) that GLU1 is an extracellular enzyme.

Diplodia corticola secretes hydrolases from the three classes known to work synergistically to degrade cellulose [exoglucanases, endoglucanases, and β-glucosidases (Horn et al. 2012)], having already been described on the secretome of phytopathogenic fungi (Fernández-Acero et al. 2010; Jung et al. 2012; Wang et al. 2011) and on the secretome of wood degrading fungi (Abbas et al. 2005; Phalip et al. 2005; Sato et al. 2007).

Plant cell wall degrading enzymes require the assistance of carbohydrate esterases (Aspeborg et al. 2012) to deacetylate the substituted saccharides (esters or amides) of celluloses (Biely 2012), and of other molecules such as suberin. Suberin is a polyester biopolymer that acts as a barrier between plants and the environment. It is the main cell wall component of cork, the outer bark of the cork oak tree, up to 50 % of its dry weight (Graça & Santos 2007; Pereira 1988). The putative ferulic acid esterase (spot 9) can release ferulic acid from suberin (Jové et al. 2011). A compromised integrity of the suberin barrier may result in water vapour loss and in an increased susceptibility to the pathogen and to infection (Lulai et al. 2006).

Neuraminidase (spot 4) is an exoglycosidase that cleaves glycoconjugates, releasing the terminal sialic acid residues (Warwas et al. 2010). These enzymes are involved in the virulence of several microorganisms (Jermyn & Boyd 2002; Warwas et al. 2010; Zhou et al. 2009). While the participation of bacterial and viral neuraminidases in virulence is widely described (Vimr et al. 2004), the knowledge of the function of these enzymes in fungal pathogenesis is very limited

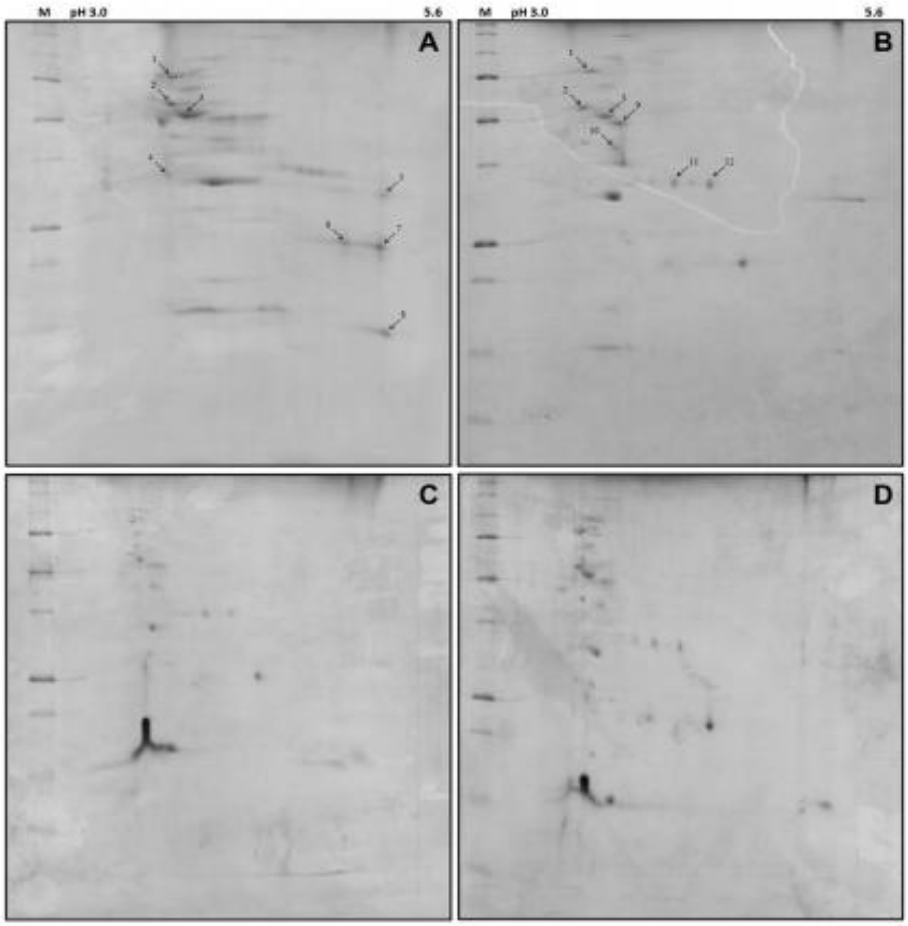

Fig 2 – 2-DE of proteins extracted with TCA–acetone (A, method 1), TCA–phenol (B, method 2), and ultrafiltration (C, method 3; D, method 5). M – Precision Plus Protein Standard (Bio-Rad, USA).

(Uchida et al. 1974; Warwas et al. 2010). In bacteria, neuraminidase is thought to aid pathogenesis by revealing carbohydrate receptors for adherence, inducing increased resistance towards host defence molecules and biofilm formation, and providing a carbon source for the bacteria – and a significant competitive advantage to the pathogen (Burnaugh et al. 2008; Dalia et al. 2010; Jermyn & Boyd 2002; Parker et al. 2009; Soong et al. 2006). In virus, neuraminidase is responsible for the release of progeny virus from infected cells (Upadhyay et al. 2011). The role of neuraminidases in fungal life cycle or pathogenesis is currently unknown. Although, there is controversy concerning the presence of sialic acid on plant cell walls (Zeleny et al. 2006), it has been shown that *Botryosphaeriaceae* fungi such as *M. phaseolina* recognise and infect host plants via a sialic acid binding lectin (Bhowal et al. 2006; Bhowal et al. 2005). A similar role for *D. corticola* neuraminidase, involving the removal of sialic acids from plant cell wall glycoproteins, can be hypothesised, but the real significance of neuraminidase in *D. corticola* pathogenesis remains unclear.

Traditionally proteases were not seen as key partners on fungal phytopathogenesis. Nonetheless, it is known that filamentous fungi increase protease secretion in the presence of plant extracts (Espino et al. 2010; Phalip et al. 2005; Zorn et al. 2005), emphasizing their importance on fungal pathogenicity strategies. Plant cell walls and extracellular matrices contain glycoproteins and proteoglycans that interpenetrate networks of structural polysaccharides (Lamport et al. 2011). The degradation of these proteins – as is the case of extensins – can lead to cell softening aiding fungal hyphal penetration (Espino et al. 2010).

Additionally, the successful plant colonization by a pathogen benefits from the existence of proteases and peptidases that impair the plant proteins and allow the fungus to evade plant defence mechanisms (Pietro et al. 2009). Additionally, amino acids release supports the pathogen growth demands (Espino et al. 2010; Faulkner & Robatzek 2012; Jung et al. 2012).

Besides the obvious function on basal metabolism, the peptidases found on *D. corticola* secretome (Table 2) can also

Table 2 – Summary of proteins identified by *de novo* sequencing. Peptide similarity search was performed with FASTS algorithm (Mackey *et al.* 2001) ($p < 0.05$ scores were considered significant).

Spot	Protein	Accession number	Organism	Theoretical pI[a]	Subcellular localization[b]
1	Glucoamylase	K2S7L9	*Macrophomina phaseolina* (strain MS6)	5.37	Extracellular
2	Glycoside hydrolase family 71	K2R498	*Macrophomina phaseolina* (strain MS6)	4.84	Extracellular
3	Putative carboxypeptidase S1	R1GF60	*Neofusicoccum parvum* UCRNP2	4.45	Extracellular
4	Neuraminidase	K2SSW0	*Macrophomina phaseolina* (strain MS6)	4.27	Extracellular
5	Putative serine protease	R1GM11	*Neofusicoccum parvum* UCRNP2	6.07	Extracellular
6,7	Peptidase M35 deuterolysin	K2SDQ0	*Macrophomina phaseolina* (strain MS6)	5.34	Extracellular
8	Uncharacterized protein	K2RZ98	*Macrophomina phaseolina* (strain MS6)	5.59	Extracellular
9	Putative ferulic acid esterase	R1EDH3	*Neofusicoccum parvum* UCRNP2	4.79	Extracellular
10	Putative glucan-β-glucosidase	R1GIC9	*Neofusicoccum parvum* UCRNP2	4.73	Extracellular
11, 12	Sporulation-specific family 4	K2RK67	*Macrophomina phaseolina* (strain MS6)	4.04	Extracellular

a Compute pI/Mw, ExPASy (Gasteiger *et al.* 2005).
b BaCelLo (Pierleoni *et al.* 2006).

be involved on host colonization. These enzymes are known for playing major roles in physiologic and pathologic scenarios in a wide range of organisms (Sarmento *et al.* 2009). Their functional diversity (exo and endoproteases) reflects their synergistic interplay (Girard *et al.* 2013) and the diverse nature of their substrates. Serine carboxypeptidase S1 (spot 3) is an exoprotease that seems to efficiently work in an acidic environment (Fig 2A). The serine endopeptidase (spot 5) has already been described in other plant infection models (Billon-Grand *et al.* 2002; Li *et al.* 2012). Similarly, the Zn^{2+} metalloendopeptidase deuterolysin (spots 6 and 7) was described as a virulence factor not only in pathogenic fungi (Monod *et al.* 2002), but also in bacteria (Arnadottir *et al.* 2009).

We identified a sporulation-specific family 4 protein (spots 11, 12) previously reported in *Magnaporthe oryzae* secretome (Jung *et al.* 2012). This protein is involved in sporulation, and is usually linked to starvation; nonetheless, usually follows infection to spread the fungus through the host (Wilson & Talbot 2009). More studies need to be performed to understand the function of this sporulation-inducing protein, which has two isoforms on *D. corticola* secretome (Fig 2).

The interaction between fungi and plants is mediated by a variety of molecules secreted by each organism. The identification of these molecules is crucial to understand how pathogen and host's cells interact and in the case of plant pathogens, how we can alter the balance of this interaction towards a decrease of virulence.

Despite the efforts and achievements made in the last years regarding fungal phytopathogens' secretome identification, we remain largely unaware of the secretory mechanisms and of the secretome of these organisms.

More efforts, to increase the fungal annotated databases, are necessary. Particularly concerning the *Botryosphaeriaceae* family, improving these data will boost homology search and protein identification rates.

This is the first report describing the secretome of *D. corticola* and the second one describing the secretome of a *Diplodia* species (Cobos *et al.* 2010). Proteomics is increasingly gaining importance in the investigation of infection markers – it allows deciphering the relationship between fungal pathogens and their hosts. The use of complementary techniques to gel based proteomics and the application of proteomics to other strains of *D. corticola* will help expanding the knowledge of the infection strategies of this organism. For instance, the comparative analysis of an infection-induced secretome profile may contribute to assess putative virulence factors that can be further validated and/or detected with a multiple reaction monitoring (MRM) mass spectrometry approach.

Acknowledgements

This study was supported by FEDER funding through COMPETE program and by national funding through FCT within the research project PROMETHEUS (PTDC/AGR-CFL/113831/2009 and FCOMP-01-0124-FEDER-014096) and Pest (PEst-C/MAR/LA0017/2013). FCT also financed AC Esteves (BPD/38008/2007) and I Fernandes (BD/66223/2009).

Appendix A. Supplementary data

Supplementary data related to this article can be found at http://dx.doi.org/10.1016/j.funbio.2014.04.006

REFERENCES

Abbas A, Koc H, Liu F, Tien M, 2005. Fungal degradation of wood: initial proteomic analysis of extracellular proteins of *Phanerochaete chrysosporium* grown on oak substrate. *Current Genetics* 47: 49–56.

Alves A, Correia A, Luque J, Phillips A, 2004. *Botryosphaeria corticola*, sp. nov. on *Quercus* species, with notes and description of *Botryosphaeria stevensii* and its anamorph, *Diplodia mutila*. *Mycologia* 96: 598–613.

Arnadottir H, Hvanndal I, Andresdottir V, Burr S, Frey J, Gudmundsdottir B, 2009. The AsaP1 peptidase of *Aeromonas salmonicida* subsp. *achromogenes* is a highly conserved deuterolysin metalloprotease (family M35) and a major virulence factor. *Journal of Bacteriology* 191: 403–410.

Aspeborg H, Coutinho P, Wang Y, Brumer H, Henrissat B, 2012. Evolution, substrate specificity and subfamily classification of glycoside hydrolase family 5 (GH5). *BMC Evolutionary Biology* 12: 186–202.

Bhowal J, Ghosh S, Guha AK, Chatterjee BP, 2006. Infection of jute seedlings by the phytopathogenic fungus *Macrophomina*

phaseolina mediated by endogenous lectin. *Research Journal of Microbiology* 1: 51–60.
Bhowal J, Guha AK, Chatterjee BP, 2005. Purification and molecular characterization of a sialic acid specific lectin from the phytopathogenic fungus *Macrophomina phaseolina*. *Carbohydrate Research* 340: 1973–1982.
Biely P, 2012. Microbial carbohydrate esterases deacetylating plant polysaccharides. *Biotechnology Advances* 30: 1575–1588.
Billon-Grand G, Poussereau N, Fevre M, 2002. The extracellular proteases secreted *in vitro* and *in planta* by the phytopathogenic fungus *Sclerotinia sclerotiorum*. *Journal of Phytopathology* 150: 507–511.
Blanco-Ulate B, Rolshausen P, Cantu D, 2013. Draft genome sequence of *Neofusicoccum parvum* isolate UCR-NP2, a fungal vascular pathogen associated with grapevine cankers. *Genome Announcements* 1: 3.
Burnaugh AM, Frantz LJ, King SJ, 2008. Growth of *Streptococcus pneumoniae* on human glycoconjugates is dependent upon the sequential activity of bacterial exoglycosidases. *Journal of Bacteriology* 190: 221–230.
Chevallet M, Diemer H, Dorssealer A, Villiers C, Rabilloud T, 2007. Toward a better analysis of secreted proteins: the example of the myeloid cells secretome. *Proteomics* 7: 1757–1770.
Cobos R, Barreiro C, Mateos R, Coque J, 2010. Cytoplasmic- and extracellular-proteome analysis of *Diplodia seriata*: a phytopathogenic fungus involved in grapevine decline. *Proteome Science* 8: 46–62.
Dalia AB, Standish AJ, Weiser JN, 2010. Three surface exoglycosidases from *Streptococcus pneumoniae*, NanA, BgaA, and StrH, promote resistance to opsonophagocytic killing by human neutrophils. *Infection and Immunity* 78: 2108–2116.
Damm U, Crous P, Fourie P, 2007. *Botryosphaeriaceae* as potential pathogens of *Prunus* species in South Africa, with descriptions of *Diplodia africana* and *Lasiodiplodia plurivora* sp. nov. *Mycologia* 99: 664–680.
Erjavec J, Kos J, Ravnikar M, Dreo T, Sabotic J, 2012. Proteins of higher fungi: from forest to application. *Trends in Biotechnology* 30: 259–273.
Espino JJ, Gutierrez-Sanchez G, Brito N, Shah P, Orlando R, Gonzalez C, 2010. The *Botrytis cinerea* early secretome. *Proteomics* 10: 3020–3034.
Faulkner C, Robatzek S, 2012. Plants and pathogens: putting infection strategies and defence mechanisms on the map. *Current Opinion in Plant Biology* 15: 699–707.
Fernández-Acero F, Colby T, Harzen A, Cantoral J, Schmidt J, 2009. Proteomic analysis of the phytopathogenic fungus *Botrytis cinerea* during cellulose degradation. *Proteomics* 9: 2892–2902.
Fernández-Acero F, Colby T, Harzen A, Carbu M, Wieneke U, Cantoral J, Schmidt J, 2010. 2-DE proteomic approach to the *Botrytis cinerea* secretome induced with different carbon sources and plant-based elicitors. *Proteomics* 10: 2270–2280.
Fu H, Feng J, Aboukhaddour R, Cao T, Hwang SF, Strelkov SE, 2013. An exo-1,3-beta-glucanase GLU1 contributes to the virulence of the wheat tan spot pathogen *Pyrenophora tritici-repentis*. *Fungal Biology* 117: 673–681.
Gasteiger E, Hoogland C, Gattiker A, Wilkins M, Appel R, Bairoch A, 2005. Protein identification and analysis tools on the ExPASy server. In: Walker J (ed.), *The proteomics protocols handbook*. Humana Press, pp. 571–607.
Girard V, Dieryckx C, Job C, Job D, 2013. Secretomes: the fungal strike force. *Proteomics* 13: 597–608.
Gonzalez-Fernandez R, Aloria K, Valero-Galvan J, Redondo I, Arizmendi JM, Jorrin-Novo JV, 2014. Proteomic analysis of mycelium and secretome of different Botrytis cinerea wild-type strains. *Journal of Proteomics* 97: 195–221.
Gonzalez-Fernandez R, Jorrín-Novo J, 2012. Contribution of proteomics to the study of plant pathogenic fungi. *Journal of Proteome Research* 11: 3–16.
Graça J, Santos S, 2007. Suberin: a biopolyester of plants' skin. *Macromolecular Bioscience* 7: 128–135.
Horn S, Vaaje-Kolstad G, Westereng B, Eijsink V, 2012. Novel enzymes for the degradation of cellulose. *Biotechnology for Biofuels* 5: 45–58.
Huser A, Takahara H, Schmalenbach W, O'Connell R, 2009. Discovery of pathogenicity genes in the crucifer anthracnose fungus *Colletotrichum higginsianum*, using random insertional mutagenesis. *Molecular Plant-microbe Interactions* 22: 143–156.
Islam M, Haque M, Islam M, Emdad E, Halim A, Hossen Q, Hossain M, Ahmed B, Rahim S, Rahman M, Alam M, Hou S, Wan X, Saito J, Alam M, 2012. Tools to kill: Genome of one of the most destructive plant pathogenic fungi *Macrophomina phaseolina*. *BMC Genomics* 13: 493–509.
Jermyn WS, Boyd EF, 2002. Characterization of a novel *Vibrio* pathogenicity island (VPI-2) encoding neuraminidase (nanH) among toxigenic *Vibrio cholerae* isolates. *Microbiology* 148: 3681–3693.
Jové P, Olivella M, Cano L, 2011. Study of the variability in chemical composition of bark layers of *Quercus suber* L. from different production areas. *BioResources* 6: 1806–1815.
Jung Y, Jeong S, Kim S, Singh R, Lee J, Cho Y, Agrawal G, Rakwal R, Jwa N, 2012. Secretome analysis of *Magnaporthe oryzae* using *in vitro* systems. *Proteomics* 12: 878–900.
Laemmli UK, 1970. Cleavage of structural proteins during the assembly of the head of bacteriophage T4. *Nature* 227: 680–685.
Lamport DT, Kieliszewski MJ, Chen Y, Cannon MC, 2011. Role of the extensin superfamily in primary cell wall architecture. *Plant Physiology* 156: 11–19.
Lemos MF, Soares AM, Correia AC, Esteves AC, 2010. Proteins in ecotoxicology - how, why and why not? *Proteomics* 10: 873–887.
Letunic I, Doerks T, Bork P, 2012. SMART 7: recent updates to the protein domain annotation resource. *Nucleic Acids Research* 40: D302–D305.
Li B, Wang W, Zong Y, Qin G, Tian S, 2012. Exploring pathogenic mechanisms of *Botrytis cinerea* secretome under different ambient pH based on comparative proteomic analysis. *Journal of Proteome Research* 11: 4249–4260.
Linaldeddu B, Sirca C, Spano D, Franceschini A, 2009. Physiological responses of cork oak and holm oak to infection by fungal pathogens involved in oak decline. *Forest Pathology* 39: 232–238.
Lulai E, Weiland J, Suttle J, Sabba R, Bussan AJ, 2006. Pink eye is an unusual periderm disorder characterized by aberrant suberization: A cytological analysis. *American Journal of Potato Research* 83: 409–421.
Mackey A, Haystead T, Pearson W, 2001. Getting more from less: algorithms for rapid protein identification with multiple short peptide sequences. *Molecular & Cellular Proteomics* 1: 139–147.
Marincowitz S, Groenewald J, Wingfield M, Crous P, 2008. Species of *Botryosphaeriaceae* occurring on *Proteaceae*. *Persoonia* 21: 111–118.
Martin K, McDougall BM, McIlroy S, Chen J, Seviour RJ, 2007. Biochemistry and molecular biology of exocellular fungal β-(1,3)- and β-(1,6)-glucanases. *FEMS Microbiology Reviews* 31: 168–192.
Medina ML, Kiernan UA, Francisco WA, 2004. Proteomic analysis of rutin-induced secreted proteins from *Aspergillus flavus*. *Fungal Genetics and Biology: FG & B* 41: 327–335.
Mehl JW, Slippers B, Roux J, Wingfield MJ, 2011. *Botryosphaeriaceae* associated with *Pterocarpus angolensis* (kiaat) in South Africa. *Mycologia* 103: 534–553.
Monod M, Capoccia S, Lechenne B, Zaugg C, Holdom M, Jousson O, 2002. Secreted proteases from pathogenic fungi. *International Journal of Medical Microbiology* 292: 405–419.
Niekerk JMV, Fourie PH, Halleen F, Crous PW, 2006. *Botryosphaeria* spp. as grapevine trunk disease pathogens. *Phytopathology Mediterranea* 45: S43–S54.

Parker D, Soong G, Planet P, Brower J, Ratner AJ, Prince A, 2009. The NanA neuraminidase of *Streptococcus pneumoniae* is involved in biofilm formation. *Infection and Immunity* 77: 3722–3730.

Pereira H, 1988. Chemical composition and variability of cork from *Quercus suber* L. *Wood Science and Technology* 22: 211–218.

Phalip V, Delalande F, Carapito C, Goubet F, Hatsch D, Leise-Wagner E, Dupree P, Dorsselaer A, Jeltsch J, 2005. Diversity of the exoproteome of *Fusarium graminearum* grown on plant cell wall. *Current Genetics* 48: 366–379.

Pierleoni A, Martelli P, Fariselli P, Casadio R, 2006. BaCelLo: a balanced subcellular localization predictor. *Bioinformatics* 22: e408–e416.

Pietro A, Roncero M, Roldán M, 2009. From tools of survival to weapons of destruction: the role of cell wall-degrading enzymes in plant infection. In: Deising H (ed.), *Plant Relationships*, 2nd edn. Springer, pp. 181–200.

Reuveni M, Sheglov N, Eshel D, Prusky D, Ben-Arie R, 2007. Virulence and the production of endo-1,4-β-glucanase by isolates of *Alternaria alternata* involved in the moldy-core disease of apples. *Journal of Phytopathology* 155: 50–55.

Rogowska-Wrzesinska A, Le Bihan M, Thaysen-Andersen M, Roepstorff P, 2013. 2D gels still have a niche in proteomics. *Journal of Proteomics* 88: 4–13.

Sarmento AC, Lopes H, Oliveira CS, Vitorino R, Samyn B, Sergeant K, Debyser G, Van Beeumen J, Domingues P, Amado F, Pires E, Domingues MR, Barros MT, 2009. Multiplicity of aspartic proteinases from *Cynara cardunculus* L. *Planta* 230: 429–439.

Sato S, Liu F, Koc H, Tien M, 2007. Expression analysis of extracellular proteins from *Phanerochaete chrysosporium* grown on different liquid and solid substrates. *Microbiology* 153: 3023–3033.

Sergeant K, Samyn B, Debyser G, Van Beeumen J, 2005. *De novo* sequence analysis of N-terminal sulfonated peptides after in-gel guanidination. *Proteomics* 5: 2369–2380.

Slippers B, Smit WA, Crous PW, Coutinho TA, Wingfield BD, Wingfield MJ, 2007. Taxonomy, phylogeny and identification of Botryosphaeriaceae associated with pome and stone fruit trees in South Africa and other regions of the world. *Plant Pathology* 56: 128–139.

Soong G, Muir A, Gomez MI, Waks J, Reddy B, Planet P, Singh PK, Kaneko Y, Wolfgang MC, Hsiao YS, Tong L, Prince A, 2006. Bacterial neuraminidase facilitates mucosal infection by participating in biofilm production. *The Journal of Clinical Investigation* 116: 2297–2305.

Standing K, 2003. Peptide and protein *de novo* sequencing by mass spectrometry. *Current Opinion in Structural Biology* 13: 595–601.

Suarez MB, Sanz L, Chamorro MI, Rey M, Gonzalez FJ, Llobell A, Monte E, 2005. Proteomic analysis of secreted proteins from *Trichoderma harzianum*. Identification of a fungal cell wall-induced aspartic protease. *Fungal Genetics and Biology: FG & B* 42: 924–934.

Tannu N, Hemby S, 2007. *De novo* protein sequence analysis of *Macaca mulatta*. *BMC Genomics* 8: 270.

Uchida Y, Tsukada Y, Sugimori T, 1974. Production of microbial neuraminidases induced by colominic acid. *Biochimica et Biophysica Acta – Enzymology* 350: 425–431.

Upadhyay A, Chompoo J, Kishimoto W, Makise T, Tawata S, 2011. HIV-1 integrase and neuraminidase inhibitors from *Alpinia zerumbet*. *Journal of Agricultural and Food Chemistry* 59: 2857–2862.

Úrbez-Torres J, Gubler W, 2009. Pathogenicity of *Botryosphaeriaceae* species isolated from grapevine cankers in California. *Plant Disease* 93: 584–592.

Vimr ER, Kalivoda KA, Deszo EL, Steenbergen SM, 2004. Diversity of microbial sialic acid metabolism. *Microbiology and Molecular Biology Reviews* 68: 132–153.

Wang Y, Wu J, Park Z, Kim S, Rakwal R, Agrawal G, Kim S, Kang K, 2011. Comparative secretome investigation of *Magnaporthe oryzae* proteins responsive to nitrogen starvation. *Journal of Proteome Research* 10: 3136–3148.

Warwas M, Yeung J, Indurugalla D, Mooers A, Bennet A, Moore M, 2010. Cloning and characterization of a sialidase from the filamentous fungus, *Aspergillus fumigatus*. *Glycoconjugate Journal* 27: 533–548.

Wilson R, Talbot N, 2009. Under pressure: investigating the biology of plant infection by *Magnaporthe oryzae*. *Nature Reviews Microbiology* 7: 185–195.

Yajima W, Kav NN, 2006. The proteome of the phytopathogenic fungus *Sclerotinia sclerotiorum*. *Proteomics* 6: 5995–6007.

Zeleny R, Kolarich D, Strasser R, Altmann F, 2006. Sialic acid concentrations in plants are in the range of inadvertent contamination. *Planta* 224: 222–227.

Zhang J, Xin L, Shan B, Chen W, Xie M, Yuen D, Zhang W, Zhang Z, Lajoie G, Ma B, 2012. PEAKS DB: *de novo* sequencing assisted database search for sensitive and accurate peptide identification. *Molecular & Cellular Proteomics* 11 M111.010587.

Zhou H, Yu Z, Hu Y, Tu J, Zou W, Peng Y, Zhu J, Li Y, Zhang A, Yu Z, Ye Z, Chen H, Jin M, 2009. The special neuraminidase stalk-motif responsible for increased virulence and pathogenesis of H5N1 influenza A virus. *PLoS ONE* 4: e6277.

Zorn H, Peters T, Nimtz M, Berger R, 2005. The secretome of *Pleurotus sapidus*. *Proteomics* 5: 4832–4838.

POSTER AND ORAL COMMUNICATIONS

2012 IUFRO Conference Division 5 Forest Products, 8-13 July, Estoril (Portugal)

Fernandes, I., Alves, A., Devreese, B., Correia, A., Esteves, A. (2012) The threat of *Diplodia corticola* to cork oak – how does infection occur? – *Poster presentation*

EuPA2013 Scientific Meeting, 14-17 October, Saint Malo (France)

Fernandes, I., Alves, A., Devreese, B., Correia, A., Esteves, A. (2013) Secretome of a cork oak pathogen, *Diplodia corticola* – *Poster presentation*

MICROBIOTEC'13, 6-8 December, Aveiro (Portugal)

Fernandes, I., Alves, A., Devreese, B., Correia, A., Esteves, A. (2013) Comparison of *Diplodia corticola* secretome in an infection-like environment – *Poster presentation*

MICROBIOTEC'13, 6-8 December, Aveiro (Portugal)

Fernandes, I., Alves, A., Devreese, B., Correia, A., Esteves, A. (2013) When fungal proteomics meets cork oak decline – *Poster presentation and oral communication*